



Angelidis, Orestis (2025) *5th generation district heating and cooling for holistic energy system decarbonisation: Novel system designs and detailed techno-economic assessment*. PhD thesis.

<https://theses.gla.ac.uk/84916/>

Copyright and moral rights for this work are retained by the author

A copy can be downloaded for personal non-commercial research or study, without prior permission or charge

This work cannot be reproduced or quoted extensively from without first obtaining permission in writing from the author

The content must not be changed in any way or sold commercially in any format or medium without the formal permission of the author

When referring to this work, full bibliographic details including the author, title, awarding institution and date of the thesis must be given

Enlighten: Theses

<https://theses.gla.ac.uk/>
research-enlighten@glasgow.ac.uk

**5th Generation District Heating and Cooling for Holistic Energy System
Decarbonisation: Novel System Designs and Detailed Techno-economic
Assessment**

Orestis Angelidis

Submitted in fulfilment of the requirements for the
Degree of Doctor of Philosophy

School of Engineering
College of Science and Engineering
University of Glasgow



University
of Glasgow

13th September 2024

Abstract

To limit climate breakdown, decarbonising the heating and cooling sector in a cost-effective manner represents a crucial challenge. Holistic energy system decarbonisation is recognised as a key solution, relying on sector coupling, energy reuse and energy storage. 5th Generation District Heating and Cooling (5GDHC) presents a promising pathway for holistic decarbonisation. It utilises an ambient temperature water network with decentralised heat pumps to exploit synergies between heating and cooling, to harness low temperature waste heat and allow sector coupling with the electricity grid. However, questions remain on 5GDHC's hydraulic design, operational stability, economic viability, and overall performance against alternative supply options.

This PhD thesis addresses these gaps by developing and experimentally validating a novel hydraulic design and operational methodology for 5GDHC systems. This design focuses on decentralised variable speed pumping and a centralised passive balancing unit to ensure system stability. Detailed simulation models for the proposed design are also developed and experimentally validated, which are made open access. Additionally, a techno-economic assessment tool, the Centralisation Analysis Tool for Heat Pump Systems (CATHeaPS), is created to evaluate the economic viability of 5GDHC against other thermal supply options. CATHeaPS is also made open access.

To complete these tasks,

1. A systematic literature review is conducted and integrated with views from leading industry and academic professionals in the field, collected during bespoke interviews on the opportunities and challenges of 5GDHC for holistic decarbonisation. It is found that further research is required on quantifying the range of operational boundaries that make 5GDHC more techno-economically viable, hydraulic design and operation standardisation as well as a business structure redefinition.
2. A novel hydraulic design and suitable control philosophies are developed and experimentally validated. The experiments showed stable operation over a period of 20 hours for all demand regimes without control instabilities. A discussion is conducted on generalisability of findings and full-scale implementations.

3. Bespoke Modelica models are created and validated by building a digital twin of the experiment. A stepwise validation of the assembled digital twin demonstrates that the developed Modelica components effectively capture the behaviour of 5GDHC, with a Coefficient of Determination (R^2) for the primary pump flowrates exceeding 0.88 in all cases. The similarity of the results is also seen through an analysis of the overall system behaviour.
4. For the techno-economic comparison of 5GDHC against alternative energy supply strategies for decarbonising heating and cooling, CATHeaPS is employed. CATHeaPS is verified using a direct comparison of outputs and the theoretical results/analysis verification approaches. Economic and environmental analyses are conducted highlighting the impact of cooling and access to waste heat sources. When there is no cooling, 5GDHC performs worse than 4th Generation District Heating (4GDH) for any network topology and consumer class configuration. An annual cooling to heating demand share of 30% (with a demand overlap coefficient of 16%) is required for 5GDHC to start performing better for a higher number of connections per property.
5. A real-world case study with heating and cooling loads and a waste heat source/sink during the winter/summer is used to demonstrate the application of the developed models and methodologies. It quantifies the techno-economic performance of 5GDHC against alternative supply options for the project area. 5GDHC shows a better economic performance than 4GDH with individual Air-Condition units for cooling (4GDH&AC) with 227£/MWh compared to 257£/MWh. It is less energy efficient than 4GDH&AC, having an additional 81 tonnes of CO₂ over a 40-year period. However, having reversible BHP units at each prosumer allows for a smaller electric capacity requirement, reducing the impact on the electricity grid. A discussion is also present on space constraints, operational complexity, and expansion flexibility.

Altogether, this research delivers a comprehensive framework for designing, simulating, and assessing 5GDHC systems. It facilitates their understanding and ultimately assists the efforts for a holistic energy system decarbonisation.

Contents

Abstract	i
Contents	iii
List of Tables	viii
List of Figures	xi
Acknowledgements	xviii
Author’s Declaration	xix
Data Availability	xx
List of papers and contributions	xxi
Paper I – Published – Scientific journal	xxi
Paper II – Submission – Scientific journal.....	xxi
Paper III – Published – Conference paper.....	xxi
Paper IV – Published – Scientific journal	xxi
Paper V – Notional Paper.....	xxii
Connection between papers	xxii
Contribution I – Submission – Book.....	xxiv
Contribution II – Published – Report.....	xxiv
Abbreviations	xxv
List of Symbols	xxvii
Variables with units.....	xxvii
Subscripts	xxviii
1 Introduction	1
1.1 Background	1
1.2 Aims and research objectives.....	7
1.3 Overview of structure.....	8
1.4 Novelty of project	10
2 Systematic Literature Review on 5GDHC for Holistic Energy System	
Decarbonisation	13
2.1 Methodology for SLR and stakeholder interviews	13
2.2 5GDHC system operation and control	17
2.3 5GDHC techno-economic comparison to other supply options	21
2.4 Thermal grid as a flexibility element to the electricity grid.....	25
2.4.1 TES role for sector coupling	25

2.4.2	HP and TES operation for a smart grid	27
2.4.3	DSM for 5GDHC	29
2.5	Business models for holistic 5GDHC system	30
2.6	SLR key findings	33
2.7	Discussion based on stakeholder interviews	36
2.8	Research gaps addressed in this thesis	39
3	5GDHC system: Design, Operation and Simulation.....	41
3.1	5GDHC system design	41
3.2	5GDHC control philosophy	46
3.3	5GDHC system simulation	48
3.3.1	Modelica for 5GDHC simulation.....	48
3.3.2	5GDHC component design methodology	50
3.3.3	Prosumer simulation model.....	51
3.3.4	BU simulation model	57
3.3.5	Hydraulic interface simulation model	59
3.3.6	FMUs of prosumers and BU	61
3.3.7	Exemplary use case of simulation models	62
3.3.8	Implementation of PHIL with developed simulation models	64
3.3.9	Discussion of developed simulation models	66
4	Experimental Validation of Proposed 5GDHC Design and Operational Philosophies	69
4.1	Experimental setup.....	70
4.2	Control implementation and component testing	73
4.3	Hypothesis for experiment	75
4.4	Experimental results.....	77
4.4.1	Overall hydraulic behaviour.....	77
4.4.2	BU experimental behaviour	79
4.4.3	BHP experimental behaviour	80
4.5	Experimental validation	83
4.5.1	Control errors during experiment.....	83
4.5.2	Statistical analysis of experimental measurements	88
4.6	Discussion of experimental findings.....	90
4.6.1	Key findings and control approach comparison.....	91
4.6.2	Generalisability and considerations for larger applications	92
5	Experimental Validation of 5GDHC Modelica Models.....	95

5.1	5GDHC simulation models validation methodology	96
5.1.1	Hydraulics (Hy).....	98
5.1.2	Hydraulics & Prosumers (HyP)	106
5.1.3	Hydraulics & Prosumers & BU (HyPB)	108
5.1.4	Full Model (FM)	110
5.2	5GDHC simulation models validation results.....	111
5.3	5GDHC simulation models validation discussion	123
6	Techno-economic Modelling: CATHeaPS	126
6.1	Background on techno-economic assessments for 5GDHC systems.....	126
6.1.1	Review of existing TEMs	128
6.1.2	Introducing CATHeaPS	131
6.2	CATHeaPS methodology.....	132
6.2.1	Energy demand assessment in CATHeaPS.....	133
6.2.2	Hydraulic design in CATHeaPS	136
6.2.3	Energy supply assessment in CATHeaPS.....	140
6.2.4	Economic analysis in CATHeaPS.....	144
6.3	CATHeaPS verification	147
6.3.1	CATHeaPS verification methodology	147
6.3.2	CATHeaPS verification results and discussion.....	150
6.3.3	CATHeaPS verification sensitivity analysis	156
6.4	CATHeaPS for economic and environmental analyses	159
6.5	CATHeaPS for economic analysis – BEP	165
6.5.1	BEP of ‘heating only’ districts with access to an ambient temperature waste heat source.....	166
6.5.2	BEP of ‘heating only’ districts.....	169
6.5.3	BEP of heating and cooling districts.....	170
6.5.4	Discussion of BEP outputs and wider considerations.....	174
6.6	CATHeaPS for environmental analysis – Monte Carlo simulations	175
6.6.1	Discussion of environmental analysis outputs	178
6.7	Discussion on CATHeaPS limitations and future improvements	180
7	Case Study: D2 Grids Ambient Loop Project in Clyde Gateway, Glasgow	182
7.1	Introduction to the case study	182
7.1.1	Case study background	182
7.1.2	Supply options in case study project area	184
7.1.3	Case study aim and objectives	186

7.2	Energy demand assessment of case study project area	187
7.3	WWTP waste heat utilisation.....	192
7.4	5GDHC design and operation for case study	198
7.4.1	Analysis and simulation of prosumers for 5GDHC	201
7.4.2	Analysis and simulation of BU for 5GDHC	206
7.4.3	Energy share of the WWTP for 5GDHC	212
7.4.4	Ambient network sizing for 5GDHC	214
7.5	Techno-economic modelling of case study.....	219
7.5.1	Electricity use and CO ₂ emissions of supply options considered in the case study	221
7.5.2	Economic performance of supply options considered in the case study.....	225
7.6	Sensitivity analysis of case study variables	228
7.6.1	Sensitivity analysis of techno-economic variables	228
7.6.2	Sensitivity analysis of WWTP capacity.....	230
7.7	Discussion on case study outputs.....	233
7.7.1	Miscellaneous factors affecting supply option selection	233
7.7.2	Overall techno-economic performance of supply options considered in the case study	234
7.7.3	5GDHC for areas with low heating and cooling demand co-occurrence.....	235
7.7.4	Limitations of the case study analysis.....	236
8	Conclusion, Context and Future Research	237
8.1	Conclusion	237
8.2	Context	246
8.3	Future research	247
9	References	249
10	Appendix A - Stakeholder interview details	273
10.1	Appendix A1 - Participant information sheet	274
10.2	Appendix A2 - Consent form.....	279
11	Appendix B – Experiment schematics, photos and drawings	281
11.1	Appendix B1 - P&ID	281
11.2	Appendix B2 – Equipment photos	283
11.2.1	Heating prosumer	283
11.2.2	Cooling prosumer.....	285
11.2.3	ASHP and BU TES	287
11.2.4	Grid connector.....	288

11.3	Appendix B3 – LabView screenshots	289
11.3.1	Main virtual instrument interface	289
11.3.2	BU sub VI	291
11.3.3	Heating prosumer sub VI	292
11.3.4	Cooling prosumer	295
12	Appendix C – CATHeaPS Data	297

List of Tables

Table 2.1: SLR search strategy.	14
Table 2.2: Stakeholder engagement details.....	16
Table 2.3: Opportunities and barriers of 5GDHC in terms of techno-economic performance, sector coupling facilitation and market uptake (adapted from [144]).....	34
Table 4.1: Legend for data referencing.	69
Table 4.2: Description of control elements from Figure 4.3.....	74
Table 4.3: Setpoints used for key control variables in the experiment.	76
Table 4.4: Energy and SCOP for BHP.....	82
Table 4.5: R^2 values for experimental accuracy (values with an asterisk (*) next to them have been adjusted).	90
Table 5.1: Validation steps description.....	97
Table 5.2: Pipework lengths for pipe sections 3-8 from Figure 5.5.....	102
Table 5.3: Elements of hydraulic resistance for pipe sections 3-8 from Figure 5.5.	102
Table 5.4: Values of ζ for different hydraulic resistance elements.....	103
Table 5.5: Cumulative ζ for pipe sections 3-8 from Figure 5.5.	103
Table 5.6: Δp at nominal flowrate of 30l/min for pipe sections 3-8 from Figure 5.5.....	105
Table 5.7: PI controller parameters for simulation and experiment.....	105
Table 5.8: Heating prosumer's TES pipe connections' levels.	108
Table 5.9: BU's TES pipe connections' levels.	110
Table 5.10: Computational time for validation cases: simulation time 72,000s (20h).	111
Table 5.11: R^2 values for Hy, HyP and HyPB flowrates.....	116
Table 5.12: R^2 values for Hy, HyP and HyPB flowrates (* values have been adjusted).	118
Table 5.13: Comparison of power and energy outputs for BHP and ASHP for FM digital twin.	118
Table 5.14: R^2 for energy outputs for BHP and ASHP for FM digital twin.....	121
Table 6.1: Summary of tools for heat network supply options assessment.	130
Table 6.2: Input data and their description.	133
Table 6.3: Factors included in CATHeaPS supply options.	146
Table 6.4: Building schedule of Network 1.	148
Table 6.5: Pipe schedule and network layout for Network 1.....	149
Table 6.6: Pipe Schedule and network layout for Network 2.	149

Table 6.7: 4GDH&AC supply option verification using Network 1 ('heating only' districts).....	151
Table 6.8: Verification of ASHP and GB using IEA published data [224].	152
Table 6.9: Verification of 5GDHC using published CAPEX data [4].	155
Table 6.10: Parameters included in the sensitivity analysis.....	156
Table 6.11: Sensitivity analysis on 40-year LCOE with social costs for 'heating only'.	157
Table 6.12: Sensitivity analysis on 40-year LCOE with social costs for heating and cooling.....	158
Table 6.13: Average computational time for CATHeaPS for different number of properties.....	165
Table 6.14: 4GDH&AC vs 5GDHC for different shares of cooling demand.....	171
Table 7.1: Case study objectives.....	186
Table 7.2: Building schedule of project area.	187
Table 7.3: Demand assessment outputs.	189
Table 7.4: Capacity of BHP and TES.	203
Table 7.5: Electricity use and SCOP of BHP in prosumer substations.....	205
Table 7.6: Plant sizing for BU for 5GDHC-1 and 5GDHC-2.....	208
Table 7.7: Control setpoints for ASHP and SWSHP in the BU based on TES temperature.....	208
Table 7.8: Energy use for BU for full built-out.	209
Table 7.9: Share of energy from WWTP.	213
Table 7.10: Trench lengths and pipe diameters for each topology.	216
Table 7.11: Trench lengths and pipe diameters for 4GDH&AC option.	219
Table 7.12: 4GDH&AC supply option equipment sizing.....	220
Table 7.13: ASHP supply option equipment sizing.....	220
Table 7.14: SPF for counterfactual energy supply scenarios.....	221
Table 7.15: CATHeaPS outputs – LCOE components.....	225
Table 7.16: CATHeaPS outputs – total absolute costs.....	226
Table 7.17: Parameters included in the sensitivity analysis.....	228
Table 7.18: Sensitivity analysis on 40-year LCOE with social costs.....	229
Table 7.19: 5GDHC-1 BU's new demand.....	230
Table 7.20: Impact on BU's energy supply for WWTP sensitivity.....	231
Table 7.21: Impact of WWTP capacity on LCOE.....	232
Table 12.1: Key technical data used in CATHeaPS.....	297

Table 12.2: Key cost data used in CATHeaPS.	298
--	-----

List of Figures

Figure 1.1: Progression of district heating – 1 st to 4 th generation [21].....	3
Figure 1.2: Progression of district cooling – 1 st to 4 th generation [22].	3
Figure 1.3: Ambient network with decentralised BHPs supplying heating and cooling prosumers.	5
Figure 1.4: Schematic of PhD structure.	11
Figure 2.1: SLR Methodology.	15
Figure 2.2: VOS Viewer map of SLR keyword co-occurrence by publication year.	15
Figure 2.3: Stakeholder interview themes.....	16
Figure 2.4: Comparison of bidirectional 5GDHC system and reservoir network.	20
Figure 3.1: 5GDHC with decentralised and centralised pumping using an active BU for thermodynamic balancing.	42
Figure 3.2: Pump hunting phenomena in a bidirectional grid.....	42
Figure 3.3: 5GDHC with decentralised pumping and passive BU for balancing.	44
Figure 3.4: Prosumer pump interaction example in proposed hydraulic setup.....	45
Figure 3.5: Schematic of control strategy for $T_{GridFloat}$	47
Figure 3.6: Schematic of control strategy for $T_{GridFix}$	47
Figure 3.7: Modelica components used for 5GDHC system development.....	51
Figure 3.8: 5GDHC prosumer Modelica model.....	52
Figure 3.9: Schematic of control methodology for BHP.	54
Figure 3.10. TES operation under modulation of the BHP.....	56
Figure 3.11: 5GDHC BU Modelica model.	57
Figure 3.12: Schematic of control methodology for BU.....	58
Figure 3.13: Hydraulic interfaces for prosumer, BU and hydraulic model for the 5GDHC grid.....	60
Figure 3.14: Exemplary case study of developed 5GDHC Modelica models.	63
Figure 3.15: PHIL for a prosumer using a HEX.	65
Figure 4.1: Experimental setup schematic.	71
Figure 4.2: BHP schematic detail with InPu _{BHP}	72
Figure 4.3: Control elements and PHIL setup.....	73
Figure 4.4: BHP and ASHP operation based on TES temperature levels.....	75
Figure 4.5: Demands resulting from PHIL simulation models.	77
Figure 4.6: Hot and cold grid pipe temperatures and flowrate through the BU.....	78
Figure 4.7: BU TES temperature profile.....	80

Figure 4.8: BHP operation and heating prosumer's TES temperature profile.....	81
Figure 4.9: BHP energy profile.....	82
Figure 4.10: Pump control setpoints and measurements for $T_{GridFix}$	84
Figure 4.11: Pump control setpoints and measurements for $T_{GridFix}$, detail on BHP operation.....	85
Figure 4.12: Pump control setpoints and measurements for $T_{GridFix}$, detail on HEX _{DC} operation.....	85
Figure 4.13: Pump control setpoints and measurements for $T_{GridFloat}$	86
Figure 4.14: Pump control setpoints and measurements for $T_{GridFloat}$, detail on BHP startup.....	87
Figure 4.15: Pump control setpoints and measurements for $T_{GridFloat}$, detail of HEX _{DC}	88
Figure 4.16: Calculation of the theoretical prosumer grid flowrate.....	88
Figure 4.17: Experimental and adjusted theoretical flowrates of prosumers' grid pumps.....	91
Figure 5.1: Modelica digital twin of the experiment.....	95
Figure 5.2: Schematic of validation steps.....	96
Figure 5.3: Hy validation step Modelica simulation model.....	98
Figure 5.4: Schematic for step Hy validation variables.....	99
Figure 5.5: Schematic of the experimental setup with numbers for pipe sections of interest.....	101
Figure 5.6: Pump curve for heating prosumer [172].....	104
Figure 5.7: Pump curve for cooling prosumer [169].....	104
Figure 5.8: HyP validation step Modelica simulation model.....	106
Figure 5.9: Schematic for Hydraulics & Prosumers validation variables.....	107
Figure 5.10: HyPB validation step Modelica simulation model.....	109
Figure 5.11: HyPB BU Modelica simulation model.....	109
Figure 5.12: Validation results for Hy against experimental outputs.....	112
Figure 5.13: Validation results for HyP against experimental outputs.....	113
Figure 5.14: Validation results for HyPB against experimental outputs.....	114
Figure 5.15: Validation results for Hy, HyP and HyPB against experimental outputs.....	115
Figure 5.16: Detail of cooling prosumer flowrate for $T_{GridFloat}$ for hours 1 to 2 in the Hy step.....	116
Figure 5.17: Detail of heating prosumer flowrate for $T_{GridFix}$ at the 3 rd hour in the HyP step.....	117

Figure 5.18: Detail of heating prosumer flowrate for $T_{GridFloat}$ at BHP startup in the HyP step.	117
Figure 5.19: $T_{GridFix}$ BHP and ASHP power and energy outputs.	119
Figure 5.20: $T_{GridFloat}$ BHP and ASHP power and energy outputs.	120
Figure 5.21: BU's TES temperature profile for $T_{GridFix}$ and $T_{GridFloat}$	122
Figure 6.1: Schematic of different heat supply options.	127
Figure 6.2: Schematic of CATHeaPS methodology.	132
Figure 6.3: Diversification curve for DHW, space heating and space cooling.	135
Figure 6.4: Flowchart for pipe sizing algorithm for 4GDH.	137
Figure 6.5: Flowchart for pipe sizing algorithm for 5GDHC.	138
Figure 6.6: Connection methodology for 4GDH and 5GDHC systems in CATHeaPS.	139
Figure 6.7: Connection methodology for residential units with multiple connections for 4GDH and 5GDHC systems in CATHeaPS (adapted from [43]).	139
Figure 6.8: Normalised hourly demand profiles from FLEXYNETS [69].	142
Figure 6.9: Normalised monthly demand profiles from FLEXYNETS [69].	142
Figure 6.10: Example of BU balancing requirements for a fictitious 5GDHC scheme.	143
Figure 6.11: Electricity emission factors [17].	144
Figure 6.12: LCOE of Network 1 (A) and Network 2 (B) (heating demand).	150
Figure 6.13: LCOE of Network 1 (A) and Network 2 (B) (heating and cooling demand).	153
Figure 6.14: 'Heating only' scenario's BU share for 5GDHC in Network 1.	154
Figure 6.15: Heating and cooling scenario's BU share for 5GDHC in Network 1.	154
Figure 6.16: Normalised sensitivity analysis outputs ('heating only').	157
Figure 6.17: Normalised sensitivity analysis outputs (heating and cooling).	158
Figure 6.18: Break-even point example for 4GDH and 5GDHC networks.	160
Figure 6.19: AN schematic.	162
Figure 6.20: Supply options considered for 'heating only' districts with access to an ambient temperature waste heat source.	163
Figure 6.21: Supply options for 'heating only' districts.	164
Figure 6.22: Supply options for heating and cooling districts.	165
Figure 6.23: BEP for 4GDH to become more economical than other energy supply options.	166
Figure 6.24: Preliminary energy supply performance comparison of ASHP-AN-4GDH.	167
Figure 6.25: Preliminary energy supply performance comparison of GB-AN-4GDH.	168

Figure 6.26: Sensitivity analysis on BEP for ASHP-AN-4GDH.....	168
Figure 6.27: Sensitivity analysis on BEP for GB-AN-4GDH.....	169
Figure 6.28: DOC for different annual shares of cooling and heating demand.	171
Figure 6.29: Heating and cooling demands overlaid on the BU's share. Annual cooling demand is 10% of the annual heating demand.....	172
Figure 6.30: Heating and cooling demands overlaid on the BU's share. Annual cooling demand is 50% of the annual heating demand.....	172
Figure 6.31: Preliminary energy supply performance comparison of ASHP-5GDHC-4GDH&AC for annual cooling demand of 10% to 50% of heating demand.	173
Figure 6.32: Preliminary energy supply performance comparison of GB&AC-5GDHC-4GDH&AC for annual cooling demand of 10% to 50% of heating demand.....	173
Figure 6.33: CO ₂ Emissions from Monte Carlo simulations excluding GB&AC (A) 'heating only' districts with access to an ambient temperature waste heat source, (B) 'heating only' districts and (C) heating and cooling districts.	176
Figure 6.34: Emissions from Monte Carlo simulations (A) 'heating only' districts with access to an ambient temperature waste heat source, (B) 'heating only' districts and (C) heating and cooling districts.	177
Figure 6.35: Normalised standard deviation of CO ₂ emissions for all three scenarios when (A) the number of properties is kept constant and (B) when the density is kept constant.	179
Figure 7.1: Project regeneration area in Glasgow [232].	183
Figure 7.2: Constructed ambient network, EC and WWTP abstraction point [233].	183
Figure 7.3: Building schedule for case study.	184
Figure 7.4: 5GDHC Network with decentralised BHP plantrooms.....	185
Figure 7.5: 4GDH network with centralised EC and individual AC for cooling.....	185
Figure 7.6: Reversible ASHPs on building level for heating/cooling.....	185
Figure 7.7: Ambient air temperature, solar direct and diffused radiation.	188
Figure 7.8: Values for step functions probability method for DHW demand analysis.....	189
Figure 7.9: Specific Energy demand per building.	190
Figure 7.10: Specific peak demand per building.	190
Figure 7.11: Total annual heating and cooling demand and their co-occurrence (DOC).....	191
Figure 7.12: Demand phasing from start year to full built-out.	191
Figure 7.13: Average daily final effluent temperature.	192
Figure 7.14: 5GDHC scenarios for using the WWTP as a heat source/sink.....	193

Figure 7.15: 5GDHC-1 restrictions for utilising WWTP through a HEX.	194
Figure 7.16: Histogram of WWTP’s final effluent flow temperatures.	195
Figure 7.17: 5GDHC-1 temperature profile during heating and cooling season.	196
Figure 7.18: WWTP’s final effluent and temperature profile and available thermal power.	196
Figure 7.19: Building heating and cooling demands, WWTP energy share and demand co-occurrence.	197
Figure 7.20: Demand co-occurrence from prosumer demands and WWTP.	197
Figure 7.21: Methodology of 5GDHC design for yielding inputs for TEM.	199
Figure 7.22: Prosumer setup schematic.	201
Figure 7.23: Prosumer simulation using ProHMo models.	202
Figure 7.24: BHP and Heating TES operation for meeting heating requirements.	203
Figure 7.25: BHP and Cooling TES operation for meeting cooling requirements.	204
Figure 7.26: Electricity use for buildings for each year accounting for phasing.	205
Figure 7.27: Energy supply from BU for 5GDHC-1 and 5GDHC-2 for full built-out.	206
Figure 7.28: BU Models in ProHMo.	207
Figure 7.29: Operation of 5GDHC-2 BU units during hours 30 to 70.	210
Figure 7.30: 5GDHC-2 BU’s TES power and energy profile during hours 30 to 70.	211
Figure 7.31: Annual temperature profile in BU’s TES.	211
Figure 7.32: Energy transformation units’ electricity use for 5GDHC-1 and 5GDHC-2.	212
Figure 7.33: 5GDHC-1 network layout.	215
Figure 7.34: 5GDHC-2 network layout.	215
Figure 7.35: Network topology 5GDHC-1.	217
Figure 7.36: Network topology 5GDHC-2.	218
Figure 7.37: Total electricity use for different supply options at full built-out.	222
Figure 7.38: Annual (solid) and cumulative (dashed) CO ₂ emissions for each supply option.	223
Figure 7.39: Installed power capacity for each supply option.	223
Figure 7.40: Electricity grid capacity in project area.	224
Figure 7.41: CATHeaPS outputs – LCOE.	226
Figure 7.42: Normalised outputs of sensitivity analysis on LCOE with social costs.	229
Figure 7.43: WWTP capacity sensitivity on co-occurrence of building demand and WWTP available power.	230

Figure 11.1: (Left) Grid pump for heating prosumer (Right) Flowmeter on the return of the BHP.....	283
Figure 11.2: (Left) Connection to and out from the BHP (Right) Connection from the BHP to the TES.....	284
Figure 11.3: Connection from the TES to the DHW and space heating loads.....	284
Figure 11.4: Connection to the space heating and DHW loads, each having a HEX dedicated to it for the load emulation.....	285
Figure 11.5: (Left) HC for replicating cooling prosumer (Right) HC inlet and outlet.	286
Figure 11.6: Connection to and from the HC, back to the HEX _{DC} (Right) HEX _{DC} and flowrate sensor.	286
Figure 11.7: Cooling prosumer grid pump.....	287
Figure 11.8: (Left) ASHP indoor and outdoor unit along with air chamber for air intake (Right) BU TES.....	287
Figure 11.9: Grid connection (for hot and cold pipes), combining the BU TES, BHP and HEX _{DC} flows.	288
Figure 11.10: VeriStand inputs (from IC sensors) and LabView control sub-VIs.	289
Figure 11.11: VeriStand outputs for IC.....	290
Figure 11.12: PHIL VeriStand outputs.	290
Figure 11.13: LabView control logic when the ASHP is off.....	291
Figure 11.14: LabView control logic when the ASHP is on.....	291
Figure 11.15: ASHP control parameters front panel.....	292
Figure 11.16: LabView control logic when the BHP is on.....	292
Figure 11.17: LabView control logic when the BHP is off.	293
Figure 11.18: BHP control parameters front panel.	293
Figure 11.19: Heating prosumer grid pump control logic for $T_{GridFloat}$ (control on pump flowrate).....	293
Figure 11.20: Heating prosumer grid pump control logic for $T_{GridFix}$ (control on return temperature).	294
Figure 11.21: Heating prosumer grid pump control parameters front panel.....	294
Figure 11.22: DHW control logic.	294
Figure 11.23: Heating coil operation and cold prosumer control logic.	295
Figure 11.24: Cooling prosumer control parameters front panel.	295
Figure 11.25: Cooling prosumer control logic for $T_{GridFloat}$ (control on flow temperature to heating coil).	296

Figure 11.26: Cooling prosumer control logic for $T_{GridFix}$, (control on return temperature of HEX _{DC}).	296
---	-----

Acknowledgements

This thesis constitutes the final product of many years of work and summarizes my PhD journey. A journey that has seen me spending hours in front of a computer screen in a tiny flat in London to draining mug after mug of coffee in a lab in Munich, hoping that the experiment will run on the last days of my stay. But what I will remember the most from these years, are the amazing people I got to meet; they have made me a better person.

Firstly, I want to thank my supervisors. I advise anyone considering starting a PhD to focus on their supervisors. I sincerely hope they are as fortunate as I have been. My primary supervisor, Professor Gioia Falcone, and my secondary supervisor, Professor Daniel Friedrich, have been exceptionally helpful throughout my PhD. Other than the advice and help they have offered, they have set the highest standards of professionalism. My tertiary supervisor, Dr. Anastasia Ioannou, and my industrial supervisor, Alan Thomson, have offered invaluable technical and editorial support, and it has been a joy to collaborate with them. This supervisory team has provided me with a platform to develop and realise my ideas. Their working ethos and guidance has shaped me as a scientist and a professional.

I would also like to thank my colleagues in the Technical University of Munich for providing me the facilities to conduct my experiments in the CoSES centre for combined energy systems. I would like to thank Professor Thomas Hamacher and Professor Christoph Goebel for welcoming me in their research groups. I cannot overstate my gratitude to Dr. Daniel Zinsmeister for his help in shaping and undertaking the experiment. Rushing through the open door between our offices to sketch a new idea on each other's whiteboards is one of the sweetest memories I have. I would like to thank everyone at TUM's CoSES and EMT teams, for making my Munich stay the highlight of my PhD.

I would also like to thank the Energy Technology Partnership (ETP), the University of Glasgow, and Ramboll for funding this work. I would like to thank the Ramboll Foundation for its financial support and my Ramboll UK Energy Systems colleagues for their technical support and guidance.

Finally, I want to thank my friends and family for their love and support throughout this journey. Their understanding, patience and interest has been instrumental in completing this work.

Author's Declaration

I declare that all work presented in this thesis is entirely my own, unless clearly stated to be the contribution of others through referencing in accordance with the University's guidance on good academic conduct.

Signed:

Orestis Angelidis

September 2024

Data Availability

All experimental data presented in this work are made openly available at the University of Glasgow's Enlighten Repository with DOI:10.5525/gla.researchdata.1659 available at <https://researchdata.gla.ac.uk/id/eprint/1659> [1].

All developed Modelica simulation models for 5GDHC are made openly available at the University of Glasgow's Enlighten Repository at <https://researchdata.gla.ac.uk/1639> [2].

All techno-economic models developed for analysing 5GDHC and alternative supply options are made openly available at the University of Glasgow's Enlighten Repository at <https://researchdata.gla.ac.uk/id/eprint/1638> [3].

List of papers and contributions

This chapter aims to provide information about publications and contributions arising from this PhD and the plan for future ones.

Paper I – Published – Scientific journal

2023. District heating and cooling networks with decentralised energy substations: Opportunities and barriers for holistic energy system decarbonisation.

Angelidis, O., Ioannou, A., Friedrich, D., Thomson, A., Falcone, G.,
Energy 269, 126740. <https://doi.org/10.1016/j.energy.2023.126740>

Paper II – Published – Scientific journal

2025. Comparative technoeconomic analysis of centralised and decentralised water source heat pump systems using CATHeaPS.

Angelidis, O., Ioannou, A., Friedrich, D., Thomson, A., Falcone, G.,
Heliyon 11, e41396. <https://doi.org/10.1016/j.heliyon.2024.e41396>

Paper III – Published – Conference paper

2023. 5th Generation District Heating and Cooling Modelica Models for Prosumer Interaction Analysis.

Angelidis, O., Zinsmeister, D., Ioannou, A., Friedrich, D., Thomson, A., Falcone, G.,
Modelica Conferences 607–616. <https://doi.org/10.3384/ecp204607>

Paper IV – Published – Scientific journal

2024. Development and experimental validation of a hydraulic design and control philosophies for 5th generation district heating and cooling networks.

Angelidis, O., Zinsmeister, D., Ioannou, A., Friedrich, D., Thomson, A., Ganslmeier, U.,
Falcone, G.,
Energy 308, 132835. <https://doi.org/10.1016/j.energy.2024.132835>

My paper contributions.

	Conceptualisation	Methodology	Formal Analysis	Investigation	Writing - draft	Writing Review & editing	Visualisation
Paper I	3	3	3	3	3	3	3
Paper II	3	3	3	3	3	3	3
Paper III	3	3	3	3	3	3	3
Paper IV	3	3	3	3	3	3	3

Levels of contribution

None	0
Little	1
Moderate	2
High	3

In addition to these 4 papers, there is 1 more notional paper that should be derived from this thesis.

Paper V – Notional Paper

Notional paper on the conceptual design of 5th Generation District Heating and Cooling for D2 Grids Ambient Loop Project in Clyde Gateway, Glasgow. The work has been presented in the 10th Smart Energy Systems conference where it received positive feedback.

Connection between papers

Paper I investigates the opportunities and barriers related to techno-economic performance, sector coupling facilitation and market uptake of district heating and cooling networks with decentralised energy substations. It follows a systematic literature review and integrates its findings with insights from interviews held with stakeholders from leading academic and industrial institutions in the field. It establishes the foundation of the project. It presents a series of further research topics following a critical discussion of the key findings and opening the way for extensive research opportunities, helping to clarify their benefits and operational details.

Paper II provides the design decisions and methodology for thermal networks featuring water source heat pumps along with a completed techno-economic model for scenario appraisal. It sets the components required for a break-even analysis. It covers the design process for thermal systems ranging from energy demand assessment and hydraulic design to economic evaluation and sensitivity analysis. It provides a preliminary indication of beneficiary operation for different thermal zoning scenarios when only heating is considered. The model developed will be used when obtaining the results from the detailed simulations of heating and cooling networks examined in paper III.

Paper III presents the developed simulation models to accurately capture 5th generation district heating and cooling networks with decentralised energy stations with simultaneous heating and cooling loads. To accurately capture the effect of “energy trading” formed by the interaction of different prosumers (points of connection that supply and consume energy) the Modelica language is used. New hydraulic designs and control strategies are implemented in the models, capturing thermofluid and energy flows. These models allow a study of energy use and sector coupling opportunities with the electricity grid.

Paper IV presents novel control methodologies for the operation of district heating and cooling networks with decentralised energy stations. In addition, it describes their experimental validation using the power hardware in the loop approach shown in Paper III.

Paper V is the final planned output from this PhD, which will combine the developed designs and models for a detailed techno-economic analysis of a real project area in Glasgow. It follows a conceptual level design of the proposed designs and operation shown in Paper IV, utilising the simulation models shown in Paper III to characterise it. Then, its techno-economic performance against alternative supply options is assessed using the techno-economic model shown in Paper II.

Other than the first author papers discussed above, my work during this PhD has contributed to other outputs. These are outlined below.

Contribution I – Submission – Book

The work during this PhD informed my co-author contribution to the Elsevier book *Geothermal Energy Engineering: Technology Transfer from the Oil and Gas Industry*, in the *Geothermal production, injection and storage engineering* chapter. My work focused on the integration of geothermal systems with district thermal energy networks. It investigated the impact of centralising thermal energy supply units and sources as well as the opportunities for different types of thermal networks to be coupled with geothermal sources.

Contribution II – Published – Report

Scottish Enterprise commissioned Ramboll to analyse the capital costs and value across the supply chain for design, build and delivery of 4th and 5th generation heat networks. As the third author, I focused on the technical aspects and the development of potential cost/supplier trends. The industrial report was published in January 2024 and is made open accessed* [4].

* Available online at: <https://www.scottish-enterprise.com/learning-zone/research-evaluation-and-insight/2024/cost-analysis-of-a-typical-4th-and-5th-generation-heat-network>.

Abbreviations

Abbreviation	Meaning
3WV	3-Way Valve
4GDC	4 th Generation District Cooling
4GDH	4 th Generation District Heating
4GDHC	4 th Generation District Heating and Cooling
5GDHC	5 th Generation District Heating and Cooling
AN	Anergy Network
ASHP	Air Source Heat Pump
BEP	Break-Even Point
BHP	Booster Heat Pump
BU	Balancing Unit
CAPEX	Capital Expenditure
CO ₂	Carbon Dioxide
DESNZ	Department for Energy Security and Net Zero
DH&AC	District Heating with Air-Conditioning units
DHC	District Heating and Cooling
DNO	Distribution Network Operator
DOC	Demand Overlap Coefficient
DSM	Demand Side Management
EC	Energy Centre
EER	Energy Efficiency Rating
EHV	Extra High Voltage
ESCo	Energy Supply Company
FFC	Feed Forward Control
FM	Full Model
FMI	Functional Mock-Up Interface
FMU	Functional Mock-Up Unit
GB	Gas Boilers
GB&AC	Gas Boilers with Air-Conditioning units
HC	Heating coil
HEX _{DC}	Direct Cooling Heat Exchanger
HIU	Heat Interface Unit
HP	Heat Pump
HV	High Voltage

Abbreviation	Meaning
Hy	Hydraulics (Modelica models validation step)
HyP	Hydraulics & Prosumers (Modelica models validation step)
HyPB	Hydraulics & Prosumers & Balancing Unit (Modelica models validation step)
IEA	International Energy Agency
InPu _{BHP}	Internal Pump on Booster Heat Pump's Evaporator
KPI	Key Performance Indicator
LCOE	Levelised Cost of Energy
LMTD	Logarithmic Mean Temperature Difference
MILP	Mixed Integer Linear Programming
MPC	Model Predictive Control
NPV	Net Present Value
OHL	Overhead Lines
OPEX	Operational Expenditure
P&ID	Pipe and Instrumentation Diagram
PHIL	Power Hardware in the Loop
PI	Proportional – Integral
PID	Proportional – Integral – Derivative
PV	Photovoltaic
R ²	Coefficient of Determination
REPEX	Replacement Expenditure
RES	Renewable Energy Systems
RO	Research Objective
SCOP	Seasonal Coefficient of Performance
SEER	Seasonal Energy Efficiency Rating
SPF	Seasonal Performance Factor
SWSHP	Sewer Water Source Heat Pump
TEM	Techno-economic Model
TES	Thermal Energy Store
TESTL	Thermal Energy Store Temperature Layer
VSD	Variable Speed Drive
WSHP	Water Source Heat Pump
WWTP	Waste Water Treatment Plan

List of Symbols

Variables with units

Symbol	Meaning, Unit
A	Surface area, m ²
AHD	Annual heating demand with losses, kWh
COP_c	Cumulative coefficient of performance, dimensionless
cp	Specific heat capacity, J/(kgK)
D	Pipe diameter, m ²
DF_{SHC}	Space heating/cooling diversity factor, dimensionless
E	Energy, J
f	Darcy friction coefficient, dimensionless
h_o	heat transfer coefficient of water, W/m ² K
hp_{oh}	Heat pump's operational hours, hr
hp_s	Heat pump's share of heating/cooling supply, %
L	Length, m
mf	Modulation factor, %
n	Efficiency, %
N	Number of non-domestic properties, dimensionless
n_{HEX}	HEX _{DC} efficiency, %
P	Power, W
p	Pressure, Pa
q	Flowrate, m ³ /s
q_d	Diversified design flow rate for domestic hot water demand calculation, l/min
q_f	Peak flow rate for domestic hot water demand calculation, l/min
q_m	Weighted mean flow rate for domestic hot water demand calculation, l/min
r	Discount rate, %
SF	Safety factor, dimensionless
T	Temperature, °C
t	Timestep, s

Symbol	Meaning, Unit
t_{dis}	Discharge period, s
$TESTL$	Thermal Energy Store Temperature Layer, dimensionless
t_y	Number of years since the start of the project, years
α	Parameter for counterflow heat exchanger efficiency calculation, m^3/kg
β	Parameter for heat balance between the two counterflowing streams, Jkg/sm^3K
Δp	Pressure drop, Pa
$\Delta p/L$	Pressure drop per meter of pipe, Pa/m
ΔT	Temperature difference, °C
ζ	Pressure loss coefficient, dimensionless
θ	Probability of draining during peak load for domestic hot water demand calculation, %
ρ	Density, kg/m^3

Subscripts

Symbol	Meaning
$5GDHC$	5GDHC Network
Af	ASHP flow pipe
Ar	ASHP return pipe
$ASHP$	Air source heat pump
BHP	Booster heat pump
BU	Balancing unit
bui	Building
C	Cold pipe
cal	Calculated analytical value
co	Cooling
$CPro$	Cooling prosumer
el	Electric
exp	Experimental measurement
FFC	Feed forward control
H	Hot pipe
he	Heating

Symbol	Meaning
<i>HEX</i>	Heat exchanger
<i>hi</i>	High
<i>HP_{ro}</i>	Heating prosumer
<i>lo</i>	Low
<i>max</i>	Maximum setpoint
<i>min</i>	Minimum setpoint
<i>pri</i>	Primary network (ambient grid)
<i>ref</i>	Reference
<i>sec</i>	Secondary network (between BHP and TES)
<i>set</i>	Setpoint
<i>sim</i>	Simulation output
<i>sink</i>	Thermal sink
<i>source</i>	Thermal source
<i>startHP</i>	Control setpoint for starting the heat pump
<i>stopHP</i>	Control setpoint for stopping the heat pump
<i>sup</i>	Supply
<i>SWSHP</i>	Sewer water source heat pump
<i>ter</i>	Tertiary network (flow through heating/cooling load).
<i>TES</i>	Thermal energy store
<i>th</i>	Thermal
<i>WWTP</i>	Waste water treatment plant

1 Introduction

This chapter introduces the need for a widespread decarbonisation of the thermal sector centred around energy reuse and sector coupling. It provides background on the concept of 5th Generation District Heating and Cooling (5GDHC) and how it could provide a pathway for holistic decarbonisation. The aims and objectives of this PhD thesis are clearly set out followed by an overview of the thesis' structure and a discussion on the novelty of the work.

1.1 Background

One of the major challenges of our times is to keep global temperature levels within 1.5°C and limit the effects of climate change. The key pathway to achieve this is through mitigation, adaptation, finance and collaboration as proposed by the 6th IPCC report on climate change [5]. International efforts are underway to achieve these targets as highlighted by the EU Green Deal [6] and the international agreement on COP28 to transition away from fossil fuels [7]. Despite the progress made in the electricity sector to realise this energy transition, the challenges of decarbonising heat in a cost-effective manner are delaying the transition in the thermal sector [8]. Heat for the domestic, industrial and commercial sector accounts for almost a third of EU's energy Carbon Dioxide (CO₂) emissions [5,9]. At the same time, the impact of cooling emissions is expected to grow, with cooling being the fastest growing energy use in buildings. Space cooling in Europe expected to triple due to the climate change and the heat island effect in urban centres by 2050 [10,11]. In 2023, fossil fuels account for the biggest share of heating and cooling generation with only 25% relying on Renewable Energy Systems (RES) according to Eurostat's latest available data [12]. The main emitter are urban centres, with a total of 75% of emissions arising from cities due to large urbanisation trends over the past decades, since they constitute the global economic engine in both developed and developing countries [13]. The International Energy Agency (IEA) has stated in their report on urban net zero futures that acting in such urban centres could lead to a staggering 90% overall emission reduction by 2050 [13].

Most heating and cooling decarbonisation solutions rely on the decarbonisation of the electricity network with several countries progressing to ban gas and oil boilers in new homes [14]. However, if simple, individual solutions are used, such as direct electric

units (for heating and cooling), the electrification of the heating system would induce significant pressures on the electricity grid [14,15]. For instance, if direct electric heating is used, an additional 50GW of electricity peak in the UK is expected, which would require a 50% increase in the national electricity generation capacity [16]. Additionally, relying on simple, low efficiency decentralised solutions could drive more people into fuel poverty due to high electricity prices. Electricity prices in the UK are considerably higher than gas (3-5 times higher depending on the region), and expected to rise further over the following years as the grid decarbonises [17].

Therefore, the concept of a holistic energy system approach to decarbonisation arises. A holistic energy system considers sector coupling of cross-sectoral, inter-sectoral, and intra-sectoral energy flow and energy storage [18]. Holistic thermal systems aim to minimise the impact of heating and cooling decarbonisation on other utilities, particularly the electricity grid. This is achieved by exploiting all possible synergies between thermal and electricity grids to facilitate overall energy system cost reduction (RES capital costs and consumer tariffs), grid stability and the realisation of ambitious decarbonisation targets [19]. Sector coupling allows interconnecting utilities to achieve such a holistic energy system through digitisation and smart controls and underpinning the most effective urban planning policies [8].

The evolution of district heating and district cooling networks has at its centre increased system-wide efficiency progressing from simple, centralized networks to sophisticated, multi-source systems capable of sector coupling. 4th Generation District Heating (4GDH) and 4th Generation District Cooling (4GDC) enable sector coupling via multi-source supply capability and coordinated interaction of energy sources, distribution and consumption. They utilise centralised Heat Pumps (HP) and Thermal Energy Storage (TES) to supply heating and cooling through a network of insulated flow and return pipes [20]. The progression of district heating and district cooling systems can be seen in Figure 1.1 and Figure 1.2 respectively.

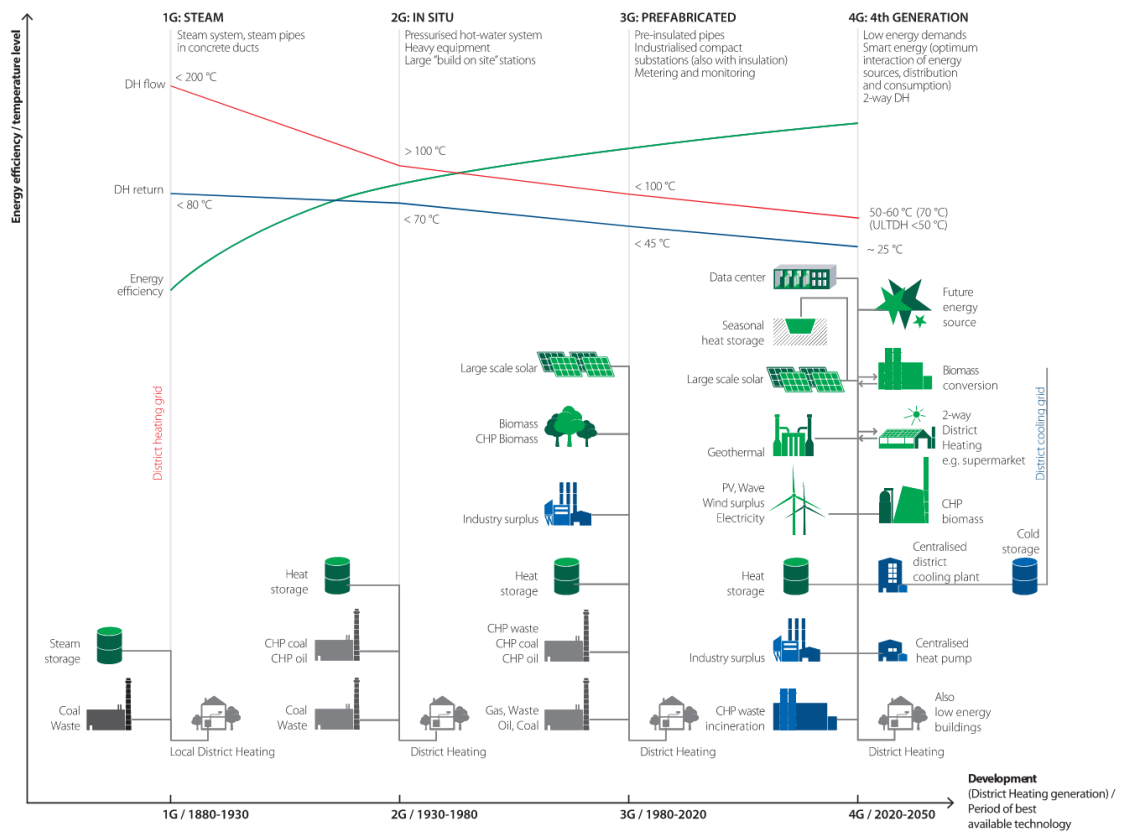


Figure 1.1: Progression of district heating – 1st to 4th generation [21].

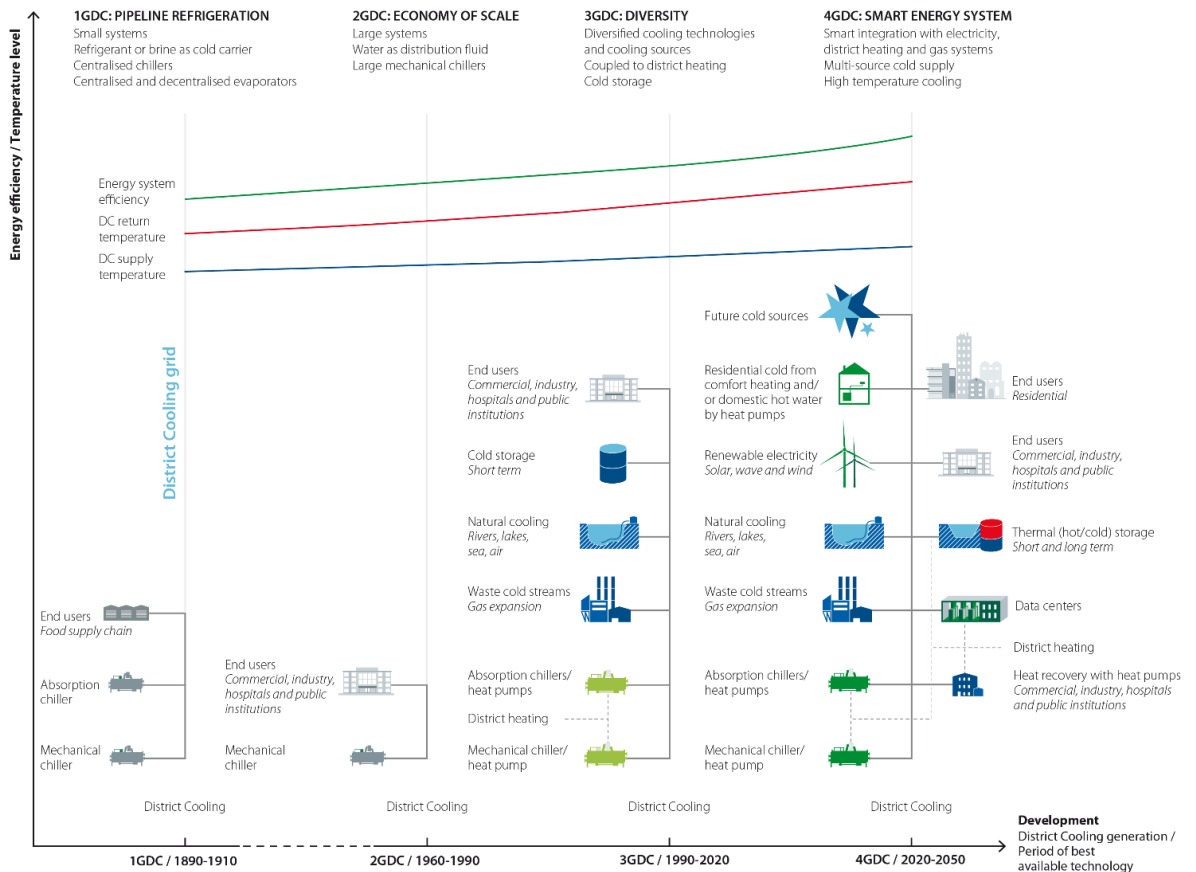


Figure 1.2: Progression of district cooling – 1st to 4th generation [22].

The concept of combining 4GDH and 4GDC networks into one system has sparked interest, essentially taking sector coupling in smart cities a step forward by meeting heating and cooling demands via the same thermal network [23]. This integrated system relies on an ambient temperature network and decentralised Water Source Heat Pumps (WSHP), referred to as Booster Heat Pumps (BHP), at flat/building/district level. These BHPs upscale the temperature of the hot/cold line from the ambient grid to supply the heating/cooling demands of the properties. Since no system has always perfectly balanced heating and cooling demands, a Balancing Unit (BU) provides the missing energy requirements, ensuring system wide thermodynamic balance. This BU can be an equipment-based BU such as an Energy Centre (EC) comprising large energy transformation units (reversible HPs, electric boilers, electric chillers etc.), or an equipment-free one using a seasonal TES or a combination of the two.

The key difference from a conventional 4GDH or 4GDC system is that the ambient temperature network allows circular economy practices by using low-grade thermal resources and introducing the “energy trading” concept, since heating and cooling are met by the same system, making each point of connection a prosumer (producer and consumer) [9,23,24]. It also allows for capturing scattered low exergy waste heat without the need for upgrading its temperature through Heat Exchangers (HEX) [15]. Such a system also allows a shift from a monopolistic energy market to an open access one comprising active prosumers [25]. It can finally cater to the rise of cooling needs, by relying on the same infrastructure for supplying heating and cooling demands [26]. This system is illustrated in Figure 1.3.

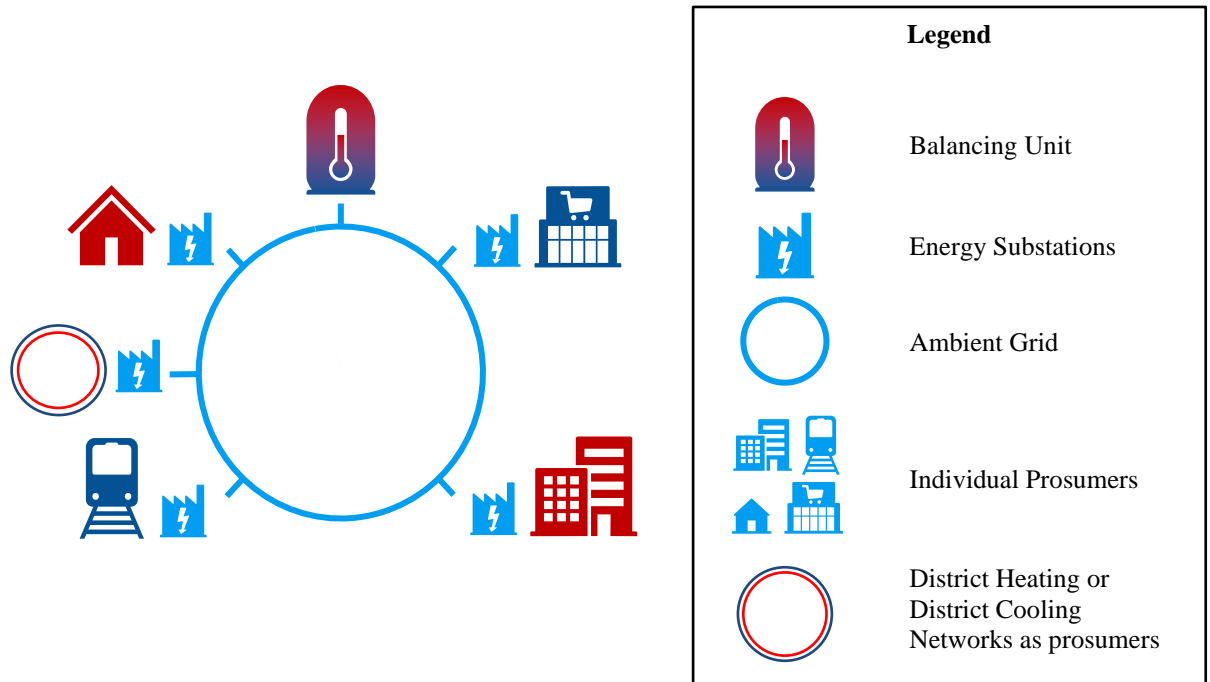


Figure 1.3: Ambient network with decentralised BHPs supplying heating and cooling prosumers.

However, this integrated approach to thermal systems may not be universally applicable as its economic and environmental performance is often inferior to conventional centralised thermal networks [27]. When only heating or cooling demands are present there are no energy synergies, meaning that the additional infrastructure and energy transformation units lead to a lower economic and environmental performance. Districts having properties with only heating or only cooling demands are referred to as ‘only heating’ and ‘only cooling’ districts respectively. Gudmundsson et al. (2022) [28] indicate that centralised 4GDH solutions will always perform economically better than an ambient network with decentralised BHPs when only heating demand is present. Even in cases where heating and cooling demand are present, demand seasonality may prove an issue. Demand seasonality (heating demand in winter and cooling demand in summer) means that demand co-occurrence on an hourly basis is limited [29]. This in turn means that the opportunities for demand synergies may also be limited. Zhang et al. (2023) [30] highlight that only 0.1% of the building stock in Europe has a demand co-occurrence of over 30%, arguing that this ambient network system has limited application. Still, these studies do not account for ambient temperature waste heat sources, the effect of utilising seasonal TES and shallow geothermal energy, the impact on the electricity grid or the rise of cooling needs (especially within urban centres).

The role of such system within the heat decarbonisation arsenal is unclear as highlighted by the uncertainty over the system's official naming, with the prevalent names being 5GDHC or 4th Generation District Heating and Cooling (4GDHC). The need for a universal definition is stressed in Sulzer et al. (2021) [31], where after a thorough bibliographic review, the term 4GDHC is proposed. However, the term 4GDHC has not been used in any other publication since 2018, with the term 5GDHC used to refer to the system. This trend of using 5GDHC is also observed in the industry, with most leading companies referring to the system as 5GDHC, mainly to differentiate the concept from the conventional 'heating only' centralised approach (4th Generation District Heating). Therefore, due to its ubiquity, the term 5GDHC is used in this work.

One of the main challenges in the design and operation of such networks arises from their strength, namely the energy sharing aspect [25]. A hydraulic design and control philosophy that could allow the utilisation of such synergies between heating and cooling without hindering the system's robustness and overall operational behaviour is still unclear. Furthermore, multiple questions are present on the impact of the decentralised nature of the energy generation equipment to the electricity grid as well as the overall economic viability of 5GDHC compared to alternative thermal system options. These alternatives comprise the aforementioned centralised (4GDH/4GDC) and decentralised solutions such as individual Air Source Heat Pumps (ASHP).

Based on the presented background the following research questions are formulated:

- What key techno-economic drivers and barriers influencing the market uptake of 5GDHC for thermal grid decarbonisation?
- How can novel hydraulic designs and operational methodologies facilitate energy sharing and system robustness in 5GDHC for thermal grid decarbonisation?
- What are 5GDHC's techno-economic performance characteristics against alternative decarbonisation solutions for varying project and operational conditions?

Given the lack of a complete assessment and the challenges regarding operational stability and economic viability, a comprehensive analysis of 5GDHC is needed. This thesis provides three main contributions. Firstly, it proposes and experimentally validates

a novel hydraulic design and operational methodology that can exploit the energy-sharing potential of 5GDHC while maintaining system robustness. Secondly, it provides a set of open access, experimentally validated simulation models allowing a detailed thermofluid simulation of 5GDHC systems. Finally, it provides an open access Techno-economic Model (TEM) to evaluate the economic and environmental viability of 5GDHC compared to alternative thermal systems, as well as its impact on the electricity grid. These outputs will contribute to a rounded understanding of 5GDHC's potential for decarbonizing the thermal grid.

1.2 Aims and research objectives

The PhD's main aim is to develop and assess novel 5GDHC system designs for effective holistic energy system decarbonisation. To provide a complete qualitative and quantitative assessment that will highlight the boundaries of beneficial application against other decarbonisation strategies, the following Research Objectives (RO) are set:

- RO 1.** Evaluate 5GDHC's opportunities and shortfalls for a holistic energy system decarbonisation. Focus on characteristics of operation as well as its technical and business-related features that could facilitate a holistic approach to decarbonising the energy grid. A Systematic Literature Review (SLR) and stakeholder interviews (policymakers, industry and academic experts) will be used.
- RO 2.** Investigate 5GDHC hydraulic designs, focusing on maximising energy synergies and sector coupling. Understand suitable operational methodologies, comprising control philosophies and equipment interaction, ensuring hydraulic stability.
- RO 3.** Assess different modelling methodologies to accurately simulate 5GDHC's physics of operation along with the proposed hydraulic designs and operational philosophies. Emphasise on their capacity to be used in different model architectures to allow the creation of 5GDHC digital twins and a higher-level system analysis.
- RO 4.** Examine TEMs for evaluating the Levelised Cost of Energy (LCOE) of 5GDHC against other supply options, with a focus on transparency and ease of use to facilitate market uptake. They should allow for detailed economic and environmental comparisons of 5GDHC with other supply options. This can facilitate a techno-economic analysis to develop trends for what conditions are

required to choose 5GDHC over other supply options for different project area variables.

RO 5. Utilise a case study to showcase the hydraulic design, system operation and techno-economic performance of a 5GDHC system using all developed methodologies and models.

1.3 Overview of structure

The thesis is structured to best address the project aim presented above, with different chapters emphasizing on different ROs.

Chapter 2 - RO 1.

Chapter 2 offers an SLR to evaluate the opportunities and barriers that 5GDHC presents for a holistic energy system decarbonisation through sector coupling. The outputs are synthesised with the insights of stakeholders from leading institutions in the field to provide qualitative arguments from empirical knowledge, obtained through interviews.

Chapter 3 - RO 2, RO 3

Chapter 3 presents in detail the novel hydraulic design and operational methodologies for 5GDHC (RO 2). It covers a description of the equipment required in the prosumer substations, the BU and the grid topology. It also discusses two control philosophies for hydraulic stability. One with a constant ambient grid Temperature Difference (ΔT), and the other with free floating temperatures. Following this, the chapter delves into the development of comprehensive Modelica models for all key elements of 5GDHC systems (prosumers, hydraulic interface, and BU) allowing system simulations (RO 3). Methodologies are presented for Power Hardware in the Loop (PHIL) implementations, allowing the interface of the models with hardware and thus their experimental validation.

Chapter 4 - RO 2

Chapter 4 covers the experiments used to validate the novel hydraulic design and operational philosophies. For the validation, the experimental setup of the heating & cooling prosumers, BU and ambient grid hardware is presented. The component testing along with the control implementation is then discussed. The expected results are

mentioned, followed by the experimental outputs and a thorough discussion on the validation process.

Chapter 5 - RO 3

Chapter 5 includes a thorough experimental validation of the developed Modelica models. First, the overall methodology for a progressive validation of a digital twin of the experiment is presented. It employs the gradual addition of model components and levels of complexity in four stages. Then, results are shown for each validation stage with a discussion on model accuracy, computational time and key sources of error leading to inaccuracies.

Chapter 6 - RO 4

Chapter 6 presents CATHeaPS, a Centralisation Analysis Tool for Heat Pump Systems. This TEM allows a complete multivariable comparison of 5GDHC with: (a) centralised 4GDH with Air Conditioning (AC) units for cooling; (b) individual reversible ASHPs for heating and cooling; and (c) individual Gas Boilers (GB) and AC units for heating and cooling respectively. CATHeaPS' methodology is first outlined through its key aspects: energy demand assessment, hydraulic design, energy supply assessment and economic analysis. Two case studies are used for model verification. An economic break-even analysis and an environmental analysis using Monte Carlo simulations are presented for three project area scenarios. (i) A 'heating only' district with access to an ambient temperature waste heat source; (ii) a typical 'heating only' district; and (iii) a typical project area with heating and cooling demands.

Chapter 7 - RO 5

Chapter 7 presents a real project case study, where the developed designs and models are utilised to propose a 5GDHC design and capture its techno-economic performance. A 5GDHC conceptual design is developed for the D2 Grids Ambient Loop Project expansion scenario in Clyde Gateway, Glasgow. The project area features multiple consumer classes with heating and cooling demands and a low temperature waste heat source (Wastewater treatment plant). 5GDHC's techno-economic feasibility is quantified against counterfactual energy supply options (4GDH with AC units for cooling and decentralised reversible ASHPs). The design specifications are presented in detail, along

with a data analysis focusing on the impact of 5GDHC design elements on its economic and environmental performance.

Chapter 8

Chapter 8 concludes this dissertation by summarising how the ROs are addressed, presents a wider context discussion and finally suggests areas for future research.

A schematic of the thesis' structure is shown in Figure 1.4. The respective ROs and research papers (published/submitted/notional as described in the List of papers and contributions section) that correspond to each chapter are also included.

1.4 Novelty of project

This PhD thesis presents several novel contributions that can significantly advance the development and implementation of 5GDHC systems for holistic energy system decarbonisation.

The main novelty of this research is addressing the current research gap on a clear system-wide hydraulic design and control regime for 5GDHC. The proposed hydraulic design and operational philosophy promotes prosumer interaction through bidirectional flows and decentralised pumping without compromising hydraulic stability. This minimisation of hydraulic issues and maximisation of system efficiency could act as a basis for industrial and academic applications of 5GDHC, elucidating a key system implementation challenge. The proposed hydraulic design and control methodologies form a basis for 5GDHC and opens the way for their future research and industrial implementation.

In addition to the experimentally validated design, this work delivers a set of open access 5GDHC simulation models for analysing 5GDHC systems. These Modelica models allow a detailed characterisation of 5GDHC systems and can be used in different architectures to study different components. They could be used to develop digital twins of 5GDHC systems, to capture the detailed thermofluid behaviour of a bidirectional flow system. Unlike simulation models that focus on energy flows, they include hydraulic components that capture pressure and flow variations (which occur at the speed of sound) using a simulation timestep of 10^{-5} s.

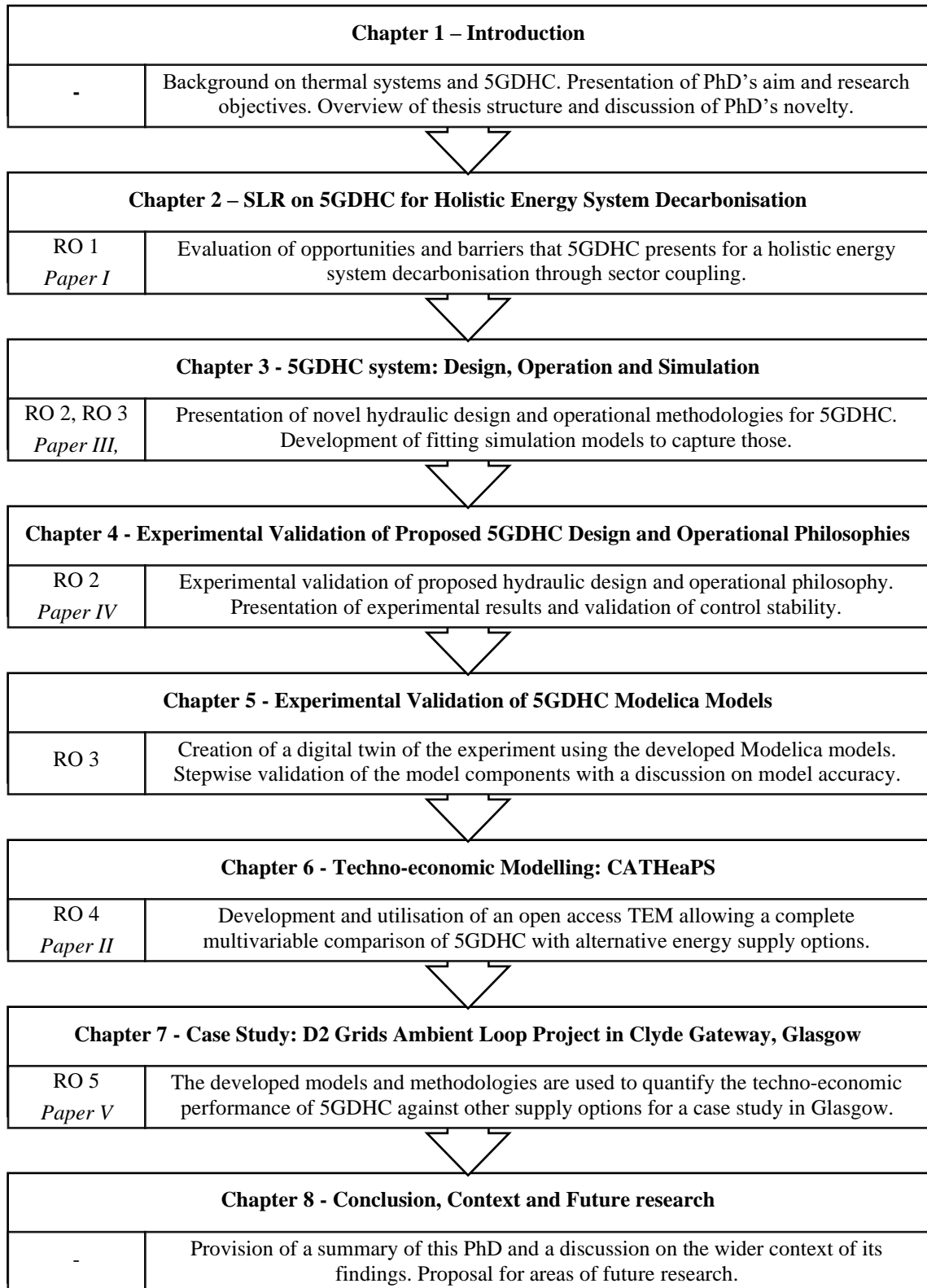


Figure 1.4: Schematic of PhD structure.

They could also be used through different system architectures for a conceptual stage analysis, focusing on annual energy flows while achieving low computational times. These are the first open access models that include hydraulic and thermal models for the

prosumers, the network, and the centralised BU along with system wide controls. Moreover, they can act as a basis for researching the impact of other system components to 5GDHC operation.

The developed TEM allows for preliminary techno-economic comparisons of different heat decarbonisation strategies. It is structured in a transparent, easily editable, and user-friendly way. It features a detailed database of cost and technical information, as well as a detailed cashflow analysis. No open access models are currently available for such complete preliminary techno-economic assessments. It allows non-expert stakeholders, such as members of local councils, to assess the feasibility of 5GDHC for their project area, enhancing their potential uptake. The research also provides multiple scientific contributions to the field of 5GDHC, which include:

- A comprehensive SLR focusing on the opportunities and barriers related to the design and deployment of 5GDHC for holistic sector coupling.
- The integration of the systematic literature review findings with the views of experts from both academia and industry to create a complete narrative on the opportunities of 5GDHC for holistic energy system decarbonisation.
- A methodology for conducting stakeholder interviews in compliance with UK guidelines for personal data protection, including examples of confidentiality statements and consent forms.
- A minimal hardware approach for 5GDHC experiments using PHIL for simulating heating and cooling demands for entire buildings through a HEX.
- Provision of open-access data from experiments for future comparisons by the research community.
- A pumping strategy and pipe sizing methodology tailored to 5GDHC.
- A progressive experimental validation methodology for Modelica models, allowing for precise identification of error sources in different model components.
- A methodology and fitting algorithms for automated hydraulic sizing of thermal networks by network linearisation.
- A comprehensive cost and technical database for 5GDHC systems.

Having established the aims, structure and novelty of this research, the literature review on 5GDHC for holistic decarbonisation is presented in Chapter 2.

2 Systematic Literature Review on 5GDHC for Holistic Energy System Decarbonisation

This chapter conducts an evaluation of the opportunities and barriers that 5GDHC presents for a holistic energy system decarbonisation comprising sector coupling. An SLR on 5GDHC for holistic energy system decarbonisation is undertaken that aims to:

- Highlight 5GDHC operational characteristics and compare them to conventional thermal network operational characteristics.
- Compare the techno-economic performance of 5GDHC to other decarbonisation strategies.
- Investigate the technical components that allow a holistic operation, such as TES, HP, Demand Side Management (DSM) and control methodologies.
- Present current business models, legislation frameworks and other project implementation parameters that would affect market uptake.

To ensure that this study integrates the academic and industrial needs and knowledge gaps, stakeholder interviews are undertaken from leading institutions in the field. Building on past research on district thermal networks with decentralised energy transformation units and the role of HPs in smart grids, this chapter provides insights on the potential and limitations of 5GDHC to promote sector coupling in energy systems.

2.1 Methodology for SLR and stakeholder interviews

SLRs allow for transparency and replicability, ensuring an aggregative and algorithmic methodology is followed [32]. The search strategy to get the reference database from Scopus for the SLR is based on a comprehensive set of keywords and Boolean operators to address the research questions while remaining broad enough to ensure inclusivity [33]. The selected keywords are clustered into 10 categories, shown in Table 2.1. The keywords within the same category are joint by the Boolean operator “AND”, while the categories are joint by the operator “OR”.

Table 2.1: SLR search strategy.

Keyword categories	Keywords
Category 1	District, Heating
Category 2	District, Cooling
Category 3	Ambient, Temperature, Network
Category 4	Balanced, Energy, Network
Category 5	Low-Temperature, Network
Category 6	Low, Quality, Excess, Heat
Category 7	Aenergy, Network
Category 8	Smart, Heat, Pump, Grid
Category 9	Thermal, Energy, Storage
Category 10	Bidirectional, Flow

The search is then limited to scientific peer-reviewed journals, published in English after 2012 with relevant subject areas. References from Ramboll (projects and documentation) are added, followed by an initial screening of title and abstract based on the research questions and finally a thematic full-text analysis of the references. This SLR methodology follows the work of authors from Ioannou et al. (2017) [34] and Juntunen and Martiskainen (2021) [35] and is captured in Figure 2.1. The SLR outputs are based on a search conducted in August 2024.

A scientometrics exercise (measuring and analysing scientific literature) is carried out to understand the links between the various keywords found in the SLR [33,36]. VOS Viewer software is used to visualise these links [37]. The outputs are shown in Figure 2.2. The visualisation confirms the hypothesis that a lot of fragmented research is being predominantly undertaken within the last five years. There are several clusters with concepts such as HPs, TES, energy modelling, techno-economic analysis and waste heat recovery having a small number of co-occurrences and links. This is further stressed by the large number of publications originating from different countries and institutions.

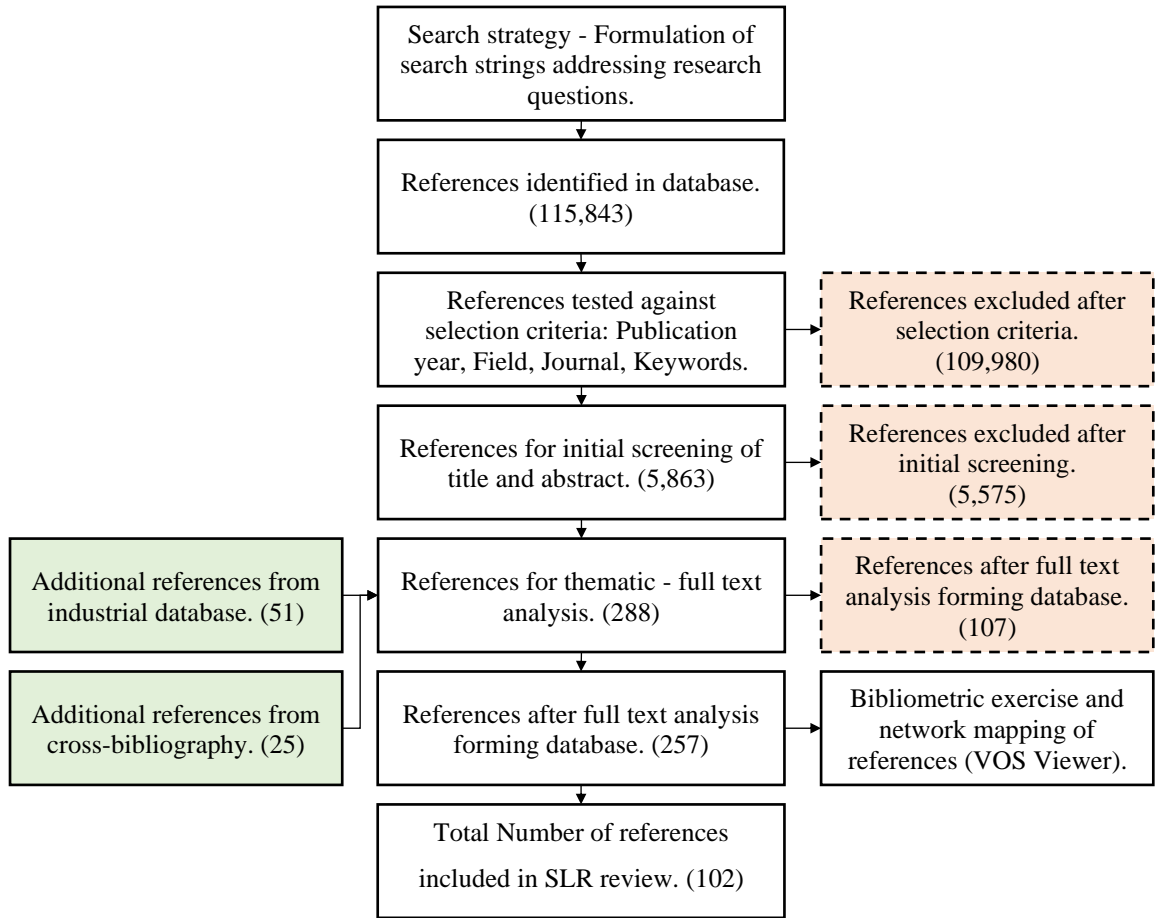


Figure 2.1: SLR Methodology.

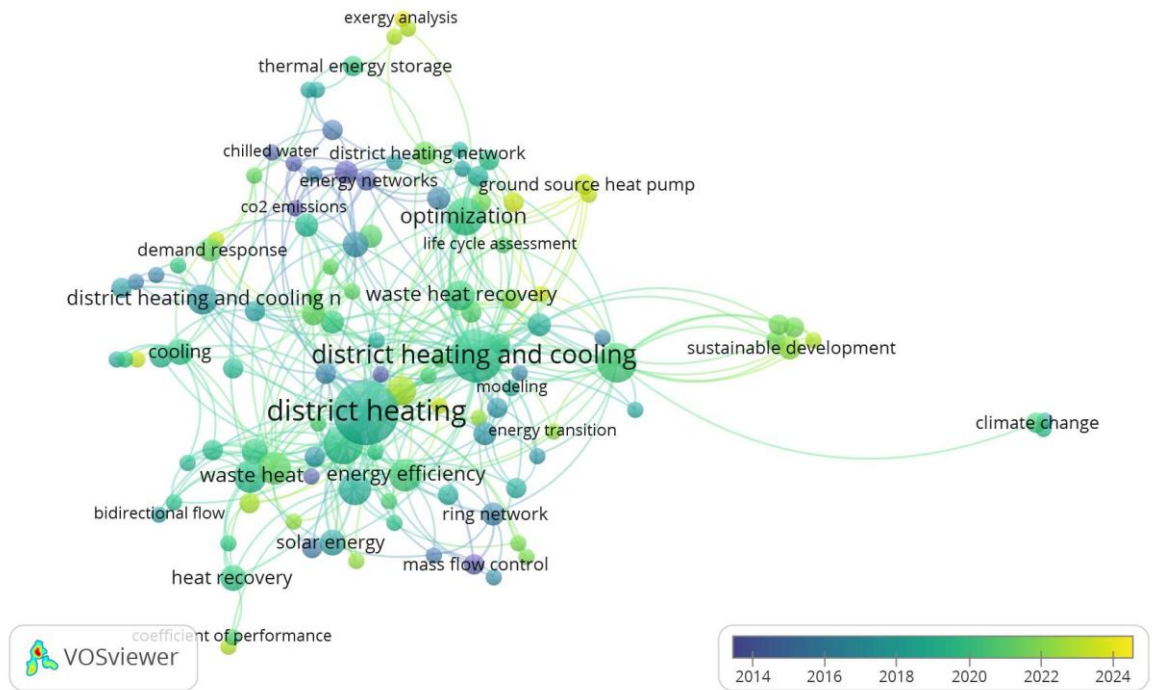


Figure 2.2: VOS Viewer map of SLR keyword co-occurrence by publication year.

To provide an additional dimension to the findings of the SLR, 18 stakeholder interviews are undertaken, focusing on the SLR research questions. The interviews are centred around five key themes captured in Figure 2.3. A different focus is given in each interview depending on the stakeholder's expertise and background, following relevant guidelines [38,39]. A detailed breakdown of the list of questions along with the items included in the participant information sheet and the consent form are presented in Sections 10.1 and 10.2, Appendix A. The interviews were conducted from May 2021 to February 2022.

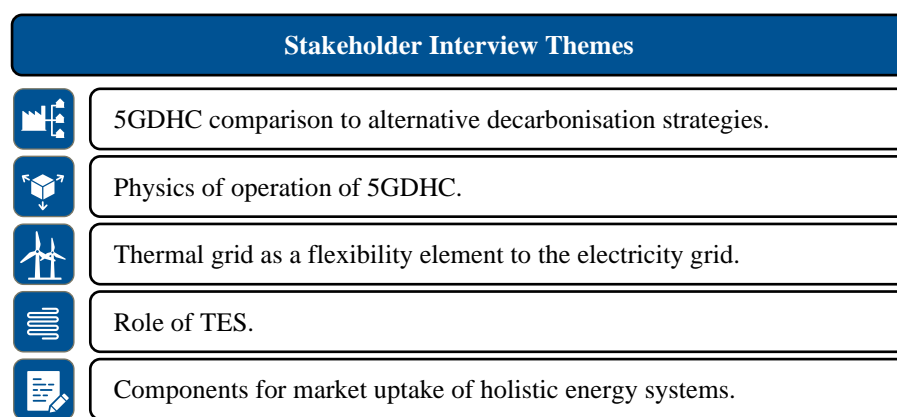


Figure 2.3: Stakeholder interview themes.

These stakeholders are industry professionals and academics in the field of thermal networks from leading institutions (universities, research centres, contractors, engineering consultants and public officials) from different countries as shown in Table 2.2. The selection criteria for their participation depended on number of relevant publications for academics and project participation and industry professionals. The resulting transcripts provide a diversified set of views, frequently conflicting each other, that give a valuable base for critical discussion of the SLR outputs.

Table 2.2: Stakeholder engagement details.

Occupation	Number	Countries
Academics	9	UK, Sweden, United States of America, Switzerland, Italy, Belgium
Contractors	2	UK
Engineering consultants	6	UK, Sweden, Denmark
Public officials	1	UK

All information collected about the participants and their responses during the research will be kept strictly confidential. Any personal data collected are susceptible to UK guidelines for personal data protection principles to ensure data security [40]. The data are anonymised using the UK Data Service’s text anonymization tool [41]. An information sheet and a consent form approved by the research ethics committee of the University of Glasgow have been signed by all participants.

2.2 5GDHC system operation and control

The operational philosophy of thermal networks is a topic that has been deeply researched with multiple papers and books addressing it. However, regarding 5GDHC networks, literature is limited, especially when combining system wide control strategies. The key difference is the energy sharing between prosumers, leading to issues on mass and energy bidirectionality, optimal topology, centralised vs decentralised pumping, characteristics of energy substations and overarching control philosophies.

Network topology is defined by graph theory as the connection arrangement of different nodes in the system (consumers) by branches/links (pipes) [42]. Traditional radial grids pipe sizing allows for diameter reductions along its length since every pipe segment “serves” less consumers, and are associated with the lowest Capital Expenditure (CAPEX) [43]. The pressure gradient identifies the critical path for all consumers in the network and there are sets of key network pressure and temperature control strategies to ensure smooth operation [44]. For 5GDHC, energy and flow bidirectionality means that any node can “produce” and “consume” energy and therefore in a branched topology, a reduction of the pipe sizing is not possible, thus moving away from the aforementioned pressure gradient diagram [45]. According to Jensen et al. (2016) [46], a ring or meshed topology are more suited to the bidirectional elements of a 5GDHC network by helping maintain more consistent pressure and flowrates throughout the network which is further confirmed by von Rhein et al. (2019) [42]. Most operational networks have such a topology such as ETH Zurich [47], Mijwater [10] and Ectogrid [48].

Having a meshed network with prosumers rises some questions as to the new pressure and temperature controls [44]. Firstly, according to Zen et al. (2021) [49], a 5GDHC network can be active or passive, depending on the existence of centralised pumping. Passive

networks depend only on decentralised pumps to modulate the flow and have lower electricity consumption due to hydraulic sub-cycles from heating/cooling balancing but are linked with dangers on hydraulic short circuiting (pump-to-pump hydraulic interactions referred to as “pump hunting”) [50]. Active networks feature centralised pumping and pressurisation units to hydraulically balance the system, with the decentralised HP substations containing a flow regulation unit to prevent continuous flow between prosumers. The key problem with decentralised pumping is highlighted by Wetter and Hu (2019) [51] and relate to pressure variations. They argue that when decentralised pumping is present, pressure variations are interfering with the operation of other pumps and lead to “pump hunting”, especially during low load operation. They proved this through detailed Modelica models. To mitigate the pressure variations caused by individual pumping stations in the network, a centralised pump working on differential pressure is used. The system led to controller instability, mainly due to the interaction of the centralised and decentralised controllers, causing cascading control errors.

To address this issue while benefiting from bidirectional mass flow and a hot and cold line, the Ectogrid network in Medicon Village described in Korsell and Ydén (2021) [52], features a slightly different hydraulic arrangement. They propose decoupling the substation’s BHP from the network by having two pumps, a variable network pump in series with a modulating valve that are responsible for flow control and a fixed speed pump for the BHP. However, only one substation is modelled and the interconnection with other substations is not completed therefore there is no complete representation of the physics of the system, not fully addressing the network pressure issues identified in Wetter and Hu (2019) [51] and Sommer et al. (2020) [53].

Regarding system controls, a centralised tool/controller could be used to tie individual substation performance with the overall network hydraulic stability. Such a controller could combine the individual control strategies of each prosumer and unify them with a governing control philosophy [54]. For the Ectogrid network, the ectocloud is used [52], while for the Mijwater, the STORM controller has been implemented. They allow peak-shaving, cell balancing (matching heating and cooling demands) and network expansion [48–50]. Such tools allow for all control points (each substation) to have a demand forecaster operating through machine learning algorithms. Data are fed over short time intervals (10 minutes) to a planner, coordinating the operation strategy through control

plans that the tracker dispatcher can deploy on substation level after a “negotiation” based on the individual substation needs. Johansson et al. (2017) [58] successfully developed machine learning algorithms and tested them using STORM project data to conclude that the forecasting ability is heavily dependent on training data. Oevelen et al. (2020) [57] highlighted that in Heerlen, through STORM’s increased cell balancing, dependency on outside sources decreased. A capacity increase of 37-45% is seen despite limited controllability of the heat loads in the test sites. The E2Districts further researched Smart Scada systems (network control) with multiple sensors, common database of weather, flow rates and other operational indicators [59]. Finally, a weighted-error approach for a Proportional – Integral – Derivative (PID) controller in each prosumer can be used, that combines temperature and power errors [60]. This approach allows controlling each substation as an independent unit, minimising prosumer interaction, considering mutual influences and network wide control objectives.

An alternative to these complicated hydraulic configurations and extended control schemes is the adoption of a unidirectional-mass network with hydraulic separation at the nodes. An in-house model is developed by Schluck et al. (2015) [61] to compare unidirectional and bidirectional mass and energy systems. They showed that for equal parameterisation, the bidirectional system showed better economical results and less energy use, allowing a 60% reduction of the electricity used for pumping. Moreover, the concept of a reservoir network is proposed by Sommer et al. (2019) [62], with a ring topology, having HPs connected in series rather than in parallel, which can consume less electricity overall for volumes of water. The main limitations of such a unidirectional network is the CAPEX associated with it given certain project areas and the system inefficiency arising from having one pipe with “lukewarm” temperature. This system would work well when there are few cooling and heating sources, but the benefits of prosumer heating and cooling synergies would be limited. A schematic of the unidirectional single pipe reservoir network and the bidirectional two pipe network with controls coordinating centralised and decentralised pumping is shown in Figure 2.4.

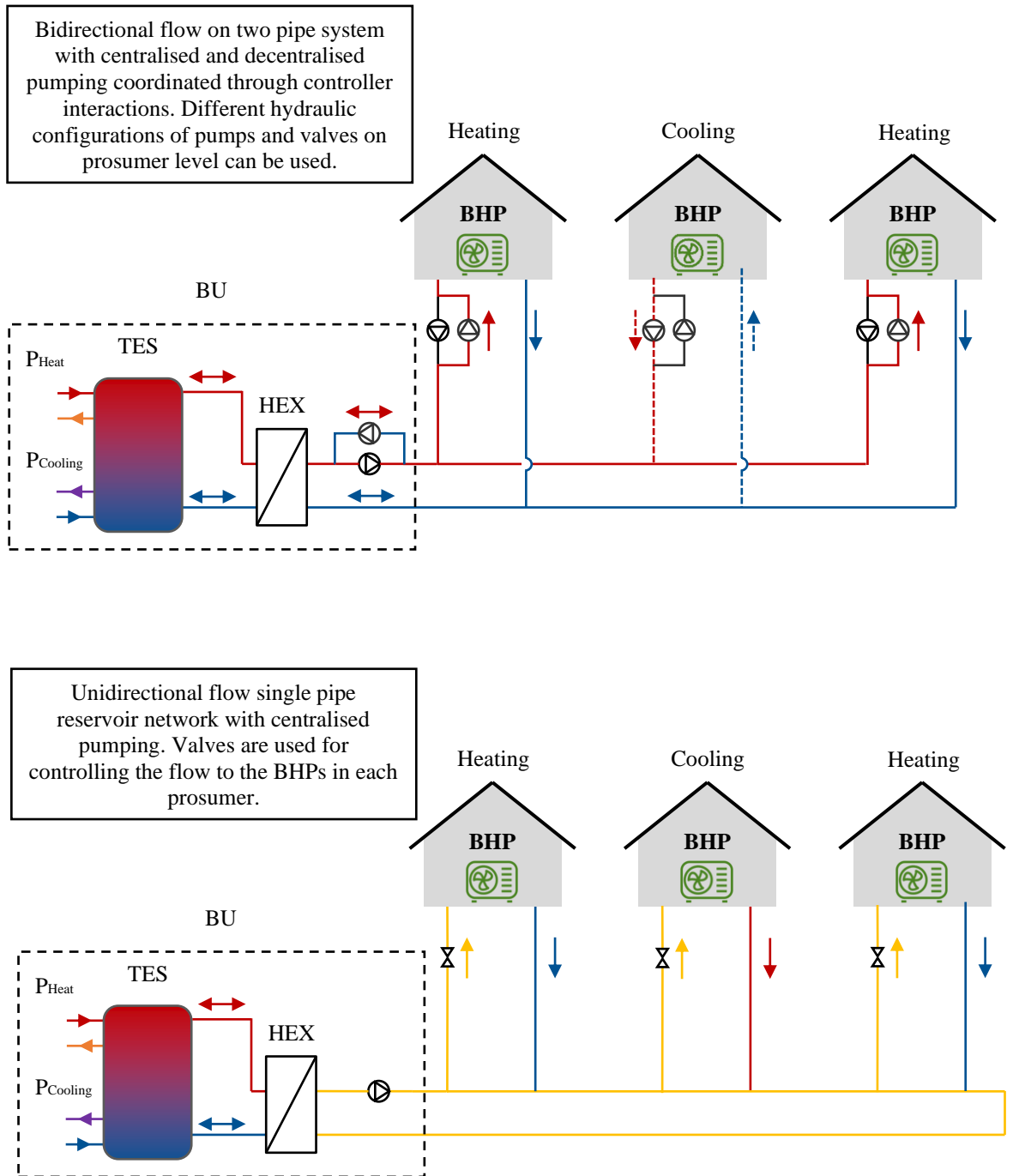


Figure 2.4: Comparison of bidirectional 5GDHC system and reservoir network.

Overall, decisions on the operational regime of the system along with the optimal topology and control philosophies are still in development, making clear the need for a standardised approach to its components design. Having a validated system wide control approach and operational philosophy similar to traditional thermal networks, that can ensure system robustness and efficient energy sharing, would facilitate the development of 5GDHC and its industrial applications. Other than the operational characteristics, it is crucial to study the techno-economic opportunities and shortfalls that 5GDHC presents.

2.3 5GDHC techno-economic comparison to other supply options

5GDHC networks rely on decentralised thermal substations comprising BHPs and local TES as well as a centralised BU to provide thermodynamic and hydraulic balance. By employing heating/cooling generation capacity relatively close to its point of use and utilising an ambient temperature in the network with lower thermal losses, the efficiency of the process could be increased compared to conventional 4GDH and 4GDC [9,63]. Utilising reversible energy transformation units, harnessing heating and cooling demand synergies and low temperature waste heat sources represents a circular economy principle to the thermal system [25]. According to the European Green Deal Investment Plan, implementing such circular economy principles in the heat sector by harvesting and distributing local excess heat that would otherwise be wasted is a crucial element for future smart cities [64]. It is shown that reductions in primary energy consumption against conventional fuel based solutions could surpass 50%, a ballpark figure that is confirmed by the findings of several studies conducted from 2018 to 2022 [9,65–67].

However, 5GDHC's techno-economic performance along with its energy use and overall quality of service is not always superior to other decarbonisation solutions [68]. As aforementioned, the key decarbonisation alternatives can be split to decentralised (direct electric heating/cooling, flat or building level ASHPs) and centralised (4GDH and 4GDC networks) solutions [15]. Decentralized solutions are often advantageous in low energy density areas, such as rural residential settings, or where multiple individual stakeholders are involved [18]. In contrast, centralized systems offer economies of scale, demand diversification, and the potential for an optimized energy transformation unit mix, leading to improved system efficiency and lower LCOE [20].

FLEXYNETS is one of the first key projects researching 5GDHC networks, covering all components of such a system in detail and highlighting their respective advantages and disadvantages [69]. It is concluded that 5GDHC networks generally perform poorly against conventional 4GDH and 4GDC when cooling and heating demand in the project area are not comparable in magnitude. This occurs because equipment-based BUs will introduce more stages of upgrading the heating/cooling to the final required levels,

increasing the sources of inefficiency, and thus lowering the overall efficiency of the system [70]. This is highlighted by Gudmundsson et al. (2021) [71], where the authors conducted a thorough techno-economic exercise comparing 5GDHC with a conventional 4GDH solution. The project area featured only heating demands and findings suggest that 5GDHC always has a higher LCOE. Authors of [26,48] identified some scenarios where the economics of 5GDHC are better, all of which included a high share of cooling. Wirtz et al. (2020) [29] further explored the idea of heating and cooling demand co-occurrence for 5GDHC system performance. They proposed the Demand Overlap Coefficient (DOC) to quantify the degree of demand balancing available for both buildings and districts and is based on mathematical relations of the demand time series' simultaneity. Based on an assessment of 63 demand scenarios excluding TES, a DOC of 0.3 is required for an economic benefit compared to traditional 4GDH and 4GDC networks. These findings are reinforced from the outputs of Calise et al. (2023) [72], where a residential development in Madrid is assessed. It features heating and cooling demands, with cooling demand being 16% of heating but because it is mainly occurring during the summer where no heating demand is present, the DOC is only 4%. Dynamic simulation models compared 5GDHC with 4GDH and 4GDC networks, and it is found that 5GDHC required more energy use with 16% higher CO₂ emissions. Achieving a DOC of 0.3 in a project area is rare due to demand seasonality. Only 0.1% of the existing building stock in Europe has such a DOC [30].

Other than the demand simultaneity, 5GDHC's decentralised energy substations comprise design influences the techno-economic performance of the system. It is dictated by heat sources' availability and seasonal temperature profile, thermal capacity and stability along with the building side thermal requirements for space heating and Domestic Hot Water (DHW) [71,73]. Decentralising the energy transformation units has the problem of a higher overall Capital Expenditure (CAPEX) but could also improve the economic feasibility of the project by allowing a phased CAPEX and lower electrical upgrade costs [74]. The network could be rolled out across the city in phases (referred to as phasing), greatly improve the economic feasibility of a project mainly due to the discount rate's effect on the Net Present Value (NPV) and the LCOE [17]. The discount rate captures the risk of future cashflows, reducing the value of future cashflows. Therefore, having CAPEX items occurring in future years reduces their impact. Furthermore, phasing increases the flexibility to incorporating future technologies and

plant diversity while it facilitates expansions by having multiple networks connecting to each other [53,75]. In addition, this decentralised approach can cater for different temperature requirements which is a key challenge in project areas with varying consumer classes and levels of retrofitting [76]. Reductions in supply temperatures results to energy savings of 0.05Eur/MWh°C to 0.50Eur/MWh°C (for a temperature reduction of 20°C that would equate to a reduction of 1Eur/MWh to 10Eur/MWh) and more efficient HP operation, significantly further reducing Operational Expenditure (OPEX) [77]. Furthermore, having a conventional ultra-low temperature 4GDH network carries the risk of legionella, bacteria that could cause health problems. Legionella has a high risk of growth between 35°C to 45°C, which is over the typical 5GDHC temperature range of 10°C to 30°C [78].

Network CAPEX is another element that is proposed as a potential benefit for 5GDHC. This is because plastic, uninsulated pipework can be used, unlike 4GDH networks that require insulated steel pipes. However, 5GDHC's network CAPEX ends up being similar to 4GDH as the reduction of cost from using plastic pipes compared to insulated steel pipes is countered by the required internal diameters being approximately 1.5 times larger [4,77]. Compared to conventional unidirectional centralised solutions, a bidirectional 5GDHC ring network cannot take advantage of demand diversification, leading to larger pipe sizing for a given area along with higher installed capacity of energy transformation units [20,79]. Larger volumes of water are also present, since similar to 4GDC networks, the ΔT is lower (typically 4 times lower than 4GDH, since a 5K to 7K ΔT is seen in 5GDHC systems compared to a ΔT of 20K in 4GDH systems) [69]. Due to the decentralised approach and the larger volumes of water being circulated within the system, the pumping requirements can increase significantly [26]. In addition, the parasitic loads for the required controls described above would be larger, increasing the electricity needs even further [80].

Moreover, one of the key advantages of 5GDHC is its capacity to harness low temperature heat from ambient or waste heat sources and upscaling it to useful levels on the prosumer's substation [81]. For example, the annual waste heat from a supermarket's refrigeration unit in Europe is equivalent to the energy needs of 200 homes [82]. Reusing waste heat has the additional benefit of reducing the heat island effect (raise of temperature due to anthropogenic activities), which in turns reduces the energy demand

for cooling [82]. The RewardHeat project's Ospitaletto network is demonstrating how a scheme integrating multiple secondary waste heat opportunities in an urban setting could operate [83]. Other ambient low exergy waste heat sources can be used in a 5GDHC, such as bodies of water and geothermal sources, each linked with some difficulties in fully harnessing their potential. To ensure sustainability, analysis of abstraction and injection site arrangement and flow rates is crucial. In regards to source water direction, hydrogeological assessments and cooperative planning of operation on district/wider system level are necessary [49,84,85]. Sewer waste heat recover is another source for 5GDHC, with heat recovery at sewer pipe level or Wastewater Treatment Plant (WWTP) level. Costs are highly dependent on the specific project area and can range from 3,000€/kW to 5,000€/kW depending on filtration needs, other utilities and pumping installations [4].

Finally, there is a range of other elements that need to be taken into consideration for this comparison. Space constraints occur both above and below ground. On the one hand, having multiple abstraction points and substations throughout the city could prove to be problematic for planning, but on the other hand, a large, centralised piece of land for the EC can be reduced by depending on the BU capacity [86]. Furthermore, one of the biggest limitations for projects in urban centres are the space constraints below ground for the pipes. In a 5GDHC network, the trench required would be approximately half than one comprising a four pipe system with 4GDH and 4GDC pipes considering minimum distances between them to avoid interference as specified in EN13941 [87]. The system risk is larger since it is a newer technology and requires a lot of components and sometimes complicated controls to lead to better performance [88]. In an effort to reduce risk, a detailed procurement strategy is produced by Brummer and Midiere (2021) [89] to face the several organisation and technical challenges on such a project.

Altogether, the system's performance is highly dependent on the specific conditions present in the network, from co-occurrence of demand to waste heat availability. According to Buffa et al. (2019) [25], the key application of a 5GDHC could be a neighbourhood-based approach, that is based on small budgets without needing a critical mass of customers while Averfalk et al. (2021) [15] suggest that 5GDHC should be used as a complement to centralised thermal networks. This dependency on local conditions suggests that the local context is essential for 5GDHC. Following the categorization of

thermal networks in terms of existing energy share [76,90], small markets such as the UK could follow city wide urban decarbonisation through the construction of multiple smaller 5GDHC networks rather than one large 4GDH or 4GDC spine. The following section investigates how such a decentralised approach would influence the grid through the sector coupling capacity of 5GDHC.

2.4 Thermal grid as a flexibility element to the electricity grid

As previously discussed, holistic energy systems comprise a thermal grid that acts as a battery rather than an additional strain to the electricity grid. It facilitates its smoother operation, avoiding large increments to its infrastructure capacity and disturbances to its control philosophy [14]. In 5GDHC systems HPs in combination with TES (daily and seasonal) provide ancillary services to the power grid (grid-friendly operation), facilitate integration of RES on building and network level and could benefit from operation under variable electricity prices [91]. Additionally, the thermal inertia of buildings and a manipulation of the thermal request profiles, defined as DSM, can further increase peak shaving by shifting peaks to off-peak hours and load shifting [92,93].

2.4.1 TES role for sector coupling

TES plays a critical role in thermal networks, and especially in 5GDHC networks, as it allows Low Zero Carbon technologies such as HP to have higher running hours and reduce their number of start-stops, maximising in that way cost and emission reductions [94]. It also permits flattening the demand profile (less demand peaks seen in the day) by shifting peak production into hours of low demand [43]. There are two main types of TES as described in Sveinbjörnsson et al. (2019) [95], seasonal and daily energy storages.

Seasonal TES is a vital part of a 5GDHC network as it allows significant cost and emission reductions, in some cases 50% lower heat prices and 95% less CO₂ emissions are possible [95]. The lower temperatures would require larger and costlier storages than conventional medium temperature approaches, but they also allow the safe utilisation of Aquifer TES (ATES) from an environmental perspective [96]. A worked example of

ATES working as the sole energy source for a 5GDHC network is undertaken under the DATES program in Utrecht University at the Uithof campus [96,97]. The seasonal ATES utilised a cold and a warm well acting as BUs for both energy and hydraulic flows within the network, by incorporating a simple hydraulic connection via a HEX and pump unit [96]. They also proved that the location of the wells (inside the loop rather than outside) yielded 35% lower CAPEX for piping. Seasonal TES shows the best economic performance at substation level, especially when the demand is peaky, reducing the total network investment cost by 4% [98]. The number of wells depends on the specific project and its characteristics.

Flooded mines can play an important role in the viability of 5GDHC due to their relatively constant seasonal temperature profile (13°C-14°C) and large volume. This is especially true when considering that water needs to be actively pumped irrespective of their use due to water quality deterioration concerns [84,99]. Menéndez et al. (2020) [84] presented 7 operational schemes achieving Coefficients of Performance (COP) in the range of 3.5-5.5. In their detailed feasibility analysis on mine water usage for 5GDHC, they highlighted the technical components of both an open and closed loop system and concluded that the capacity of the mine, the depth and the proximity to the loads are the key variables influencing the balance between high pumping costs and OPEX to higher SCOP. They also concluded that a geothermal plant of less than 1MW does not reach the expected profitability of 8% Internal Rate of Return, but that this highly depends on the country's electricity prices. The hydrochemical characteristics of mines and the extraction limitations are discussed in Loredo et al. (2017) [100], with design guidelines to avoid mineral precipitation and pipe clogging.

Daily energy storage comes usually in the form of tanks and can be found on substation level. Jebamalai et al. (2020) [98] suggested that for daily storage, building storage level is optimal as it requires the smallest CAPEX, has limited space requirements, and can smooth the energy demand profile with a capacity as low as 1 hour discharge. Gabrielli et al. (2020) [47] researched the optimal operation of a multi-energy system with both seasonal and daily TES through a Mixed Integer Linear Programming (MILP) optimisation model. They showed that having both storage facilities allow for better operation of HPs, drastic reductions to CO₂ emissions (87% reduction to conventional systems) and better flexibility when heating and cooling demands are not co-occurring.

For cooling, the capacity requirements for storage are larger due to the lower system temperatures, but the effects on peak reduction are just as prevalent as 4GDH [101]. Since daily TES is an integral part of the energy substation and its effect should be studied along with HP operation, its role is further discussed in more detail in Section 2.4.2.

2.4.2 HP and TES operation for a smart grid

The operation philosophy and control methodology of HPs in combination with building level daily TES can allow for the creation of a smart thermal grid as discussed in Fischer and Madani (2017) [102]. In their extensive review of HP on smart grids, it is highlighted that smart grids can focus on grid stability, RES integration and price reductions.

For RES integration, HP operation for heating is well matched with wind power generation due to higher wind resource during winter. For Photovoltaics (PVs) without TES, despite the seasonal mismatch, self-consumption can increase by 10%-14% without significantly lowering the HPs COP while the feed-in peaks from multiple small-scale PVs can be reduced by 30%-55% [102,103]. Prasanna et al. (2017) [104] further investigated the effect of coupling localised RES such as PVs with 5GDHC networks through an MILP optimisation model and concluded that 35% of the onsite generation could be used for HP, jumping to 77% if daily TES is used. Ground Source Heat Pumps (GSHP) with shallow geothermal borehole arrays can also accommodate curtailed wind, by using the geothermal well as a thermal battery [105]. When curtailed wind is present, GSHPs can heat up the geothermal well (charge the geothermal source), to increase their efficiency during later operation (discharge of geothermal source).

Price-focus can be either static, using fixed tariffs, or dynamic, where tariffs change daily (day-ahead pricing) or on real-time (real-time pricing). Tariff structure has the capacity to incentivise the demand profile, reducing the network's OPEX [106]. In general, price focus leads to lower OPEX, but potentially to increased consumption and indoor comfort deterioration by shifting the demand peak [102,103]. Grid stability can be achieved through voltage control, congestion management and frequency regulation. HPs can be used for overcoming over-voltage problems especially prominent near PV installations. Congestion management refers to HP operating when grid voltage levels are low to avoid

transformer overloading [102]. Day ahead planning, which involves predicting and scheduling changes in electricity consumption of the HP for the next day, can lead to reductions in generation cost and infrastructure capacity. Frequency regulation through spinning and non-spinning reserve can balance demand by turning HPs on and off [102]. The time scales can vary from a few seconds to minutes, but the success of this approach depends heavily on fast performing load controllers and HP dynamics [107]. For frequency regulation, frequency containment reserve supplies instantaneous frequency restoration services supplemented after some seconds by frequency restoration reserves to balance the grid [108,109]. Apart from the technical function, there is also a market function associated with Frequency Restoration Reserves, as there are monetary incentives to participate in these energy balancing schemes through weekly audits [103]. However, for 5GDHC there are participation challenges due to hard technical requirements (HP cycles are at least 10 minutes compared to power activation demands of seconds to a few minutes) and prohibitive logistics of multi-player day-ahead heat plan generation [103,107]. In 5GDHC, HP pool operation coupled with decentralised TES can enable meeting the technical requirements of short activation times and the participation threshold of 5MW installed capacity [102]. Coordinating a pool of HPs can prove difficult due to the required integrated control strategies, but there are successful case studies of 54 HP units participating in frequency regulation markets [102]. Such a prosumer coordination for integrating electricity and heat system control variables could be facilitated through decentralised MILP method, using a two-stage robust optimization model [110]. Such a methodology could speed up the computational efficiency of the controllers by several tens of times.

Given the operation methodologies described above, a smart grid relies on the interaction of controls on all three levels of the network (power system, building, and energy substation) with variations arising on the autonomy level of individual energy substations. Passive systems rely on direct control with set values being centrally sent to individual units. Passive intelligent systems use a centrally sent cost signals to set a boundary within which the individual units try to optimise operation. In active systems, units as seen are individual entities, and their control actions are negotiated interactively to achieve both network wide and individual goals of operation [102,103]. The exact control methodology can be shaped so that DSM measures can be applied and thus benefits of coupling the thermal and electricity grid are maximised for 5GDHC [111].

2.4.3 DSM for 5GDHC

DSM measures can vary from retrofitting buildings to Indirect DSM (by modifying the tariff structure) and Direct DSM (modifying on/off schedule of energy units and applying a different regulation strategy) [92]. For 5GDHC, there is an increased interest on the impact of DSM programs, which can lead to peak shaving of 20%-30% in the domestic sector, and energy requirements can be reduced by up to 5% [69,92,112]. However, emission and cost reductions depend heavily on HP and TES size as well as the overall dynamic properties of the network [92]. The speed of response is limited by the rate of change of the compressor speed, turndown ratio (minimum load the HP can supply), minimum on-off pause time, and maximum number of on-offs within a year to avoid reducing the lifetime of the unit [102].

One of the most intricate and challenging components of Direct DSM is decision intelligence, especially for aggregating a pool of buildings which is applicable to 5GDHC networks [92]. Agent based control performed through MILP showed that a fixed temperature allows for a reduced OPEX by exploiting the coordinated balancing efforts from the individual substations [25,113–115]. To accommodate the non-linear characteristics found in 5GDHC networks, other approaches could be more suitable. In Buffa et al. (2021) [44], a detailed literature review of network control strategies determined that despite multi agent systems require less data manipulation and are easier to develop and use. Model Predictive Control (MPC) has the capacity to include more parameters in the optimisation problem such as weather forecasting, consumer profiles and system disturbances. Artificial Neural Network MPC could also be used for smart charging a 5GDHC substation's TES based on a receding prediction horizon [112]. Despite some improvements in terms of lower costs (3.5%) and higher peak shaving (13%), the research is limited to a single substation without exploring the interconnection with other substations and the effect that could have. Hering et al. (2021) [116] combined Python with Modelica to test the effect of an MPC to an entire 4GDH network supplied by HP and coupled with local PVs which resulted in energy cost savings of 5%. An additional feature to DSM would be to incorporate behavioural demand response analysis, to predict the expected behaviour of building occupants to DSM actions [117].

Prosumers can aggregate their asset activity to provide flexibility to the grid by using forecasting and day ahead trading, which becomes beneficial especially when a pool of consumers are bidding together [118,119]. The coupling potential of DSM in 5GDHC networks is further researched by Edtmayer et al. (2021) [118]. They simulated a HP led network of 2,200 houses and evaluated the flexibility offered to the grid with response to thermal comfort (internal temperature between 20-24°C as stated in DIN EN ISO 7730 [120]). The installed heat supply systems role is tested through step response tests (radiators take 240 seconds to cool down while underfloor heating takes 1,950 seconds) and polynomial equations for heat up and cool down times where determined that could be used in an MPC algorithm. However, financial compensation alone to exploit DSM is not sufficient to incentivise participation of prosumers, so additional benefits are required [92,119].

Currently, there are few holistic smart energy grids where the electricity network is seen as a key vector in its planning, especially within a 5GDHC setting which as claimed by Olivier et al. (2020) [121] could provide true local heat to urban centres. There is an increased effort in understanding and modelling these utility interrelations and capabilities with few simulation models currently available. Other than the technical aspects of sector coupling, the business models required to realise such a holistic approach need to be studied.

2.5 Business models for holistic 5GDHC system

This section investigates the inherent business intricacies of 5GDHC that need to be addressed, current barriers and potential opportunities for its effective widespread adoption. Despite the focus on technical aspects mentioned so far and efforts to increase the efficiency of the system and thermal networks in general, a key obstacle to the widespread adoption of these technologies is economic and legislative [122]. In a workshop carried out by Vázquez et al. (2021) [76] with key stakeholders from various Horizon 2020 programs on 5GDHC, 55% of the attendees considered local authorities to be the key actors for facilitating thermal networks and 90% considered financial issues as the key obstacles to their extensive roll-out. This is also highlighted by Galindo Fernández et al (2021) [123], where the first key success factor to integrate RES and waste energy to thermal grids is national policies and a supportive regulation and legal

framework. For example, Wahlroos et al. (2018) [81] state that multiple data centres are planning to utilise their waste heat to 4GDH networks, but find it difficult due to the lack of structure and transparency on current business models.

As stated in Pellegrini and Bianchini (2018) [124], for a bidirectional system to be effective, a novel business model is necessary. 5GDHC presents the opportunity for a new business model based on the notion of prosumers [74,125]. The benefits from having active substations, as mentioned in Buffa et al. (2019) [25], include a shift from the current monopolistic energy model, where large Energy Supply Companies (ESCOs) sell heat to consumers, to a more involved open access market [126]. Such a switch offers a greater bargaining opportunity to the prosumers, and opportunities to energy suppliers by providing energy as a service, essentially selling comfort [82]. This open access market can adopt a bottom-up approach rather than a top down where the citizens are actively participating in the energy market as demonstrated by the DRIMPAC project. At the same time, there are multiple challenges present in such a switch including cost and asset allocation, energy exchange tracking and restrictions, market clearing processes as well as simulating and controlling such a network [127,128]. Averfalk et al. (2021) [15] suggest that ESCOs potentially fail to develop new business models as they make a shift in technologies due to limited awareness and short-term profit orientation.

To best capture this bottom up approach of active consumers, other than a strictly economic dimension, a complete shift in paradigm of the role of the citizen is necessary, something that is outlined in IEA's latest report on smart cities [13]. Therefore, a sociotechnical approach to energy communities where citizens have control and even ownership of their energy supply is recommended. In this way, the necessary digitalisation of the energy sector is undertaken in a democratic way, neither alienating its population, nor leading to monopolies that can only lead to increased fuel poverty [13,129]. Examples of such energy communities have been explored throughout Europe, trying to redefine the ownership structure while following the Business Model Canvas to investigate partnerships, resources and revenue streams [38]. In Jaegerspris, Denmark, the heat network for the town belongs to the consumer-owned Jaegerspris Kraftvarme 4GDH utility and is operated by the Heat Supply Act's non-for-profit principle, where all profits are translated to lower heat tariffs [123]. The main obstacles to such business

models are both technical (data models and standards) and business related (consumer risks and tariff structure), especially when the legal frameworks have yet to be updated [78].

Setting up a new tariff structure is challenging as striking a balance between benefit and cost is necessary to overcome limited prosumer engagement [15]. The smaller networks present in 5GDHC, with circular economy and decentralised assets in their core, make novel economic models such as doughnut economics possible [130], allowing the smart city to reach its participatory and co-constructed targets [131]. Even the financing of such projects can be constructed in a different manner. Crowdfunding in the energy sector is initiated in 2012 and has reached over 300 million EUR of funding, but it has not been significantly used in the heating market [38]. Non-financial and financial crowdfunding are available depending on whether the individual's contribution is associated with a financial return [132]. The Community-based development schemes for geothermal energy project (CROWDTHERMAL) project highlights the benefits of co-financing, co-ownership and collective responsibility for geothermal energy projects [133]. As part of the project, a set of digital support tools for financing and risk mitigation along with relative guidelines for geothermal projects are made open access to help stakeholders [134]. Their impact on successful project implementation and social acceptance are showcased through three European case studies.

Some additional aspects that can be facilitated through a different market structure within a smart city network are Artificial Intelligence, Blockchain, and the Internet of Things [135]. Such platforms allow the use of extensive metered data to unlock the potential for digitalising an open business model through their collection and management, especially when combined with Cloud computing, leading to new patterns of trade [126,136,137]. Another method to facilitate the large number of control variables and individual prosumers is Blockchain [138]. Prosumers could benefit from Blockchain's strength in optimising decentralised data records in a transparent transmission and storage capacity, as it does not rely on a central entity, but rather on multiple writers being able to modify the database. There are no case studies at the time of writing of such schemes, but there are suggestions to implement Blockchain in a pilot site [139].

It is evident that a discussion about a switch to a holistic system is inherently tied with socioeconomical parameters rather than strictly technical. Redefining the role of a citizen within the energy market and assessing different tariff structures, asset management and costing schemes is required. The Energy Citizens for Inclusive Decarbonization (ENCLUDE) project researched the notion of energy citizenship in the decarbonisation efforts and the typologies that arise [140]. A key finding is that “*an energy citizenship that is won or earned is good imagery for an energy system that remains unjust*” [141]. As a proposal to overcome this, it is suggested to have a clear typology of energy citizens based on access to energy, consumption, production and politics to define the role of citizens in the energy transition [142]. In addition, integrating perspectives and views of citizens and stakeholders in the analysis and modelling of energy systems is critical for capturing the full decarbonization picture [143]. By incorporating such participatory elements in the modelling, analyses can better reflect the complex realities of different decarbonisation solutions for different energy citizen groups.

2.6 SLR key findings

The key findings of the SLR are summarised in Table 2.3 and overlaid to the stakeholders’ views on the following section (2.7) to provide a comprehensive and inclusive review.

Table 2.3: Opportunities and barriers of 5GDHC in terms of techno-economic performance, sector coupling facilitation and market uptake (adapted from [144]).

Topic	Indicators	Opportunities	Barriers
System operation and control	Robustness and flexibility of application	Various levels of retrofitting (temperature requirements) supplied by same network [76].	Complicated controls that could lead to hydronic instabilities (pump hunting) [44,50].
		Multiple networks connecting to each other [53,75].	Prosumer technical complexities of energy exchange between multiple stakeholders [127].
		Various topology and connection methodology options [42,46,62].	
Techno-economic performance	Economic performance	Phasing of CAPEX in urban scale [74].	Need for seasonal co-occurrence of heating and cooling demands [29,71,72].
		No centralised EC [86].	
		Reversible BHP units for meeting heating and cooling demands [66].	No demand diversification - larger pipe sizing & higher installed capacity of energy transformation units [20,79].
	Energy use	Hydraulic sub-cycles for lower exergy losses and higher security of supply [50]. Controls allowing peak-shaving, cell balancing (matching heating and cooling demands) and network expansion [44,60].	Typically, lower system SCOP than centralised solutions if low heating and cooling demand co-occurrence and no waste heat source availability [29,71,72]. Higher pumping requirements than conventional centralised system and parasitic loads [26,80].
	Excess heat utilisation	Ability to harness low exergy sources (both natural and urban sources) [83,129]. Reduction of heat island effect [82].	High dependency on excess heat for thermal balancing and efficient operation [51,69]. Hydrogeological assessments and cooperative planning requirements [49,84,85].
Sector coupling facilitation	TES utilisation	Safe utilisation of ATES from an environmental perspective [96]. Utilisation of abandoned flooded mines [84,99]. Daily storage for peak shaving and PV utilisation [25,98].	High capacity requirements for cool storage [101]. The hydrochemical characteristics of sources and extraction limitations [100].
	HP operation	Grid stability through voltage control, congestion management and frequency regulation [102,107].	Participation and coordination challenges due to multi-player day-ahead heat plan generation [103,107].

Topic	Indicators	Opportunities	Barriers
	DSM	Peak shaving and energy requirements reduction [69,92,112,117]. Prosumers can aggregate their asset activity to provide flexibility to the grid by using forecasting and day ahead trading [118,119].	Decision intelligence, especially for aggregating a pool of buildings with non-linear characteristics [92]. Financial compensation is not sufficient an incentive to exploit DSM [92,119].
Market uptake	Legislation	Political design decisions [67].	Legal frameworks have yet to be updated [78].
	Business models	Opportunity for a new business model based on the notion of prosumers [74,125]. More involved open access market [126]. Energy communities [38,123]. Novel economic models (doughnut economics) [127,130].	Lack of structure and transparency on current business models [81]. Cost and asset allocation, energy exchange tracking and restrictions, market clearing processes [127]. Financial viability [76].
	Financing	New patterns of trade [126,136,137].	Larger risk by having multiple stakeholders and various levels of asset ownership [127,128].
	Public engagement	Citizens actively participating in the energy market [141,142].	

2.7 Discussion based on stakeholder interviews

5GDHC is a complex system with multidimensional parameters as highlighted in the literature findings, a notion that is also prevalent during the stakeholder interviews. In this section, a critical discussion of the SLR findings superimposed onto stakeholders' views is presented.

There is a rise in interest for 5GDHC projects throughout Europe indicated by multiple EU funded schemes, the uptake of the 5GDHC from large ESCOs and innovative start-ups and the research spike in 5GDHC over the last 5 years. Despite this increased attention for 5GDHC, many stakeholders emphasized the difficulty of deploying combined centralized heating and cooling solutions. They noted that locations with sufficient energy density to support such systems would be rare. An engineering consultant on energy systems mentioned that finding the right seasonal balance between heating and cooling would occur in 1 out of 100 projects. They argued that the benefits of phasing, lower losses and scattered waste heat opportunities are countered by larger costs for substations, larger pipe diameters, and the overall complexity of the network, which increases the risk of investment, a view that is in line with the SLR findings. In addition, the larger number of HPs and space requirements for evaporators could limit the feasibility of projects, especially in urban centres with listed buildings. There is a fear that more focus is given on this technology in recent years simply because it is "*the new shiny thing but it can lead to a dead end*". Opportunities of local excess heat harnessing are wider with 5GDHC however they are linked with more stakeholders and intricate contracts that could block rather than facilitate thermal network uptake. Some stakeholders suggested that a community-based smart city model, rather than one with a centralized city-wide network, could be preferable in some regions. They attributed this to citizens' expectations of the energy market, which are influenced by historical and political factors. The system's boundaries of social, economic, technical and environmental performance compared to conventional thermal networks are still unclear with more research needed.

The challenges related to the physics of operation of the system are still not fully resolved within the industrial and academic community. There are multiple components

that need to be considered to maximise energy recirculation between the system and optimise thermodynamic and hydraulic performance. Providing standards for connection methodologies and specifications for contractors seems highly challenging; specifically, the investigation of the substation pump and valve optimal operation point for handling pressure disturbances would be of interest. Advanced building automation systems and data manipulation are critical for the operation of 5GDHC, but there is a gap in control competence between academia, pilot projects, and industrial applications. It is crucial to standardise the control systems and detail how multiple sensors and energy data can be utilised in a transparent and practical way. As one academic argued, 5GDHC systems are in the process of simplifying the original idea to find the best configuration “*Hydraulics are more like art. Complexity is not the solution, rather it is simplicity and elegance.*”

HPs and TES can add grid stability and allow the widespread integration of RES. Most engineering consultants mentioned that additional research is needed on the integration of thermal networks with the electricity network. In general, the two utilities are viewed semi-separately from a design point of view, with different experts focusing on each without much overlap. Regarding DSM, there are few applied cases despite that most available models are better than the controllers employed nowadays (on/off and proportionate). For single building control, research is so far ahead from the industry, with MPC or similar controls being a necessary step to “*getting rid of archaic rules of thumb and simplistic controls*”. On the one hand, decentralising the energy transformation units would remove flexibility from the grid since the energy consumption is larger, at lower individual capacities and with more complicated controls to synchronise actions of turning HPs on and off. The benefits of co-operation with PVs are stripped by the seasonality mismatch and the electricity costs could be lower for big connections since it is easier to have 4 HPs rather than 1000 individual connections. On the other hand, a leading academic on thermal systems added that it depends on the structure of the electricity grid and how it has incorporated RES. If there is a focus on local level with multiple building level PVs, flexibility is added since local self-use can be increased. Moreover, when discussing net zero schemes, conventional 4GDH schemes would typically depend on electric boilers rather than gas boilers for their back-up supply, potentially requiring massive electricity substation capacity upgrades, a cost that could be avoided in a decentralised 5GDHC network.

TES is an integral part of 5GDHC by maximising HPs' hours of operation and allowing shifting production profiles. Some seasonal TES systems, such as ATEs and flooded mines, are unique to low temperature networks, providing both thermodynamic and hydraulic balancing capacities. There are several questions related to the costs and technical viability of seasonal TESs that need to be taken into consideration especially in an urban environment. They can sometimes be viewed as a *“panacea for thermal networks, but they should only be considered as a storage, not a source”*. For lower temperature networks, the volume of the TES is increased dramatically compared to traditional 4GDH, due to much lower temperature differences between flow and return. Daily storage via thermal tanks faces similar space constraint challenges, especially due to the large number of required substations which are related to both floor area and height constraints, due to water stratification concerns.

Finally, all stakeholders agreed that improvements in legislation and redefined business models are the way forward for thermal networks. According to some stakeholders, 5GDHC is a solution to more localised systems compared to urban centres, pushed by some ESCo. They argue it is not seen as a competitor to 4GDH due to its better efficiency, but rather as a potential solution to consumers that cannot be reached with centralised networks. It is also suggested that some resistance might be present from current operators to switch to 5GDHC, not wishing to move away from current, profitable solutions where they have more control on the system and less complicated ownership agreements with prosumers for both the assets and heating/cooling agreements themselves. Having such a paradigm shift from a monopolistic to an open access market, adopting a bottom-up approach, would redefine the role of the citizen within the energy sector, requiring a more active citizen participation. Some stakeholders argued that simplicity and robust quality of service are the pinnacles of interest, avoiding complex equipment and an intricate business model. *“Frankly, having dedicated ESCo running the networks and owning all assets is the right paradigm. Why would the council, let alone the citizens, be involved in it? They are not experts; they want someone to wave a magic wand to shake and decarbonise the system.”* Countering this view, some stakeholders mentioned that citizens would be willing to connect and have a more active role if less variable electricity costs and less susceptibility to volatile electricity prices could be achieved. Going a step further, an engineering consultant mentioned that *“in the future, consumers will be willing to pay more for environmentally clean solutions, having*

a more community-based approach.” Finding the right balance between participatory smart city approaches, including energy communities, and simple service delivery is essential for 5GDHC to meet our societies ambitious decarbonisation targets.

2.8 Research gaps addressed in this thesis

The findings of this chapter indicate that 5GDHC has the capacity to provide a holistic solution to the energy sector decarbonisation problem our society faces but there are multiple challenges on its effective application.

Altogether, despite its poorer economic performance when little seasonal energy co-occurrence is present, 5GDHC can be beneficial if phasing and varying levels of retrofitting within the project area are taken into consideration. This is especially true for new markets with increasing cooling demands, little industrial waste heat available and a prevalence of scattered low temperature waste heat opportunities. However, the complex physics of operation arising from mass/energy bidirectionality can result in hydronic misbalancing, pressure instabilities and increased OPEX for pumping. Therefore, network topology and pipe sizing, substation design, and overall control methodology are critical. Controls are tied to individual energy substations’ operation, which is inherently tied to the electricity grid via the use of HPs. A coordinated HP led thermal grid coupled with daily and seasonal TES and employing DSM practices can support the evolution of the energy grid to one comprising multiple distributed generation points by offering voltage control and frequency balancing opportunities. In addition, distributed daily TES and a centralised seasonal TES allows optimal operation of 5GDHC networks, increasing peak shaving and demand shifting potentials while providing thermodynamic and hydraulic balancing. The economic feasibility of the system relies on the business models, legal frameworks and modes of financing. Some business models have emerged that facilitate decarbonisation by the presence of prosumers in the network. However, there is no cohesive plan currently in place which suggests this field is open to extensive research. Overall, a neighbourhood approach to 5GDHC would allow to harness the benefits of energy trading and scattered waste heat while avoiding technical risks of hydronic imbalances and HP coordination. A limited pool of prosumers can offer grid flexibility and implement new business models with novelties on asset ownership and tariff structure. Such a neighbourhood approach could allow a phased, bottom-up energy

system development, especially fit to new markets and provide an economically viable holistic decarbonisation of the thermal grid.

Based on these findings, this thesis is tackling the following research gaps which are in line with the ROs analysed in Section 1.2:

- Providing standardised design and operation methodologies for 5GDHC that allow bidirectional flows.
- Developing fitting simulation models that can capture bidirectional flow regimes and heating and cooling synergies.
- Exploring the implementation of the developed design and operation methodologies in an experimental setup, offering methodologies for PHIL to test 5GDHC digital twins.
- Investigating quantified techno-economic boundary conditions for when to prefer 5GDHC over alternative supply options in a range of project area scenarios.
- Highlighting the techno-economic performance of 5GDHC for a real case study with heating and cooling demands and an ambient temperature waste heat source/sink, accounting for the impact on the electricity grid.

The critical challenge of providing a comprehensive system-wide hydraulic design with fitting control strategies and simulation models is presented in Chapter 3.

3 5GDHC system: Design, Operation and Simulation

As highlighted in the SLR, one of the main challenges in the design and operation of 5GDHC networks arises from their strength, namely the energy sharing aspect. What hydraulic design and control philosophy could allow the utilisation of such synergies between heating and cooling without hindering the system's robustness and overall operational behaviour? In addition, how could any proposed designs be captured in the modelling sphere, allowing a precise simulation of 5GDHC systems?

This chapter explores novel designs for 5GDHC and control philosophies. It proposes a hydraulic design for decentralised pumping along with two fitting control philosophies. It then presents a set of novel Modelica models for system simulation, capturing all the proposed 5GDHC system components. An exemplary model architecture is also presented as well as a methodology for how the components can be used for hardware experiments testing 5GDHC systems.

3.1 5GDHC system design

As highlighted in the SLR, the current proposed bidirectional 5GDHC design is a system with decentralised pumping in prosumer level and centralised pumping at BU level for modulating the system in terms of flowrate and pressure requirements. The BU supplies heating or cooling to the system, contingent to its requirements. A HEX is present between the BU pumps and the BU TES, hydraulically separating it from the network. Two separate pumps are used for pumping in each connection, one for heating and one for cooling. A single pump with appropriate valve configuration could be used but it would introduce further control complications. The dual pump setup is used in this design as is the simplest concept to prove and establish the hydraulic basis, reducing the sources of potential errors. This configuration is shown in Figure 3.1.

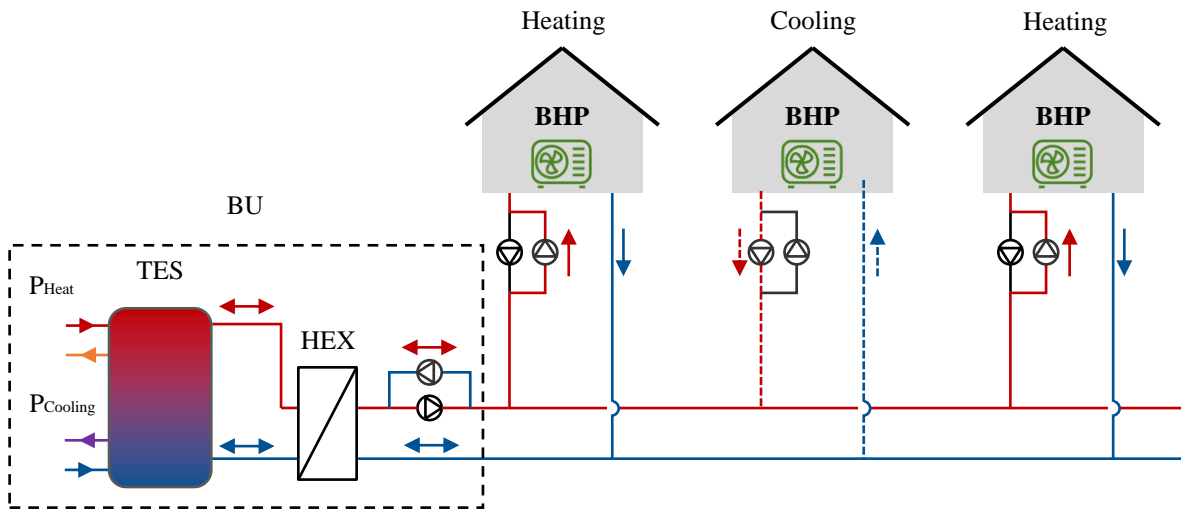


Figure 3.1: 5GDHC with decentralised and centralised pumping using an active BU for thermodynamic balancing.

When the speed of one of the decentralised pumps changes, the characteristic curve of subsequent pumps changes. Figure 3.2 shows the interaction of two pumps in a bidirectional grid, where one pump changes its pump speed.

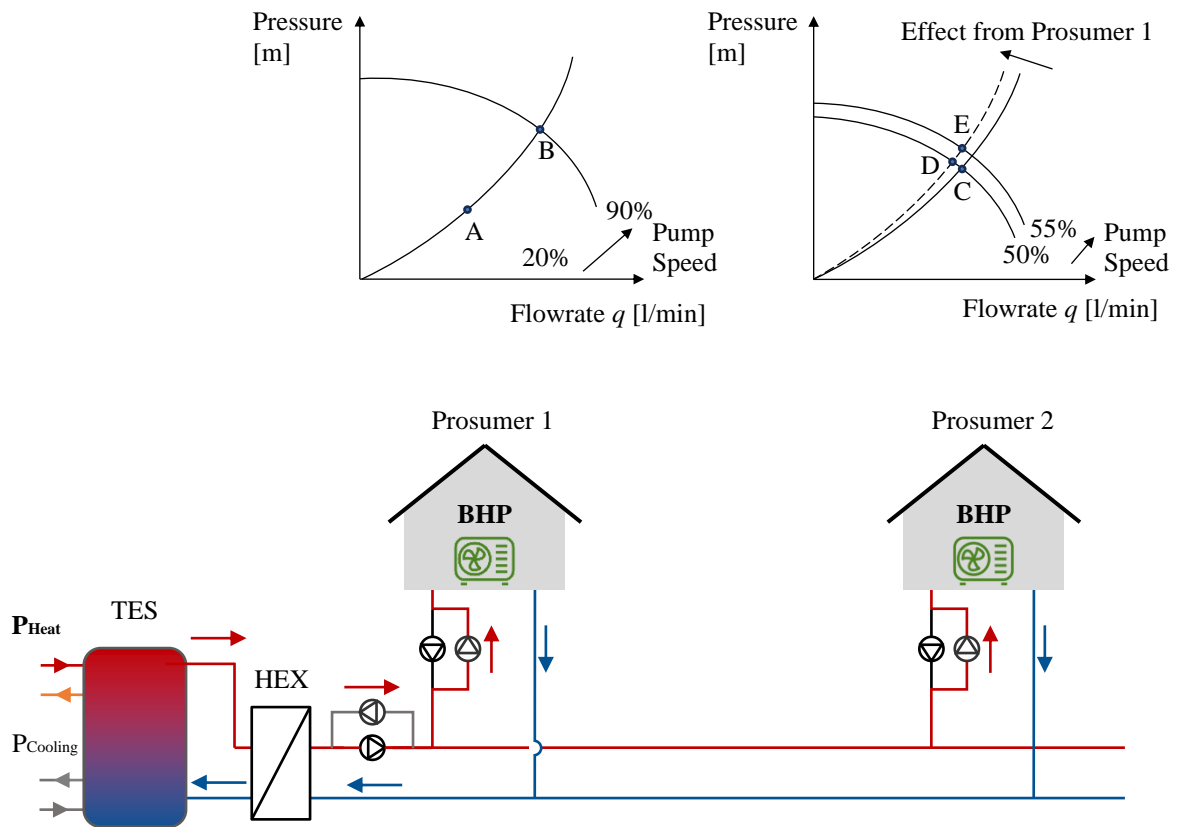


Figure 3.2: Pump hunting phenomena in a bidirectional grid.

The coupling of both pumps can lead to the pump hunting phenomena as analysed in Wetter and Hu (2019) [51]. Namely, the modulation of one pump is altering the system characteristic curve of subsequent pumps. In this example, an increase in the demand of prosumer 1 leads to the pump ramping up from point A (20% speed) to point B (90% speed). This instantaneously changes the system characteristic curve of prosumer 2's pump, making it steeper since the hydraulic resistance has increased in the network (higher flowrates lead to higher pressure drops along the pipes). In turn, despite the demand remaining unchanged for prosumer 2, the operational point shifts from point C to point D. However, this new point D does not provide the flowrate required in the system ($q_C > q_D$), so the pump needs to increase its speed to point E, so that the flowrate needed can be supplied for the new system curve ($q_C = q_E$).

In the current proposal shown in Figure 3.1 with an active BU, the centralised pumps try to modulate any control instabilities by regulating the flowrate and pressure of the system. However, due to the transient behavior of water, changes within the network require time to propagate to the BU. Therefore, hysteresis is likely to occur, where the centralised pumps are attempting to solve past issues, leading to system instability ("pump hunting"), between the centralised and decentralised pumps as thoroughly explained in the work of Sommer et al. (2020) [53]. Controlling such a system necessitates a complex control hierarchy, with a centralised controller continuously communicating with individual pumps to ensure stability. It would also require weighted PID controllers to account for flowrate, pressure and thermal power measurements [60].

To prevent these problems, the proposed solution involves a passive BU, without centralised pumping that is not hydraulically separated from the ambient grid. In this configuration, the hot grid line connects to the top of the TES at the BU, while the cold line connects to the bottom. Flow direction through the BU depends on the grid, where any "remaining" flowrate can pass through the passive BU. The stratified TES operates so that its top and bottom temperature levels, match the hot and cold pipe temperature respectively. Figure 3.3 depicts this system, where a passive BU supplies heating or cooling depending on the flow direction in the grid, a direct result of the energy balance between the prosumers. A critical aspect of this design is that the responsibility for meeting the system's pressure head is entirely assigned to the decentralised pumps. Consequently,

pressure losses within the pipes and HEX must be small, to minimise pump oversizing and inefficiencies.

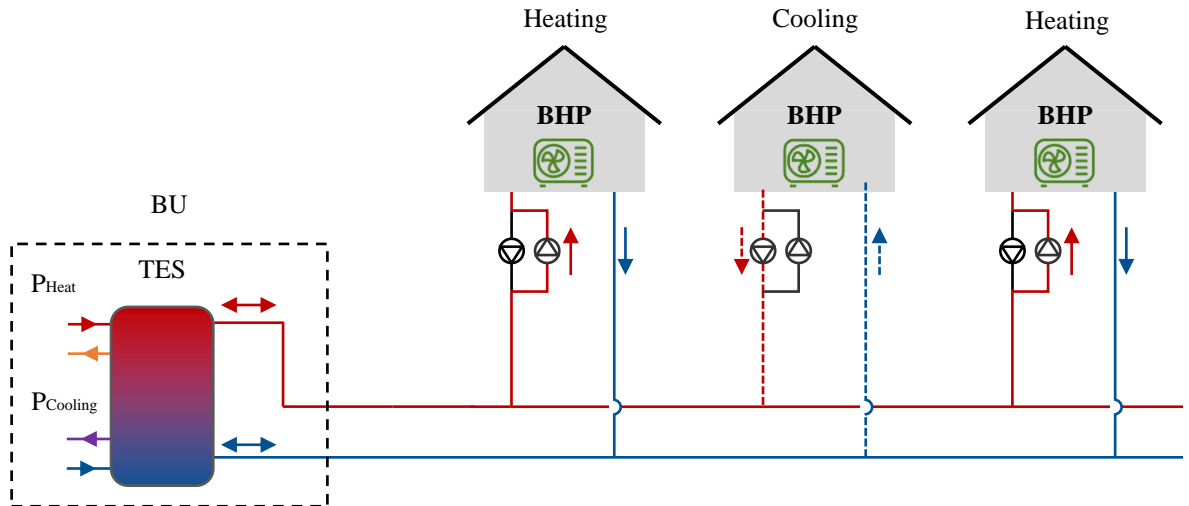


Figure 3.3: 5GDHC with decentralised pumping and passive BU for balancing.

The key difference from the current hydraulic designs other than having the passive BU, is that only the pump speed of a Variable Speed Drive (VSD) pump is used to meet temperature or pressure control signals. There is no need for a central distribution pump and modulating control valves to regulate the flow. This concept is in line with patent US 6,607,141 B2 for decentralised pumping systems [145]. Furthermore, this concept of decentralised pumping is investigated by Dolstan and Havlena (2014) [146], where decentralised pumps are used for a domestic hydronic system and by Paarporn (2000) [147] for industrial applications. Having decentralised pumps could result in inefficient pumping operation due to larger heads for relatively small flow rate. However, this problem is present in all cases of bidirectional flow and lower grid temperature [15]. Decentralised pumping could even lead to reduced electricity costs, since instead of utilising the throttling of balancing valves to change the system curve, only pump speed control is utilised [146]. Altogether, even if inefficient pumping operation is present, the overall impact on the system's techno-economic performance is small compared to the energy savings made possible by energy sharing between different prosumers [29].

Revisiting the example of Figure 3.2, the interaction of two pumps in the proposed design is shown in Figure 3.4.

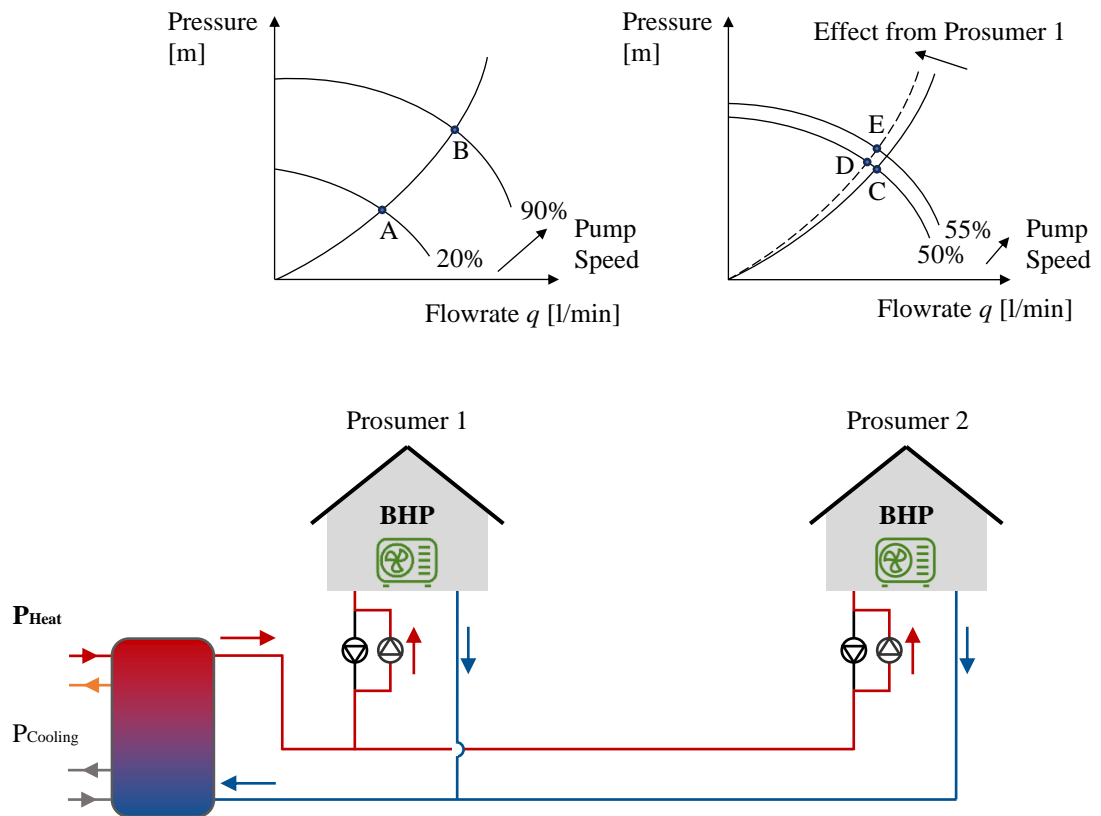


Figure 3.4: Prosumer pump interaction example in proposed hydraulic setup.

As previously, an increase in the demand of prosumer 1 leads to the pump ramping up from point A (20% speed) to point B (90% speed). This instantaneously changes the system characteristic curve of prosumer 2's pump, with the operational point shifting from point C to point D. This new point D does not provide the flowrate required in the system ($q_C > q_D$), so the pump needs to increase its speed to point E. In the proposed design, the surplus flow can “escape” to the BU while any pressure variations are absorbed by the water mass in the TES of the BU. This interaction of pumps and passive calibration from the BU's TES is a continuous process. The key challenge is to develop a lenient control regime for the prosumer pumps that can prevent system instability.

To decrease control stiffness, control could be based on return temperature. This way, the thermal inertia of the water allows for a larger time interval until the changes of the new operating point's flowrate (q_D) are seen. Due to the thermal inertia of the transfer station, a change in the transferred power (e.g. due to changed volume flow or changed demand) only slowly changes the outlet temperature. The temperature deviation is then seen by the PI controller which in turn changes its speed. The resulting change in speed of the pump leads to a slight change in the pressure drop across it. However, the stiff coupling of the

hydraulic system described above is with this control approach less problematic, as the thermal inertia relaxes the control system. The pumps therefore will continuously ramp up and down to meet the new operating point, but this is done in a slow and controlled manner, especially if the variations are small.

Developing control strategies that explore both temperature and flowrate control variables in the proposed hydraulic design is critical. These strategies, structured around the characteristics of the passive BU and decentralised pumping are discussed below.

3.2 5GDHC control philosophy

There are two possibilities to control the heat power extracted/deposited from/to the grid: one involves adjusting the flow rate going through the prosumer, and the other the return temperature. If the return temperature is controlled, that would require a constant ΔT on the ambient grid. If the flowrate is adjusted without accounting for the return temperature, the grid temperatures can freely fluctuate. The controls need to account both for active energy transfer units (BHP for heating and/or cooling) and passive Direct Cooling Heat Exchanger (HEX_{DC}). It has been shown that their use in 5GDHC is instrumental to the system's efficient operation [148].

To start with, for the case where the grid ΔT is not fixed, the BHP needs to be modulated on its flowrate. The flowrate setpoint from the BHP based on the prosumer demand is used as the control input in a Proportional – Integral (PI) controller and the return temperature is allowed to fluctuate. For the HEX_{DC} , since there is no flowrate setpoint, the flowrate of the prosumer pump is controlled based on the flow temperature to the cooling load. This results in a free-floating supply and return temperature in the grid, depending on the prosumers' power demand. Figure 3.5 showcases this control strategy, with the BHP in heating mode and the HEX_{DC} used for cooling. This control strategy is referred to as

$T_{\text{GridFloat}}$.

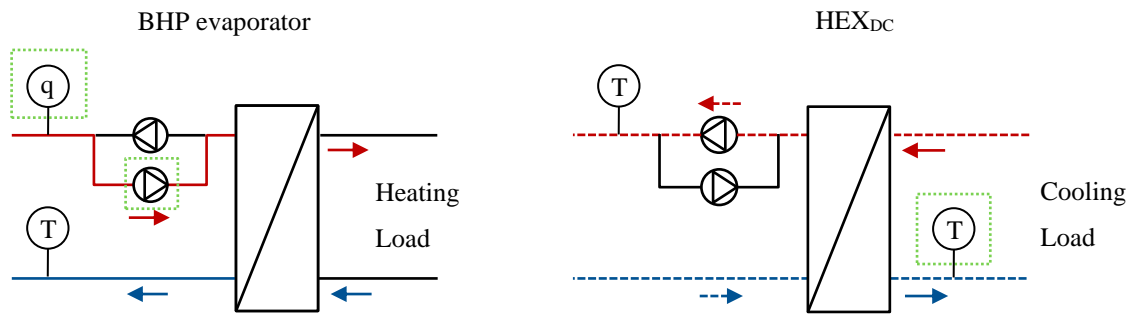


Figure 3.5: Schematic of control strategy for $T_{GridFloat}$.

Alternatively, the ΔT on the grid is fixed. In this case, the prosumer primary pumps are controlled through the return temperature. A return temperature setpoint is assigned to the pumps' PI controller, with its speed (and thus flowrate) varying based on the error from the measured value. The same control is implemented on the BHP and the HEX_{DC} . For example, for a BHP in heating mode, if more thermal power is requested by the prosumer, the return temperature on the grid drops. This in turn leads to an increase in the PI error, which is corrected by increasing the pump's speed. An advantage of this approach is that the grid temperature can be optimised to maximize efficiency for different project areas or different periods in the year [65]. This control strategy is referred to as $T_{GridFix}$ and is shown in Figure 3.6.

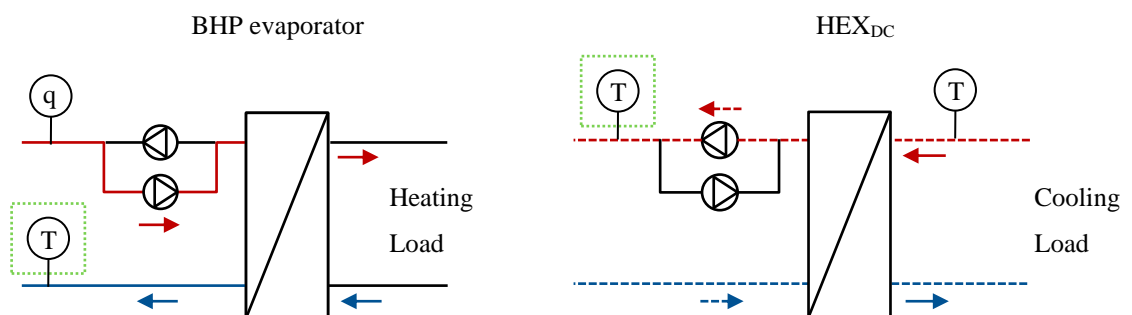


Figure 3.6: Schematic of control strategy for $T_{GridFix}$.

Having developed these designs and control methodologies, it is crucial to develop computer models that can simulate their behaviour. This will allow a first indication of whether they are valid and a valuable resource for modelling 5GDHC systems.

3.3 5GDHC system simulation

The development of bespoke simulation models for 5GDHC is discussed below. The models are made open access[†] [2]. First, a review of potential modelling environments for 5GDHC simulation and the respective available models is conducted. It is followed by a description of the modelling components development, capturing the proposed hydraulic designs and control strategies. An exemplary use case of the components for a simple 5GDHC system with two prosumers and a BU is then showed. The methodology for PHIL setups using the developed models and requiring minimal hardware is discussed. These setups can allow the experimental analysis of prosumer interaction. A discussion on strengths and limitations of the developed models is finally conducted.

3.3.1 Modelica for 5GDHC simulation

Simulating prosumer-dominated 5GDHC systems presents a significant challenge, compounded by the lack of a clearly defined system design as described in Section 3.1. This simulation challenge involves capturing complex interactions such as cross-sector energy flows, hydraulic dynamics, and control strategies within acceptable computational timeframes [44,149,150]. The key simulation challenges are rooted to the prosumer nature of nodes, leading to a complex model with bidirectionality influencing hydraulic interactions and consecutively energy flow characteristics.

To capture the operational complexity of such systems, it is key to accurately model thermofluid behaviour. Bünning et al. (2018) [65] propose the use of Modelica for modelling 5GDHC systems after conducting a thorough comparison of Modelica with multiple modelling environments including EnergyPlan. They argue that detailing hydraulic and energy flow interaction coupled with overarching controls is a challenge that fits the multi-engineering scope of the Modelica simulation language [151]. These findings are strengthened by a more recent SLR by Kuntuarova et al. (2024) [152] on proposed modelling environments for different thermal systems' simulations. Modelica allows for accurate simulation of the system dynamics including bidirectionality of flow, pressure constraints, flow characteristics and energy interactions between heating and cooling. It is

[†] Available online at: <https://researchdata.gla.ac.uk/1659/>.

recognised by the IEA as one of the key computational models for building system modelling [153]. Modelica features multiple open access libraries with validated components for buildings and community heating and cooling energy systems, including the Buildings [154] and AixLib [155] libraries, summarised in one library under BESMod [156].

Authors from [51,62] researched the hydraulic constraints and opportunities for new topologies in Modelica while von Rhein et al. (2019) [42] developed a model for 5GDHC topology comparisons in Modelica. These models are associated with high computational times but, despite capturing the performance of the system, they cannot be used for a larger project area or for a long simulation time horizon. Hinkelman et al. (2021) [157] suggested that modelling simplifications can be made in Modelica to allow for lower computational times, combining the ability to capture the non-linearities of plants and flow behaviour with acceptable computational times. Following a detailed SLR of the modelling methodologies of 5GDHC networks, Abugabbara et al. (2020) [33] suggest that the computational time for 5GDHC networks could be reduced by 63%. To achieve this, better coupling of district and building energy models is needed, along with co-simulation. The concept of co-simulation is also adopted by Buffa et al. (2020) [112]. In their work, TRNSYS is coupled with LabView to create a digital model of a 5GDHC substation with a TES and a reversible HP calibrated with a physical model. The model's limitations are mainly the interconnection with other substations and the overall simulation of operation of the system as well as a limited prediction horizon and real-time pricing.

Overall, publications on 5GDHC Modelica systems have focused on describing modelling methodologies and subcomponent development, aimed mainly at studying particular elements [45,158,159]. However, these studies have limitations. The developed models are not provided for reuse, nor include a comprehensive explanation of the interplay between control regimes and prosumer, BU, and decentralised pumping station interaction. Furthermore, they have been mostly case-specific, with only some Buildings library components providing limited insights on BHP and TES interaction and overarching control. Finally, prosumer interaction, the function of the BU and the effects of decentralised pumping to system performance has not been experimentally validated. This is mainly due to the large number of units and hardware components required to study such

interactions. PHIL provides a method for combining simulation models with real hardware, interfacing through digital and analogue input/output signals, that could facilitate system-wide experiments with the use of minimal hardware. Facilitating such experiments through the provision of bespoke Modelica models for 5GDHC would be a step forward in understanding and quantifying the complex behaviour of such systems.

3.3.2 5GDHC component design methodology

The development of the Modelica components is guided by usability, scalability, accuracy, flexibility, reliability & validity [153]. The prosumer and BU models are based on equipment from the thermal Prosumer House Model (ProHMo) library [160]. The ProHMo library includes experimentally validated components from the Centre for Combined Smart Energy Systems (CoSES) lab. It is based on the Green City library from the commercial Modelica environment Simulation X [160]. The library uses a thermal only approach to simplify the models and shorten simulation time, where pressure influences are neglected. This simplification is valid for heating systems within buildings [160,161].

To model the interaction of prosumers in a 5GDHC network with several prosumers, it is important to capture pressure losses and bidirectionality of flow. For this purpose, the building models of ProHMo are coupled with hydraulic components through a communication interface sub-model, referred as hydraulic interface. The hydraulic interface serves as an accurate and comprehensive representation of the hydraulic components within the system, their behaviour and interaction. It comprises interconnected hydraulic elements (pumps, valves, sensors, pipes and elements of hydraulic resistance), facilitated by hydraulic connectors, and replicates all relevant elements encountered in real-world applications. To connect the hydraulic interfaces with the thermal only models, input/output connectors are used for flowrate, temperature and control signals.

Furthermore, the developed control strategies are captured in all components for different grid operations. These bespoke Modelica components for 5GDHC allow the creation of digital twins of real systems. An example of such a digital twin for a 5GDHC system with two prosumers is shown in Figure 3.7.

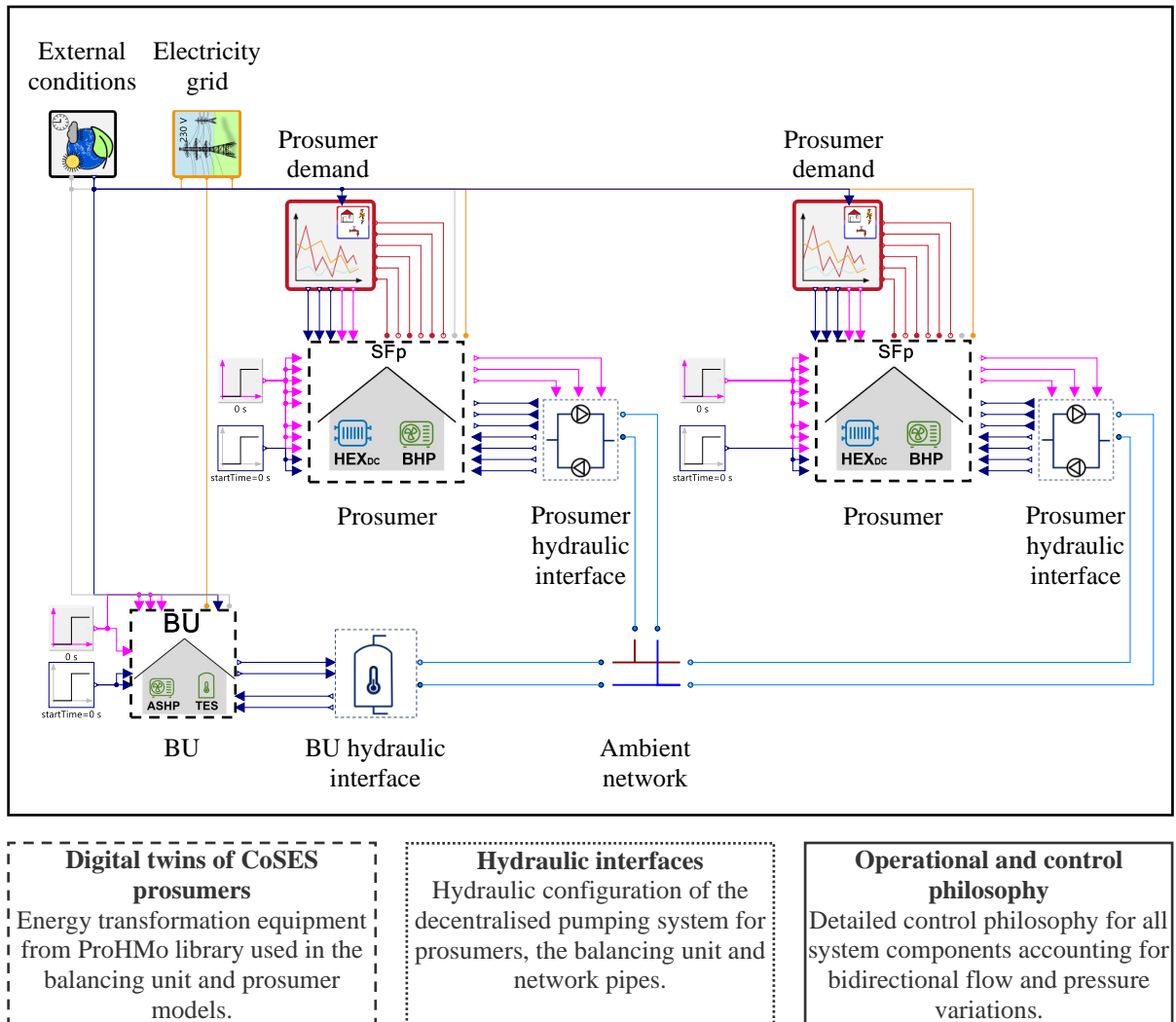


Figure 3.7: Modelica components used for 5GDHC system development.

3.3.3 Prosumer simulation model

The prosumer model includes energy transformation units, TES and energy demands. It can capture space heating, space cooling and DHW demands. The Modelica prosumer model is shown in Figure 3.8.

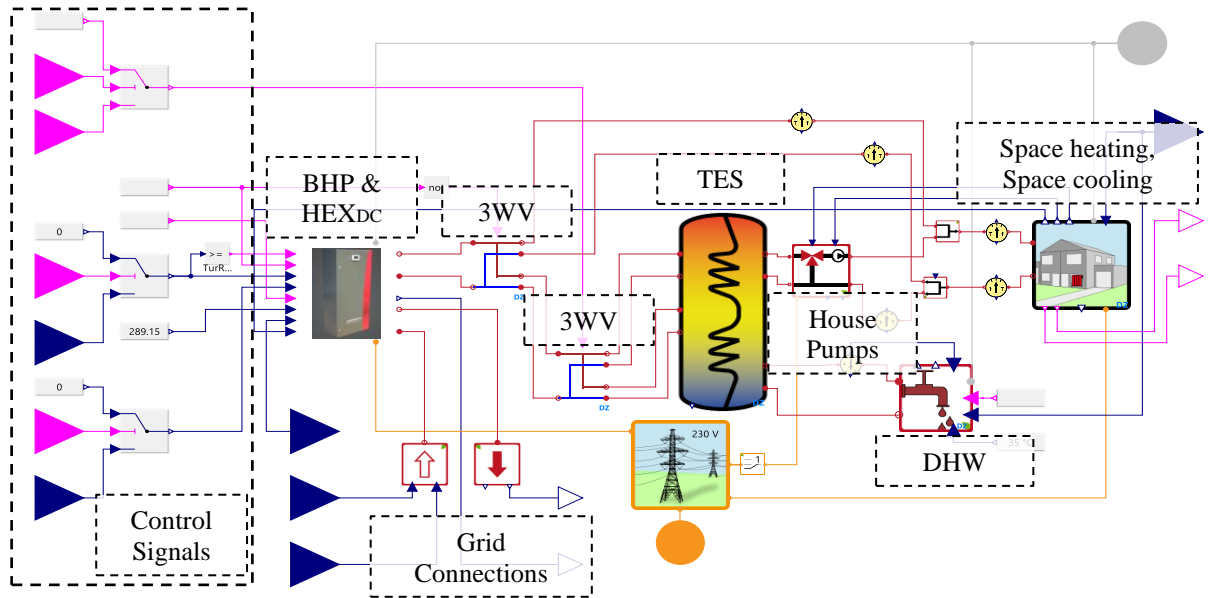


Figure 3.8: 5GDHC prosumer Modelica model.

The operation of the BHP and the HEX_{DC} is the focal point in the prosumer component. HEX_{DC} allows for direct utilisation of the cooling from the network's cold pipe (if low enough) without upscaling it via a BHP. For space heating and DHW, the load is to be supplied mainly from the BHP with any additional loads supplied by an auxiliary heater (electric resistance) placed within the BHP unit. For heating, the energy transformation units are connected in series with the TES which is discharged to the heat sinks (buildings). Cooling is directly supplied by the energy transformation units (HEX_{DC} or BHP) without going through the TES. Component sizing in the model is user-defined based on project-specific parameters, reflecting the scalable nature of the components. Default values are based on the equipment present in the CoSES lab, which served as the prototype for the digital twins in the ProHMo library.

The BHP model is based on measurements of a commercial BHP found in the CoSES lab, reproducing its efficiency and dynamics. The TES model has also been experimentally validated [160] and is represented by a one dimensional stratified model, where the TES is split into multiple TES Temperature Layers (TESTL) of uniform size. 10 TESTL are used in the ProHMo library to match the number of temperature sensors in the physical unit in the lab. The minimum temperature, seen at TESTL 10, is set to 60°C . This value satisfies both DHW supply and legionella avoidance requirements [43]. A hydraulic switch, namely a 3-Way Valve (3WV), can change the charging TESTL based on temperature in the TES. Space heating is from TESTL 5 (Flow) and TESTL 1 (Return) since a low temperature

heating system is assumed (underfloor heating) and TESTL 10 (Flow) and TESTL 1 (Return) for DHW. The discharge of the TES is modulated by a pump valve setup based on temperature and flow requirements from the heat sinks.

The space heating and space cooling demands are captured by adapted Green City library models which allow for different number of residents, construction characteristics, building type and terminal units. The default is set to new buildings with underfloor heating/cooling systems which is most relevant for 5GDHC prosumers with heating and cooling demands [144]. Additionally, models for inputting heating/cooling demand in the form of time series are also available. The flow and return temperature depend on the flowrate supplied by the tertiary pumps (variable flowrate pumps in the building) but are designed for 40-30°C for heating and 16-24°C for cooling. Both space heating and space cooling are modulating around a temperature setpoint (21°C for heating and 23°C for cooling) by varying the request inlet flowrate. Similarly, DHW is modelled, requiring a temperature of 60°C and, based on the consumption, returning a cooled down water at varying flowrates. There is a HEX between the end DHW consumption and the water from the TES. DHW is dependent on the number of residents and can be switched off during cooling operation (if no DHW is required during cooling periods). At each time step, there can only be heating or cooling supply. A 3WV is alternating between BHP or HEX_{DC} when in cooling mode depending on the grid's cold line temperature (if low enough, the HEX_{DC} is used). Therefore, there cannot be at the same timestep heating and cooling being drawn from the ambient grid. However, there can be heating and cooling supply to the prosumer at the same time (i.e. space cooling and DHW) since the TES decouples heat supply from generation.

The control strategy for modulating the BHP in heating mode is built around the discharging rate of the TES. The goal for the control is to keep a stratified TES, minimise the starts and stops of the BHP, keep a minimum temperature of 55°C on TESTL 9 for legionella concerns and maximise system efficiency. Based on these objectives, the control uses a 3WV to charge the top or middle of the TES, with priority given to charging the top TESTL. To avoid on/off control with hysteresis (system lagging to the input signal), a novel control method is proposed with the modulation of the BHP as a function of the reference TESTL. By introducing this operational area with an upper and lower temperature limit, oscillation around a control setpoint, with the equipment turning on and off once it goes over/under the setpoint, is avoided. Equation 3.1 shows how the

modulation factor is determined by the ratio between the actual and maximum temperature difference for the respective TESTL against set maximum and minimum values:

$$mf = \left(\max \left(0, \min \left(1, \left(1 - \frac{T_{TESTL,ref} - T_{sup,min}}{T_{sup,max} - T_{sup,min}} \right) \right) \right) \right) \quad (3.1)$$

where mf is the modulation factor for the BHP, $T_{TESTL,ref}$ is the reference TESTL, $T_{sup,min}$ is the minimum temperature value for the reference TESTL and $T_{sup,max}$ the maximum temperature value for the TESTL. When the reference temperature is equal to the maximum allowed temperature, the modulation factor is zero. Conversely, when the temperature matches the minimum allowed temperature, the modulation factor is 1. To ensure the modulation factor stays within the bounds of 0 and 1, a max-min definition is applied. This approach accounts for cases that the temperature levels in the TES exceed the upper limit (e.g., on start-up).

To maintain TES stratification, the prosumer component utilises two modulation factors: one for the top for DHW and one for the middle for space heating, as shown in Figure 3.9. Depending on the setting of the 3WV, the respective modulating factor is used, with the reference TESTL set to layer 7 for charging of the top of the TES and layer 4 for the middle, chosen to limit hysteresis and the impact of water inflow to/outflow from the TES.

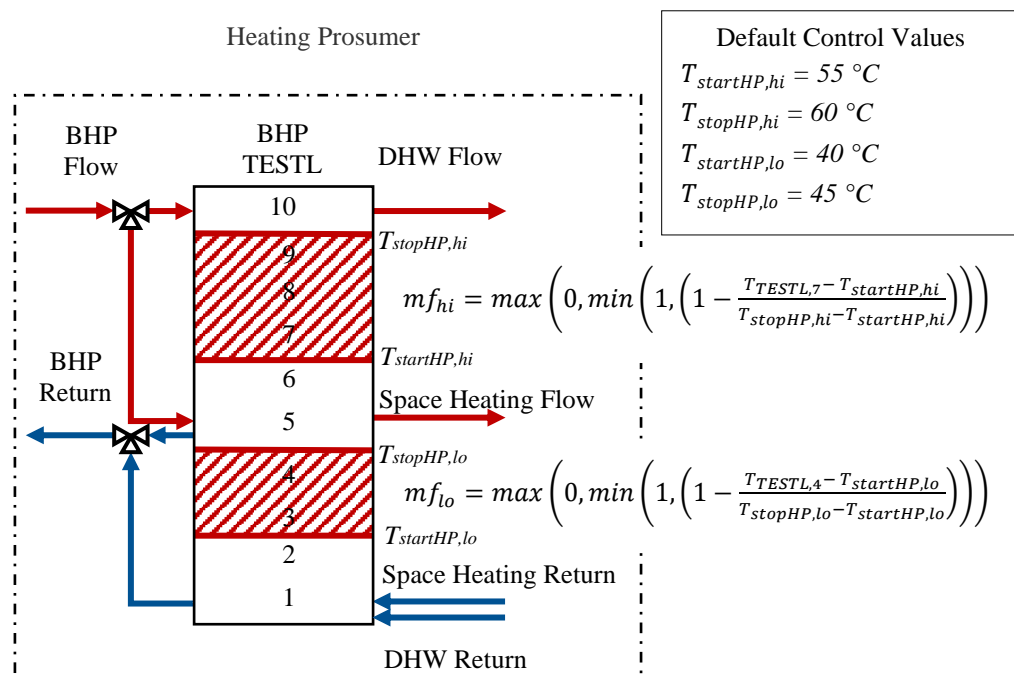


Figure 3.9: Schematic of control methodology for BHP.

It is seen that the higher TES modulation factor mf_{hi} is utilising a temperature band between the start and stop temperature setpoints, $T_{startHP,hi}$ and $T_{stopHP,hi}$ respectively. In a similar manner, the lower TES modulation factor mf_{lo} is determined by a lower temperature range $T_{startHP,lo}$ and $T_{stopHP,lo}$. The maximum of the two is set to the mf that the BHP sees. This control strategy allows for a stratified TES, maximisation of continuous BHP operation and abiding to minimum temperature requirements for legionella concerns. An operation example for 1 day is shown in Figure 3.10. This figure indicates how the modulation of the HP impacts the power output (plot A) and its relation to the temperature profile inside the TES.

Plot A indicates how the power demanded is followed while plot B indicates all TESTL temperatures. In this example, plot B shows that the TES remains stratified during both periods of BHP operation and idle times. The variable mf allows for a smoother operation of the BHP without many starts and stops. The difference between TESTL 4 and TESTL 5 occurs due to the water outflow from the TES for space heating demands occurring at TESTL 5. The COP of the HP for the different modulation factors is shown in plot C, giving higher values for operation between 60% and 30% and a cut-off at 25% power modulation. This is in line with measurements from the HP unit [160].

For space cooling, at default settings, priority is given to HEX_{DC} over the BHP (in cooling mode). The choice of switching to the use of the BHP if the room is not cooled after a designated time (defined by the user) is also provided.

Finally, a further control option has been added for the operation of the BHP. This allows for operation of the evaporator and/or the compressor under constant temperature difference or flowrate, both of which are available for commercial BHP units. Depending on the operation, the power modulation is achieved by varying the non-fixed variable within limits set by the user. The equations governing these behaviours have been modified in the models utilizing conditional functions ("if" statements) to adapt their operation accordingly. By implementing these adjustments, the BHP and grid inlets can be dynamically controlled, enabling greater flexibility in their operation. This adaptability allows for improved system performance and optimization tailored to the specific use case, with due consideration given to external factors such as flowrate and temperature differences.

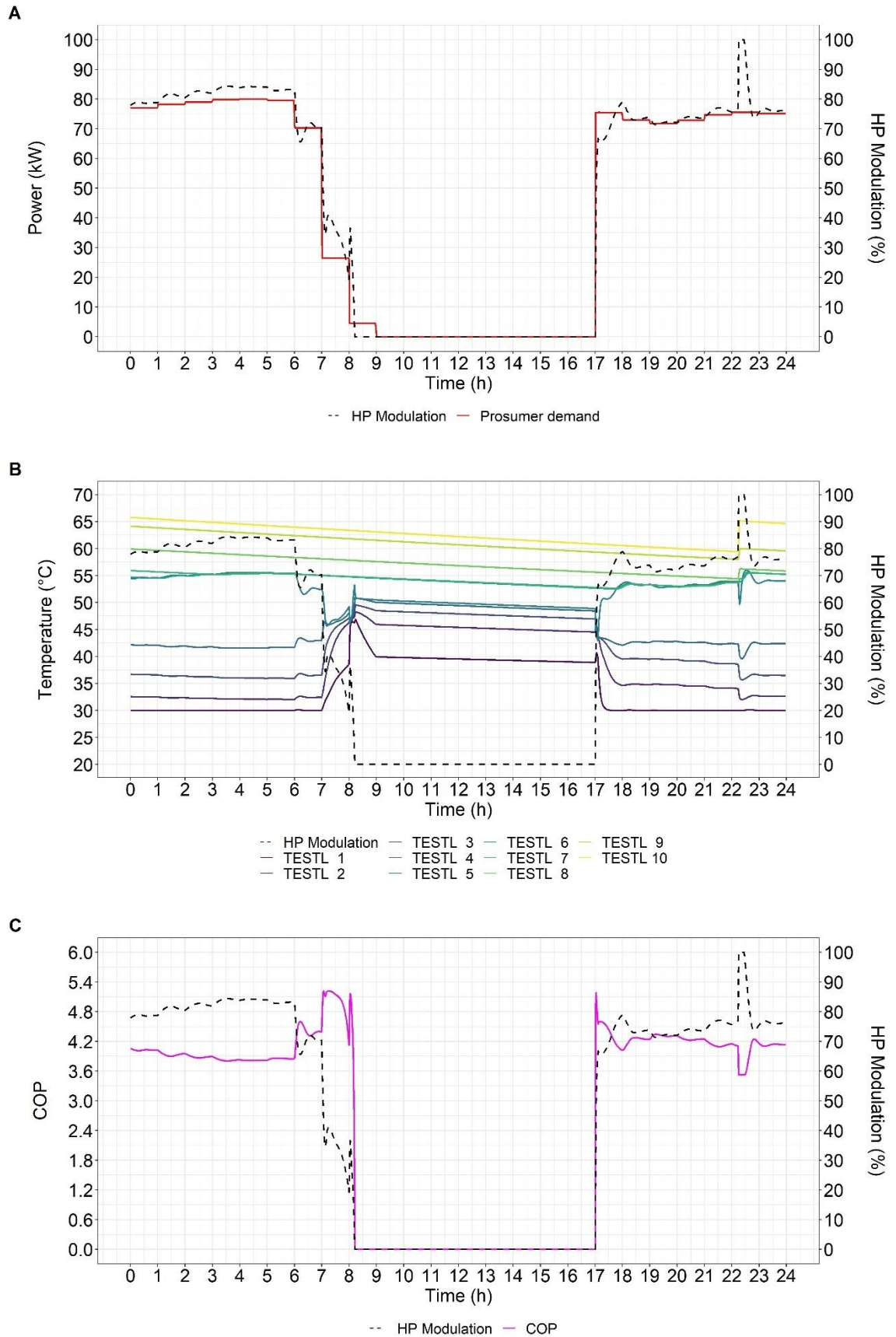


Figure 3.10. TES operation under modulation of the BHP.

3.3.4 BU simulation model

The BU is responsible for providing thermal and hydraulic balance to the network. The Modelica model is captured in Figure 3.11 and described below.

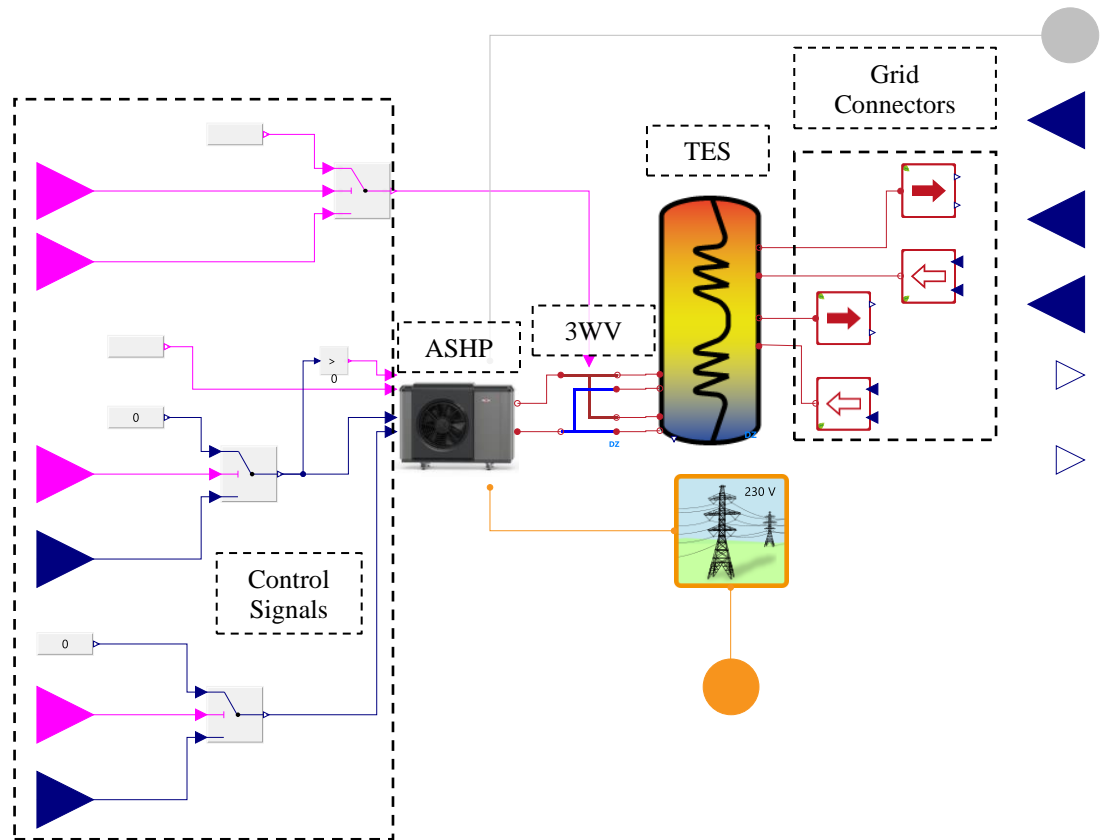


Figure 3.11: 5GDHC BU Modelica model.

An ASHP is connected in series with a TES that acts as a passive interface between the hot and cold pipes as described in the hydraulic design. This setup with the TES directly connected to the hot and cold pipe of the network (hot grid pipe at the top of the TES and cold grid pipe at the bottom), provides a passive hydraulic balance, critical for the operational integrity of the system featuring decentralised pumps and energy transformation units. Depending on the thermal balance needed by the network, the TES is cooling down (during heating balance needed) or heating up (during cooling balance needed). The ASHP needs to keep the TES temperature within the operational limits by recharging the top or bottom of the TES with heating or cooling respectively.

To achieve this operational strategy, the ASHP is connected in series with the TES where a 3WV can change the which TESTL is supplied based on mode of operation of the ASHP. Therefore, charging for heating uses TESTL 9 for flow and TESTL 6 for the return, while for cooling it uses TESTL 2 for flow and TESTL 5 for return. This setup allows for unidirectional flow through the ASHP while keeping a stratified TES without mixing when variations between heating to cooling dominant system operation occurs. The mode of the ASHP depends on the flow direction of the grid, with cooling activated when the flow leaves the bottom of the TES, and heating when the flow leaves from the top.

The ASHP operation is following the same rule-based control for the modulation factor as the one described in equation (3.1). The operation of the BU is captured in Figure 3.12.

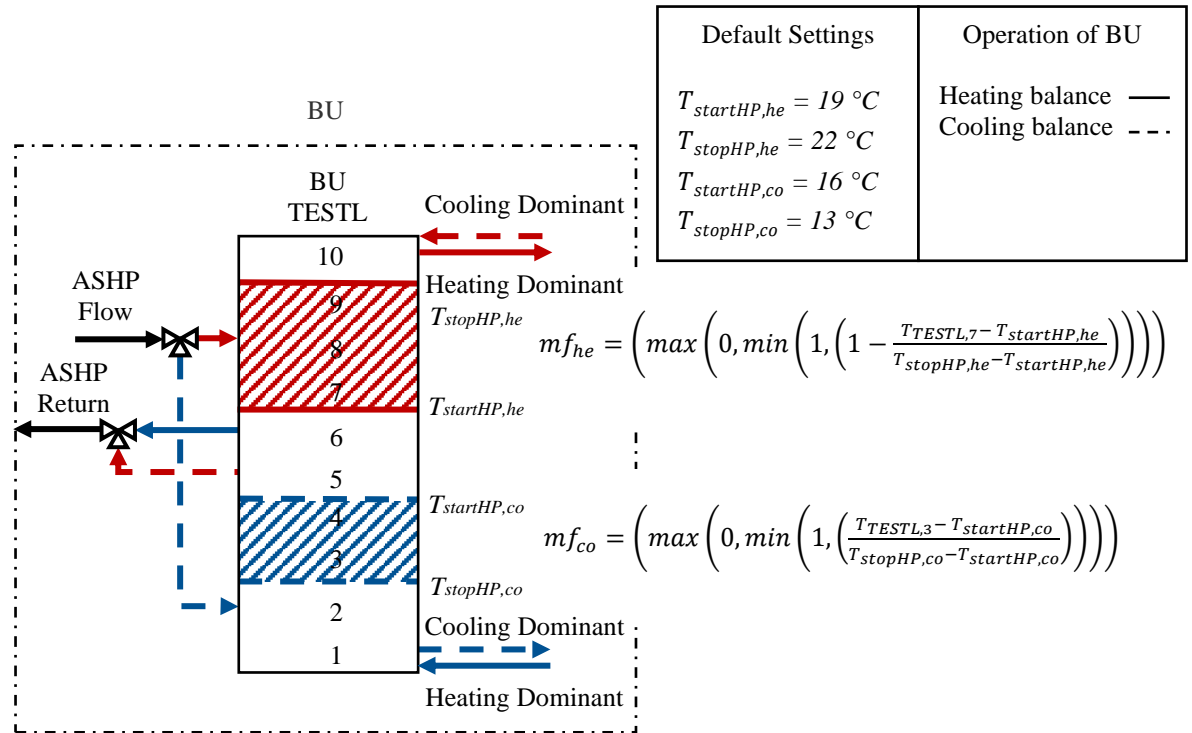


Figure 3.12: Schematic of control methodology for BU.

Like the BHP heating setup, there are two modulation factors for the ASHP, in this case depending on the operation mode (heating or cooling). During heating, the flow going through the TES is from the bottom to the top with the ASHP in heating mode. The ASHP draws water from the middle of the TES (TESTL₆) and supplies at the top (TESTL₉). The heating modulation factor (mf_{he}) is used which is calculated based on equation (3.1) with the upper and lower temperature bands being $T_{startHP,he}$ and $T_{stopHP,he}$. For cooling, flow

is reversed in the grid, with hot water coming in at the top of the TES and cold one coming out at the bottom. Therefore, the ASHP is in cooling mode, cooling down the lower half of the TES. The ASHP draws water from the middle of the TES (TESTL₅) and supplies at the bottom (TESTL₂). For the modulation factor during cooling (mf_{co}) there is no need to subtract the ratio of the reference temperature from 1 since it directly responds to the cooling power requirements. This operation also allows for a stratified TES that can respond to dynamic changes in heating/cooling balance requirements.

3.3.5 Hydraulic interface simulation model

The hydraulic interface is needed for the connection of Modelica components with thermal connectors to a system with hydraulic connectors that can capture bidirectional flow as well as pressure variations.

The hydraulic interface can avoid utilising library components that are only available in Simulation X, therefore open access Modelica standard library and Buildings library components are preferred. The functionality of the interface follows the methodology presented in the ProsNet library [162], where the primary and secondary side communicate through a set of input/output signals.

A key modelling approach developed in this work is the introduction of a thermal volume to represent the prosumer, considering thermal inertia and pressure variations of the system. This thermal volume element from the standard Modelica library is linked to the prosumer model through input/output connectors, providing temperature and flowrate setpoints. This follows the concepts of co-simulations analysed above. Therefore, we can combine the benefits of utilising thermal only connectors in the prosumer and BU components (low computational times and lower complexity) without compromising the hydraulic performance of the system nor the overall accuracy. At the same time, this setup allows for a clear separation between the thermal only models utilising Simulation X components that can be turned into Functional Mock-Up Units (FMU) as discussed in the next subsection. The hydraulic interfaces for the prosumer, the BU, and the grid model are illustrated in Figure 3.13.

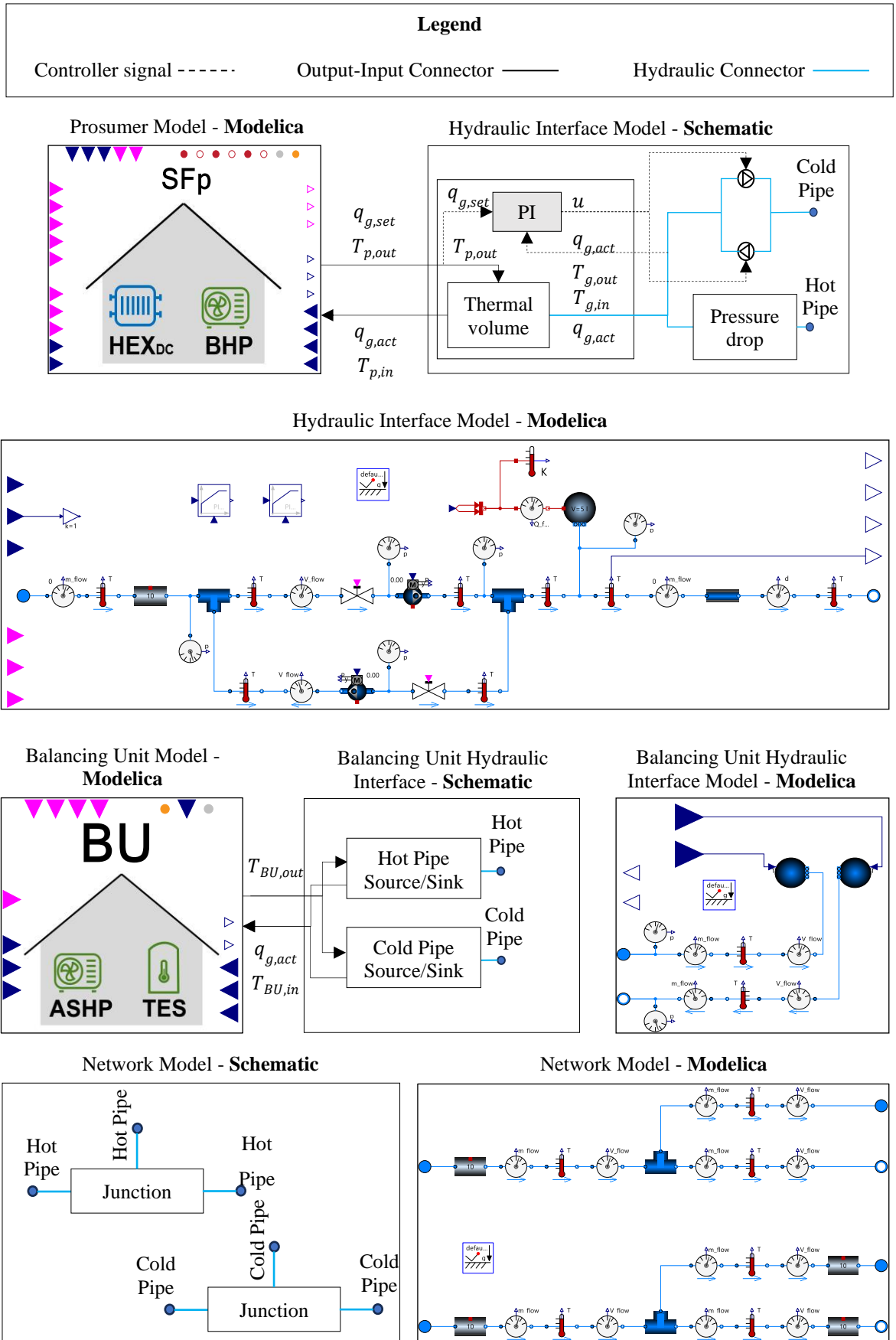


Figure 3.13: Hydraulic interfaces for prosumer, BU and hydraulic model for the 5GDHC grid.

For the prosumer hydraulic interface unit, the key inputs and outputs from the hydraulic interface are temperature and flowrate. Signals for the set flowrate $q_{g,set}$ asked by the prosumer and the output temperature $T_{p,out}$ from the prosumer are sent to a volume representing the prosumer, allowing for thermal inertia to be accounted for, resulting in the temperature the grid actually sees from the prosumer, $T_{g,out}$. Depending on the instantaneous demand mode (heating or cooling), the respective pump from the interface becomes active and flow is thus changing direction respectively. We use a PI controller to give the setpoint u to the respective pump, considering the actual $q_{g,act}$ and set flowrate $q_{g,set}$. Then, $q_{g,act}$ and $T_{g,in}$ are fed back to the prosumer as inputs.

For the BU's hydraulic interface, the key input is the temperature from the BU. The temperature corresponds to the top or bottom of the TES, depending on the flow direction, namely the sign of $q_{g,act}$. If $q_{g,act}$ is positive, which means there is dominant heating demands in the grid (flow from cold to hot port), then the hot pipe volume acts as a source with $T_{BU,out}$ being equal to the temperature at the top of the TES. $T_{BU,in}$ equal to the temperature of the cold pipe flows at the bottom of the TES. The opposite happens when there is cooling dominant operation and thus a negative $q_{g,act}$, with the cold pipe volume becoming a source and the hot pipe volume becoming a sink.

The pipe network, namely the grid model, comprises dynamic pipes, sensors and junctions to allow for the connection of the prosumers and the BU. The grid model allows for parallel connection between loads and includes ports for both the hot and cold pipes.

3.3.6 FMUs of prosumers and BU

To further increase the usability of the model, both prosumer and BU models are developed so that they can be exported to FMUs, allowing for their use through the Functional Mock-up Interface (FMI) standard for application in all Modelica environments [163]. With FMUs for these components, an arbitrary size of network can be built, with varying topologies and design and operational characteristics. However, the benefits from using a FMU come at a cost of transparency and editability. The components become "black boxes" that have specific elements that can be edited, significantly limiting the flexibility of the models to change. To maximise their usability, a set of key parameters

have been made editable in the FMU. These follow the ProHMo library methodology as described in Zinsmeister and Perić (2022) [160], and include:

- Inputs for individual control setpoints.
- Weather files.
- Consumption parameters.
- Energy generator unit capacities.
- TES dimensions.

3.3.7 Exemplary use case of simulation models

To showcase the usability of the produced models, a simple system is used. It involves a heating and cooling prosumer as well as a BU connected through a grid element in parallel. This setup is the one shown in Figure 3.8, Section 3.3.2. A constant temperature difference is kept between the cold and the hot pipe, and the grid pipes are modulated based on variable flowrate. HEX_{DC} is used for the cooling prosumer (since underfloor cooling with a flow temperature of 16°C is assumed) while the BHP is used for the heating prosumer (connected in series to the TES).

The simulation is performed for one day, with an aim to observe the behaviour of the system and qualitatively verify its operation. Figure 3.14 displays key outputs, namely the temperature levels of the top and bottom TESTL of the BU TES, the temperature in the living zones of the prosumers as well as the temperature and flowrate values on the grid's junction. The simulation lasted 3.15min.

Plot A indicates the fluctuations of the temperatures at key TESTLs in the BU's TES, responding to heating and cooling requirements in the grid while keeping the upper (22°C) and lower (13°C) temperature limits. The spikes observed occur during ASHP start-up, with a momentary large intake. Plot B shows that the temperatures in both prosumer's living areas are maintained at the target reference temperatures (21°C for heating and 23°C for cooling). Larger deviations are observed during cooling due to the controller setting, underfloor cooling system behavior and the building pump's flowrate capacity.

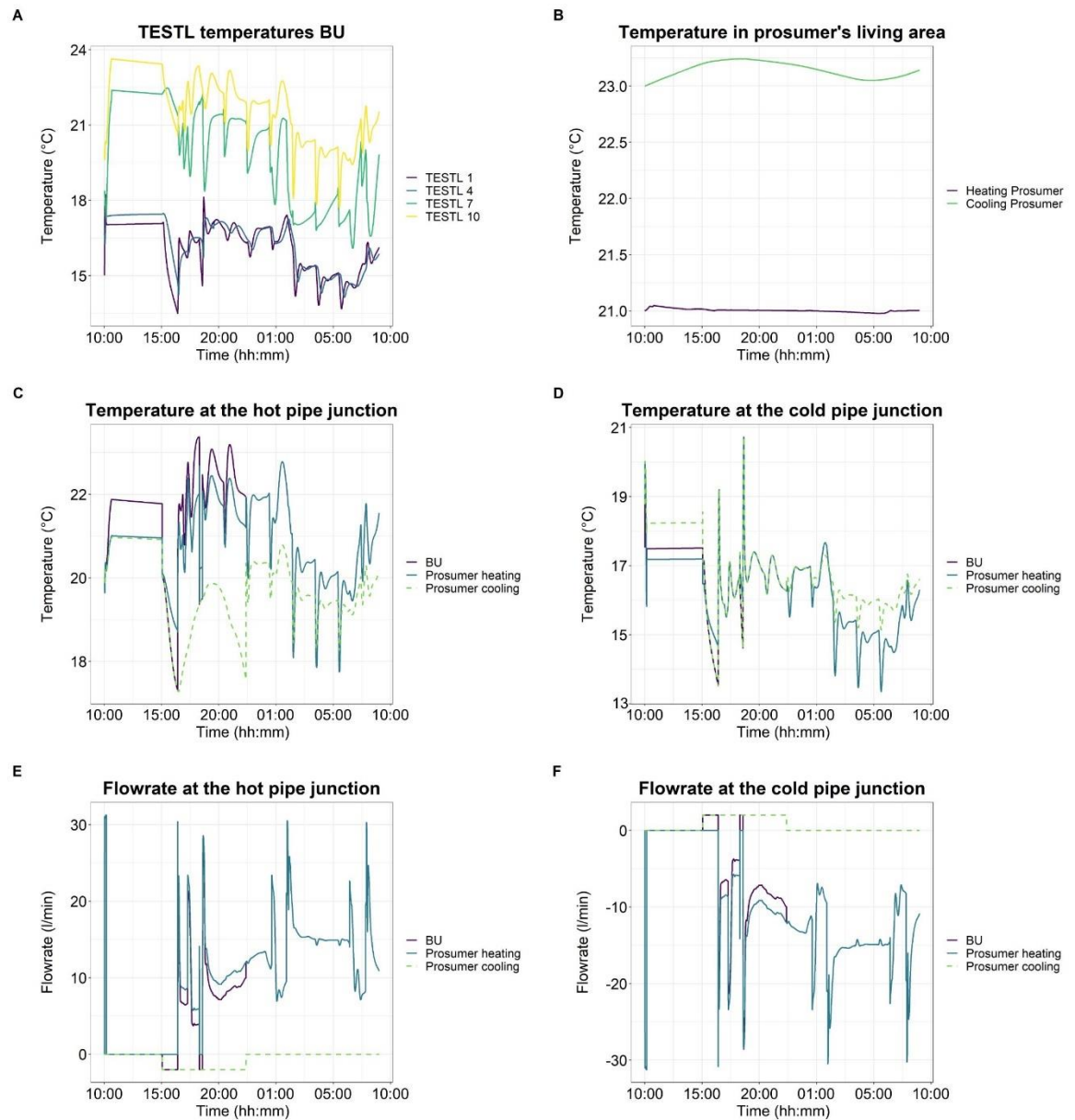


Figure 3.14: Exemplary case study of developed 5GDHC Modelica models.

Plots C and D present temperature levels at both the hot and cold pipes. In plots E and F, flow halts for the cooling prosumer after 23:00, causing the respective pipe temperatures to track ambient temperatures and those of the segment preceding it. During the flow interruption until 15:00, the BU remains idle, with the TES temperature slightly decreasing due to energy losses.

Overall, hydraulic and thermodynamic balances are kept in the system. The temperatures are maintained in the prosumers and bidirectionality of flow is captured. The BU can

operate both in heating and cooling mode ensuring that the top and bottom TESTL temperature setpoints are kept. It is shown that the components provide a working basis for investigations of different design cases and operation strategies. The next section describes how such designs can be validated with minimal hardware utilising PHIL approaches.

3.3.8 Implementation of PHIL with developed simulation models

A key research gap in 5GDHC systems is understanding prosumer behaviour and prosumer interactions under varying design conditions and control methodologies. Experimentally validating models would require multiple BHPs and buildings with both heating and cooling demands as well as the ancillary equipment (valves, pipes etc.) for developing a thermal network. Components are designed to allow PHIL applications with minimal hardware requirements, facilitating experimental assessments of prosumer interaction under varying control and design philosophies. Figure 3.15 illustrates how PHIL can be used for experimentally simulating a prosumer with only a HEX.

The HEX is sending metered signals to the prosumer simulation model for the flowrate and temperature present both on the primary and secondary side of the HEX. These are converted to standard unit values via a conversion module and fed to Modelica, which in turn sends back control signals. For the conversion and control modules, various software/hardware interaction methodologies are available. For example, the CoSES lab utilises Industrial Controllers for the hardware, communicating in real-time with NI VeriStand for the conversion of logged data and control setpoints, as thoroughly explained in Zinsmeister et al. (2023) [161]. Regarding hardware, other than the HEX, energy transformation units are required to raise/drop the temperature for both the prosumer and grid side.

The BHPs and HEX_{DCS} of the prosumers can be emulated with a PHIL setup. As mentioned in Section 3.3.3, the prosumer model features a BHP and HEX_{DC}, controlled in either constant flowrate or temperature difference. For the HEX_{DC} operation, based on the measured flowrate and temperature, the set return temperature of the building $T_{h,set}$ is calculated based on the heating/cooling system of the building and the building and outdoor temperature. The 3WV mixes water from the supply side to reach $T_{h,set}$. A signal is also provided for the grid pump $q_{g,set}$, as explained in Section 3.3.5. For the BHP

emulation, the grid pump is still operated according to the control signal $q_{g,set}$ but the building side operates differently. The 3WV is closed, so that it doesn't mix water from the supply into the return line and the pump on the building side is operated to supply $q_{h,set}$ to achieve the outlet temperature of the HP on the grid side.

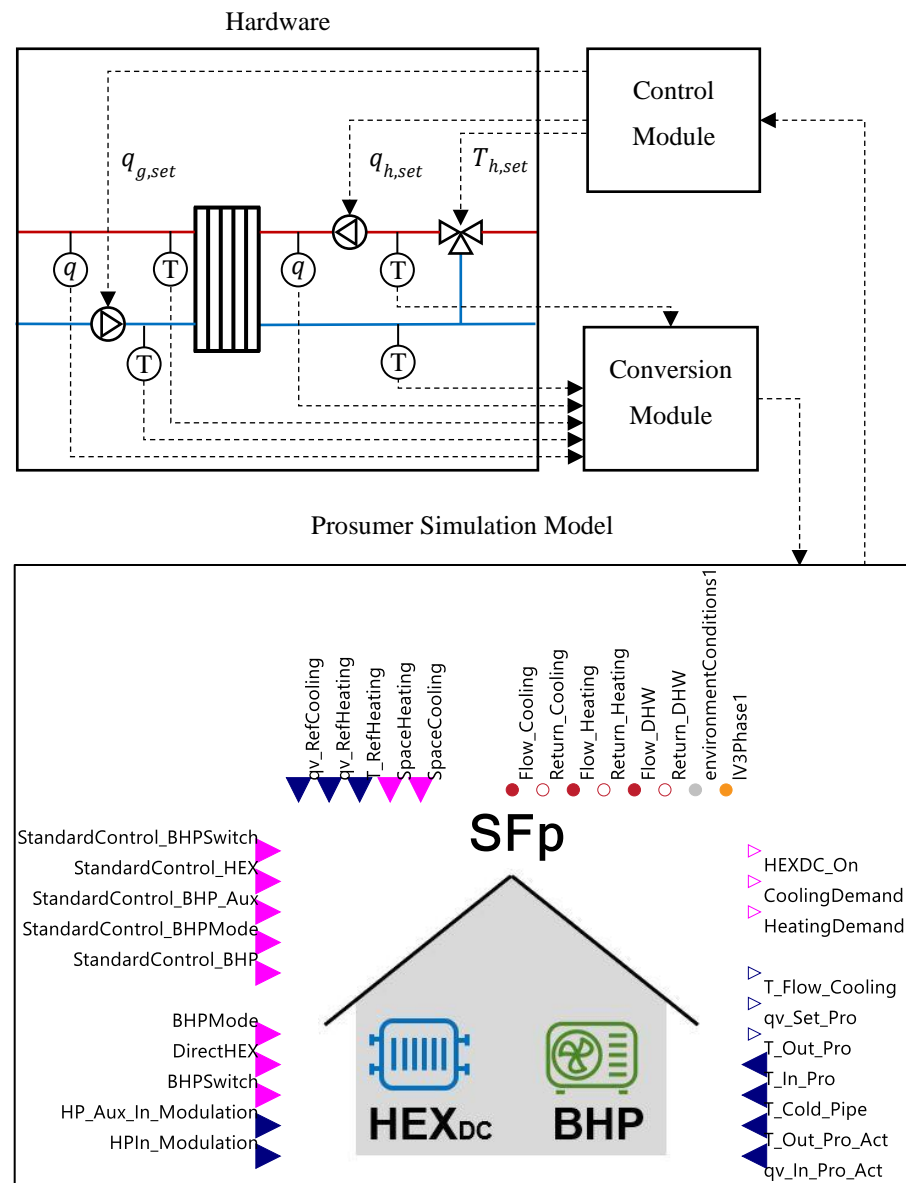


Figure 3.15: PHIL for a prosumer using a HEX.

Further implementations are possible that follow the same principles as the ones mentioned above. These could include multiple HEXs connected in series or in parallel to study the interaction of various prosumers. In addition, the BU could be connected in a similar approach to study its characteristics. Even an entire network with multiple prosumers and

BUs could be included as a simulation model on the grid side which would allow for investigating the impact of single/multiple prosumers on larger grids.

3.3.9 Discussion of developed simulation models

The following sections provide some insight on strengths and limitations of the developed models as well as a discussion on their potential applications.

3.3.9.1 Strengths of developed simulation models

These components utilise validated models from the ProHMo library that are modular and can provide a detailed representation of component operation and building behaviour. They provide a good rule-based control allowing for BHP operation with low number of starts and stops for a longer component lifetime and a stratified TES. Start up and slew times are included as well as solutions for hysteresis. Computational time is kept low since we are using hydraulic equations only for the network, significantly reducing the complexity of the model. The models are made open access and have platform independent FMUs where commercial components are used. They can be coupled with various grid models and elements such as seasonal TES.

Another key benefit that is arising from these models, is the capacity for PHIL experimentations with minimal hardware to study prosumer interaction. The models can be used to emulate both building and BHP/HEX_{DC} behaviour. Different levels of detail for PHIL experiments allow a detailed analysis of grid behaviour and component interaction with low costs, space requirements and overall complexity.

3.3.9.2 Limitations of developed simulation models

The key limitations of the components come from the use of the ProHMo library. As aforementioned the ProHMo library is used since it is the only open access experimentally validated prosumer models with BHPs and TES. However, ProHMo is built in Simulation X which is not an open access Modelica environment. This limits the capacity to freely edit the components. FMU provision has been presented as a workaround, but it does not fully open the “black box” of the component and does not allow for simple drag and drop of the individual components for use on any Modelica environment. The prosumer and BU

component models could be integrated into other libraries which are using open access components, while keeping the methodology of their operation intact.

The building models are focused on residential properties and may not accurately represent different consumer classes such as office blocks or retail properties. Moreover, the operational behaviors of the energy transformation components are tied to the physical units present in the CoSES lab, which are designed for household-scale applications. Consequently, when attempting to model much larger units or units with different technical specifications (e.g., refrigerants), the scalability and accuracy of the models may be compromised.

3.3.9.3 Potential applications of developed simulation models

The main benefit of these models is the provision of bespoke models and methodologies that facilitate the studying and analysis of 5GDHC systems. They can be used to create digital twins of 5GDHC systems or different model architectures to study specific elements of 5GDHC. They can act as a basis for the creation of research cases on the impact of several parameters on the overall performance of the system.

For example, they could be used to investigate different network topologies and the effect that network behaviour has on the hydraulic operation. The effect of including different consumer classes as prosumers as well as the seasonal co-occurrence of their heating/cooling demands could also be studied. The models could be used to replicate bespoke networks for industrial applications with given building schedules. Detailed operational strategies could also be investigated, identifying the effect of the hydraulic setup on the creation of thermodynamic subcycles and pump hunting phenomena. By developing relevant network and ground models, the effect of the ground type on the network performance can be studied for different insulation levels of the pipework, with a focus on the capacity for thermal losses under different network temperature regimes, insulation series and pipe materials. The impact on the number and location of BUs as well as the introduction of passive BUs such as seasonal energy storage (e.g., aquifers) can be quantified. The level of centralisation can also be studied, by changing the consumption parameters, allowing for a deeper investigation of the thermal zoning effect and combination of 4GDH with 4GDC and 5GDHC networks.

Altogether, the novel hydraulic designs, controls and simulation models presented in this section can elucidate a key implementation challenge of 5GDHC. However, it is crucial to experimentally validate these operational methodologies and observe the systems hydraulic stability and overall behaviour. Chapter 4 delves into such an experimental validation, focusing on the proposed system's hydraulic stability.

4 Experimental Validation of Proposed 5GDHC Design and Operational Philosophies

To experimentally validate the proposed 5GDHC system design and operational philosophies, the CoSES lab at the Technical University of Munich is visited. Two experiments are conducted in the lab, each lasting 20 hours. One for $T_{GridFix}$ (fixed grid return temperatures) and the other for $T_{GridFloat}$ (free floating grid temperatures). A comprehensive lab book is kept throughout the experiment, thoroughly detailing all setup proposals, control logic developments and component testing leading to the experiments.

A large variety of data is referenced, including experimental measurements, control setpoints and calculated figures. Table 4.1 provides a legend for the subscripts used to distinguish the different data types for T , q and P .

Table 4.1: Legend for data referencing.

Legend			
Subscript 1 - Data type		Subscript 2 – Prosumer/BU	
<i>exp</i>	Experimental measurement	<i>Cpro</i>	Cooling prosumer
<i>set</i>	Control setpoint	<i>Hpro</i>	Heating prosumer
<i>cal</i>	Calculated analytical value	<i>BU</i>	Balancing unit
Subscript 3 – Network		Subscript 4 – Pipe	
<i>pri</i>	Primary network (ambient grid)	<i>H</i>	Hot pipe
<i>sec</i>	Secondary network (BHP to TES)	<i>C</i>	Cold pipe
<i>ter</i>	Tertiary network (flow through heating/cooling load).	<i>Af</i>	ASHP flow pipe
		<i>Ar</i>	ASHP return pipe

The experimental setup is first presented. It is followed by the control implementation and component testing. The experimental results are then presented, covering the overall hydraulic and the energy transformation units (BHP & ASHP) behaviour. A detailed validation is undertaken, including an analysis of control variable errors and a statistical analysis of the primary pumps' flowrates. Finally, a discussion on the key findings and the generalisability of the results is shown.

4.1 Experimental setup

For the experiments, two prosumers are connected to a passive BU through a bidirectional ambient temperature grid. The experiments consider a heating only (heating prosumer) and a cooling only (cooling prosumer) load, meaning that one prosumer is demanding heating while the other cooling. Since these experiments aim to study the system's responsiveness to different load conditions, focus is given on exploring the system's behaviour to different demand regimes in the grid. These include dominant heating, dominant cooling, only heating, only cooling or no demand at all.

PHIL is used to simulate real building loads, following the methodology described in Section 3.3.8. Unlike typical predefined demand profiles, the building demands in this experiment depend not only on ambient conditions but also on the received energy. The prosumer models simulate a realistic building where if the received energy is lower than demanded, the demand accumulates, leading to a higher demand in the next time step. Therefore, the power demand the apparatus sees in each timestep will never be identical for different experiments. This dynamic behaviour allows to assess the control system's ability to meet the demands in real-time. The Modelica building models used in the PHIL are openly available in the ProHMo library, as well as the demand profiles observed during the experiment, which are presented in the experimental results (Section 4.4), in Figure 4.5.

A combination of Industrial Controllers and software (VeriStand and LabVIEW) is used for controlling, monitoring, and logging information. This setup allows for real-time interaction between simulation models as discussed in detail Zinsmeister et al. (2023) [161]. The schematic of the experiment is shown in Figure 4.1, while the complete Pipe and Instrumentation Diagram (P&ID) is found in Section 11.1, Appendix B. Equipment and experimental setup photos can also be found in Section 11.2, Appendix B.

Temperature is measured through 4-wire PT100 resistance sensors [164], quality class A with an error of ± 0.15 °C at 0°C and ± 0.25 °C at 50°C, while flowrates are measured using electromagnetic flowmeters Proline Promag E 100 [165], with errors of ± 0.5 % namely ± 0.15 l/min at nominal flowrate of 30 l/min. Both TES have 10 temperature sensors distributed along their height (only sensor 1 and 10 are shown for clarity) [166,167].

Electric power (P_{el}) is measured through voltage and current sensors on each of the three phases and thermal power (P_{th}) is measured for both the ASHP and BHP. The total ambient grid length is 3,830mm with pipe diameters of 20mm. The pipe lengths are measured in the lab using a measuring tape, with a reading error of ± 20 mm.

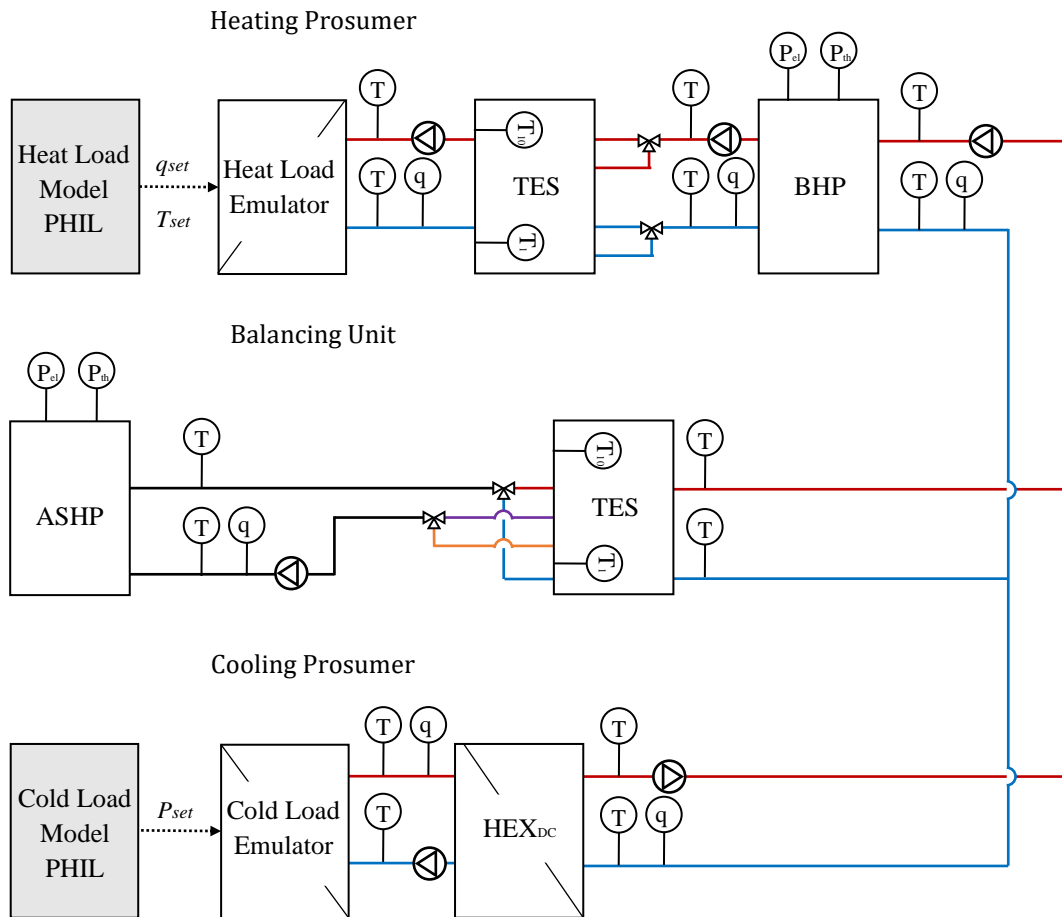


Figure 4.1: Experimental setup schematic.

The cooling prosumer extracts cooling from the grid using a HEX_{DC} (SWEP 60kW Single Phase Water-Water B80Hx20/1P) [168]. For the cooling prosumer's primary pump (grid) and tertiary pump (heating coil), a VSD pump is used with rated flowrate and head of $3.31\text{m}^3/\text{h}$ and 5.76m respectively (IMP Pumps unit NMT PLUS ER 25/60-180) [169]. A stainless steel direct electric Heating Coil (HC) is used as the cooling load emulator, with a maximum power of 9kW [170].

The heating prosumer features a BHP (20kW Ratiotherm WP Max-HiQ) [171] connected in series with a TES (750l Ratiotherm Oskar^o 10) [166]. The hydraulic separation with the main grid occurs at the BHP evaporator. The grid pump of the heating prosumer is a VSD

pump with rated flowrate and head of $2.04\text{m}^3/\text{h}$ and 18.01m respectively (Grundfos unit CME 1-2 A-R-G-E-AQQE S-A-D-N) [172]. A set of 3WVs are used to charge the middle or the top of the TES based on the control logic. The secondary and tertiary pumps used for supplying the TES and the heating load emulator respectively, are the same as the cooling prosumer's pumps (IMP Pumps unit NMT PLUS ER 25/60-180) [169]. A key characteristic of the BHP is its capacity to operate with a constant or flexible ΔT on the grid. The evaporator's ΔT is 3.5K , however a small internal pump referred to as InPu_{BHP} , allows the BHP to operate with a larger grid ΔT as shown in Figure 4.2. The exact setup can be seen in the system wide P&ID found in Section 11.1, Appendix B.

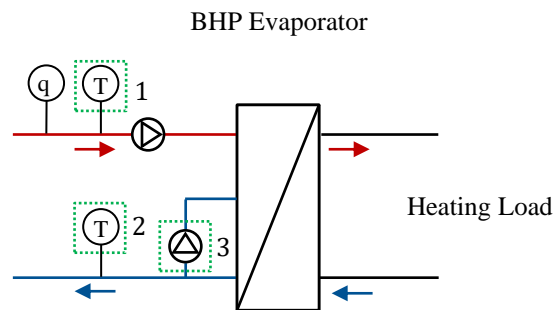


Figure 4.2: BHP schematic detail with InPu_{BHP} .

If the ΔT required across the hot and cold line in points (1) and (2) is higher than 3.5K , InPu_{BHP} (3) turns on, mixing the return water with the supply water to provide the setpoint ΔT of 3.5K . The higher flowrate counters the reduced ΔT through the evaporator, allowing for the same power to be supplied. In this way, the spread of the grid can be altered while the BHP operates with a constant evaporator ΔT . However, this leads to an efficiency drop, since the pump consumes more electricity for the same thermal power output and more importantly, the temperature in the BHP inlet drops, lowering the COP.

The BU has a reversible ASHP (10kW Wolf CHA 10) [173] connected in series with a TES (7851 Wolf BSP-800) [167]. The BU is directly connected at the top with the hot line and at the bottom with the cold line. Flow can change direction through it, or completely stop, depending on the flow regime in the grid. A set of 3WVs is used to control which TESTL is charged based on the mode of operation of the ASHP.

4.2 Control implementation and component testing

LabVIEW and VeriStand Environments allowed for logging data, real-time communication with hardware and PHIL implementation. The execution rate of the controller is 100 Hz. The controls of individual elements follow the descriptions in Section 3.2. For the HC of the cooling prosumer, Feed Forward Control (FFC) is implemented, with the control variable being the power setpoint from PHIL. The variable used in the FFC is calibrated based on return temperatures from the HC. The key control elements are shown in Figure 4.3, along with the PHIL setup. The schematic should be read in conjunction with Table 4.2 where the control elements of Figure 4.3 are described.

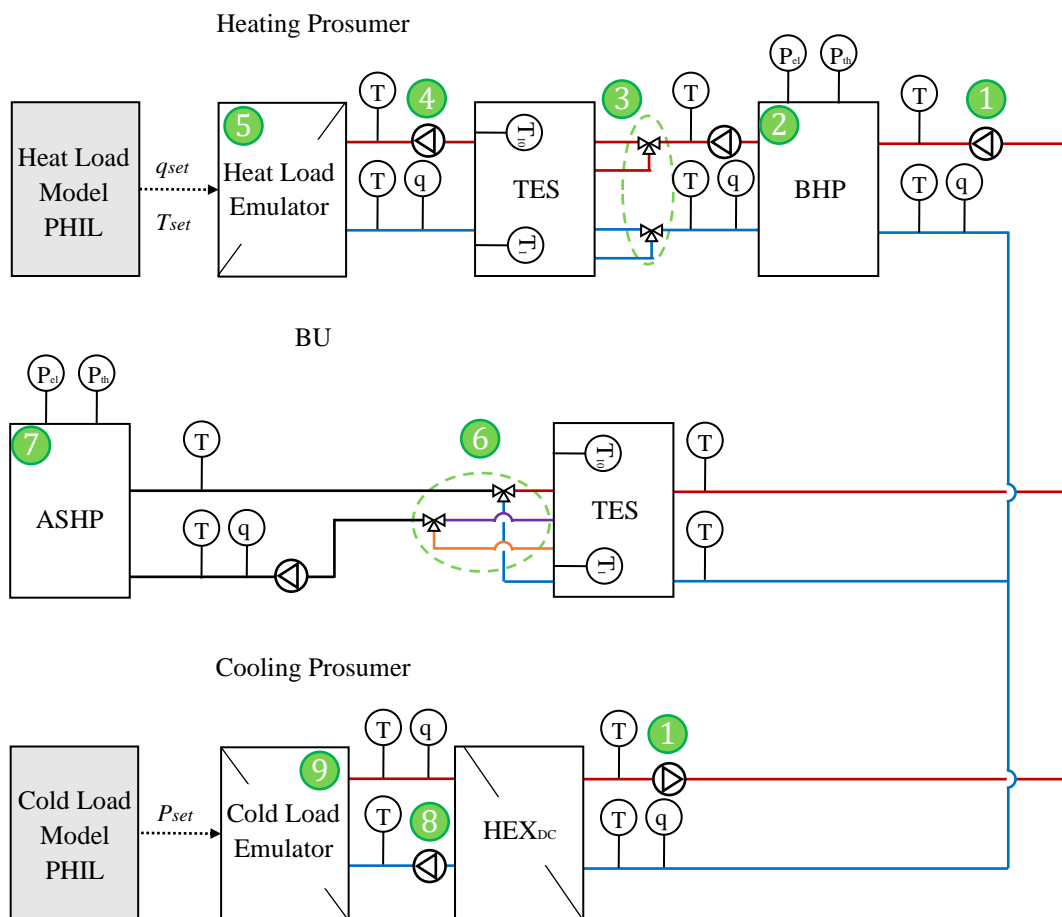


Figure 4.3: Control elements and PHIL setup.

Table 4.2: Description of control elements from Figure 4.3.

Control Element	Description
1	Prosumer primary pumps PID controller: $T_{GridFix}$ – Control on grid return temperature. $T_{GridFloat}$ – Control on flowrate for BHP and prosumer flow temperature for HEX _{DC} .
2	BHP power modulation based on temperature level of defined TESTLs.
3	BHP 3WV for charging TES based on temperature level.
4	Heating prosumer tertiary pump modulation based on the flowrate setpoint from heating load model (PHIL).
5	Heating load emulator to reach temperature setpoint.
6	BU 3WV for charging TES based on ASHP mode of operation.
7	ASHP power modulation based on temperature level of TES.
8	Cooling prosumer tertiary pump modulation.
9	Cooling load emulator using a HC based on the power setpoint from cooling load model (PHIL). Controlled with a feed forward controller with the current cooling consumption as setpoint.

Before conducting the experiments, component testing is performed for each prosumer and the BU. This allows tuning the PI controllers using the empirical method, confirming the minimum flowrates for the pumps, and ensuring no flow through non-return valves. The empirical method for PI controller tuning involved a stepwise trial and error methodology. The Proportional (P) parameter is set to reach the required setpoint, while the Integral (I) parameter is altered to obtain a steady state response without large oscillations [174].

For the BHP and the ASHP operation, the temperature levels in the respective TES are used following the methodology detailed in Section 3.3. For the BHP, if the top of the TES is charged, the 3WV is open (flow to the top part of the TES), with the power output set to 10kW. If the middle is charged, the 3WV is closed (flow to the middle part of the TES), with a power output set to 7kW. Equivalently, for the ASHP, when in heating mode (flow from bottom to top of TES) the top of the TES needs to be charged; the 3WVs open with the ASHP in heating mode having a power output of 13kW. When in cooling mode (flow from top to bottom of TES) the bottom of the TES needs to be kept at a certain temperature range; the 3WVs are closed with the ASHP operating in cooling mode. This operation of the BHP and ASHP and their respective TES is shown in Figure 4.4.

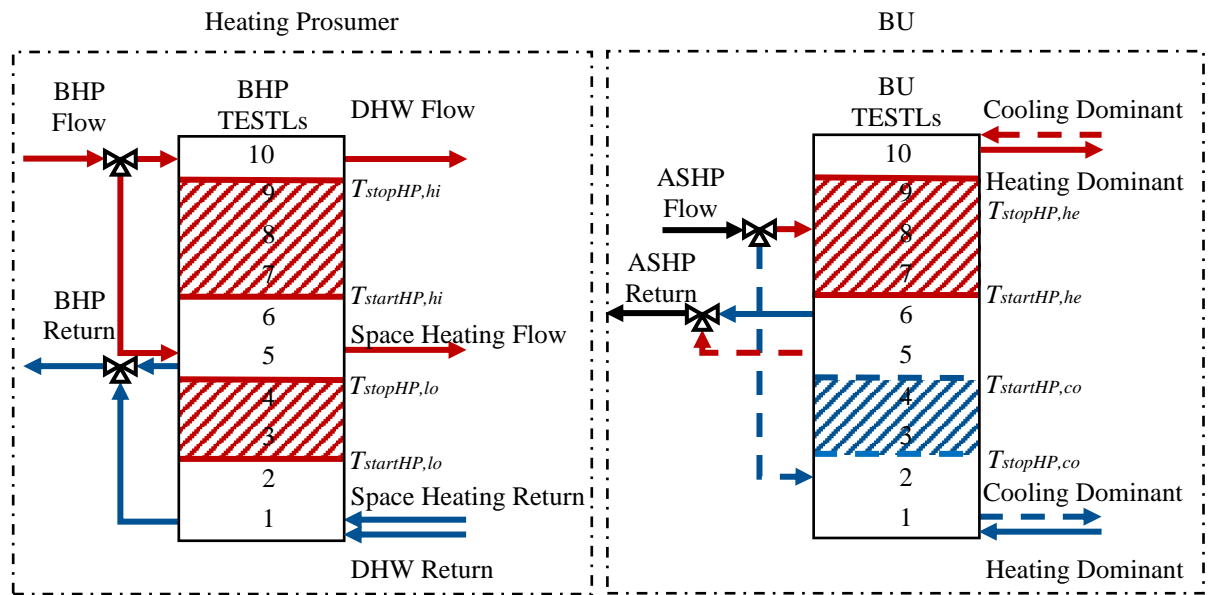


Figure 4.4: BHP and ASHP operation based on TES temperature levels.

The key control values are summarised in Table 4.3, while the screenshots of the LabVIEW interface including all control parameters and their interconnections are found in Section 11.3, Appendix B.

Using this setup, two experiments are conducted in the lab to compare the control strategies presented, both for 20 hours. A hypothesis for the systems' behaviour is followed by the experimental results comprising BU, BHP and overall hydraulic behaviour.

4.3 Hypothesis for experiment

The TESs for both the BU and the BHP are expected to be well stratified and within the temperature limits set out in Table 4.3. $T_{GridFix}$ is expected to have a constant temperature on the return pipes of both prosumers irrespective of the prosumer demand. Bidirectionality of flow is expected to not influence the behaviour of the BU, with direction of flow automatically changing based on the decentralised pumps' net behaviour. The ASHP is expected to have multiple starts and stops due to the BU TES having a short temperature band for the top TESTLs during heating (19°C -22°C) and bottom TESTLs during cooling (13°C -15°C). The COP for the BHP is expected to be slightly lower in $T_{GridFix}$ compared to $T_{GridFloat}$ due to the bypass pump reducing the

evaporator inlet temperature to keep an evaporator ΔT of 3.5K. At times of no flow in the grid (due to no demand), the temperature in the uninsulated grid is expected to try to reach the ambient lab temperature of 22°C.

Table 4.3: Setpoints used for key control variables in the experiment.

Control Family	Control Element	Name	Unit	Value	
BU	BU temperature setpoints	$T_{set,BU,startHP,he}$	°C	19.0	
		$T_{set,BU,stopHP,he}$	°C	22.0	
		$T_{set,BU,startHP,co}$	°C	15.0	
		$T_{set,BU,stopHP,co}$	°C	13.0	
	ASHP power modulation	$P_{thset,BU,ASHP}$	kW	13.0	
		$P_{coSet,BU,ASHP}$	kW	10.0	
Heating Prosumer	TES temperature setpoints	$T_{set,HPro,startHP,hi}$	°C	55.0	
		$T_{set,HPro,stopHP,hi}$	°C	60.0	
		$T_{set,HPro,startHP,lo}$	°C	40.0	
		$T_{set,HPro,stopHP,lo}$	°C	45.0	
	BHP power modulation	$P_{thset,BHP,mf,hi}$	kW	10.0	
		$P_{thset,BHP,mf,lo}$	kW	7.0	
	Heating prosumer primary pump min/max setpoints	$q_{set,Hpro,pri,max}$	l/min	30.0	
		$q_{set,Hpro,pri,min}$	l/min	6.0	
	Heating prosumer secondary pump flowrate setpoint	$q_{set,Hpro,sec}$	l/min	15.0	
	Heating prosumer primary return temperature setpoint (for $T_{GridFix}$)	$T_{set,Hpro,pri,C}$	°C	15.0	
	Heating prosumer primary pump setpoint (for $T_{GridFloat}$)	$q_{set,Hpro,sec}$	l/min	18.0	
	Cooling Prosumer	Cooling prosumer primary pump min/max setpoints	$q_{set,Cpro,pri,max}$	l/min	15.0
			$q_{set,Cpro,pri,min}$	l/min	6.0
HC FFC Variable		HC_{FFC}	constant	2.0	
Cooling prosumer primary return temperature setpoint (for $T_{GridFix}$)		$T_{set,Cpro,pri,H}$	°C	20.0	
Cooling prosumer tertiary flow temperature setpoint (for $T_{GridFloat}$)		$q_{set,Cpro,ter}$	°C	16.0	

4.4 Experimental results

Both experiments ran without unexpected behaviours and followed the hypothesis. All experimental data are made open access in the University of Glasgow's Enlighten Repository[‡] [1].

The total demands for a period of 20h are 32kWh for heating and 21kWh for cooling for both experiments. Figure 4.5 shows the demands the apparatus sees, having periods of simultaneous heating and cooling demands (hours 0-1 and 10-11), only cooling (hours 1-10) and only heating (hours 11 to 20). As discussed earlier, the reason the graphs are slightly different is due to the power supplied to the prosumer varying during the experiments, affecting the internal temperature of the building. The following subsections include a detailed analysis of the experimental results covering overall hydraulic behaviour, BU and BHP behaviour.

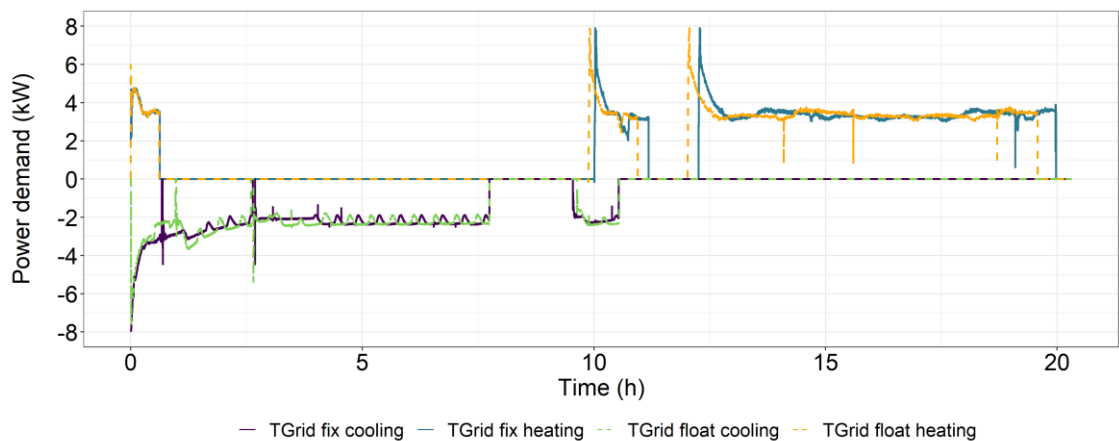


Figure 4.5: Demands resulting from PHIL simulation models.

4.4.1 Overall hydraulic behaviour

To examine the systems' overall hydraulic behaviour, the net flowrate reaching the BU along with the respective grid temperature is studied. Figure 4.6 shows these key measurements, with graphs C and D focusing up to hour 10 for clarity.

[‡] Available online at: <https://researchdata.gla.ac.uk/id/eprint/1659>.

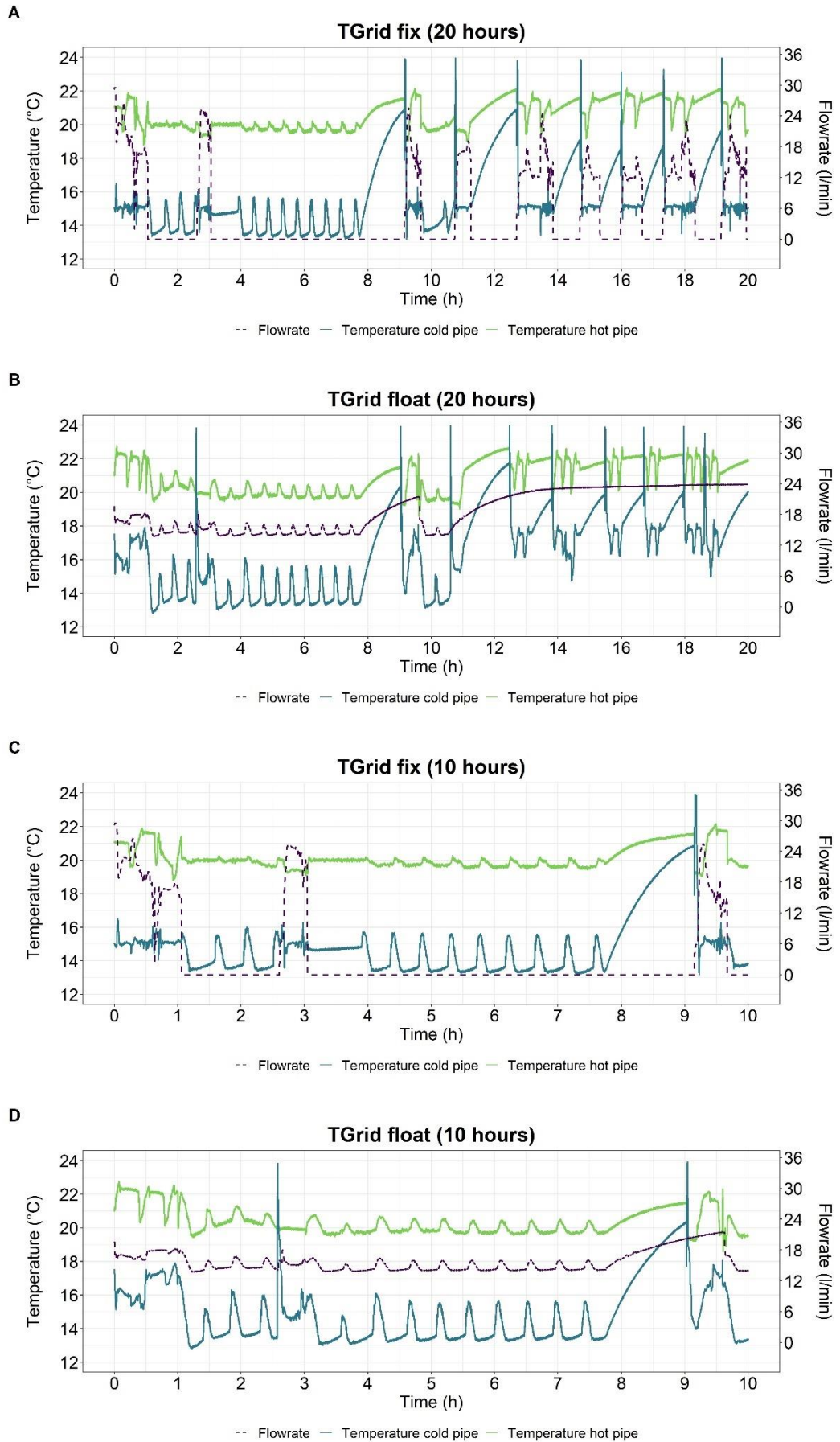


Figure 4.6: Hot and cold grid pipe temperatures and flowrate through the BU.

$T_{GridFloat}$ has a variable return temperature, unlike $T_{GridFix}$. This is best seen between hours 0.0 and 1.0 as well as 9.0 and 10.0 when there is simultaneous heating and cooling. During these periods, when there is dominant heating (flowrate is greater than zero), the temperature entering the BU is that of the cold line. For $T_{GridFix}$, it remains around 15°C while for $T_{GridFloat}$ it fluctuates from 16°C to 18°C. The control on the return temperature is also observed in hours 3.0 to 4.0, where there is only cooling, leading to a flow in the BU from the hot to the cold line (negative flowrate). There, the return line being the hot line remains at 20°C for $T_{GridFix}$ while it fluctuates from 20°C to 21°C for $T_{GridFloat}$. Between hours 2.5 and 3.0, there is a sudden change from dominant cooling to dominant heating. The flowrate direction changes, with $T_{GridFix}$ as expected adjusting to the controlled setpoint of 15°C while for $T_{GridFloat}$ the free-floating temperature settles at around 14°C. In addition, this abrupt change in demands, changing the flow direction, led to no control instabilities.

4.4.2 BU experimental behaviour

The supply temperature from the BU, fluctuates based on the setpoints of the TES for the ASHP operation. To observe if this variation of the TESTLs is within the expected setpoints and how the ASHP modulates it, Figure 4.7 is studied. A 3-hour window (hours 0.0 to 3.0) is used for clarity, where all cases of demand are present.

As expected, when there is a positive flowrate (flow from cold to hot line) the ASHP is coming on (in heating mode) when the temperature in TESTL 9 drops below 19°C. For cooling, a similar behaviour is observed when the temperature in TESTL 2 surpasses 15°C. The small power drop in each start of the ASHP is due to its start-up behaviour, where certain minutes are needed to enter steady-state operation. A similar operation is seen after the shutdown signal, where the ASHP is entering a ramp-down period. In both cases the TES is stratified with clear top middle and bottom temperature layers.

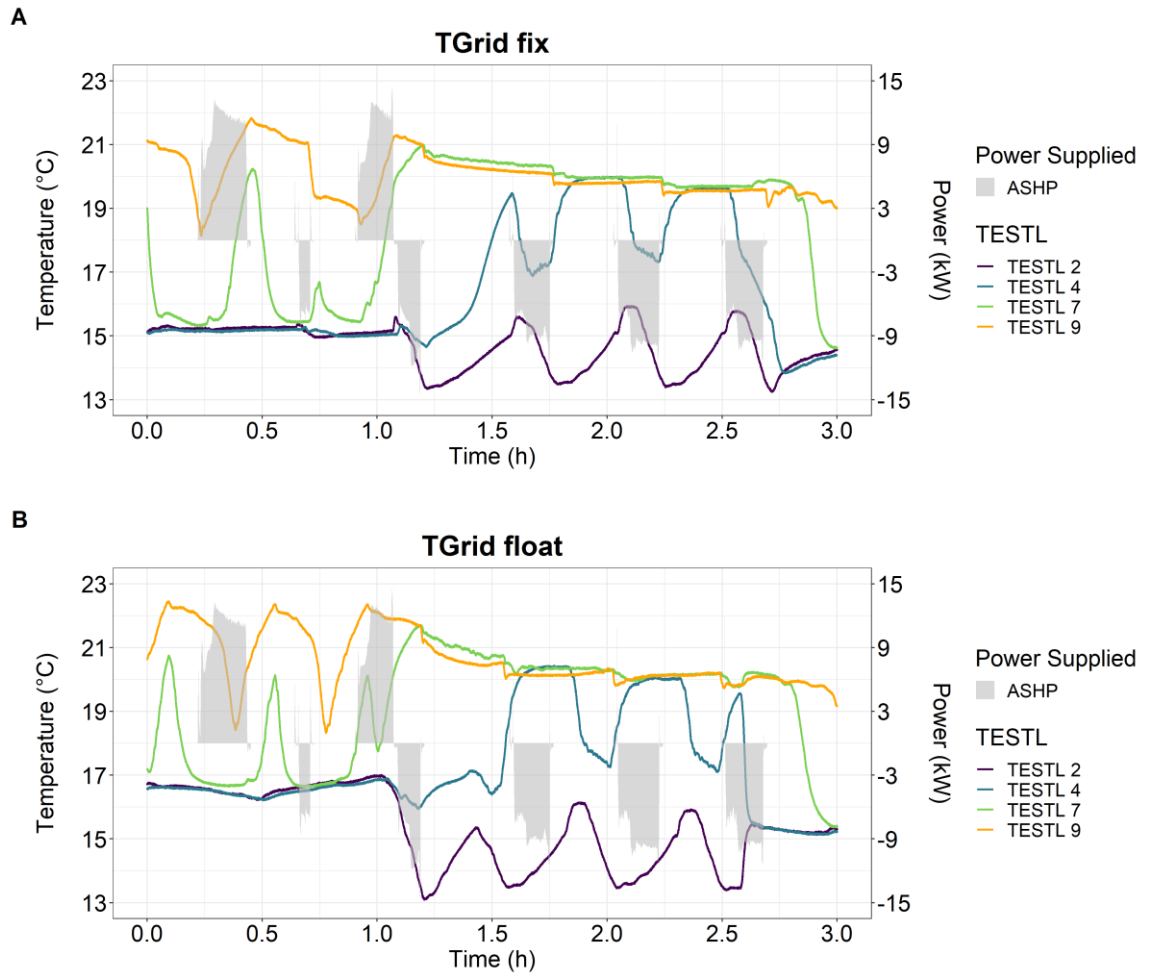


Figure 4.7: BU TES temperature profile.

4.4.3 BHP experimental behaviour

For the BHP, the operation is following the rule-based controls on the TES temperature set out in Table 4.3 as shown in Figure 4.8. When the top part needs to be charged, the power output is 10kW while when the middle is charged is 7kW.

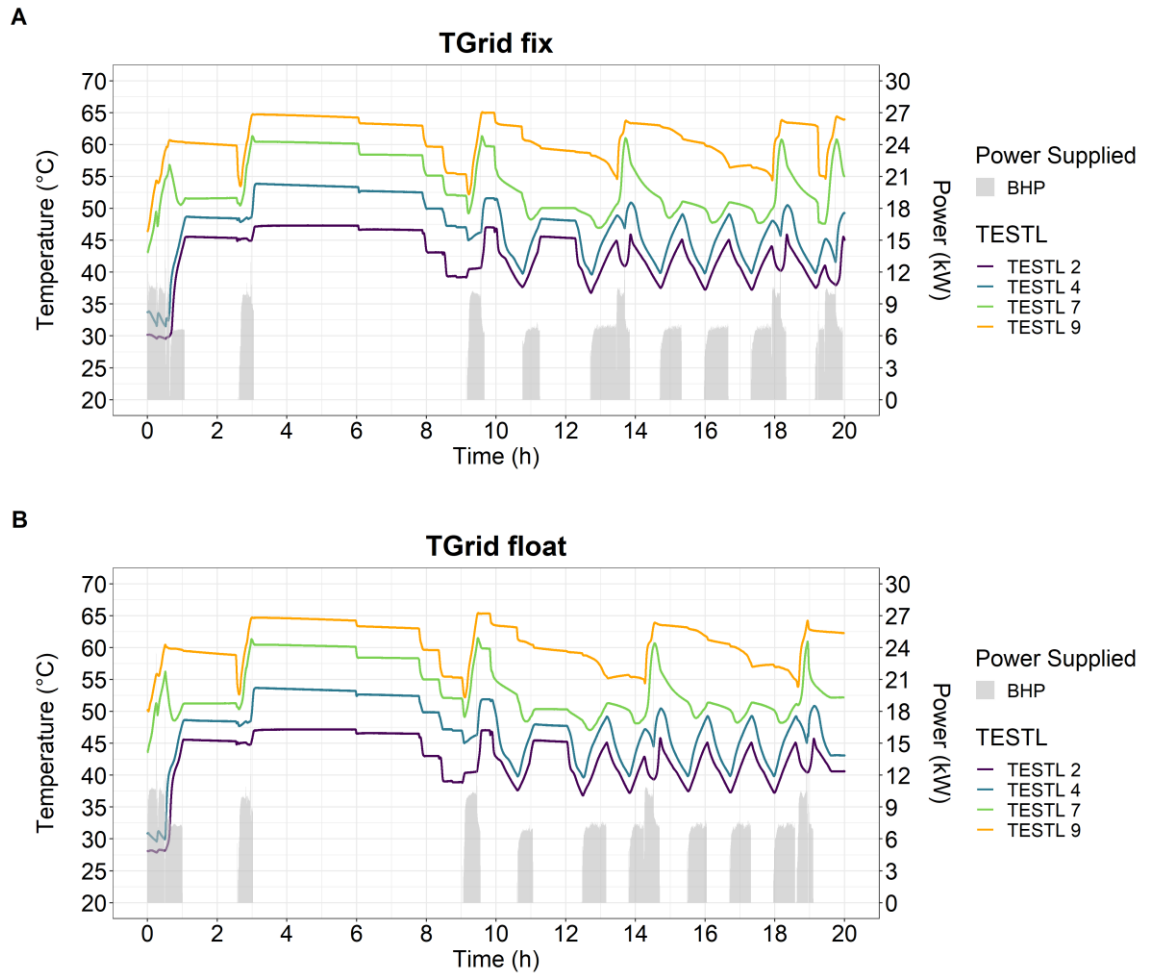


Figure 4.8: BHP operation and heating prosumer's TES temperature profile.

Finally, it is interesting to observe the operation of the BHP in terms of its energy transformation profile (electric input and thermal output) to observe the system's efficiency. These are illustrated below in Figure 4.9 along with the SCOP. The SCOP at a time (t) is defined as:

$$SCOP(t) = \frac{\sum_{i=1}^t Energy\ Thermal_i}{\sum_{i=1}^t Energy\ Electric_i} \quad (4.1)$$

The energy and SCOP values for 4-hour period brackets are also captured in Table 4.4.

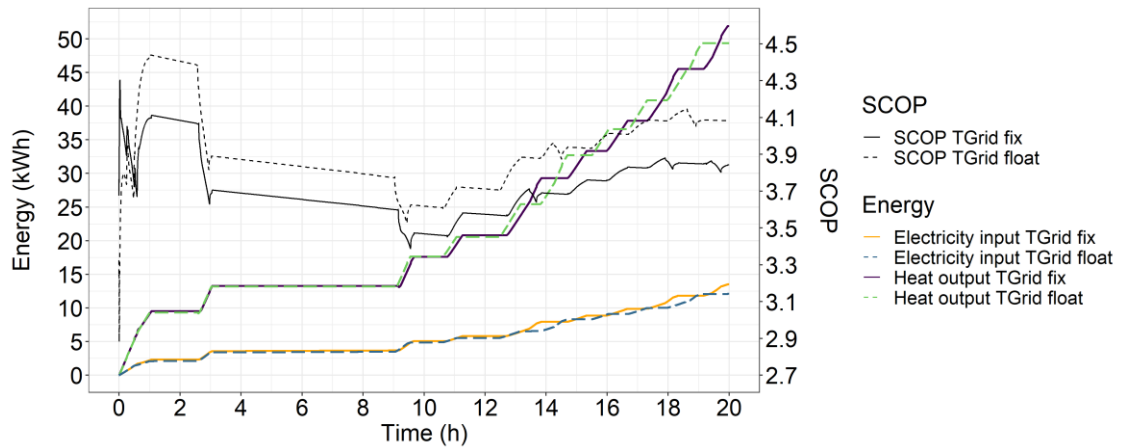


Figure 4.9: BHP energy profile.

Table 4.4: Energy and SCOP for BHP.

Period (hours)	Heating supplied (kWh)		Electricity used (kWh)		SCOP	
	$T_{GridFix}$	$T_{GridFloat}$	$T_{GridFix}$	$T_{GridFloat}$	$T_{GridFix}$	$T_{GridFloat}$
0-5	13.3	13.2	3.6	3.4	3.7	3.9
5-10	4.3	4.5	1.5	1.5	3.0	3.1
10-15	13.5	15.1	3.3	3.4	4.1	4.4
15-20	20.8	16.7	5.2	3.8	4.0	4.4
Total	51.9	49.4	13.5	12.1	3.8	4.1

The heating supplied for both cases is almost the same (4.9% difference). This variation occurs due to slight variations in the TESTL temperatures in the two experiments. For example, from hours 10 to 15, more heating needs to be supplied to the TES for $T_{GridFloat}$, while a bit more is then required from hours 15 to 20 on $T_{GridFix}$. It is expected that during an operation of multiple days, the BHP energy produced would be identical for the two control approaches.

$T_{GridFix}$ has 10.4% more electricity consumption due to the $SCOP$ being slightly higher in all periods. The $SCOP$ for 20 hours is 3.8 for $T_{GridFix}$ and 4.1 for $T_{GridFloat}$, a 5.9% difference. This difference arises from the different operation of InP_{UBHP} in the two experiments. The evaporator of the BHP has a 3.5K operational ΔT . In $T_{GridFix}$, the return temperature setpoint of 15°C and the minimum temperature at the top of the BU of 19°C mean the grid's ΔT is always higher than the BHP's evaporator ΔT . To achieve the return temperature setpoint, InP_{UBHP} must constantly mix cold water at the BHP inlet to reach an

evaporator ΔT of 3.5K, increasing its electricity consumption for the same heat output. In contrast, $T_{GridFloat}$ has no return temperature requirement eliminating the need of InPu_{BHP}'s operation.

4.5 Experimental validation

The key objective of these experiments is to validate if the proposed hydraulic design can offer control stability. To study the control stability, other than the qualitative observation of the systems' overall behaviour seen in Section 4.4, two additional methods are used. Firstly, the error between the control setpoint and the measured value for the primary pumps is investigated, using a histogram of the errors and their probability density. Secondly, a statistical analysis is conducted to compare the primary pumps' measured flow rate with the analytically expected flow rate, using the Coefficient of Determination (R^2) as the comparison metric.

4.5.1 Control errors during experiment

For the primary pump control, it's important to study the error between the setpoint and the measured value. The measured values and setpoints for the heating and cooling prosumer along with a histogram of the errors and their probability density are described below. A bin width of 1 is used for the histograms.

Figure 4.10 shows the outputs for $T_{GridFix}$. The histograms include an error count (number of data points in each bin) as well as the data probability density of the errors. For the heating prosumer in plot (A), there is a small deviation from the setpoint of 15°C. Plot (B) shows that most errors are centred at 0%, between -5% and 5%. There is a tail with some errors reaching +70% but these are less than 50 counts (less than 0.01 error density). These errors are happening when the BHP modulation changes, where for some seconds the PI controllers are overshooting before converging at the target value. A detail of this behaviour is shown in Figure 4.11, highlighting the overshoot during modulation change (0%-60% before 12.8h and 60% to 40% around 13.7h) as well as the variations around the setpoint during normal BHP operation.

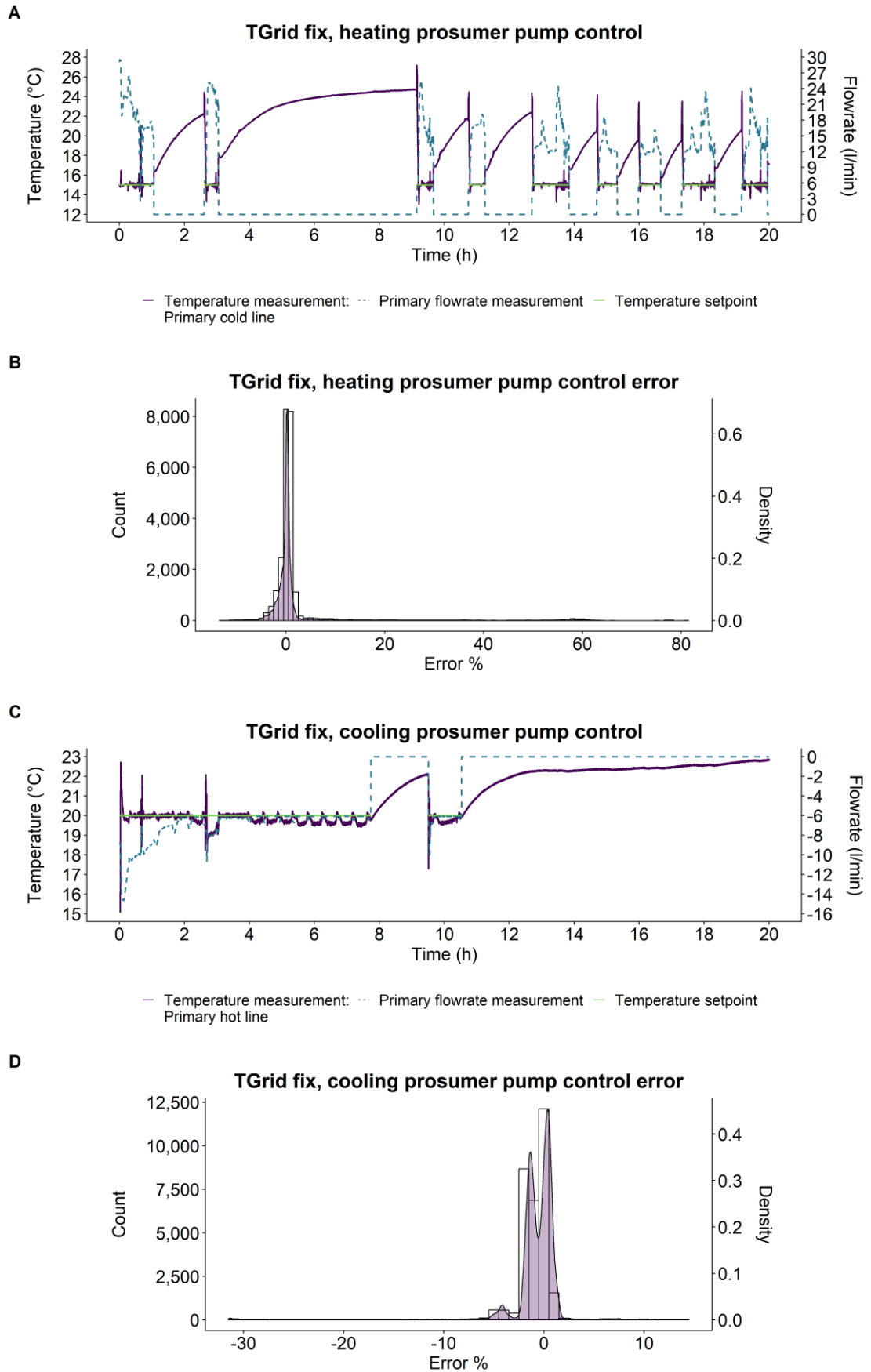


Figure 4.10: Pump control setpoints and measurements for $T_{GridFix}$.

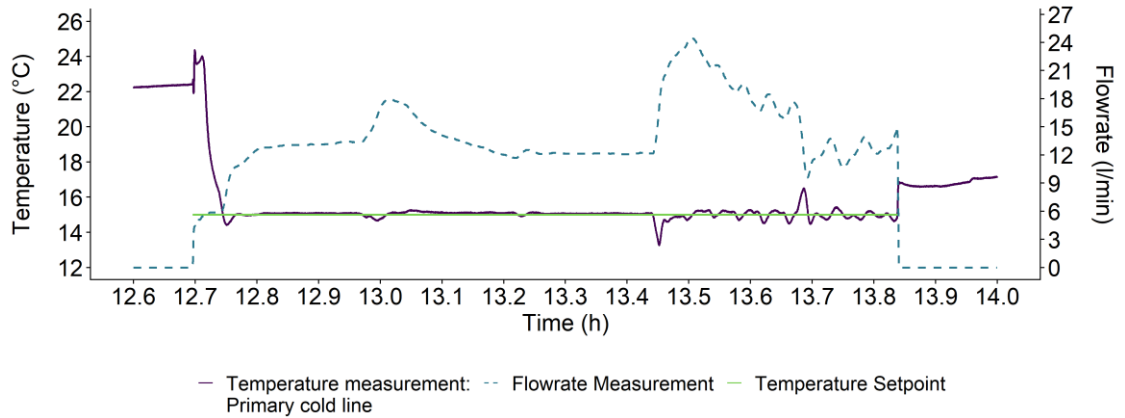


Figure 4.11: Pump control setpoints and measurements for $T_{GridFix}$, detail on BHP operation.

For the cooling prosumer in Figure 4.10, plot (C) shows how closely the setpoint of 20°C is followed. Plot (D) quantifies these errors, with most errors centred at 0%, once again between -5% and 5%. Since there is only one start for the cooling prosumer happening a bit before the 10th hour, there is only one spike of error at a bit over -30%, due to the PI controller taking some time to start. This detail is shown in Figure 4.12.

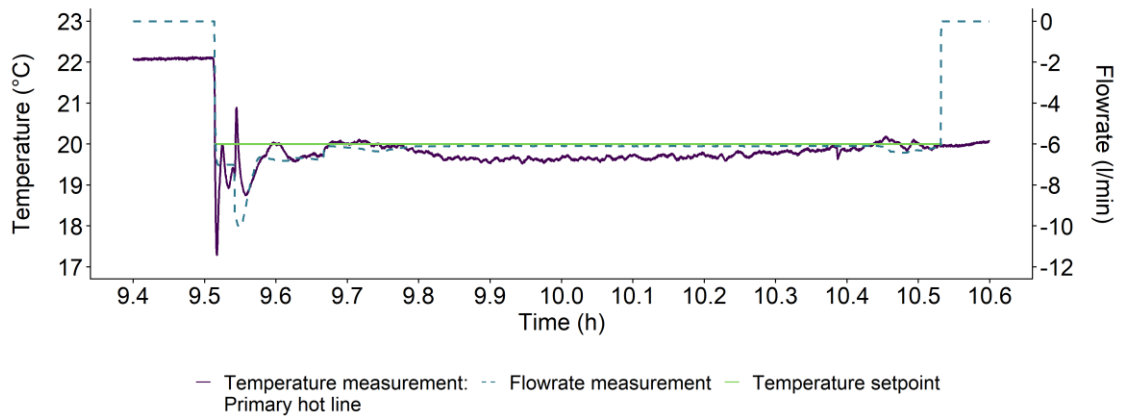


Figure 4.12: Pump control setpoints and measurements for $T_{GridFix}$, detail on HEX_{DC} operation.

The same analysis is conducted for $T_{GridFloat}$, as shown in Figure 4.13. The outputs for $T_{GridFloat}$, have greater errors than $T_{GridFix}$.

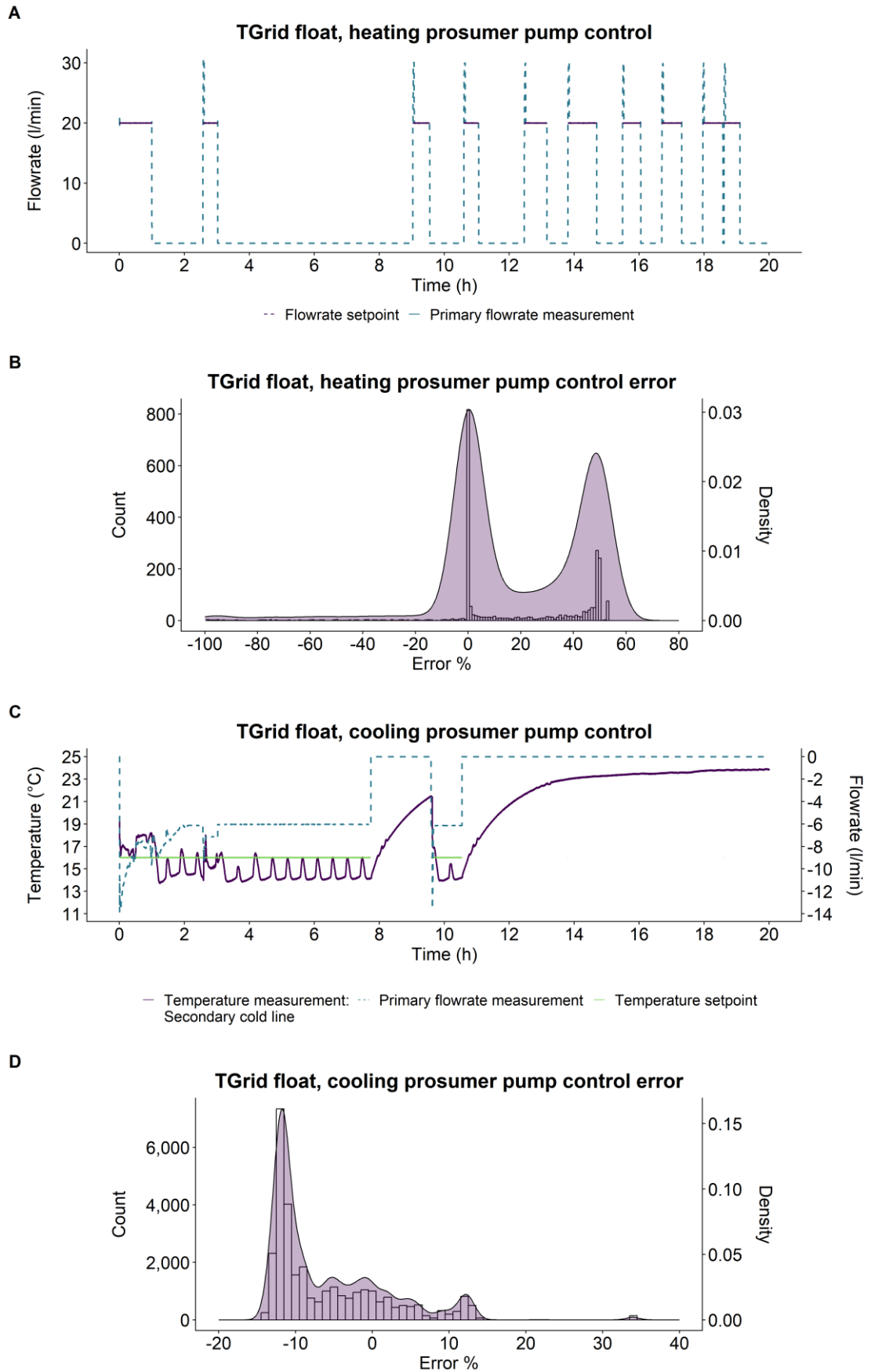


Figure 4.13: Pump control setpoints and measurements for $T_{GridFloat}$.

In Figure 4.13, Plot (A) indicates that the heating prosumer is following the setpoint with errors close to zero for most of the time. However, as plot (B) indicates, there is a considerable positive error tail, especially around 40% and 50% error. These errors occur during the startup phase of the BHP which lasts 420 seconds. During this period, there is an overshoot since the constant changes in the BHP power behaviour make controlling the flowrate challenging, with the PI controller not being able to converge the output. The detail for the BHP startup is shown below in Figure 4.14, for a startup period around the 12th hour. The negative tail reaching -100% error for a few seconds is also explained in Figure 4.15, where the slight delay of the PI controller leads to some seconds of no flow.

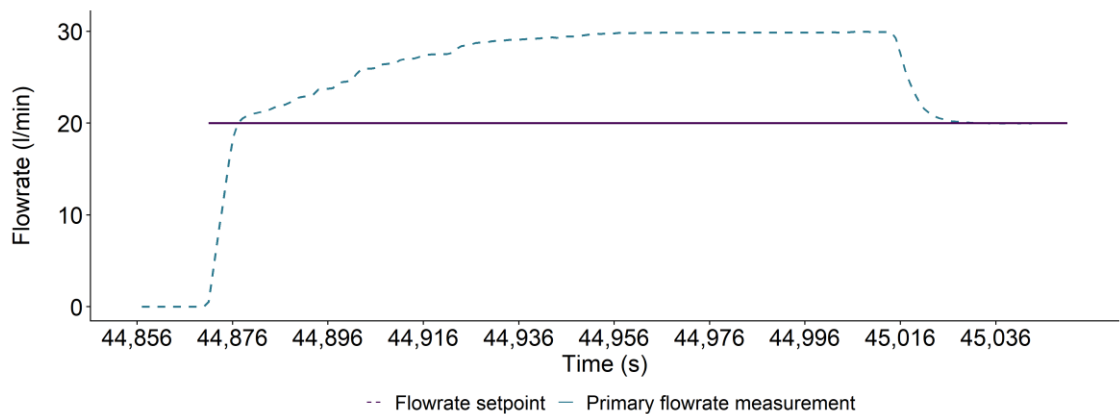


Figure 4.14: Pump control setpoints and measurements for $T_{GridFloat}$, detail on BHP startup.

For the cooling prosumer of $T_{GridFloat}$, shown in plots (C) and (D) of Figure 4.13, it is the only case where the errors' probability density is not centred around 0%. In fact, plot (D) indicates that the errors are centred around -12%, showing that for most of the time the measured temperature is lower than the setpoint. This is happening because despite having a cooling demand, it is so low that even when running at the minimum flowrate of 6l/min, not enough energy is absorbed. This leads to the control setpoint becoming obsolete and simply following the grid temperatures. Interestingly, the hours when the pump is modulating the flow are also showing an error in the measurements. The detail shown in Figure 4.15, indicates that the PI controller is responding very slowly to errors. Especially during 0.6h to 0.8h, the PI controller is not increasing the flow (from -8l/min) despite the fact that the flow temperature is much higher than the setpoint (18°C compared to 16°C setpoint). This slow response may be due to the suboptimal tuning of the PI controller.

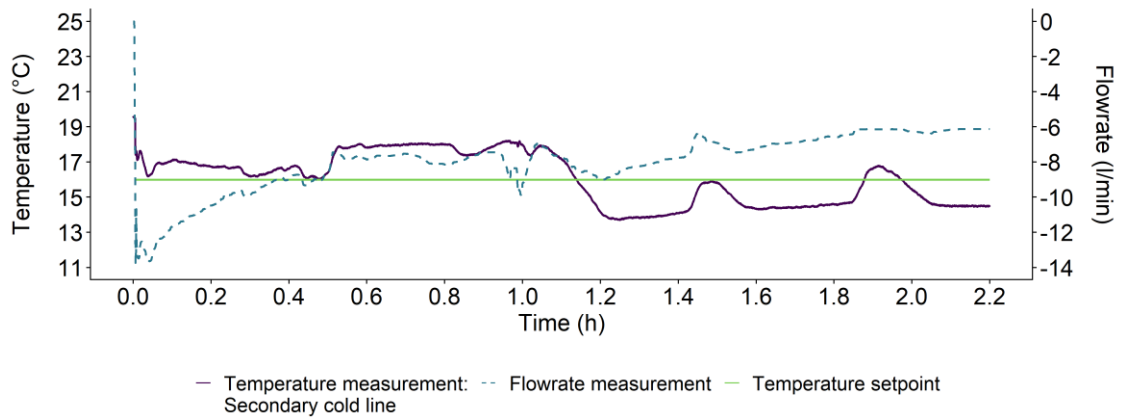


Figure 4.15: Pump control setpoints and measurements for $T_{GridFloat}$, detail of HEX_{DC} .

4.5.2 Statistical analysis of experimental measurements

A statistical analysis is finally undertaken to quantify the deviation from the analytically expected flowrate. A comparison of the experimental and calculated theoretical values is conducted using the R^2 measure [175].

4.5.2.1 Methodology for statistical analysis of experimental measurements

To obtain the theoretical flowrate that would be needed to supply the power demand in each prosumer, the heat transfer equation is used. The setpoints for temperature and flowrates in each of the control scenarios are included, with all the parameters presented schematically in Figure 4.16.

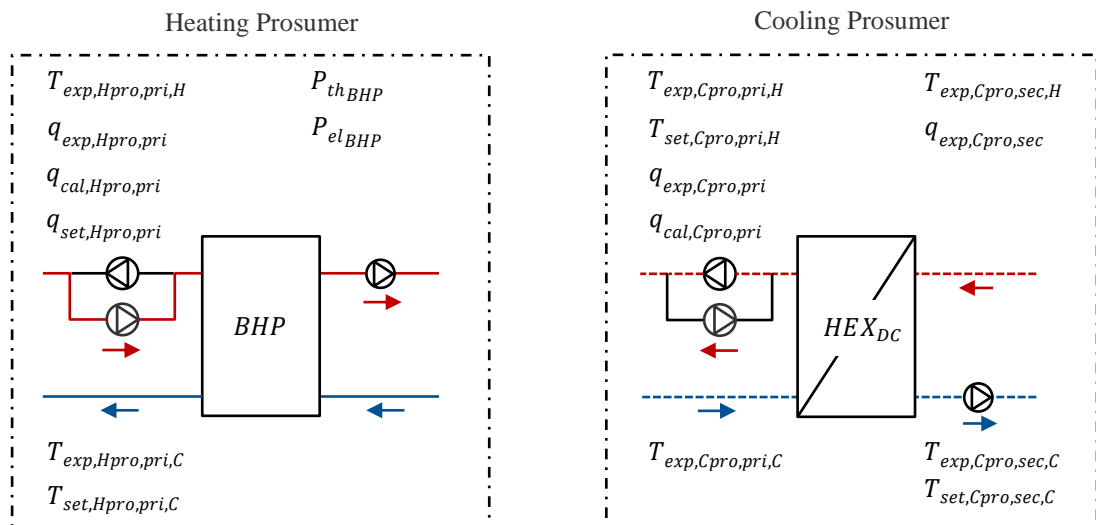


Figure 4.16: Calculation of the theoretical prosumer grid flowrate.

For the heating prosumer in $T_{GridFloat}$, the comparison is straightforward since the setpoint ($q_{set,Hpro,pri}$) can be directly compared with the measured flowrate of the prosumer's grid pump ($q_{exp,Hpro,pri}$). For $T_{GridFix}$, the theoretical flowrate can be calculated through equations (4.1) and (4.2).

$$P_{th_{cal,Hpro,pri}} = P_{th,BHP} - P_{el,BHP} \quad (4.1)$$

$$q_{cal,Hpro,pri} = \frac{P_{th_{cal,Hpro,pri}}}{c_p \rho (T_{exp,Hpro,pri,H} - T_{set,Hpro,pri,C})} \quad (4.2)$$

The power supplied by the grid ($P_{th_{cal,Hpro,pri}}$) is determined by subtracting the BHP's input electric power ($P_{el,BHP}$) from its output thermal power ($P_{th,BHP}$). Then the theoretical flowrate ($q_{cal,Hpro,pri}$) can be determined.

For the cooling prosumer, equations (4.3) to (4.5) show the methodology used for $T_{GridFix}$:

$$P_{th_{cal,Cpro,sec}} = q_{exp,Cpro,sec} c_p \rho (T_{exp,Cpro,sec,H} - T_{exp,Cpro,sec,C}) \quad (4.3)$$

$$P_{th_{cal,Cpro,sec}} = n_{HEX} P_{th_{cal,Cpro,pri}} \quad (4.4)$$

$$q_{cal,Cpro,pri} = \frac{P_{th_{cal,Cpro,pri}}}{c_p \rho (T_{set,Cpro,pri,H} - T_{exp,Cpro,pri,C})} \quad (4.5)$$

where, for $T_{GridFix}$ the power supplied to the cooling load in the experiment ($P_{th_{cal,Cpro,sec}}$) needs to be determined from the measured flow through the prosumer ($q_{exp,Cpro,sec}$) and the measured temperature difference ($T_{exp,Cpro,sec,H} - T_{exp,Cpro,sec,C}$). Then by applying the HEX_{DC} efficiency (n_{HEX}), the theoretical power supplied by the grid is found ($P_{th_{cal,Cpro,pri}}$). The theoretical primary flowrate ($q_{cal,Cpro,pri}$) can be found by applying the temperature setpoint for the return temperature ($T_{set,Cpro,pri,H}$).

For the cooling prosumer in $T_{GridFloat}$ a similar approach is taken, as shown in equations (4.6) to (4.8):

$$P_{th_{cal,Cpro,sec}} = q_{exp,Cpro,sec} c_p \rho (T_{set,Cpro,sec,H} - T_{exp,Cpro,sec,C}) \quad (4.6)$$

$$P_{th_{cal,Cpro,sec}} = n_{HEX} P_{th_{cal,Cpro,pri}} \quad (4.7)$$

$$q_{cal,Cpro,pri} = \frac{P_{th_{cal,Cpro,pri}}}{c_p \rho (T_{exp,Cpro,pri,H} - T_{exp,Cpro,pri,C})} \quad (4.8)$$

where the setpoint is on the flow temperature to the cooling prosumer ($T_{set,Cpro,sec,H}$), and the actual return temperature in the grid ($T_{exp,Cpro,pri,H}$) is used. This way, the theoretical primary flowrate ($q_{cal,Cpro,pri}$) can be determined.

4.5.2.2 Results of statistical analysis of experimental measurements

For the heating in $T_{GridFix}$ and the cooling prosumer in $T_{GridFloat}$, there are some points where the theoretical flowrate is reaching unreasonable values, causing low R^2 values (0.74 and 0.12 respectively). For the heating prosumer in $T_{GridFix}$ it is due to the ramp down of the BHP (478 timesteps out of 72,000) showing a very low electricity input for a high thermal output. For the cooling prosumer in $T_{GridFloat}$, it occurred at startups of cooling demand (38 timesteps out of 72,000), due to the temperature difference between the hot and cold grid lines being close to zero since there is no flow. The adjusted R^2 values, excluding these points, are shown in Figure 4.17, while the experimental and adjusted theoretical flowrates are found in Table 4.5. The high R^2 values (all above 90%) along with the graphs clearly indicate that no control instability is present.

Table 4.5: R^2 values for experimental accuracy (values with an asterisk (*) next to them have been adjusted).

Category	R^2
Heating Prosumer $T_{GridFix}$	90%*
Cooling Prosumer $T_{GridFix}$	93%
Heating Prosumer $T_{GridFloat}$	96%
Cooling Prosumer $T_{GridFloat}$	90%*

4.6 Discussion of experimental findings

This section delves into a thorough discussion of the results comparing the two control approaches and discussing the generalisability of the findings and considerations for applications on larger grids.

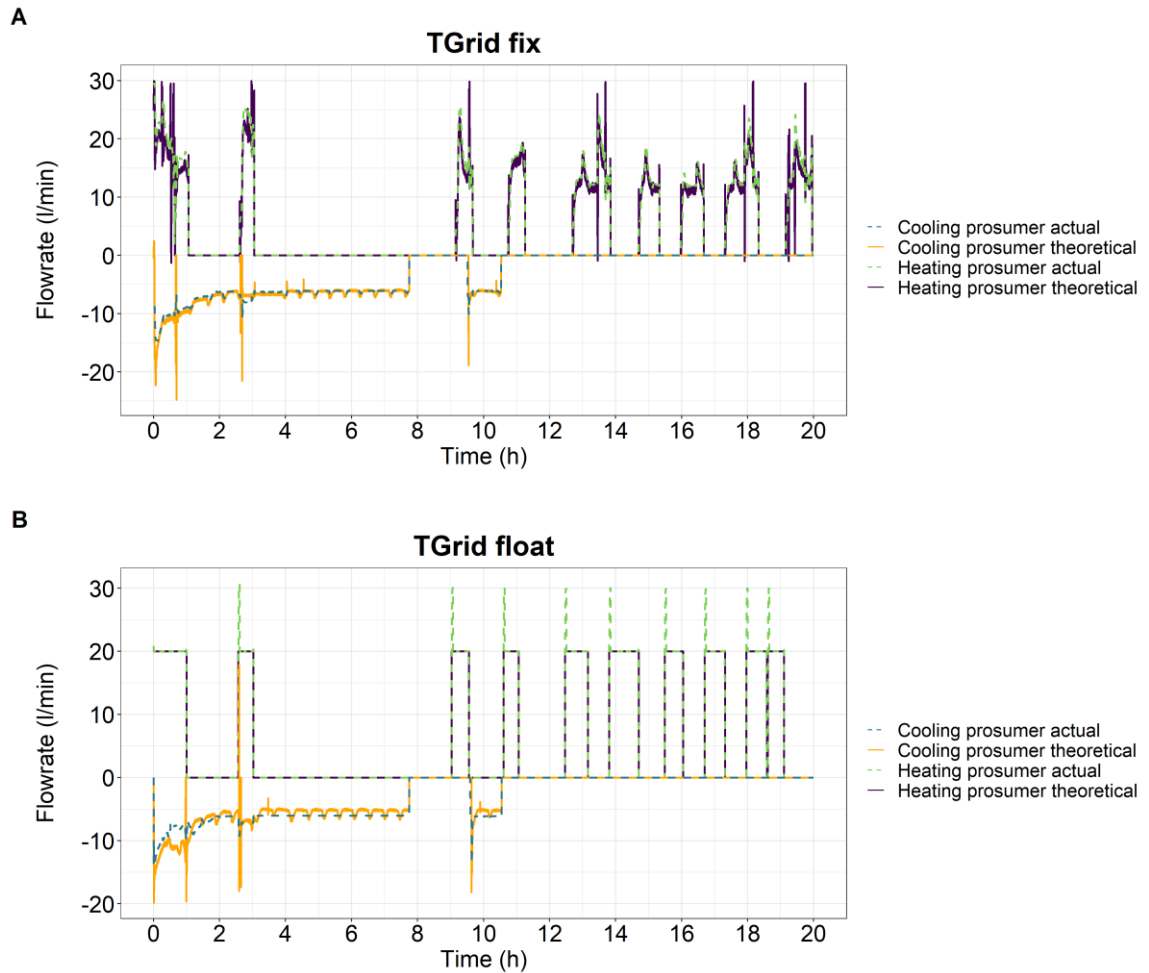


Figure 4.17: Experimental and adjusted theoretical flowrates of prosumers' grid pumps.

4.6.1 Key findings and control approach comparison

Both experiments highlight that the hydraulic design of decentralised pumps with a passive BU can allow for bidirectional operation of 5GDHC networks without hydraulic instabilities occurring due to pump hunting.

For $T_{GridFix}$, the return temperature can be controlled to a given setpoint while for $T_{GridFloat}$ the grid temperature freely floats based on the power requirements of the individual prosumers. This unpredictable variation of the return temperature for $T_{GridFloat}$ could lead to problems with prosumers down the line since it could directly affect their inlet temperatures and thus compromise their efficiency or even their operation. Furthermore, $T_{GridFix}$ could facilitate maximised operation of HEX_{DC} since the cold line grid temperature is constant, unlike $T_{GridFloat}$ where active cooling with the BHP could be required. HEX_{DC} should always be preferred to BHP as it requires no electricity input,

reducing energy use and costs [66]. From a business model standpoint, $T_{GridFix}$ could further lead to easier billability since the fixed grid temperatures and thus inlet temperatures for the BHPs allow for smaller deviations from the nominal COP. Having a controlled temperature spread can also allow for different temperature setpoints during different periods of operation, allowing for system efficiency optimisation as the one presented in Wirtz et al. (2021) [148] with small complexity.

As mentioned in the hypothesis, the BHP's SCOP for $T_{GridFloat}$ is higher than $T_{GridFix}$ due to the operation of InPu_{BHP}, causing mixing at the BHP inlet flow to ensure a fixed return temperature. This highlights that if the system is not designed correctly in $T_{GridFix}$, with the network and BHP's evaporator ΔT not matching, higher electricity uses might be present. Therefore, $T_{GridFix}$ can offer better predictability of operation but is more sensitive to variations on the network temperatures. An incorrect sizing of the evaporator/condenser of the BHP would lead to the internal pump constantly being in use, increasing electricity consumption as shown in the experiment. It can thus be argued that $T_{GridFloat}$ allows for more flexibility on the prosumer energy transformation assets.

The ASHP in the BU had multiple starts to balance the ambient grid. The small temperature difference in the network led to small control bands for the TES for both heating (19°C to 22°C at the top of the TES) and cooling (13°C to 15°C at the bottom of the TES). A better designed and sized energy supply system configuration for the BU could lead to a smoother temperature profile at the top and bottom, improving system performance. Furthermore, introducing more complex controls such as MPC or other demand response controllers could further optimise the ASHP and BHP operation [112].

4.6.2 Generalisability and considerations for larger applications

This experimental validation acts as a proof-of-concept for the proposed hydraulic design and control strategies. However, the setup's small network size, power requirements and number of prosumers may impact the system's behaviour on larger applications. The generalisability of the findings and considerations for larger applications are discussed below.

The small flows in the network (less than 30l/min) lead to a small thermal inertia compared to large networks where flows can be multiple times higher. Having controls on individual substation level, on either the return temperature or the flowrate, the larger thermal inertia is not expected to impact the control behaviour negatively. Furthermore, another source of instability are pressure variations. Since pressure variations travel at the speed of sound, the length of the network is not impacting their effect on the decentralised pumps, therefore their effect on control stability is not expected to change for larger applications.

However, having two prosumers limits the possibility of studying the potential creation of hydraulic subcycles. Hydraulic subcycles form due to points of zero flow from opposing flows within the network, forming isolated loops. These subcycles can compromise the operation of prosumers' substations as they become disconnected from the central BU's influence. Despite not being able to experimentally study hydraulic subcycles for the two control approaches, a hypothesis is made based on their control characteristics. For $T_{GridFix}$, controlling on the return temperature should minimise the issue of hydraulic subcycles and supply frontier creation. Once an area of zero flow occurs, the temperature starts going up in the subcycle, which should automatically lead to a pump adjustment breaking the flow balance between the prosumers. Therefore, the centralised unit's balancing role should not be compromised for other prosumers down the network. For $T_{GridFloat}$, the flexibility of the grid's operation does not allow a clear hypothesis on its subcycle formation and is a clear field for future work.

Scaling up the proposed hydraulic design to a larger network with multiple prosumers introduces challenges related to pump sizing and network expansion. Each prosumer pump needs to be able to circulate the water to the BU if no other pump is connected. This can lead to inefficient pump operation at normal load conditions, and variation on the sizing and operation of the prosumer pumps depending on the proximity to the BU. Furthermore, having a large deviation of the number of pumps connected to the network at different points in the year, could lead to a large seasonal deviation in the system characteristic curve. This could impact the operation of some pumps, complicating the hydraulic balancing efforts for the network. This could also compromise the flexibility for future network expansion, where the introduction of new pumps may result in a different system characteristic curve regime. This could potentially impact the pump operation of existing

prosumers and impact the system's hydraulic balance. Lastly, having larger pipe lengths leads to greater pressure drops that could lead to cavitation from areas of low pressure.

Overall, it is argued that findings for both control schemes apply to larger applications since controls are independently enacted, and the impact of pressure and low flow conditions would not alter for larger applications. However, there are questions on pump behaviour when multiple prosumers are present, or when a new load is introduced that was not accounted for in the initial balancing of the system. The scalability of the design is therefore not clear and is important to explore these issues before implementing the proposed design on large scale applications.

Following the successful experimental validation of the proposed design and operational philosophies for 5GDHC, the simulation models capturing them as detailed in Section 3.3 must be experimentally validated. Chapter 5 presents a digital twin of the experiment and uses it to analyse the accuracy of the developed Modelica models by comparing their outputs to the experimental findings.

5 Experimental Validation of 5GDHC Modelica Models

The methodology followed for comparing model outputs with experimental data is discussed in this chapter, building a digital twin progressively from basic hydraulic elements to the full digital twin of the experiment in four stages. This way, the level of inaccuracy each Modelica component adds can be studied. The validation results for all four stages are presented, along with a discussion of their accuracy and limitations. The complete digital twin is shown in Figure 5.1.

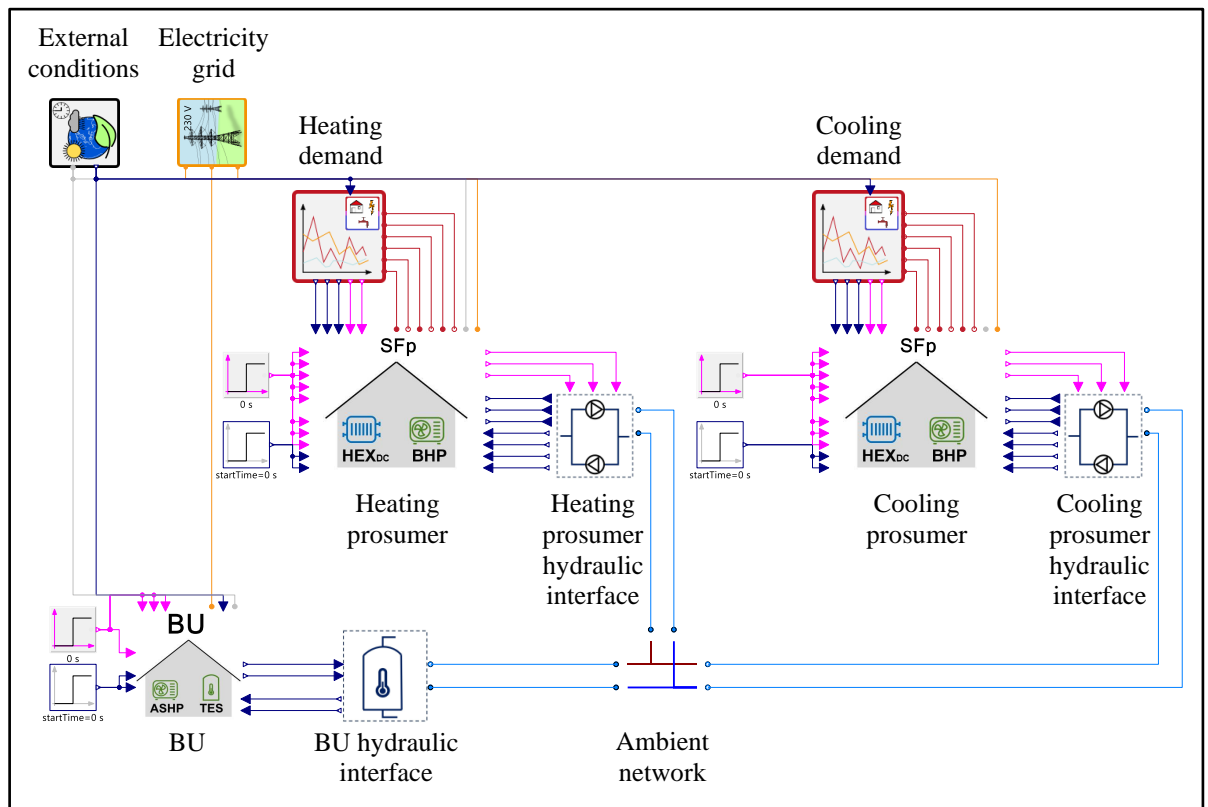


Figure 5.1: Modelica digital twin of the experiment.

Additional to the data types referenced in the previous section in Table 4.1, simulation data types are also present in this section. The Subscript 1: Data Type category has thus one additional type, *sim* for simulation outputs.

5.1 5GDHC simulation models validation methodology

To validate the developed Modelica components, a comparison of the experimental and model outputs is conducted using the R^2 methodology, same as for the experimental validation. The validation is conducted in steps, adding Modelica components to reach a full digital twin of the experiment for both $T_{GridFix}$ and $T_{GridFloat}$. This way, the impact of each Modelica component on overall accuracy can be studied. A schematic of the steps leading to developing the full digital twin is shown in Figure 5.2. Table 5.1 includes a description of each validation step; the components used; the experimental data used as inputs; and the model outputs used as validation parameters.

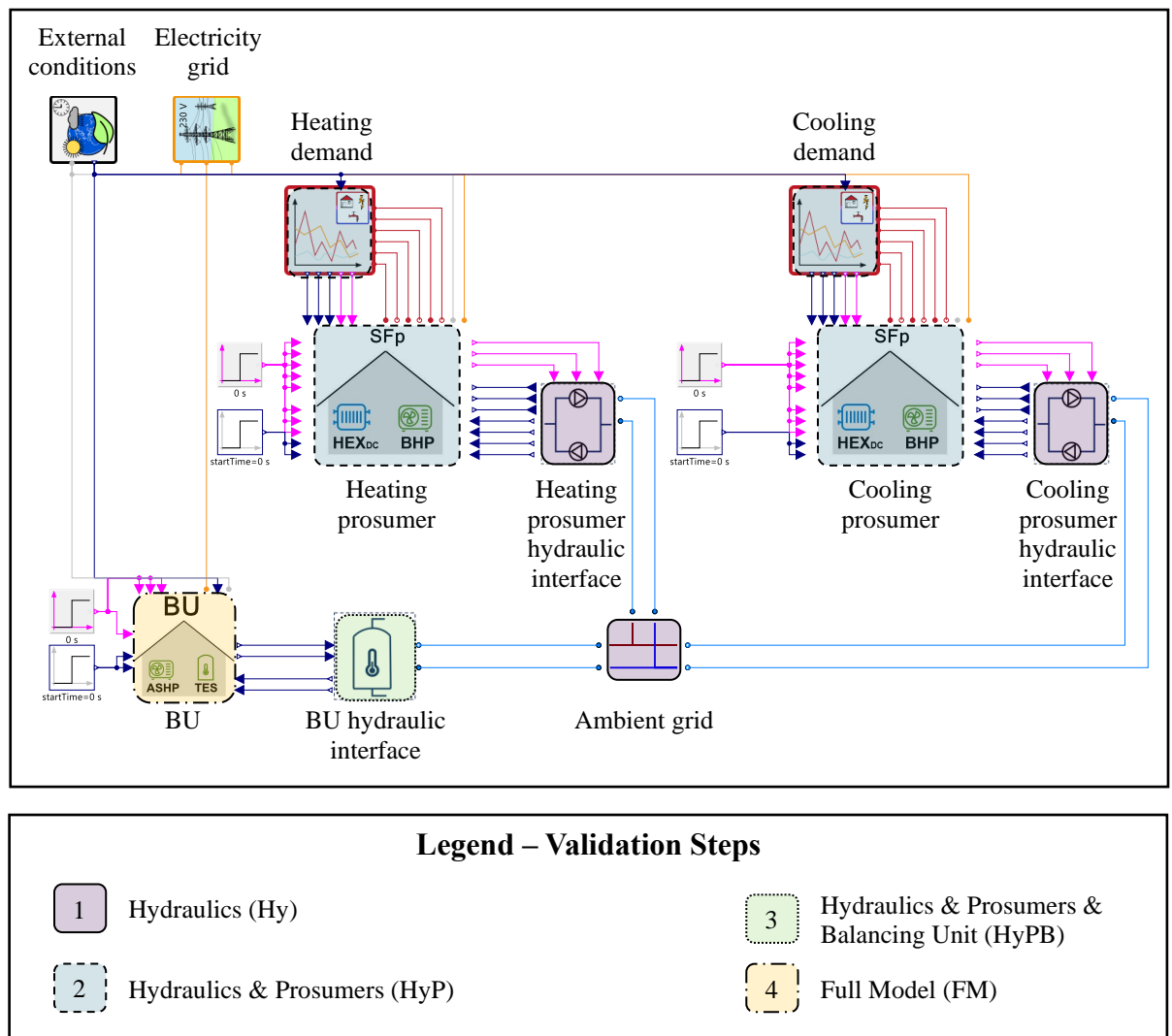


Figure 5.2: Schematic of validation steps.

Table 5.1: Validation steps description.

Step	Name	Description	Modelica Components	Experimental Data Inputs	Validation Parameters
1	Hydraulics (Hy)	Focus on hydraulic interfaces for prosumers and BU. Test the hydraulic interfaces.	Hydraulic Interface Prosumer, Hydraulic Interface BU, Ambient grid.	BU top and bottom temperatures, Calculated power consumed at BHP evaporator and HEX _{DC} .	Flowrates of prosumer grid pumps.
2	Hydraulics & Prosumers (HyP)	Step Hy & prosumer thermal components with set power setpoints for the BHP. Test prosumer model.	Hydraulic Interface Prosumer, Hydraulic Interface BU, Ambient grid, Prosumer, Demand.	BU top and bottom temperatures, Power setpoint for BHP, Heating/cooling Demand for prosumers.	Flowrates of prosumer grid pumps.
3	Hydraulics & Prosumers & BU (HyPB)	Step HyP & BU model. The BU model has the power supplied by the ASHP. Test BU's TES.	Hydraulic Interface Prosumer, Hydraulic Interface BU, Ambient grid, Prosumer, Demand, BU.	Power setpoint for BHP, Power from ASHP, Heating/cooling Demand for prosumers.	Flowrates of prosumer grid pumps.
4	Full Model (FM)	All components without power setpoints, only prosumer demands.	Hydraulic Interface Prosumer, Hydraulic Interface BU, Ambient grid, Prosumer, BU.	Demand [W] at prosumers.	Energy profile of BHP and ASHP (heating, cooling and electricity).

As it can be seen from Table 5.1, each validation step has a bespoke methodology, with different inputs and outputs to best capture the impact on the model's accuracy. In

addition, since in each level different components are added, there needs to be a parameterisation to ensure the digital twin is best capturing the system's characteristics. The following sections describe the methodology followed for validating each step along with the respective component parameterisation.

5.1.1 Hydraulics (Hy)

For the first validation step, the hydraulic interfaces and the grid are modelled. The model includes the hydraulic interfaces and grid models while the temperatures from the BU are used as direct inputs. Since the cutoff point is the HEX_{DC} and the BHP evaporator for the heating and cooling prosumer respectively, the demand needs to be calculated at that point. The model used is shown below in Figure 5.3.

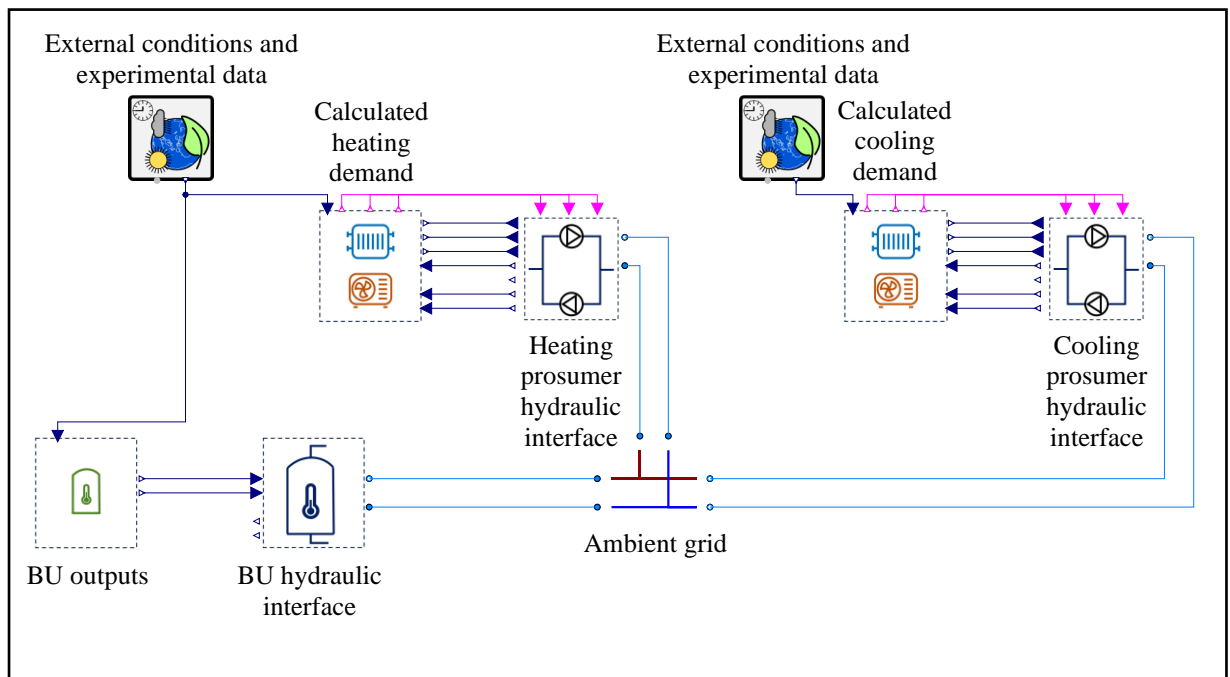


Figure 5.3: Hy validation step Modelica simulation model.

The validation parameter is the flowrate of the prosumer pumps. To make a meaningful comparison, the same power flows from the HEX_{DC} and the BHP evaporator with the grid need to be set, but at the same time ensuring the control variables for the simulation (return grid temperatures and cooling flow temperature) are influenced by changes of the validation parameter (flowrate). The relationship of the experimental and simulated

variables is explained in the following equations along with a representation in the schematic of Figure 5.4. The variable subscripts follow the convention set out in Table 4.1.

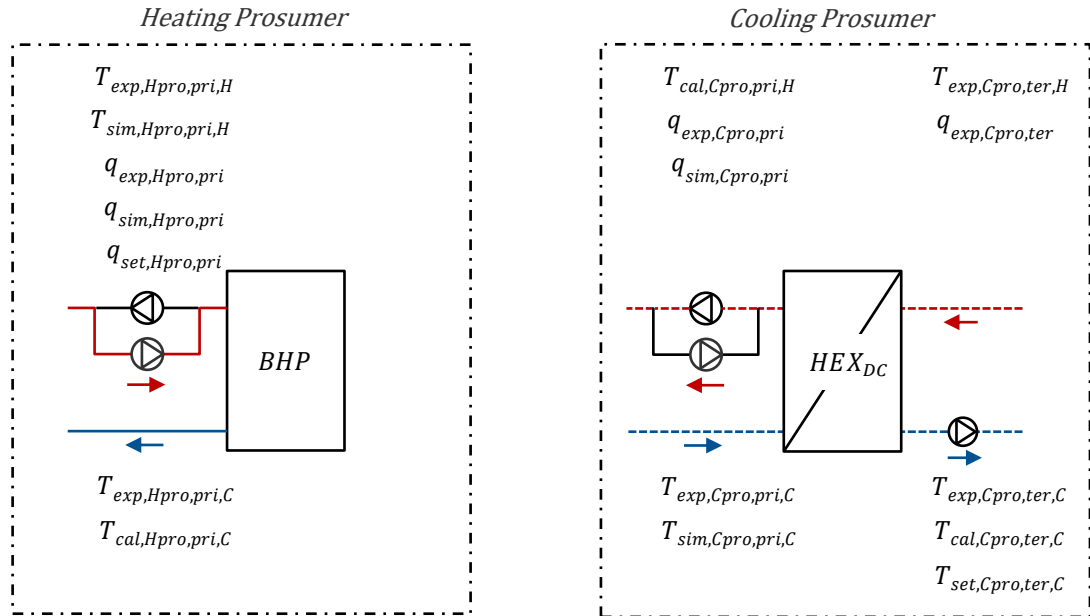


Figure 5.4: Schematic for step Hy validation variables.

For the heating prosumer in $T_{GridFloat}$, the comparison is straightforward since the setpoint ($q_{set,Hpro,pri}$) is the same for both the simulation and the experiment, so the experimental ($q_{exp,Hpro,pri}$) and simulation ($q_{sim,Hpro,pri}$) flowrates can directly be compared. For $T_{GridFix}$, the return temperature on the grid (cold pipe) that is the control variable for the PI controller of the pump, is calculated from a combination of simulation and experimental values as shown in equations (5.1) and (5.2):

$$P_{th,cal,Hpro,pri} = c_p \rho q_{exp,Hpro,pri} (T_{exp,Hpro,pri,H} - T_{exp,Hpro,pri,C}) \quad (5.1)$$

$$T_{cal,Hpro,pri,C} = \frac{P_{th,cal,Hpro,pri}}{c_p \rho q_{sim,Hpro,pri}} + T_{sim,Hpro,pri,H} \quad (5.2)$$

where the temperature on the grid's cold pipe ($T_{cal,Hpro,pri,C}$) is calculated from the experimental power supplied to the BHP's evaporator ($P_{th,cal,Hpro,pri}$) and the simulation flowrate ($q_{sim,Hpro,pri}$) in each time step.

For the cooling prosumer, for $T_{GridFix}$, the same methodology for calculating the return temperature based on the experimental power and the simulation flowrate is used, shown in equations (5.3) and (5.4):

$$P_{th_{cal,Cpro,pri}} = c_p \rho q_{exp,Cpro,pri} (T_{exp,Cpro,pri,H} - T_{exp,Cpro,pri,C}) \quad (5.3)$$

$$T_{cal,Cpro,pri,H} = \frac{P_{th_{cal,Cpro,pri}}}{c_p \rho q_{sim,Cpro,pri}} - T_{sim,Cpro,pri,C} \quad (5.4)$$

where the temperature on the grid's hot pipe ($T_{cal,Cpro,pri,H}$) is calculated from the experimental power supplied to the HEX_{DC} ($P_{th_{cal,Cpro,pri}}$) and the simulation flowrate ($q_{sim,Cpro,pri}$) in each time step.

For the cooling prosumer for $T_{GridFloat}$, the primary side's flowrate ($q_{sim,Cpro,pri}$) is affecting the tertiary flow temperature ($T_{sim,Cpro,ter,C}$) which is the control parameter for the primary pump's PI controller. To calculate the return temperatures on either side of the HEX, namely $T_{cal,Cpro,pri,H}$ for the primary side and $T_{cal,Cpro,ter,H}$ for the tertiary, a set of equations from the HEX principles of operation are used [176]. The following equations (5.5) to (5.10) capture these relationships, which are thoroughly derived from first principles in Spakovszky (2023) [176]:

$$\beta_{pri} = q_{sim,Cpro,pri} c_p \rho \quad (5.5)$$

$$\beta_{ter} = q_{exp,Cpro,ter} c_p \rho \quad (5.6)$$

$$\alpha = h_o A_{HEX} \left(\frac{1}{\beta_{pri}} - \frac{1}{\beta_{ter}} \right) \quad (5.7)$$

$$n = \frac{1 - e^{-\alpha}}{1 - \frac{\beta_{pri}}{\beta_{ter}} e^{-\alpha}} \quad (5.8)$$

$$T_{cal,Cpro,pri,H} = T_{sim,Cpro,pri,C} - n_{HEX} (T_{sim,Cpro,pri,C} - T_{exp,Cpro,ter,C}) \quad (5.9)$$

$$T_{cal,Cpro,ter,H} = T_{exp,Cpro,ter,C} + \frac{\beta_{pri}}{\beta_{ter}} (T_{sim,Cpro,pri,C} - T_{cal,Cpro,pri,H}) \quad (5.10)$$

where the simulated primary flowrate ($q_{sim,Cpro,pri}$) and experimental tertiary flowrate ($q_{exp,Cpro,ter} c_p \rho$) help calculate two parameters β_{pri} and β_{ter} respectively. The parameter α then relates them with the overall heat transfer coefficient of water (h_o) and the HEX

surface area (A_{HEX}). For the parameter known values, h_o is $5,000\text{W/m}^2\text{K}$ and A_{HEX} is 1m^2 . The efficiency of the counterflow HEX (n_{HEX}) can then be expressed as a function of the parameters α , β_{pri} and β_{ter} . Having established n_{HEX} , the return temperatures for both primary ($T_{cal,Cpro,pri,H}$) and tertiary side ($T_{cal,Cpro,ter,H}$) can be calculated.

Following the methodology for validating the model components, it's crucial to parametrise these components and ensure that the characteristics of the physical elements are replicated as closely as possible in the modelling sphere.

The details of the grid need to be captured, including lengths and elements of hydraulic resistance. In addition, the pumps and pipe characteristics need to be replicated. The medium properties must also be set as well as the system's pressure and environmental temperature. A schematic of the experimental setup is shown in Figure 5.5, with numbers indicating the different pipe sections of interest.

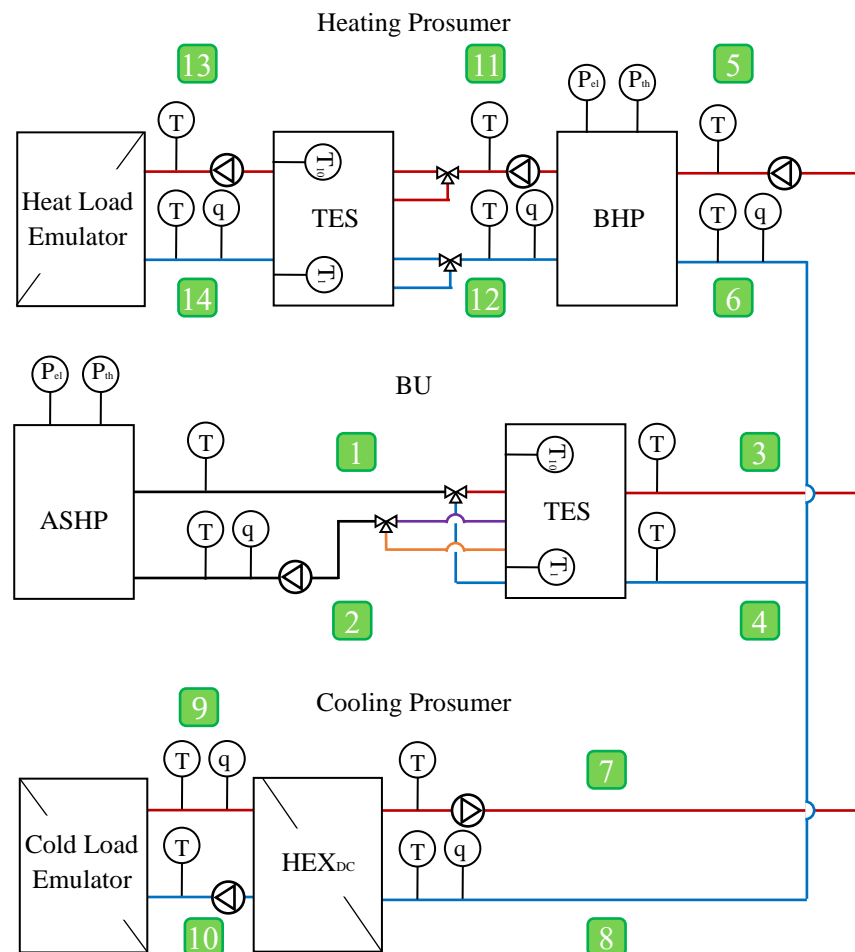


Figure 5.5: Schematic of the experimental setup with numbers for pipe sections of interest.

The hydraulic components represent pipe sections 3-8, since all the other pipe sections are captured in components where transient fluid behaviour is neglected as discussed in Section 3.3.5. The measured pipe lengths and elements of hydraulic resistance are shown below in Table 5.2 and Table 5.3 respectively, for pipe sections 3-8. The pipework lengths in Table 5.2 are split between copper and stainless-steel pipe since they each have a different roughness and pressure loss characteristics.

Table 5.2: Pipework lengths for pipe sections 3-8 from Figure 5.5.

Pipe section from Figure 5.5	Length of copper pipe (mm)	Length of stainless-steel pipe (mm)	Total pipe length (mm)
3	260	130	390
4	260	130	390
5	380	400	780
6	-	580	580
7	330	90	420
8	940	330	1,270
Total	2,170	1,660	3,830

Table 5.3: Elements of hydraulic resistance for pipe sections 3-8 from Figure 5.5.

Hydraulic resistance elements	Number of elements in each pipe segment (Figure 5.5)						
	3	4	5	6	7	8	Total
Temperature sensor	1	1	4	1	1	4	12
Pressure sensor	-	-	-	1	-	1	2
Flowrate sensor	-	-	-	1	-	2	3
Ball valve	1	1	2	2	2	3	11
Motorised valve	-	-	2	1	1	2	6
3WV	-	-	-	-	-	2	2
Isolation valve	-	-	1	-	-	2	3
HEX	-	-	2	-	-	1	3
Pump	-	-	1	-	1	-	2
Pipe connector	3	3	7	-	2	6	21
Pipe with 90° bend	3	3	15	4	5	29	59

To capture the hydraulic resistance of the various elements shown in Table 5.3, the pressure drop (Δp) is calculated using the pressure loss coefficient (ζ) through equation (5.11) [177]:

$$\Delta p = \zeta \frac{\rho}{2} q^2 \quad (5.11)$$

Therefore, for the nominal flowrate of 30l/min the following pressure drops are given in Table 5.4.

Table 5.4: Values of ζ for different hydraulic resistance elements.

Hydraulic resistance elements	Description	ζ
Temperature sensor	Electric resistance sensor. SensorShop24, PT100 [164]	None
Pressure sensor	Electric pressure sensor. DSU, DSI pressure transmitter [178]	None
Flowrate sensor	Magnetic-inductive flowmeter. Proline Promag E 100 [165]	None
Ball valve	Fully open and not modulated.	0.2 [177]
Motorised valve	Fully open in experiment.	0.2 [177]
3WV	Ball valve motorised through actuator. Actuator: AVM 105S, 115S [179].	2.4 [177]
Isolation valve	CR-Brass Bevel seat Backflow-preventer Valve, type 1431 [180].	6 [177]
HEX _{DC}	Single phase heat exchange. SWEP B80Hx20/1P [168].	Δp found in technical datasheet.
Evaporator of BHP	The evaporator is seen from the grid as a HEX. BHP model 20kW Ratiotherm WP Max-HiQ [171].	Δp found in technical datasheet.
Primary pump of heating prosumer	VSD pump with rated flowrate and head of 2.04m ³ /h and 18.01m respectively. Grundfos unit CME 1-2 A-R-G-E-AQQE S-A-D-N [172].	Δp calculated from pump curve.
Primary pump of cooling prosumer	VSD pump with rated flowrate and head of 3.31m ³ /h and 5.76m respectively. IMP Pumps unit NMT PLUS ER 25/60-180 [169].	Δp calculated from pump curve.
Pipe connector	Pipe segment connecting two pipes.	0.2 [177]
Pipe with 90° bend	Pipes with a 90° bend.	1.2 [177]

The cumulative ζ is calculated for each pipe section of interest, as shown in Table 5.5.

Table 5.5: Cumulative ζ for pipe sections 3-8 from Figure 5.5.

	Units	3	4	5	6	7	8
Cumulative ζ	-	4.4	4.4	26.2	5.4	7.0	53.8

The pipe model in Modelica includes the details for pipe losses based on the pipe diameter and velocity. The absolute roughness of pipe for the two pipe materials is 0.0025mm for the copper and 0.025mm for the corrugated stainless steel pipes [87]. The pumps' characteristic curves used are shown in Figure 5.6 and Figure 5.7.

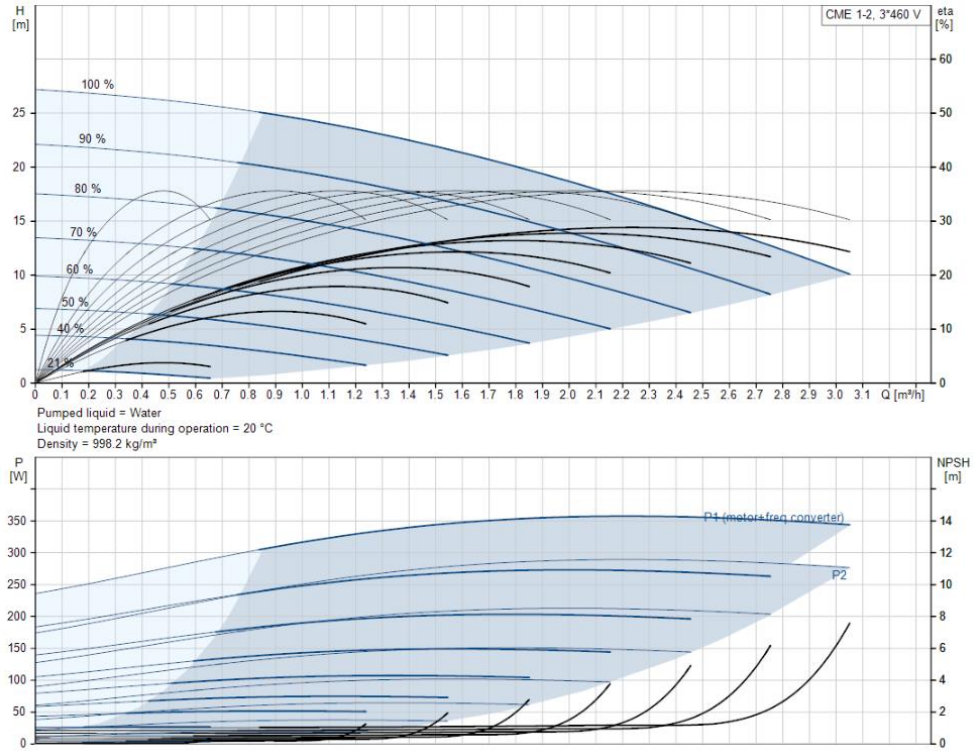


Figure 5.6: Pump curve for heating prosumer [172].

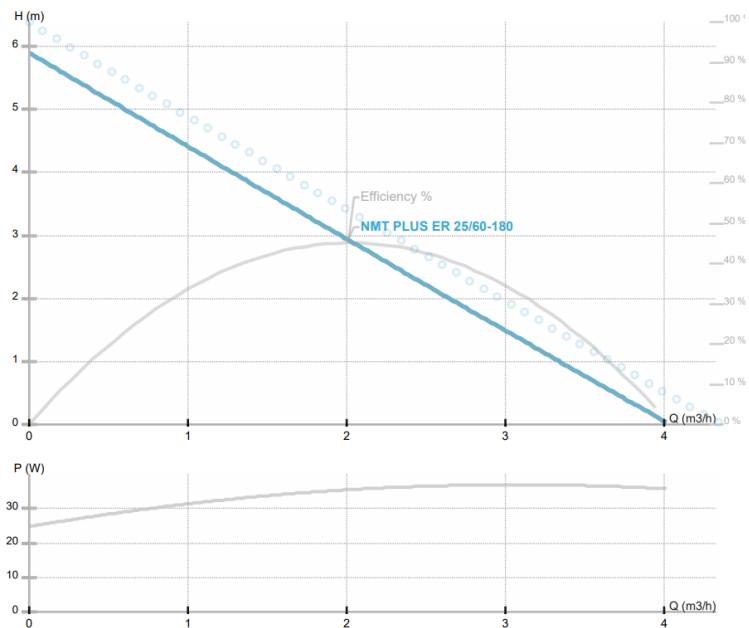


Figure 5.7: Pump curve for cooling prosumer [169].

The overall Δp per section is shown in Table 5.6. Values for pipes and pumps are outputs of the Modelica models. Since there are no active modulation valves to limit the flow, the pressure drops from elements of hydraulic resistance is low. The HEXs are the main components inducing Δp .

Table 5.6: Δp at nominal flowrate of 30l/min for pipe sections 3-8 from Figure 5.5.

	Units	3	4	5	6	7	8
Valves, sensors							
and bends.	Pa	0.15E-02	0.15E-02	0.91E-02	0.19E-02	0.24E-02	1.87E-02
HEXs.	Pa	-	-	1.30E+05	-	-	6.50E+04
Pumps	Pa	-	-	0.50E+05	-	3.00E+05	-
Pipes	Pa	0.60E+03	0.60E+03	1.00E+03	0.80E+03	0.65E+03	0.80E+03
Total Δp	Pa	6.00E+02	6.00E+02	1.81E+05	8.00E+02	3.01E+05	6.58E+04

For both experiments, the pressure rating in the primary network is 2bar while the ambient temperature is 22°C. Water with standard properties is used as the medium, following Modelica standard library components.

Finally, having arranged the models to mirror reality, the PI controllers of the grid pumps need to be tuned. The empirical method is used for tuning the PI controllers, similar to the tuning of the physical equipment in the experiment discussed in Section 4.2. The PI values for the experiment and the simulation models are different since they model an idealised component without sensor noise or errors that affect the system's response. The PI controller parameters used are shown below in Table 5.7 for both the experiment and the simulation models.

Table 5.7: PI controller parameters for simulation and experiment.

Experiment	Prosumer	Simulation values		Experimental values	
		Proportional Gain	Integral Time (min)	Proportional Gain	Integral Time (min)
$T_{GridFix}$	Heating	0.34	0.67	0.035	0.012
	Cooling	0.34	0.67	0.1	0.05
$T_{GridFloat}$	Heating	1500	0.17	0.05	0.01
	Cooling	1	0.17	0.2	0.03

A key issue that may arise is that the model is validated against experimental values, not theoretical setpoints. Therefore, errors in the experimental measurements from PI controller inaccuracies will have an impact on the R^2 value. This will be specifically

problematic for the case of the cooling prosumer in $T_{GridFloat}$. As discussed in the experimental results in Section 4.5.1 and shown in Figure 4.15, the PI controller in the experiment is not very responsive. It is thus expected to observe larger errors in $T_{GridFloat}$.

5.1.2 Hydraulics & Prosumers (HyP)

The next step is to add the prosumer models with the actual heating/cooling demands from the buildings. The prosumer models include the BHP and TES for the heating prosumer and the HEX_{DC} for the cooling prosumer along with secondary and tertiary pumping where present. The demands are modelled separately, capturing the actual power flows from the experiment. The model used is shown in Figure 5.8.

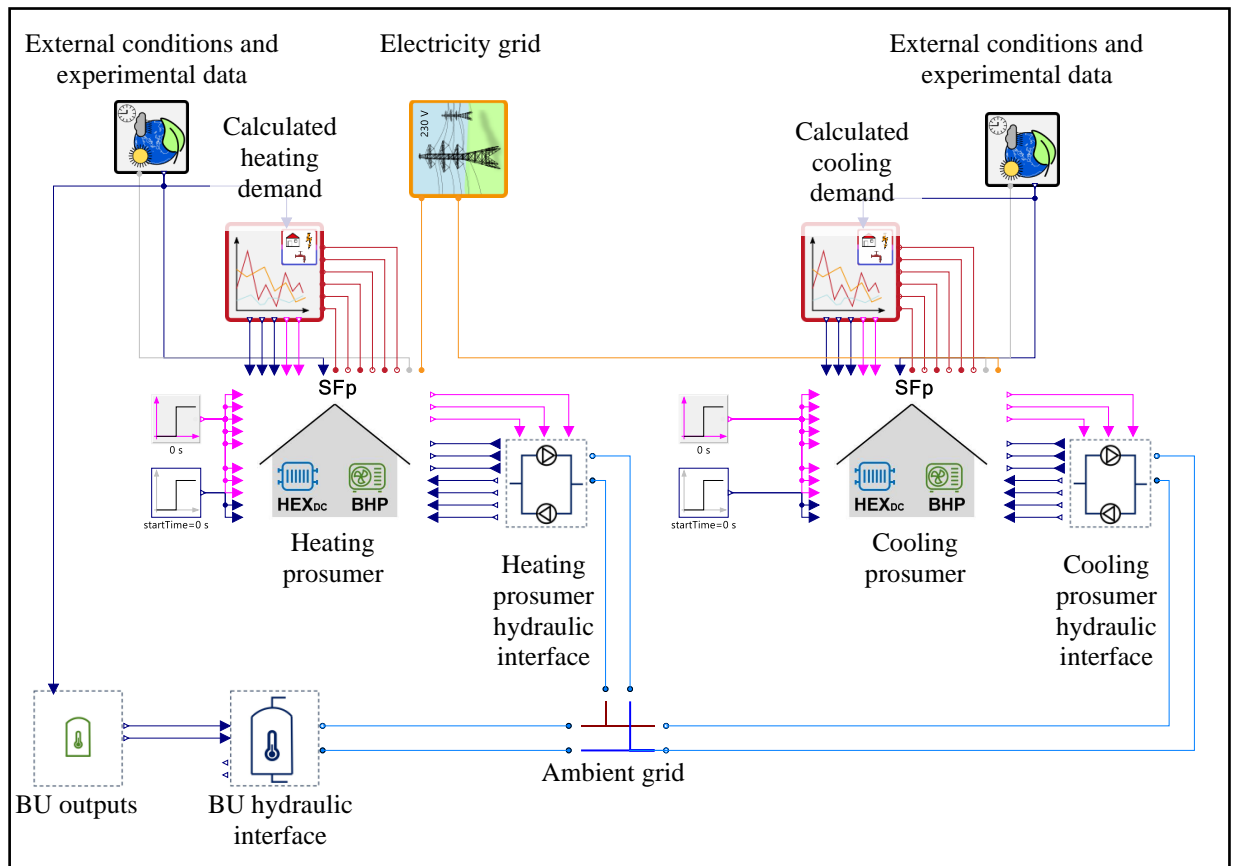


Figure 5.8: HyP validation step Modelica simulation model.

For the demands, the experimental power is calculated based on the tertiary flowrate going through the demand emulator along with the temperatures before and after it, as shown in Figure 5.9.

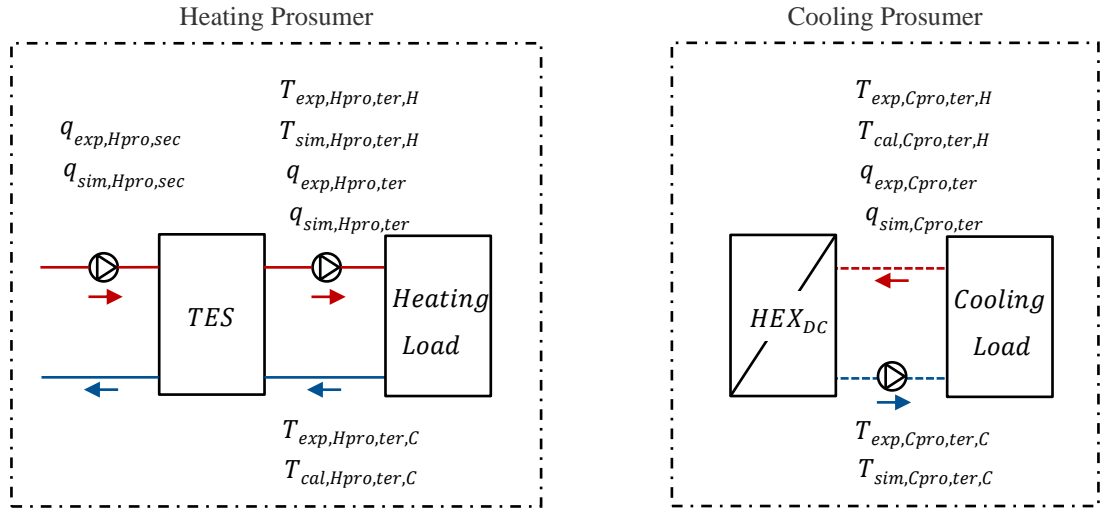


Figure 5.9: Schematic for Hydraulics & Prosumers validation variables.

For determining the power transferred to the heating/cooling loads in both $T_{GridFloat}$ and $T_{GridFix}$, equations (5.12) and (5.13) are used for the heating prosumer and (5.14) and (5.15) for the cooling prosumer:

$$P_{th_{cal,Hpro,ter}} = c_p \rho q_{exp,Hpro,ter} (T_{exp,Hpro,ter,H} - T_{exp,Hpro,ter,C}) \quad (5.12)$$

$$T_{cal,Hpro,ter,C} = \frac{P_{th_{cal,Hpro,ter}}}{c_p \rho q_{sim,Hpro,ter}} + T_{sim,Hpro,ter,H} \quad (5.13)$$

$$P_{th_{cal,Cpro,ter}} = c_p \rho q_{exp,Cpro,ter} (T_{exp,Cpro,ter,H} - T_{exp,Cpro,ter,C}) \quad (5.14)$$

$$T_{cal,Cpro,ter,H} = \frac{P_{th_{cal,Cpro,ter}}}{c_p \rho q_{sim,Cpro,ter}} - T_{sim,Cpro,ter,C} \quad (5.15)$$

where for the heating/cooling prosumer, the temperature after the heating/cooling load ($T_{cal,Hpro,ter,C} / T_{cal,Cpro,ter,H}$) is calculated from the experimental power supplied to the heating/cooling emulator ($P_{th_{cal,Hpro,ter}} / P_{th_{cal,Cpro,ter}}$) and the simulation tertiary flowrate ($q_{sim,Hpro,ter} / q_{sim,Cpro,ter}$) in each time step. The experimental tertiary flowrates are given as setpoints for the tertiary pumps.

The secondary pump's flowrate for the BHP is fixed for both experiments to 14l/min and the same setpoint is given for $q_{sim,Hpro,sec}$. The TES volume and dimensions are set to match the experimental ones, namely 720l and 0.79m diameter. The heat convection coefficient of the water layers within the TES is set to 0.5W/m²K [181] while the heat

conductance of the heat storage isolation to 30W/K in line with the manufacturer's technical datasheet [166]. The pipe connections to the BHP and the load emulator are set at the same locations as the ones in the experiment. There are a total of 3 sets of pipes, since the BHP can charge either the top (BHP at 60% modulation) or the middle (BHP at 40% modulation) depending on the TES temperature profile as the control strategy highlighted in Section 3.3.3. Table 5.8 indicates these connections, that follow the experimental hardware.

Table 5.8: Heating prosumer's TES pipe connections' levels.

Pipe	BHP at 60% modulation (Charging TES)	BHP at 40% modulation (Charging TES)	Heat Load (Discharging TES)
Flow pipe	TESTL 9	TESTL 5	TESTL 10
Return pipe	TESTL 4	TESTL 1	TESTL 1

The BHP is also set to match the details provided from the manufacturer, as described in Section 4.1 (nominal thermal power output of 19.8kW). A nominal COP of 4.5 for W10/W55 is used in line with the technical datasheet [171]. The heat losses of the BHP are set to 400W, which is in line with experimental measurements conducted in the component testing phase of the experiment. For the controls, the power setpoints from the experiment are used rather than having a dependence on the temperature of the TES as described in Section 4.2. The reason for this is to allow a direct comparison of the flowrates, ensuring the BHP turns on the same time as in the experiment will not hinder the R^2 comparisons. The same procedure is conducted for the HEX_{DC}, providing the surface area (1m²), and water volume in either side of it (0.5l in each side).

5.1.3 Hydraulics & Prosumers & BU (HyPB)

The last step before the full model includes the incorporation of the BU TES. The power flows into it are set to match those from the experiment, so the ASHP is not modelled, to limit the sources of error and focus on investigating the impact of the TES. The model used is shown in Figure 5.10.

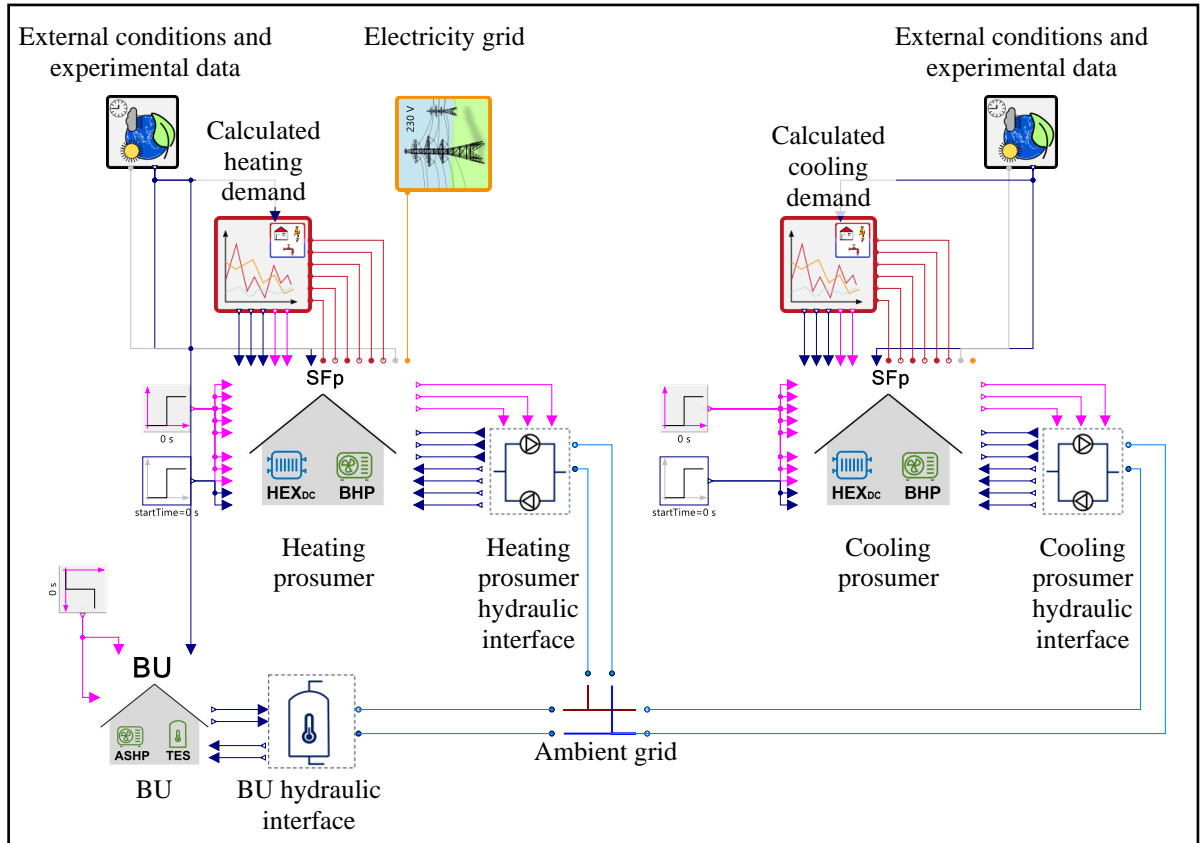


Figure 5.10: HyPB validation step Modelica simulation model.

The return temperature is calculated similarly to the demands in step HyP, with the secondary flowrate set to equal that of the experiment. As in the experiment, the power can be positive (heating) or negative (cooling), depending on the mode of operation of the ASHP during the experiment. This is shown in Figure 5.11.

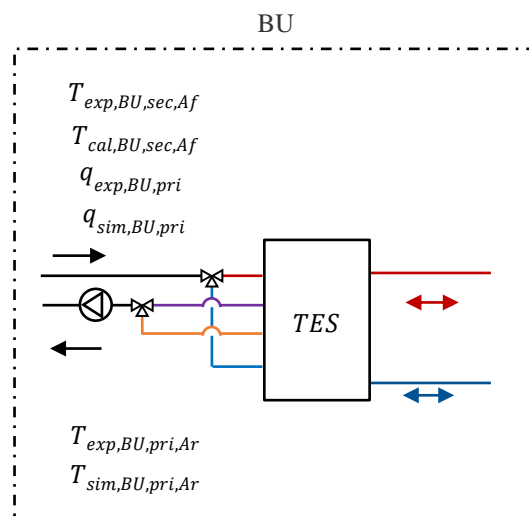


Figure 5.11: HyPB BU Modelica simulation model.

For determining the power transferred to the BU's TES in both $T_{GridFloat}$ and $T_{GridFix}$, equations (5.16) and (5.17) are used:

$$P_{th_{cal,BU,sec}} = c_p \rho q_{exp,BU,sec} (T_{exp,BU,sec,Af} - T_{exp,BU,sec,Ar}) \quad (5.16)$$

$$T_{cal,BU,sec,Ar} = \frac{P_{th_{cal,BU,sec}}}{c_p \rho q_{sim,BU,sec}} - T_{sim,BU,sec,Af} \quad (5.17)$$

where the temperature entering the BU's TES ($T_{cal,BU,sec,Ar}$) is calculated from the power supplied from the ASHP during the experiment ($P_{th_{cal,BU,sec}}$) and the flowrate through it ($q_{sim,BU,sec}$) in each time step. The power also dictates the opening and closing of the two 3WVs to charge the top (heating mode) or bottom (cooling mode) of the TES.

The BU's TES volume and diameter are set to match the experimental setup, namely 790l and 0.79m respectively. The heat convection coefficient of the water layers within the TES and the heat conductance of the heat storage isolation are the same as the heating prosumer's values, 0.5W/m²K and 30W/K respectively. The pipe locations for charging (ASHP side) and discharging (grid side) matched those from the experiment, as shown in Table 5.9.

Table 5.9: BU's TES pipe connections' levels.

Pipe	ASHP in heating mode (Charging TES)	ASHP in cooling mode (Charging TES)	Heat Load (Discharging TES)	Cooling Load (Discharging TES)
Flow pipe	TESTL 9	TESTL 2	TESTL 10	TESTL 1
Return pipe	TESTL 5	TESTL 4	TESTL 1	TESTL 10

5.1.4 Full Model (FM)

Finally, the full model can be used as a complete digital twin of the experiment, as previously shown in Figure 5.1. In this case, no setpoints or experimental values other than the prosumer demands are set. All controls described in Section 4.2 are replicated in the digital twin, including the ASHP and BHP controls, which are entirely dependent on the TESTL values.

In this case, the BU model includes an ASHP model. Its values are set to equal the ones from Section 4.1 (nominal thermal power output of 10kW for heating and cooling), confirmed during component testing prior to the experiment. A nominal COP of 4.65 for A2/W35 and a nominal Energy Efficiency Rating (EER) of 5.92 for A35/W18 are used in line with the technical datasheet [173]. Since the air and water temperatures are different, the simulated COP and EER will vary, following tables from the unit’s experimental testing that are part of the digital twin as described in Zinsmeister and Perić (2022) [160].

It is no longer possible to make a direct comparison of the flowrates using R^2 values since the TES will reach the temperatures at different timesteps. In other words, there could be delays on when the ASHP & BHP are turning on. Instead, the comparison will be made on the overall thermal energy supplied by the ASHP and the BHP, along with power outputs. By studying their behaviour, the overall similarity of the systems will be highlighted.

5.2 5GDHC simulation models validation results

All simulations are conducted on a laptop with 12 physical cores and 16 logical processors, having a maximum speed of 2.2GHz with 16GB of RAM running at Microsoft Windows 10 Enterprise. Simulation X version 4.2 is used, with CVODE C compiled integration algorithm since it offers high efficiency for thermofluid system simulation [158,182]. To determine the model’s CPU times, each model is run 10 times for 72,000 seconds (20 hours). The mean computational times for each validation step are summarised in Table 5.10, along with the number of equations. As expected, the complexity increases as more components are added to the digital twin. The individual flowrate outputs from validation steps Hy, HyP and HyPB are shown in the Figure 5.12, Figure 5.13 and Figure 5.14 respectively. Figure 5.15 combines all the flowrates in one plot for clarity.

Table 5.10: Computational time for validation cases: simulation time 72,000s (20h).

Validation case	$T_{GridFix}$		$T_{GridFloat}$	
	Number of equations	CPU time (min)	Number of equations	CPU time (min)
Hy	1,173	1.75	1,176	1.90
HyP	2,279	3.83	2,285	3.83
HyPB	2,627	4.27	2,639	4.17
FM	2,941	4.50	2,945	4.67

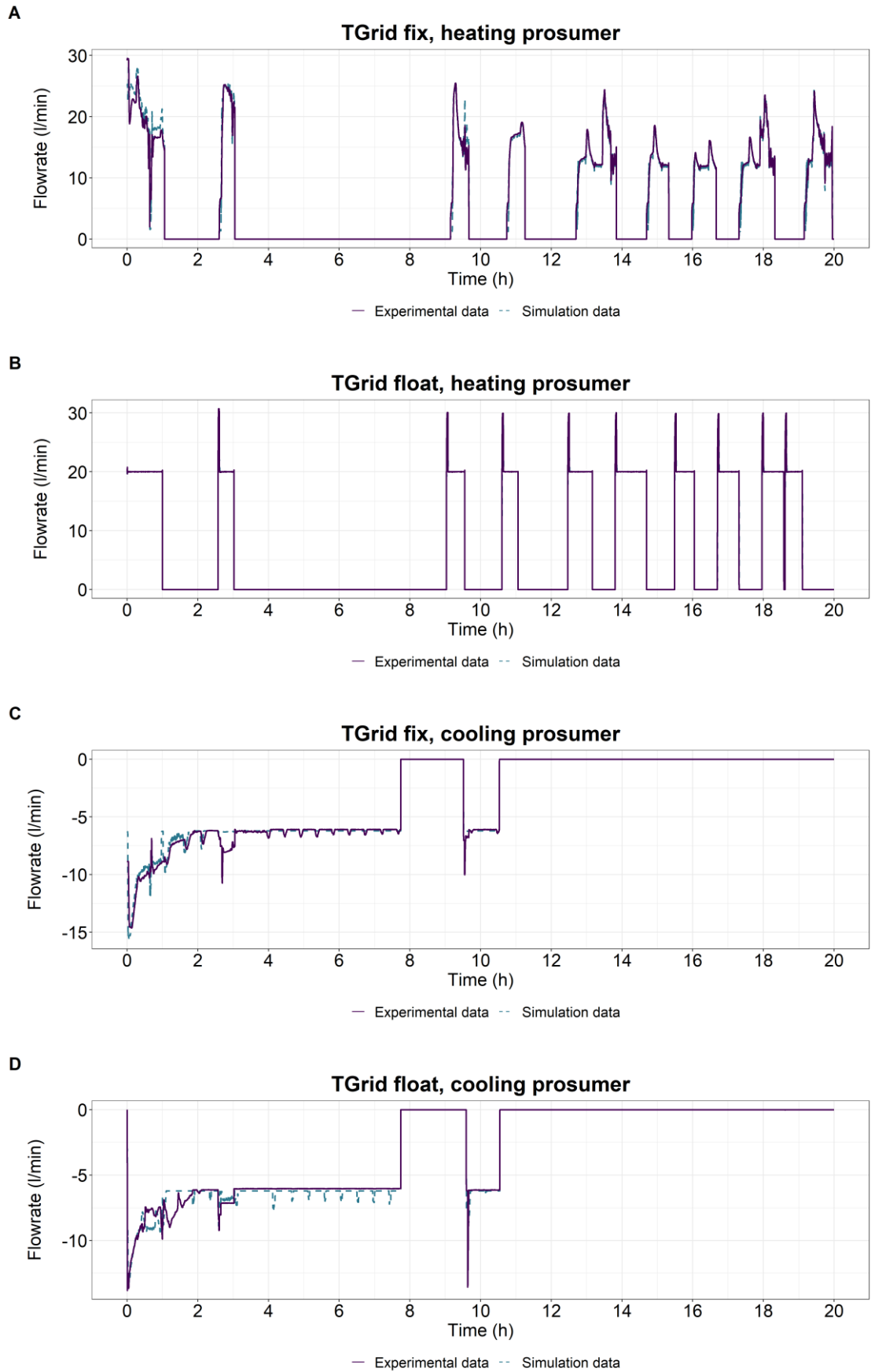


Figure 5.12: Validation results for Hy against experimental outputs.

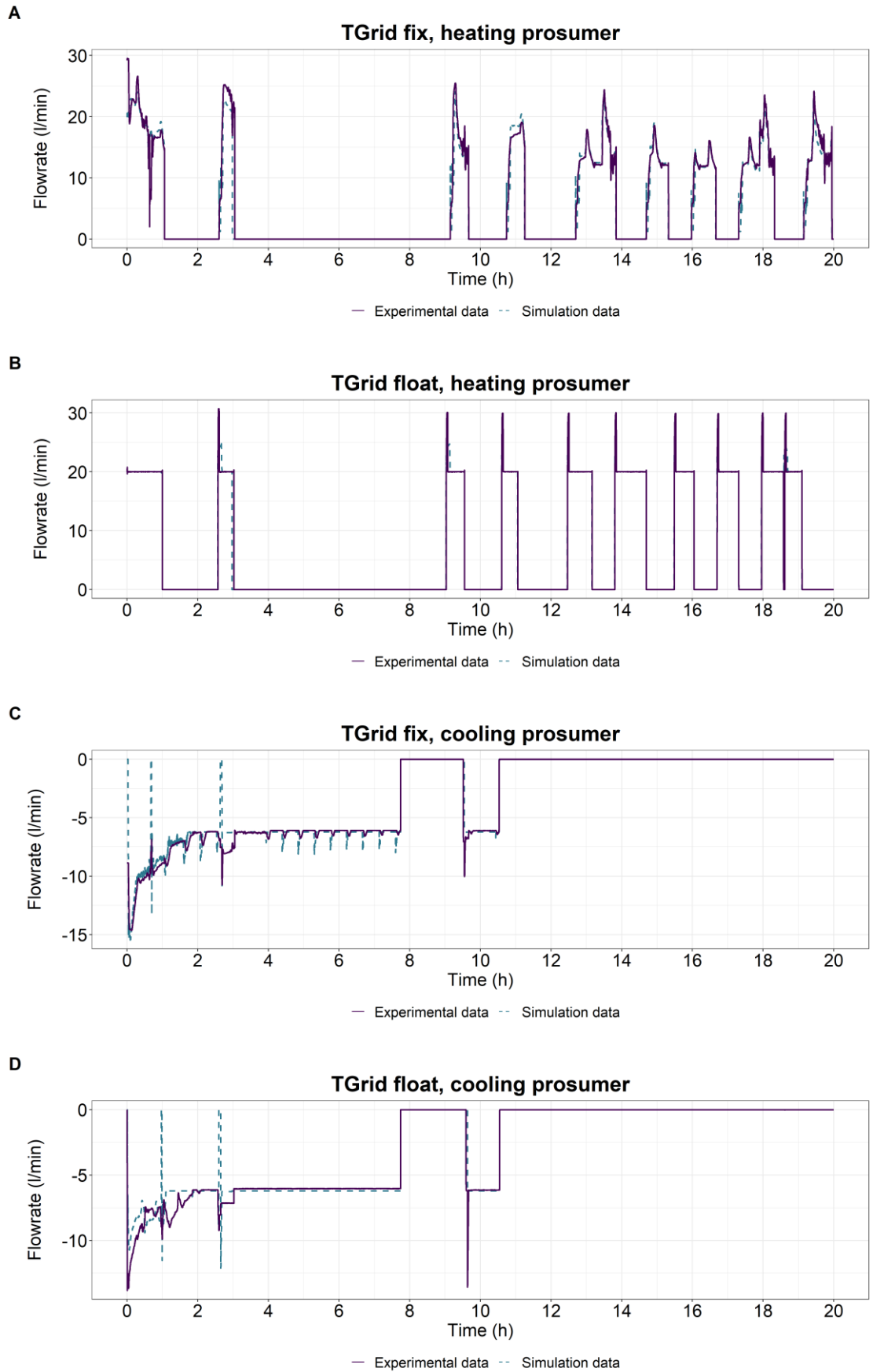


Figure 5.13: Validation results for HyP against experimental outputs.

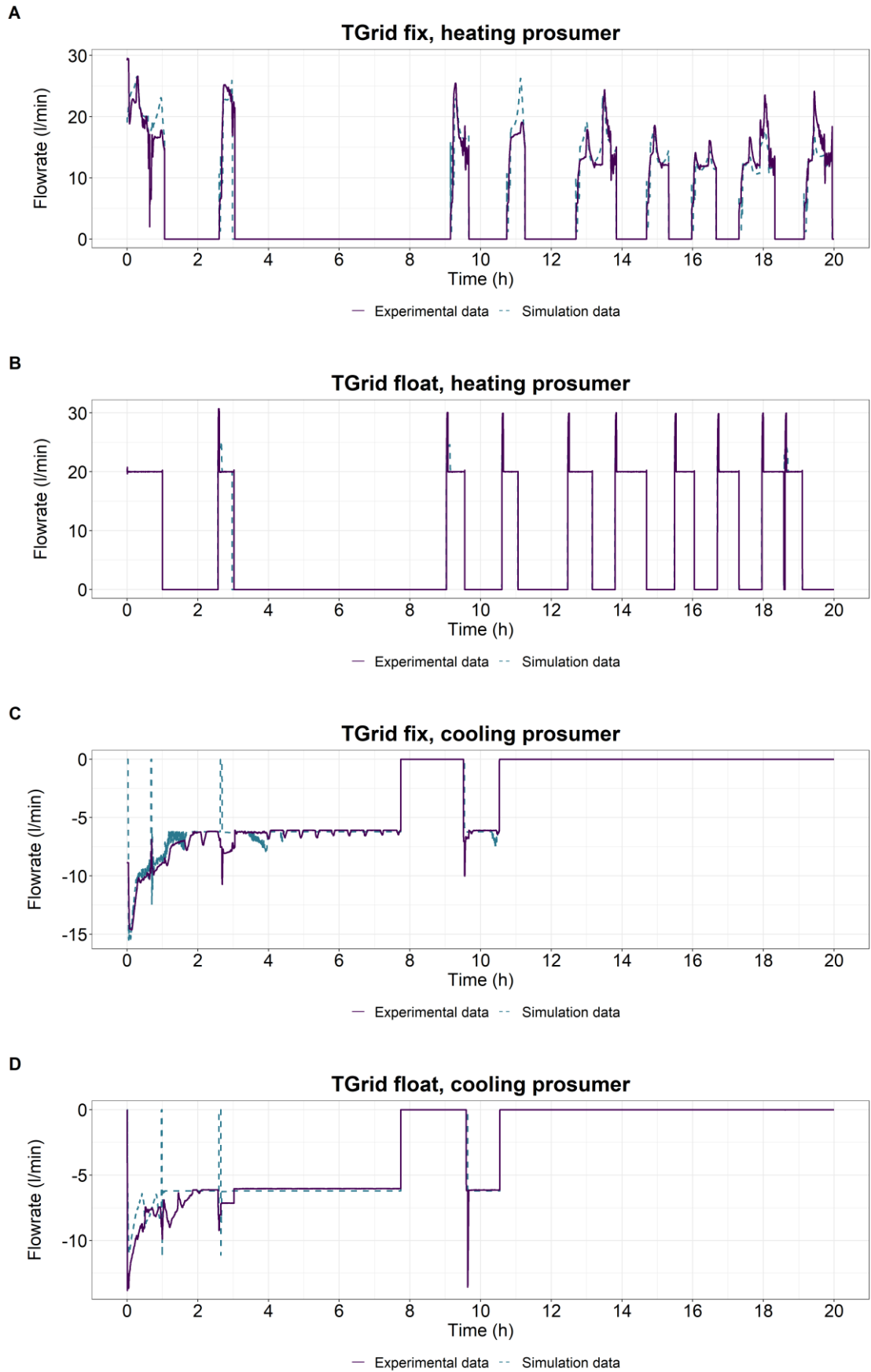


Figure 5.14: Validation results for HyPB against experimental outputs.

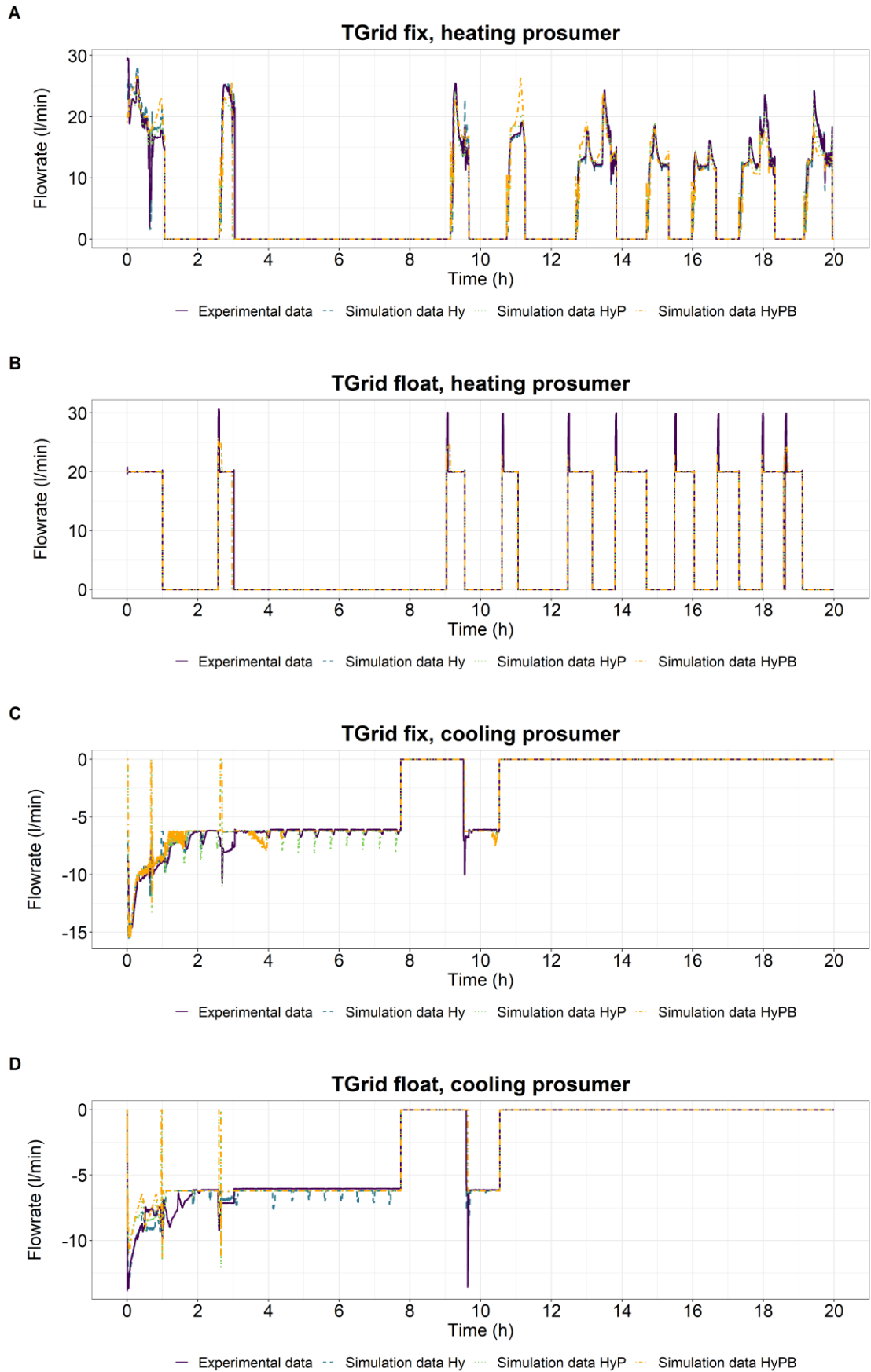


Figure 5.15: Validation results for Hy, HyP and HyPB against experimental outputs.

For the first three validation cases where the flowrate is used as the validation metric, the results for the R^2 metric are shown on Table 5.11.

Table 5.11: R^2 values for Hy, HyP and HyPB flowrates.

Validation Case	$T_{GridFix}$		$T_{GridFloat}$	
	Heating	Cooling	Heating	Cooling
	Prosumer	Prosumer	Prosumer	Prosumer
Hy	97%	98%	99%	97%
HyP	89%	95%	91%	93%
HyPB	85%	94%	91%	93%

Figure 5.12 showcases the accuracy of the hydraulic components, namely of the prosumer and BU hydraulic interfaces as well as the grid. All R^2 values are above 97%, illustrating that the PI controllers are accurately tuned, and component characteristics (pumps, pipes and pressure resistance elements) have been well captured. Expectedly, for the cooling prosumer in $T_{GridFloat}$ for hours 1 to 2, there is a difference between the simulation and experiment. The simulation is dropping quicker than the experimental flowrate, as shown in Figure 5.16. This difference occurs due to the PI controller in the experiment being less responsive, allowing a greater variation in the flow temperature from the setpoint.

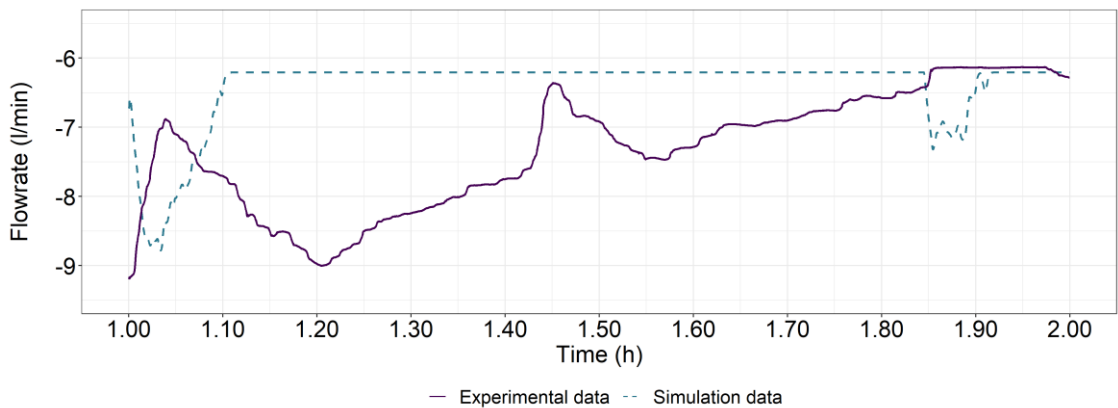


Figure 5.16: Detail of cooling prosumer flowrate for $T_{GridFloat}$ for hours 1 to 2 in the Hy step.

Figure 5.13 shows the impact of introducing the prosumer models in the digital twin. All R^2 values are above 91%, other than the heating prosumer in $T_{GridFix}$ (plot A) which is 89%. The main reason for this drop in accuracy for the heating prosumer of $T_{GridFix}$ is the cool down period of the BHP at hour 3, which has some variations to the ones from the experiment. Specifically, for 250 seconds after the BHP shut down for the first time (timesteps 10,723 to 10,973), the pump in the experiment is still running, probably due to a

delay of the PI controller, as shown in Figure 5.17. If this section is not considered (250 timesteps out of 72,000), the R^2 becomes 93%. Similarly, for the heating prosumer of $T_{GridFloat}$ (plot B), the main variation between the model and the experimental results occurs during the BHP startup. For 410 seconds (which is the BHP startup period), the pump in the model is reaching the setpoint of 20l/min quicker than the experiment. This is due to the experimental PI controller responding slowly to the variant behaviour of the BHP, as discussed in Section 4.5.1 and shown in Figure 4.15. This comparison of the experimental and simulation values for these 410 seconds are shown in Figure 5.18. For the cooling prosumer (plots C and D), as in the Hy case, there is a slight difference between hours 1-2. Additionally, the two spikes between hours 1 and 3, each lasting 60 timesteps, correspond to periods of zero demand in the experimental demand profile (shown in Figure 4.5). In the simulation, the HEX_{DC} shuts off during these periods. However, due to the brief duration of these zero-demand periods, the PI controller in the physical experiment did not trigger the pump to turn off.

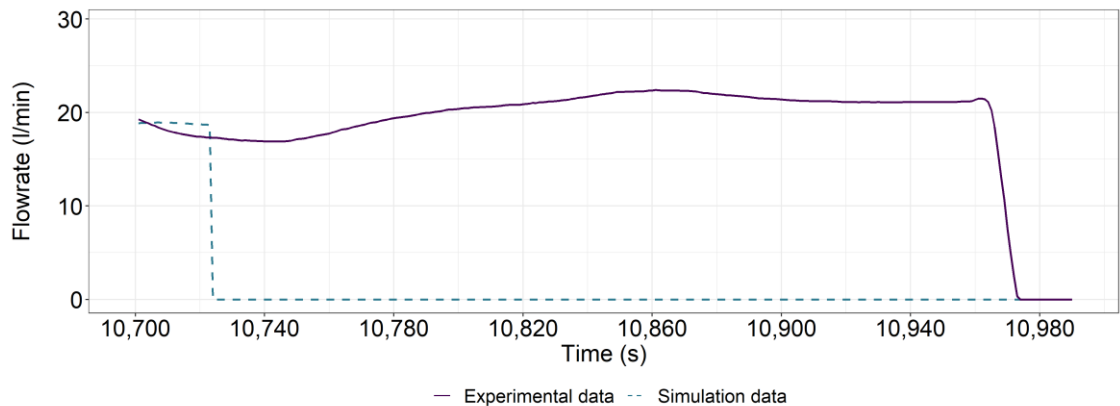


Figure 5.17: Detail of heating prosumer flowrate for $T_{GridFix}$ at the 3rd hour in the HyP step.

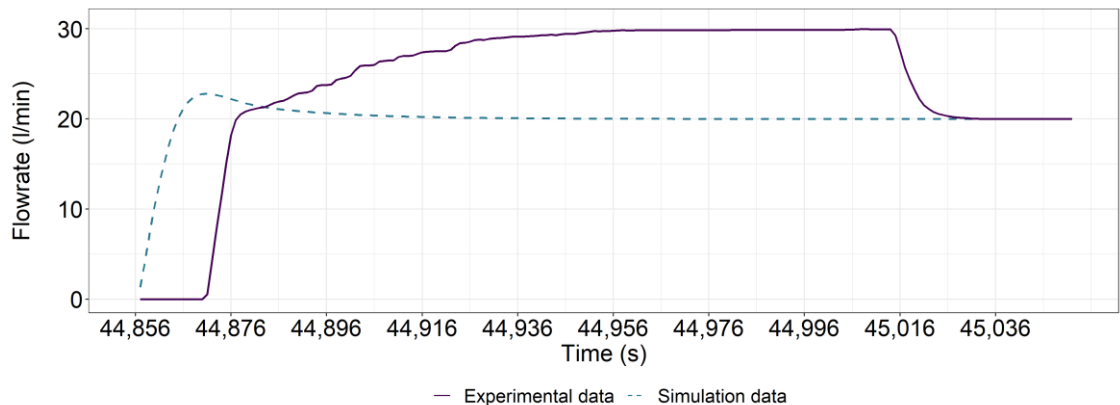


Figure 5.18: Detail of heating prosumer flowrate for $T_{GridFloat}$ at BHP startup in the HyP step.

In Figure 5.14, the BU TES model is added to the digital twin. The impact on the R^2 from HyP is almost non-existent (less than 0.2% change) other than for the heating prosumer in $T_{GridFix}$. Here, the R^2 value drops from 89% in the HyP case to 85%. This is due to the fact that the inlet temperature greatly affects the power output of the BHP and thus the return temperature to the grid. However, if the same 250 seconds are deducted from the evaluation for the reasons mentioned above, the R^2 becomes 88%.

Overall, it is seen that the simulation outputs for the flowrate closely follow the experimental outputs, as highlighted in Figure 5.15. The R^2 values with the modification on the 250 seconds for the heating prosumer in $T_{GridFix}$ are shown in Table 5.12.

Table 5.12: R^2 values for Hy, HyP and HyPB flowrates (* values have been adjusted).

Validation Case	$T_{GridFix}$		$T_{GridFloat}$	
	Heating	Cooling	Heating	Cooling
	Prosumer	Prosumer	Prosumer	Prosumer
Hy	97%	98%	99%	97%
HyP	93%*	95%	91%	93%
HyPB	88%*	94%	91%	93%

For the FM validation, the thermal outputs of the BHP and ASHP are studied. Table 5.13 includes the total energy output along with the number of times the HPs are on and in which mode. Figure 5.19 and Figure 5.20 show these outputs for $T_{GridFix}$ and $T_{GridFloat}$ respectively. The BHP outputs are shown in plots (A) and (B) while the ASHP ones in plots (C) and (D). Table 5.14 shows the R^2 values for the energy outputs.

Table 5.13: Comparison of power and energy outputs for BHP and ASHP for FM digital twin.

Item	Units	$T_{GridFix}$			$T_{GridFloat}$		
		Simulation	Experiment	Difference	Simulation	Experiment	Difference
BHP heating output	kWh	51.9	50.4	3.1%	50.4	49.2	2.4%
BHP on at 40%	times	6	6	0	6	7	1
BHP on at 60%	times	7	7	0	5	5	0
ASHP heating output	kWh	30.0	31.9	-6.1%	30.5	32.7	-6.7%
ASHP on heating	times	12	13	1	20	21	1
ASHP cooling output	kWh	20.8	19.4	7.0%	21.0	21.0	0.2%
ASHP on cooling	times	14	15	1	13	16	3

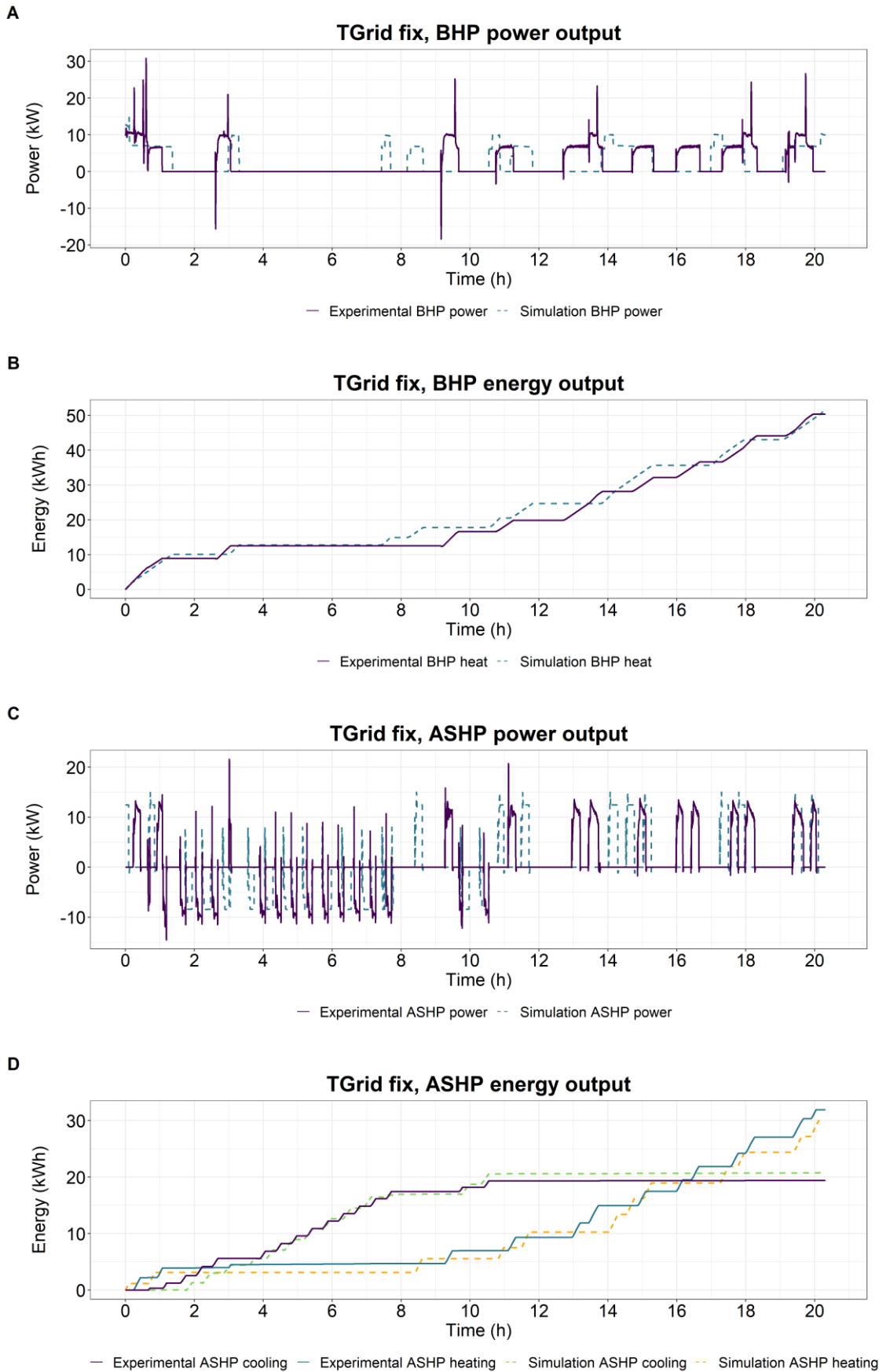


Figure 5.19: $T_{GridFix}$ BHP and ASHP power and energy outputs.

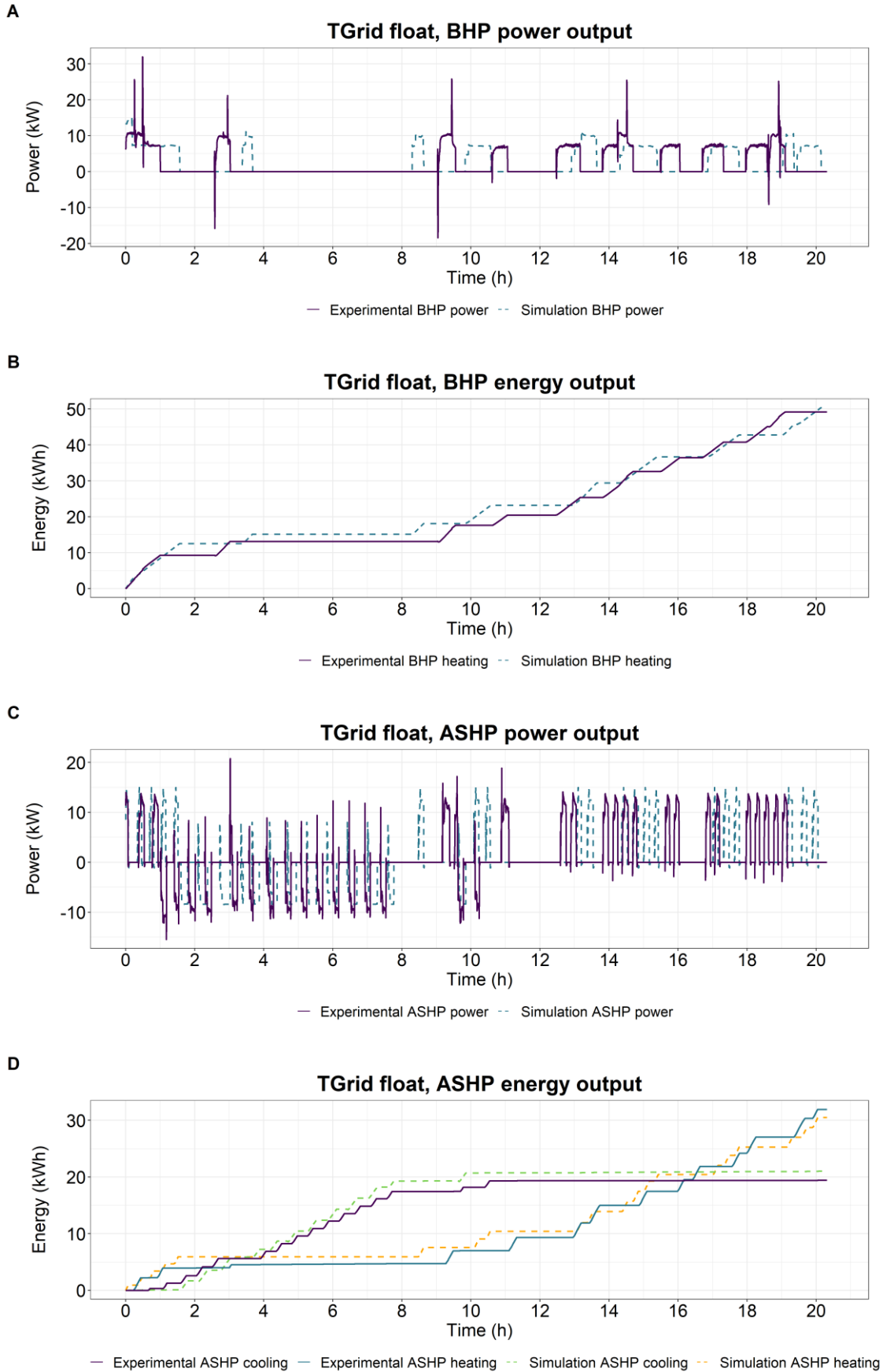


Figure 5.20: $T_{GridFloat}$ BHP and ASHP power and energy outputs.

Table 5.14: R² for energy outputs for BHP and ASHP for FM digital twin.

Energy output	$T_{GridFix}$	$T_{GridFloat}$
BHP heating	99%	99%
ASHP heating	98%	98%
ASHP cooling	99%	99%

By cross examining these figures, it's clear that there is a very similar behaviour between the experiment and simulation, with all R² values being over 97%. The BHP operation is almost identical (R² of 99%) as shown in plots (B), with a difference of 3.1% and 2.4% for the total heating energy output for $T_{GridFix}$ and $T_{GridFloat}$ respectively.

For both Figure 5.19 and Figure 5.20, Plots C and D indicate that for the ASHP, the difference in behaviour is greater. $T_{GridFix}$ has an energy difference of -1.9kWh (-6.1%) for heating and 1.4kWh (7.0%) for cooling. $T_{GridFloat}$ has an energy difference of -2.2kWh (-6.7%) for heating and 0.1kWh (0.2%) for cooling. It can be seen that the slight changes in the temperatures within the TES due to the variations of the exact flowrates and temperatures flowing in and out of the BU's TES lead to control setpoints being met at different times and for a different duration. In other words, since the control setpoint temperatures in both BU and BHP TESs happen in slightly different times, there is a slight variation on when the equipment is turning on and for how long. The temperature profiles of the TES for the TESTLs 2, 4, 7 and 9 are shown in Figure 5.21 for both $T_{GridFix}$ and $T_{GridFloat}$.

Overall, the simulated and experimental behaviour of the BU's TES exhibited good agreement for both $T_{GridFix}$ and $T_{GridFloat}$. Stratification is maintained within the control setpoints (22°C and 13°C) for TESTLs 2 and 9. However, some discrepancies are observed during cooling periods. During cooling from 2h to 8h, a larger temperature difference (up to 2.5°C) is present between TESTLs 2 and 4 in the experiment (Figure 5.21, plot A) compared to the simulation (Figure 5.21, plot B) where these TESTLs' temperatures remained almost identical. This is due to simplifications in the model regarding fluid dynamics within the tank. Similarly, for heating periods, TESTL 9 in the simulation (Figure 5.21, plot B and D) reached 21°C, unlike the experiment (Figure 5.21, plot A and C) where it reached 22°C, specifically the upper temperature bound ($T_{set,BU,StopHeat}$).

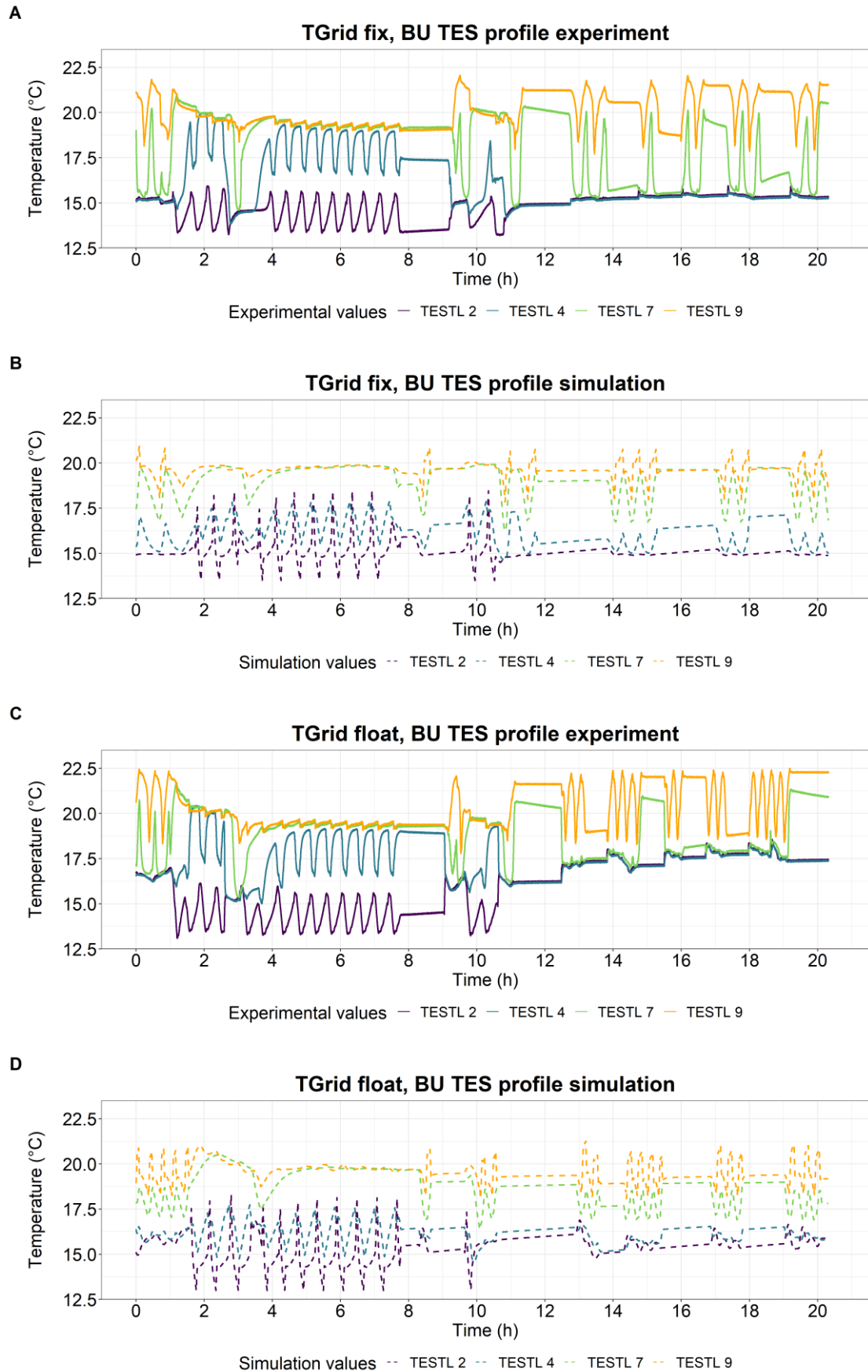


Figure 5.21: BU's TES temperature profile for $T_{GridFix}$ and $T_{GridFloat}$.

This likely happens because the control setpoint triggering the ASHP to stop is TESTL 7 reaching $T_{set,BU,StartHeat}$ rather than TESTL 9 reaching $T_{set,BU,StopHeat}$. Notably, when the ASHP is off (e.g., at 12h in all figures), the temperature stratification of the water layers in the TES is very similar, suggesting good agreement during non-operational periods.

5.3 5GDHC simulation models validation discussion

Overall, the validation process demonstrates that the developed Modelica components can be effectively used to create an accurate digital twin of the experiment. The progressive build-up of the digital twin in four steps, each increasing complexity by adding Modelica components, serves as a roadmap for identifying error sources. The full digital twin has a CPU time for 20h of simulation of 4.50min and 4.67min for $T_{GridFix}$ and $T_{GridFloat}$ respectively, which represent sufficiently fast computational speeds for most applications of such detailed thermofluid models. For larger systems with multiple prosumers, the number of equations will considerably rise, making the CPU time much higher. For such cases, more powerful computing hardware is recommended, significantly reducing CPU times.

All flowrate outputs of the Hy, HyP and HyPB validation cases showed similar behaviour to the experimental outputs, achieving an R^2 value exceeding 91%, except for the heating prosumer in step HyPB ($R^2 = 88\%$). Other than R^2 as a metric for validation, the analysis considered overall behaviour of the system. Notably, the hydraulic design and control philosophies, including equipment modulation (valves, energy transformation units and TES) are effectively replicated in the digital sphere. This resulted in similar flow, temperature, and energy profiles across both systems. Specifically, Step Hy (R^2 between 97% and 99%) of the validation process successfully captured the thermofluid behavior in the grid, with hydraulic components behaving as observed in the real system. Step HyP (R^2 between 91% and 95%) introduced the interface with the prosumer models, comprising thermal connector-only components, enabling a rapid assessment without significantly compromising model accuracy. Step HyPB (R^2 between 88% and 94%) added the BU, introducing minimal accuracy changes compared to the previous step. Finally, the full digital twin, with only prosumer demands as experimental inputs, produced a very similar energy profile to the experimental one, with energy discrepancies being less than 3.1% for the BHP and 7.1% for the ASHP. These discrepancies arise from slight variations in

energy transfer unit activation times compared to the experiment due to differences in TES control setpoints. However, over a length of time, the relative difference of the energy supplied is shrinking as the timing of the individual turn-ons has a small impact on the overall energy use. Importantly, no delays, startup/shutdown issues, or deviations in flow direction or abstraction are observed.

This progressive validation process revealed two key sources of error. Firstly, the behaviour of the BU's TES is critical to the overall behaviour of the system, since it influences ambient network temperatures that in turn affect the prosumer primary pump behaviour. The current one-dimensional model with thermal only connectors offers an efficient balance between accuracy and computational cost. However, to increase accuracy, a highly detailed TES model encompassing both hydraulic and thermal components is recommended. It would allow to better model the BU's TES behaviour, replicating hydraulic behaviours and water stratification TESTL interaction, as well as defining the precise sensor locations and the impact they have on flow recirculation and mixing within the TES. Secondly, discrepancies between the physical and modelled PI controllers for the primary pumps in the prosumers are another sensitivity variable. Accurately tuning the PI controllers requires a case-by-case procedure and can be a source of error.

The stepwise construction of the digital twin offers a valuable methodology for future development. This approach allows for error identification at each stage, pinpointing components that may require specific adjustments based on the project's unique requirements. In this validation process, no calibration is performed beyond PI controller tuning. The energy transformation units (BHP and ASHP) are part of the ProHMo library and have tables from component testing for their behaviour under various modulation values and primary/secondary water temperatures. Utilizing calibrated values for specific components, such as pump nominal flow rate or TES thermal losses, could potentially improve measurement accuracy. Furthermore, using experimental data to verify simulation outputs fosters a more critical evaluation and prevents reliance solely on simulated results. This methodology enables targeted component modifications based on the project's focus. For example, a more detailed ground model can be built if its behavior is of particular interest. This targeted approach optimizes both computational efficiency and accuracy by simplifying components outside the primary area of investigation.

Future research can investigate the impact of detailed TES models with hydraulic and thermal components, which will more accurately capture fluid dynamics and thermal TESTL stratification. Such a model could limit discrepancies in energy transfer equipment timing and operation. Future research can also expand upon the experiment by incorporating a larger network with multiple prosumers. This would elucidate the findings' generalizability, assess the impact of low flow rates in larger systems, and explore the extent of possible energy synergies. While the introduction of multiple prosumers is unlikely to drastically alter model behavior or introduce significant new error sources, it would be beneficial for broader validation. Additionally, including a reversible BHP capable of both heating and cooling operations within a prosumer would allow for validation of the dual primary pumps in the prosumer substation. Furthermore, implementing an active BHP within the cooling prosumer interfacing with the HEX_{DC} would further validate the control models. Hardware limitations prevented exploration of these scenarios. Investigating the impact of varying component detail levels, utilizing co-simulation techniques to reduce computational time, and analysing the effect of different grid and terminal temperatures on model performance are also avenues for future research.

The next critical step in quantifying the economic and environmental performance of 5GDHC systems, is a thorough techno-economic analysis. To complete this, Chapter 6 presents CATHeaPS, a TEM that can compare economically and environmentally 5GDHC against alternative decarbonisation strategies.

6 Techno-economic Modelling: CATHeaPS

This chapter introduces CATHeaPS, a Centralisation Analysis Tool for Heat Pump Systems. It presents the current literature gap on open access TEMs for 5GDHC techno-economic analyses and how they are met by CATHeaPS. It covers in detail the methodology of the model and its verification using two case studies, Network 1 and Network 2. Having verified the model, CATHeaPS is used to undertake economic and environmental analyses. These analyses are conducted on three project scenarios: (i) a 'heating only' district with access to an ambient temperature waste heat source; (ii) a typical 'heating only' district; and (iii) a typical project area with heating and cooling demands.

For the economic analysis, a break-even analysis is conducted for project scenarios comprising residential properties. This exercise provides a preliminary guide on the number of properties needed for the cost of a specific energy supply option to become lower than another. For the environmental analysis, 10,000 Monte Carlo simulations are conducted to identify trends and relationships between the supply options. Finally, a discussion is performed on the key findings.

6.1 Background on techno-economic assessments for 5GDHC systems

As mentioned, when considering a project area that needs to be supplied by a thermal system, a mix of supply options must be considered. 5GDHC is one of them but the considered supply options can feature a wide mix of technologies, ranging from fully centralised options to completely decentralised ones.

This work focuses on the UK and north European building stock, where heating is the main thermal energy demand. Therefore, the centralised option features a 4GDH network that directly supplies properties through building/flat level HEXs. For cooling, building/flat level AC units are considered. The default decentralised counterfactuals for heat network studies are typically represented by the “do minimum” and “do nothing” approaches [17,183]. The do minimum approach comprises reversible air-to-water ASHPs at each

building or flat. The “do nothing” approach includes individual Gas Boilers (GB) and AC units per property. A schematic of these four energy supply options is shown in Figure 6.1.

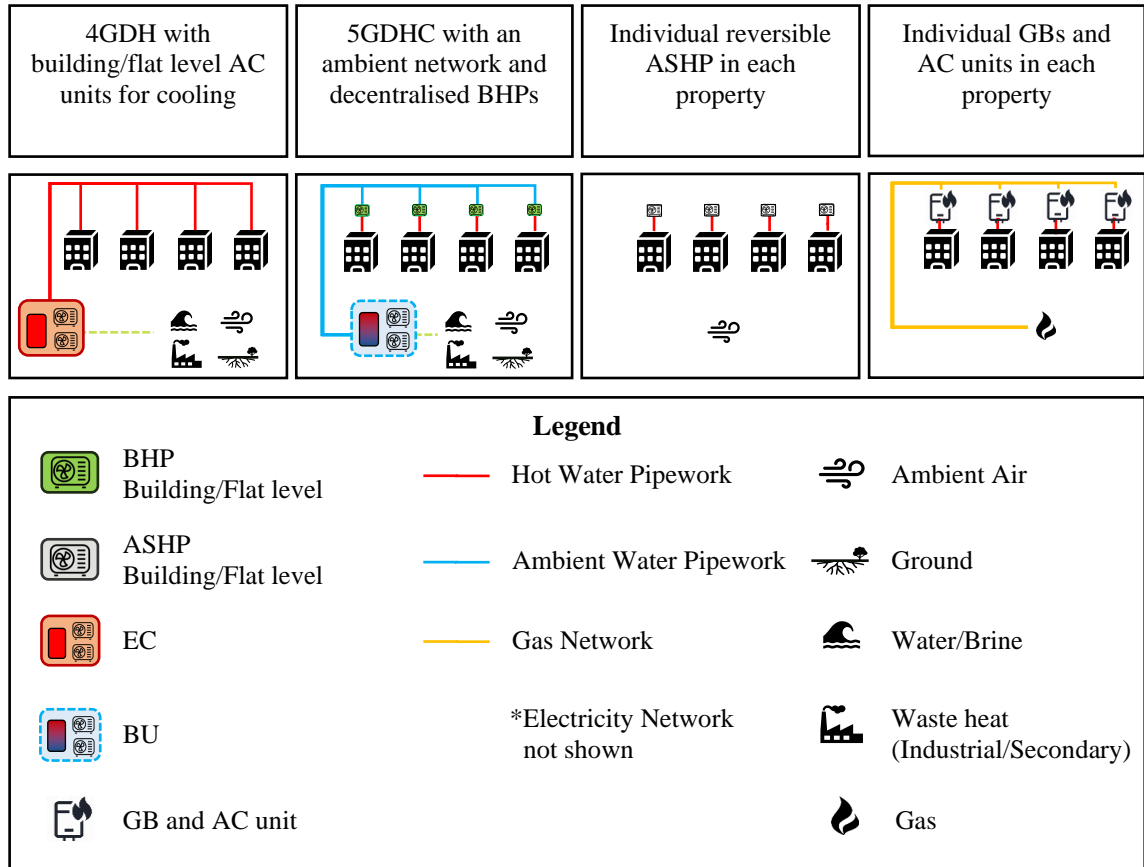


Figure 6.1: Schematic of different heat supply options.

The decision on which approach is more appropriate is site specific and influenced by the project’s bespoke building schedule. A building schedule is a listing and categorisation of the connected properties. It provides information on building consumer class (e.g. residential, office), their location and spatial density as well as the number of connections per property (capturing properties with multiple flats, such as apartment blocks).

For this decision, all the considered energy supply options need to be analysed through a bespoke techno-economic study, featuring the same methodology [43]. Such a study would include:

- Demand analysis using the bespoke building schedule.
- Energy flow analysis for determining the technology mix and capacity.
- Hydraulic modelling for sizing the distribution network of each option.

- d) A TEM to capture and utilise the above outputs to assess the economic and environmental performance of each option.

Following these design steps, the sizing and operational characteristics of the selected system can be optimised [43,184]. Depending on the level of detail and the complexity of the project, such a process can be intricate and resource intensive, requiring several months to be completed, while often utilising closed-access, in-house or commercial models and data [185]. A review of the available TEMs for conducting such studies is shown below followed by an introduction to CATHeaPS for filling the identified research gap.

6.1.1 Review of existing TEMs

There is a plethora of commercial tools available for energy supply options assessments, notably EnergyPro, NPro and TERMIS. EnergyPro provides energy supply assessment, offering an energy supply simulation which optimises energy production shares based on cost [186]. Similarly, NPro focuses on district level energy flow modelling, with the availability of load profiles, a user-friendly web-based interface, and the availability of pipe dimensioning [187]. TERMIS provides an optimised network topology along with an energy supply assessment, combining hydraulic and energy flow optimisation. It also provides a preliminary cost indication of the project [151]. All these tools focus on different aspects of the project assessment, but do not provide a full cashflow and, most critically, they are not open access.

There are some open access tools for planning district heating systems and assessing their economic feasibility as well as some publications on techno-economic comparisons of centralised and decentralised systems. THERMOS [185] is an open access tool for planning district heating networks, which focuses on optimising centralised systems; however, it lacks a transparent cashflow component that can be accessed and modified, and it utilizes a map interface instead of a simple building schedule. In addition, the open access tool can be accessed as source code requiring a GIS software and is limited to earlier versions of the project [188].

The District Heating Assessment Tool developed by the Danish Energy Agency for decision makers offers a simplified TEM that is easily accessible and editable [189].

However, it cannot undertake an energy demand, energy supply and hydraulic analysis and it does not perform cashflow calculation for multiple energy supply options. FLEXYNETS presented a cohesive pre-design open access support tool for a techno-economic analysis of low temperature District Heating and Cooling networks (DHC) that is able to undertake a hydraulic analysis [190]. Still, the tool is limited to low temperature DHC networks, a building schedule cannot be specified, no detailed cashflow is present and no counterfactual cases are analysed [69].

Molyneaux et al. (2010) [191] developed a TEM, that incorporates the lifetime environmental impact of the project in the system assessment. The model investigates the effect of integrating individual WSHPs to 4GDH schemes on the overall cost and estimates CO₂ and NO_x emissions of the system. It proved that such a combination is beneficial but did not compare the boundary cases of a completely centralised and a decentralised WSHP heat network. However, the variables that affect the network's performance are not studied and no indication is given for when one network type should be selected over another while the model is not made open access.

Regarding analysis of different supply options for WSHPs, Wang (2018) [192] presented a comparison of individual and centralised HPs in the UK. They focus on overall trends for different network sizes without considering non-residential properties, building level plantrooms with communal heat networks, connections per property nor all the cost components present. Gudmundsson et al. (2022) [28] undertook a comprehensive comparison of 4GDH with ambient networks featuring decentralised HPs but for different source temperatures, not considering different scenario mixes while the model is not made publicly available. Table 6.1 summarises these findings.

Therefore, there is a need for a user-friendly open access numerical TEM that performs a preliminary feasibility analysis of alternative heat decarbonisation options. The tool should enable the determination of the boundaries for beneficial operation of different centralisation levels of WSHPs against counterfactual thermal systems. This can in turn enable decision makers (including local authorities) to screen which alternative heat network scenario holds greater economic potential before carrying out a full-scale feasibility study of the selected project. This is an essential step to enable an informed decision during the planning phase of the project.

Table 6.1: Summary of tools for heat network supply options assessment.

Tools	Open Access	Energy & hydraulic assessment	Economic assessment	Benefits	Drawbacks
EnergyPro	No	Energy	Preliminary	Commercial tools meant for feasibility studies, specialising in energy and hydraulic analysis. Widespread use in industry.	Not open access. High barrier of entry (programming skills) and no complete cashflow analysis. High input data requirement.
NPro	No	Both	Preliminary		
TERMIS	No	Both	Preliminary		
THERMOS	Limited	Both	Preliminary	Ease of use (friendly browser-based user interface). Complete feasibility assessment.	Not entirely open access, no complete cashflow. No option of using a simple building schedule as input.
District Heating Assessment Tool	Yes	No	Detailed Cashflow	Easily accessible and editable TEM. Extensive component cost database included.	No energy demand, energy supply and hydraulic analysis. No cashflow calculation for multiple energy supply options for scenario comparison.
FLEXYNETS	Yes	Yes	Preliminary	Open access techno-economic analysis tool, including hydraulic analysis. Cost database included for multiple components.	No detailed cashflow. No option for input of a bespoke building schedule. No option for analysing counterfactual energy supply cases.
Model from Molyneaux et al. (2010) [191]	No	No	Detailed Cashflow	Lifetime environmental impact assessment. Comparison of centralised and decentralised WSHP energy supply options.	Not open access. No indication on when one network type should be selected over another.

Tools	Open Access	Energy & hydraulic assessment	Economic assessment	Benefits	Drawbacks
Model from Wang (2018) [192]	No	Yes	Detailed Cashflow	Economic comparison of individual and centralised HP supply options in the UK, focusing on overall trends.	Not open access model. Analysis for single houses only.
Model from Gudmundsson et al. (2022) [28]	No	Yes	Detailed Cashflow	Techno-economic comparison of 4GDH and 5GDHC featuring decentralised HPs for different network temperatures.	Not open access model. No analysis of multiple scenario mixes.

6.1.2 Introducing CATHeaPS

CATHeaPS is developed in this work to allow a complete techno-economic analysis of 5GDHC and alternative supply options for an area. These alternative supply options include centralised 4GDH networks with decentralised AC units for cooling, building/flat level reversible ASHPs and individual GB and AC units. CATHeaPS includes energy demand, energy supply, hydraulic and economic analysis for each considered system. The economic analysis follows the guidelines for heat network project assessment published by the UK government [183,193]. The focus is on the UK market (prices, energy projections and CO₂ contents), but the overall trends and relationships established can advise projects on other markets.

CATHeaPS is made open access with supporting documentation on the algorithms used and can be found at the University of Glasgow's Enlighten Repository[§] [3]. The model also performs data analysis and is able to run multiple scenarios with a variation on selected system variables.

[§] Available online at: <https://researchdata.gla.ac.uk/id/eprint/1638>.

6.2 CATHeaPS methodology

CATHeaPS offers a combination of simplicity, sufficient coding capacity (through VBA), and widespread availability. It is intended to allow multivariable comparison and a break-even analysis of the results by running simulations across a range of different scenarios. It provides a comprehensive and effective economic and environmental evaluation of alternative approaches to supplying heating and cooling for a user-defined area input. The methodology followed in CATHeaPS is illustrated in Figure 6.2.

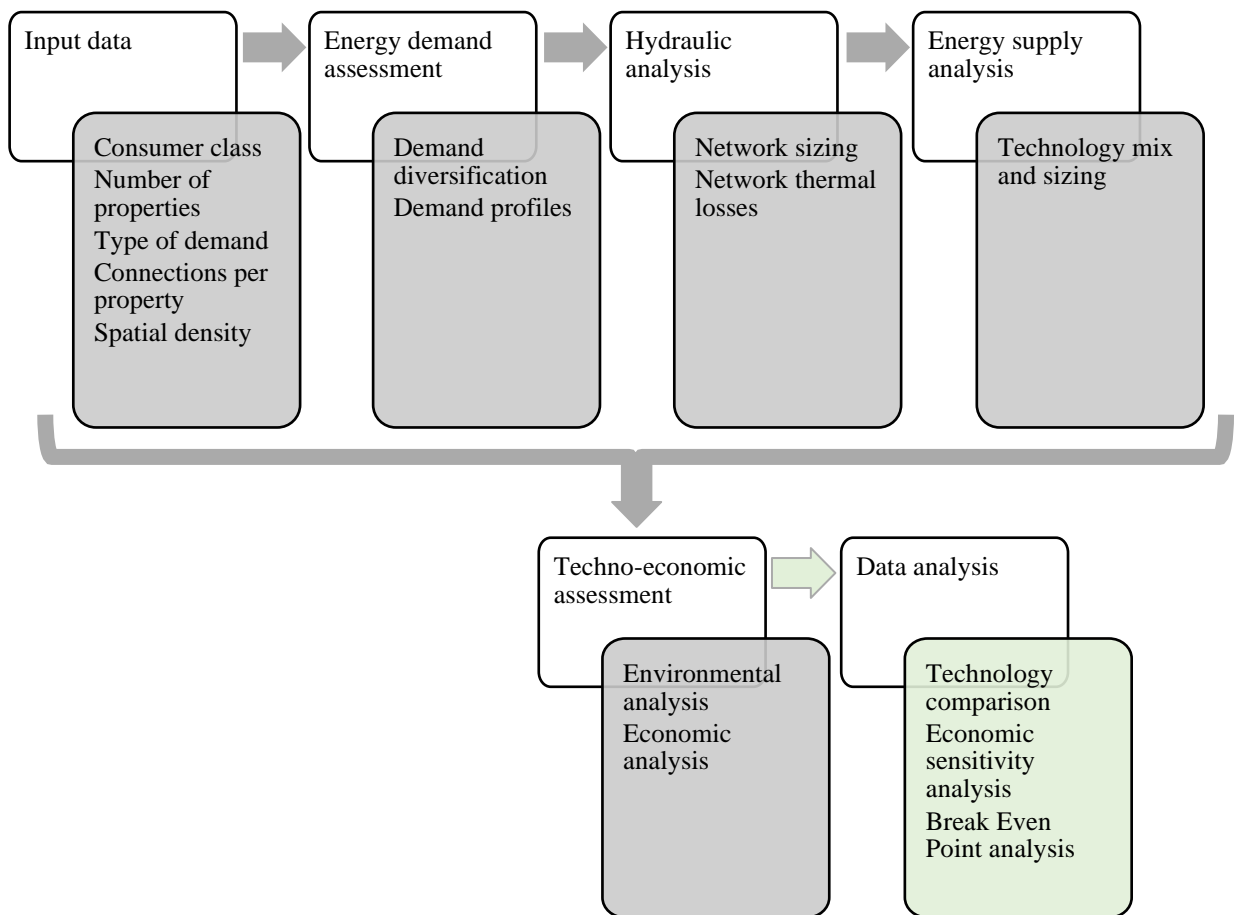


Figure 6.2: Schematic of CATHeaPS methodology.

In CATHeaPS, all networks are assumed to be linearly structured (one dimensional) rather than in an array, with uniform spatial density in line with [191]. Each property has a specified consumer class and number of connections. Retrofitting is not taken into consideration (i.e., the study accounts only for the connection of new built properties). Since the properties are newly constructed and have high insulation levels, the operating

temperatures for all 4GDH networks studied is assumed to be 60°C/40°C [43]. The cost and technical data refer to a UK case study starting in 2025 and a 40-year project lifetime.

The input data refers to information that need to be specified by the user to perform the analysis and are described in Table 6.2.

Table 6.2: Input data and their description.

Independent Variables	Unit	Description
Annual energy demand	kWh/year	This variable represents the annual energy consumption of a point of connection and mainly depends on the consumer class, the level of insulation and the outside temperature.
Peak power demand	kW	The maximum power requirement of a point of connection. For space heating/cooling this variable depends on the difference of outside and inside temperature while for DHW it depends on peak flow rate requirements [194].
Consumer class mixing	-	In each project area, there can be a range of consumer classes. The share of each consumer class in a network varies greatly and entirely depends on the specific case study.
Network alignment	-	The positioning of different properties in the network. Having properties with larger heat loads at the end of the network could influence negatively the overall economic performance due to larger diameters for larger segments of the network.
Connections in an individual property	-	The number of individual consumers in a single property. For example, a residential property could have 1 connection if it is detached or 50 if it is a large tower block with multiple flats.
Properties connected to the network	-	Total number of properties connected to the network.
Spatial density	property/m ²	Housing density of the network. The smaller the distance between consecutive properties the larger the density.

6.2.1 Energy demand assessment in CATHeaPS

The annual heating/cooling demand measured in kWh dictates the energy requirements of the network and therefore the fuel costs, heating/cooling sales and subsidy revenues (when available). Heating demand for domestic properties should be broken down into two components: DHW and space heating [195]. The reason for this distinction is that the weather usually only influences the space heating demand. DHW usage is not majorly

affected by weather conditions. Peak demand presents the instantaneous power requirements and dictates the design capacity of the energy transformation unit. When metered data are not available, the benchmark method is recommended, which involves the use of normalised values based on consumer class and floor area found in a range of international standards such as CIBSE TM46 [196] and CIBSE Guide F [197]. In CATHeaPS, CIBSE TM46 [196] is used for all commercial properties annual and peak demands. DHW is only considered for domestic properties [195]. Non-residential properties typically do not have DHW demand as it highly depends on the specific property and is common to have direct electric heaters at the point of use for it [43].

For the latter, the annual demand benchmark is set to 50kWh/m² which includes fabric efficiency measures [198]. Floor area benchmarks for non-domestic properties are set to 250m² as 75% of all non-domestic properties in the UK are less than this figure [199]. For domestic properties, the national average of 92m² equivalent to three bedroom flat is used [200].

For peak demand, 5kW per property are assumed for space heating [43] with the DHW peak set at 37kW. The design peak demand for DHW (P_{th_d}) is calculated through equation (6.1):

$$P_{th_d} = q_f \rho c_p \Delta T \quad (6.1)$$

where, ρ and c_p are set to the values for water at 55°C. ΔT is taken as the temperature of the water mains (10°C) [28] to the design DHW supply temperature (55°C). q_f is the peak flow rate which is set to 0.2 l/s corresponding to a 3-bedroom property [201]. By using one property, the DWH peak demand benchmark is found (37 kW) which is in line with literature [43].

For centralised systems, an additional process is required: the diversification of demand. This refers to the possibility of all properties requiring peak demand at the same time, which decreases as the number of properties increases. This is specifically true for DHW use where peak demand happens for some minutes in a day. This calibration of the peak demand, performed by multiplying the diversity factor with the sum of individual peak demands which can prevent oversizing of the heating supply technology and pipework, and

minimising capital and operational costs [20]. To determine the diversity factor, other than the number of properties present, the type of property and demand are needed. Bespoke curves based on metered data available from international standards can then be used. For this study, space heating, space cooling and DHW are diversified. DHW is diversified according to the methodology suggested in DS 439 [202] by calculating the design flow rate at peak demand, as shown in equation (6.2):

$$q_d = 2q_m + \theta(\sum q_f - 2q_m) + SF\sqrt{q_m\theta}\sqrt{\sum q_f - 2q_m} \quad (6.2)$$

where, q_d is the diversified design flow rate; $\sum q_f$ is the sum of all individual peak flow rates; q_m is the weighted mean flow rate (set to 0.11/s [202]); θ is the probability of draining (set to 0.0151/s [202]) during the peak load period; and SF is a safety factor (set to 3.11/s [202]). For space heating and space cooling, equation (6.3) provides the diversified peak according to Lauritsen et al. (2015) [203]:

$$DF_{SHC} = 0.62 + \frac{0.38}{N} \quad (6.3)$$

where DF_{SHC} is the space heating/cooling diversity factor and N the number of non-domestic properties. The diversifications factors for all demands are shown in Figure 6.3.

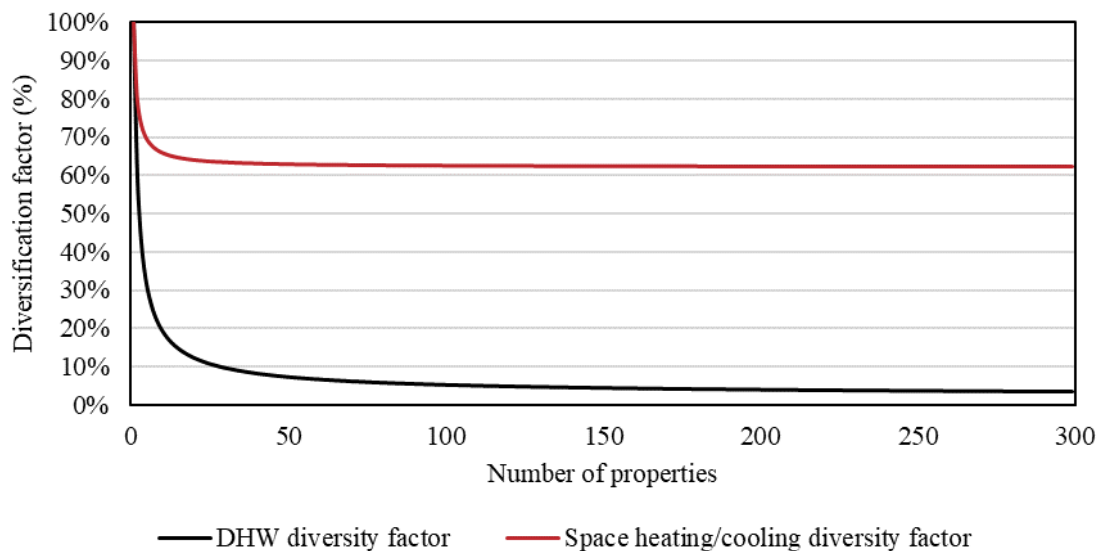


Figure 6.3: Diversification curve for DHW, space heating and space cooling.

6.2.2 Hydraulic design in CATHeaPS

The hydraulic analysis of a network comprises dimensioning pipe diameters in each network segment to ensure the pressure drop across them is below a design threshold [43]. This way, the network is able to supply the required flowrate to each individual property while abiding to pipe size dependent flowrate limitations. The expression tying the pressure drop per meter of pipe to the thermal power it needs to supply is presented in equation (6.4):

$$\frac{\Delta p}{L} = \frac{P_{th}^2 f}{D^5} \frac{8}{(c_p \Delta T \pi)^2 \rho} \quad (6.4)$$

where, the pressure drop per meter of pipe ($\Delta p/L$) is a function of the property's thermal power requirement (P_{th}), the pipe diameter (D), the Darcy friction coefficient (f), ΔT , c_p and ρ .

In this study, linearly structured (one dimensional) networks with equidistantly located loads are used as aforementioned. The minimum pipe diameter required to stay below a given pressure drop in each pipe segment is found through a bespoke algorithm. This algorithm iteratively calculates the pressure drop in each pipe segment, starting with the smallest diameter and increasing it until it falls below the threshold. A pressure drop threshold of 250 Pa/m is used [87]. Therefore, this hydraulic design of the network includes determining the smallest size of pipe that meets those restrictions for every pipe segment present in the network to minimise CAPEX without affecting consumer comfort or network lifetime.

Another element that needs to be taken into consideration, is that for a centralised branched network, the heat power requirement used to size the pipes needs to be the diversified peak demand. Since diversification is directly linked to the number of properties, towards the end of the network the pipe needs to meet the almost undiversified peak of the properties. The algorithm's logic used for sizing the 4GDH network is captured in the flowchart shown in Figure 6.4.

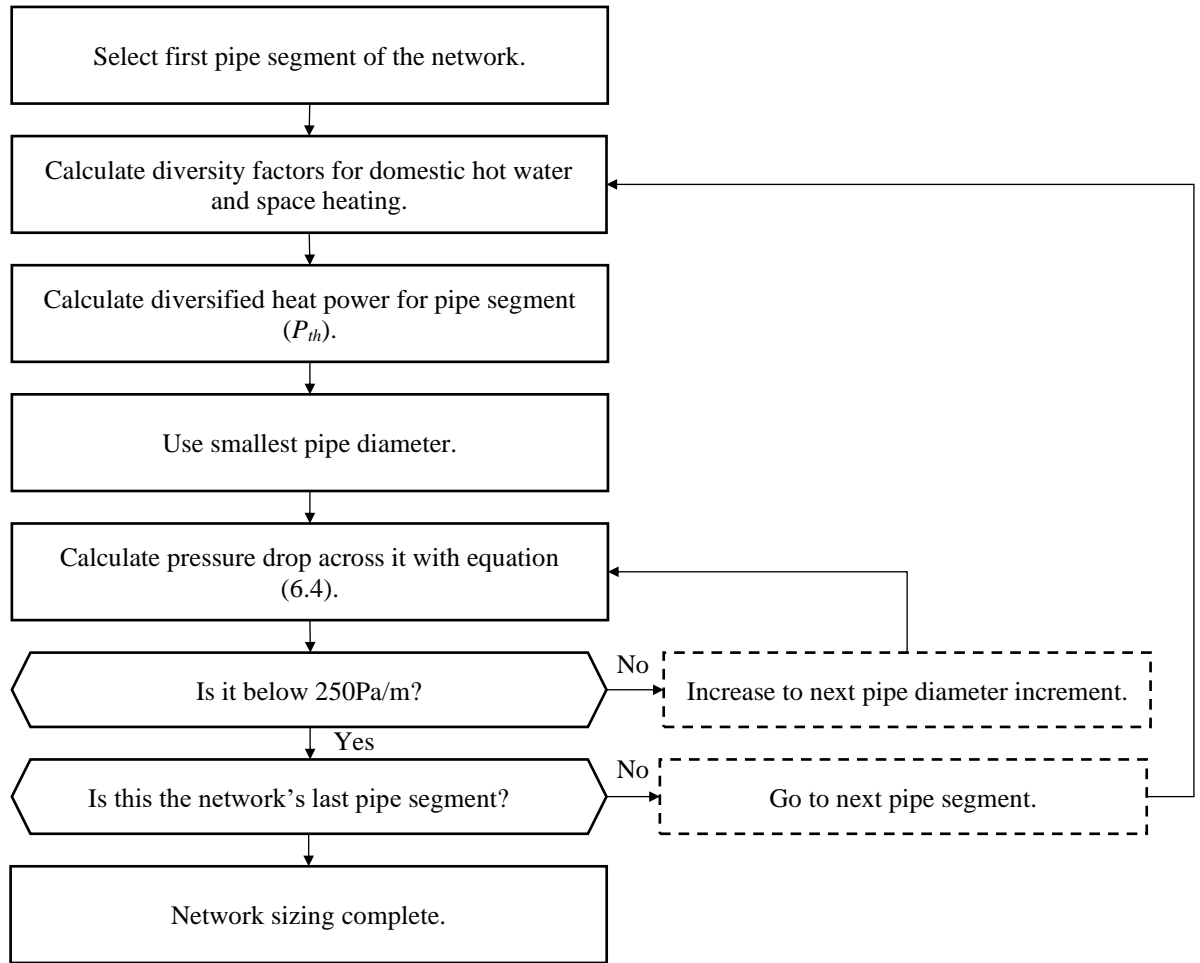


Figure 6.4: Flowchart for pipe sizing algorithm for 4GDH.

For the 5GDHC system with decentralised pumping, heating and cooling demands need to be taken into consideration. The same pipe sizing algorithm is used, only that this time, the maximum peak of heating/cooling is taken. In addition, the fact that the ambient network sees the BHP's source/sink power for heating/cooling operation rather than the building's peak power is considered. Equations 6.5, 6.6 and 6.7 capture how Q for the pipe sizing algorithm is derived for 5GDHC:

$$P_{th_{he,5GDHC}} = P_{th_{he,bui}} \left(1 - \frac{1}{COP_{BHP}} \right) \quad (6.5)$$

$$P_{th_{co,5GDHC}} = P_{th_{co,bui}} \left(1 + \frac{1}{EER_{BHP}} \right) \quad (6.6)$$

$$P_{th} = \max \left(P_{th_{he,5GDHC}}, P_{th_{co,5GDHC}} \right) \quad (6.7)$$

where $P_{th_{he,bui}}$ and $P_{th_{co,bui}}$ are the heating and cooling peaks of the buildings and $P_{th_{he,5GDHC}}$ and $P_{th_{co,5GDHC}}$ the peaks seen by the network. COP_{BHP} and EER_{BHP} are the BHP's COP and EER. The modified algorithm for pipe sizing in 5GDHC is shown in Figure 6.5.

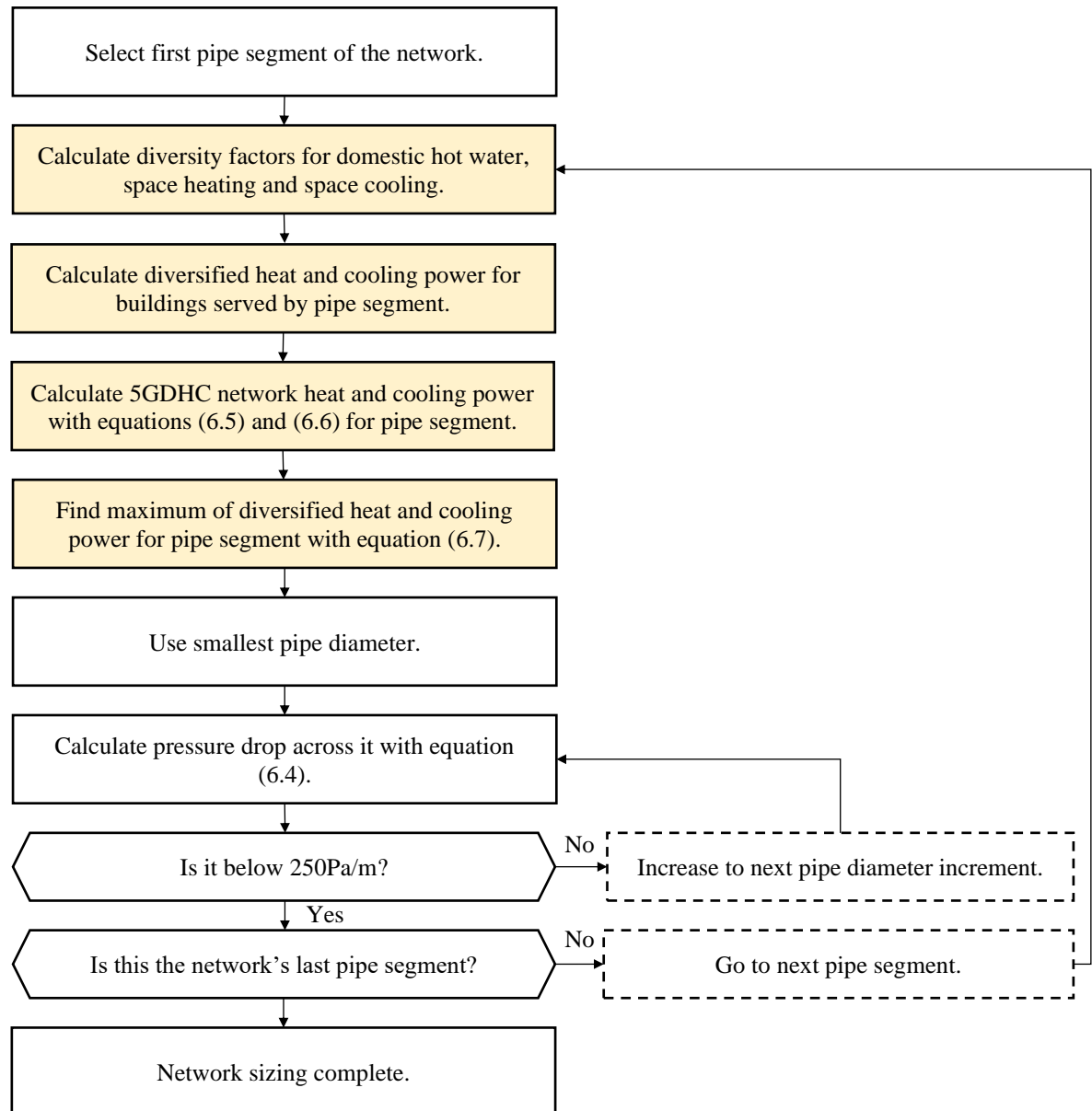


Figure 6.5: Flowchart for pipe sizing algorithm for 5GDHC.

Finally, for both centralised systems it is essential to offer localised energy control, hydraulic separation from the primary network and metering. For the 4GDH system, an indirect system with instantaneous DHW through hydraulic separation at each point of connection in the form of Heat Interface Units (HIUs) or Substations is used. For 5GDHC, building level BHPs are assumed so for residential properties with multiple flats, HIUs are

assumed in each flat. This hydraulic setup is shown in Figure 6.6 with a detail on the hydraulic connection for residential units with multiple connections in Figure 6.7.

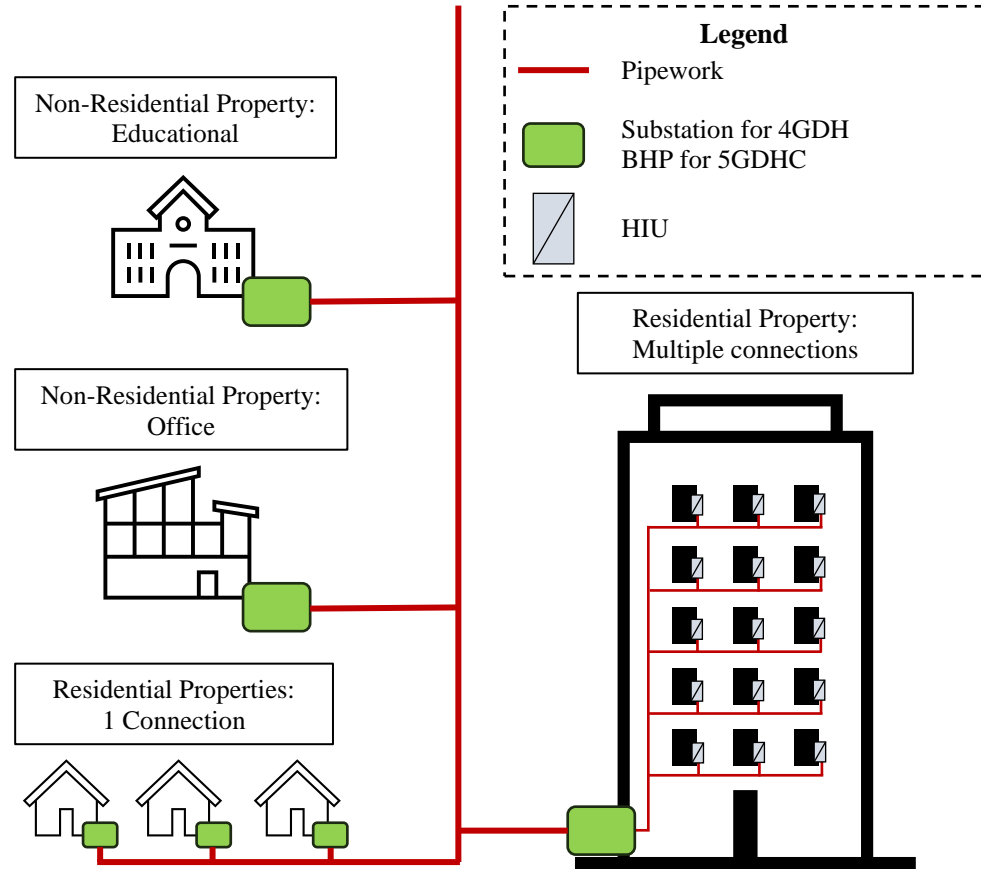


Figure 6.6: Connection methodology for 4GDH and 5GDHC systems in CATHeaPS.

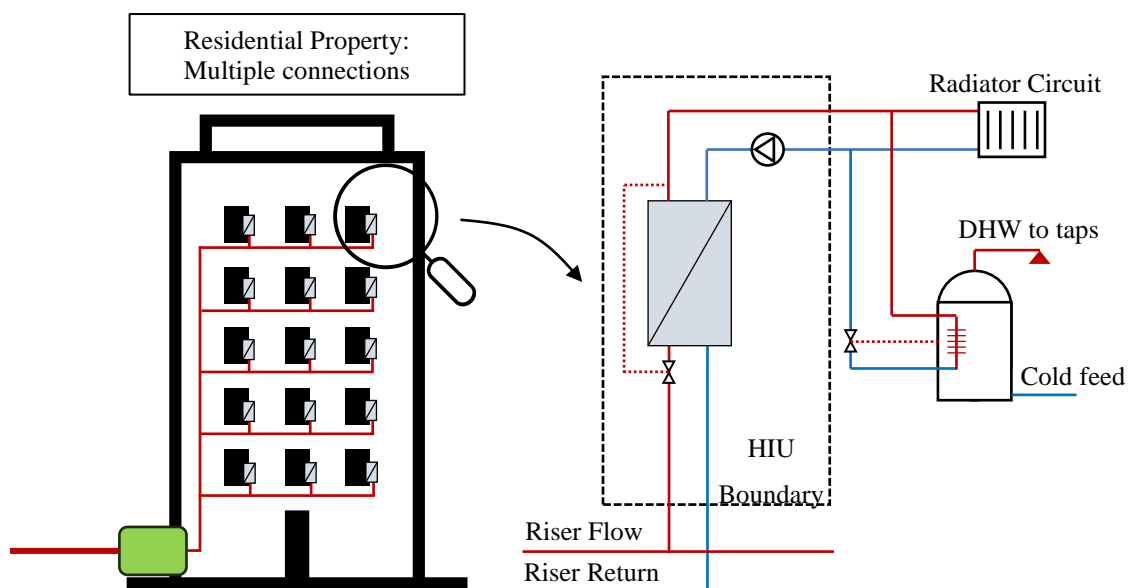


Figure 6.7: Connection methodology for residential units with multiple connections for 4GDH and 5GDHC systems in CATHeaPS (adapted from [43]).

6.2.3 Energy supply assessment in CATHeaPS

The energy supply assessment investigates the combination of a range of technologies to meet the demand requirements. For HP led schemes, thermal zoning, operating temperature levels, abstraction source characteristics and seasonal profiles along with the presence of TES are some of the parameters that indicate the capacity sizing of the equipment. An energy flow simulation is required to identify the performance of the designed system taking into consideration efficiency, turndown ratios, weather profiles, peak demand, backup and top-up capacity requirements and TES characteristics (water stratification, losses, and utilisation share). A complete operation strategy needs to be set to prioritise production of different units based on operational cost or emissions of CO₂. For this task, the outputs of the developed ProHMo models or other simulations tools could be used. However, since CATHeaPS is designed as a standalone tool, this process needs to be undertaken in the model. Since this is a high-level tool, the process needs to be simplified, while ensuring satisfactory accuracy.

For the GB&AC option, GBs and AC units are present in each property. The GBs are sized to meet both space heating and DHW demand while the AC units sized to meet the space cooling demands.

For the ASHP option, reversible units are assumed, meeting both heating and cooling demands. The DHW peak demand is met by a combination of the ASHP and a calorifier with an electric resistance [204]. The ASHP can charge the calorifier which is sized so that it can meet the instantaneous peak DHW flow rate [205]. For the residential dwelling used in this analysis of 3 bedrooms (and 2 bathrooms) with 92m² floor area [200] and corresponding to 0.20 l/s and 37kW DHW peak, a 200l cylinder is typical in the UK [206]. Such a cylinder meets the minimum storage requirement for a dwelling of this size [201]. For flats of this size, a 6kW_{thermal} HP can meet the space heating and space cooling demand. For non-residential properties the HP is sized to meet the entire heating demand as per guidance on how to perform counterfactual calculations [183].

For 4GDH&AC, the 4GDH EC comprises a ASHP with back up boilers (electric or gas) to meet the heating demand. The HP's share of heating is set to 90% and the operating hours to 6,000 which are typical design parameters for HP led 4GDH systems [43]. This setup

allows maximising its operation without oversizing the system [43]. The peaking boilers are sized to meet 80% of the peak demand [43]. This allows for sizing the ASHP's capacity ($P_{th_{HP}}$) as shown in equation 6.8:

$$P_{th_{HP}} = \frac{hp_s * AHD}{hp_{oh}} \quad (6.8)$$

where hp_s is the HP's share of heat, AHD is the annual heating demand with losses and hp_{oh} are the HP's operating hours. The AC units are sized for the individual cooling demands in each property. The efficiency and COP of each energy transformation unit is presented in detail in Appendix C, Table 12.1.

For 5GDHC, the peak demand of each building dictates the reversible BHP's capacity. As shown previously in Figure 6.6, centralised BHP are used for residential properties with multiple connections. For these communal BHPs, indirect space heating with a calorifier in each flat (with electric resistance) for DHW is assumed similar to the ASHP option. The communal BHP is sized to meet the maximum of the space heating and space cooling demands. During operation it could also feed the DHW TES tanks. For the BU, a combination of ASHP and electric boiler is assumed, sized in a similar manner to the 4GDH&AC case.

To determine the peak that the BU needs to supply, hourly profiles must be assessed, since for each project there will be a different share of heating and cooling. Data from the FLEXYNETS project are utilised [69]. The north Europe profiles are used, which are broken down to the average daily profile for winter, spring and summer season for both heating and cooling demand. In addition, the monthly shares of space heating and space cooling are used to fully characterise the hourly behaviour of the system. The daily hourly profiles are shown in Figure 6.8 while the monthly shares of space heating and cooling to the respective total demands are shown in Figure 6.9.

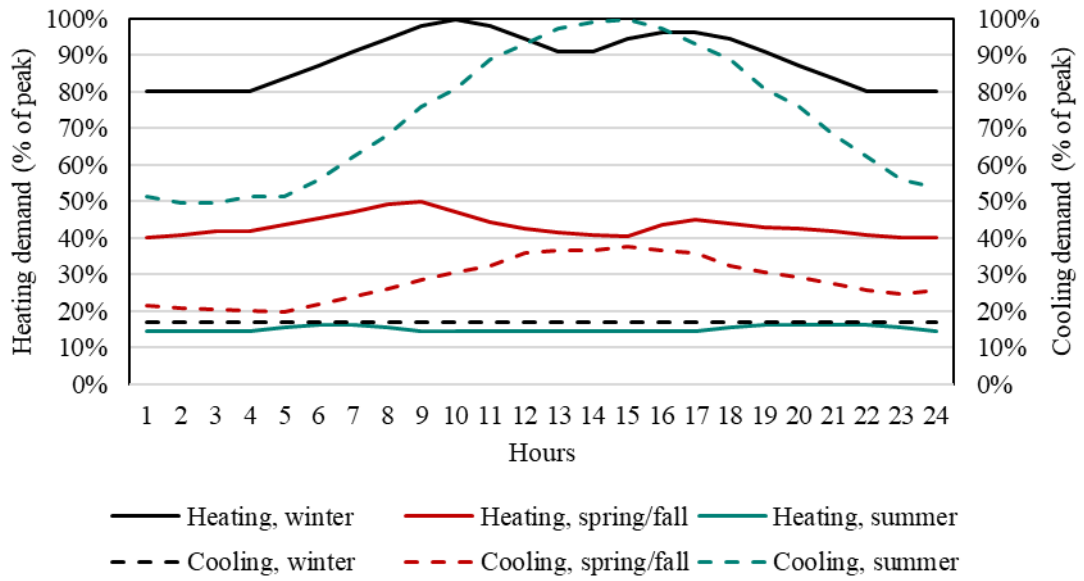


Figure 6.8: Normalised hourly demand profiles from FLEXYNETS [69].

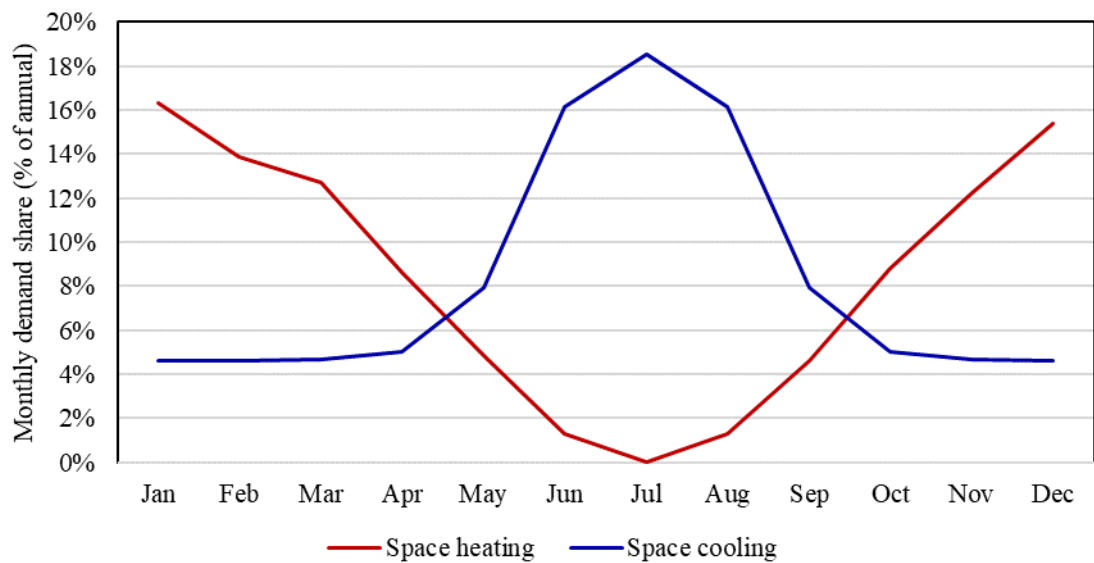


Figure 6.9: Normalised monthly demand profiles from FLEXYNETS [69].

Such an hourly analysis allows to find the maximum heating and cooling peak that occurs in the network (after the BHP’s evaporator/condenser) so that the plant can be sized. Seasonality of demand is taken into consideration too, so that co-occurrence of demand is accounted for. This is measured through the DOC in CATHeaPS, using an hourly timestep [29]. The energy that must be added to the network is thus determined, with an example of a 5GDHC system shown in Figure 6.10. Figure 6.10 includes the prosumer demands, the demands the network sees (before the BHP) and the energy supplied by the BU.

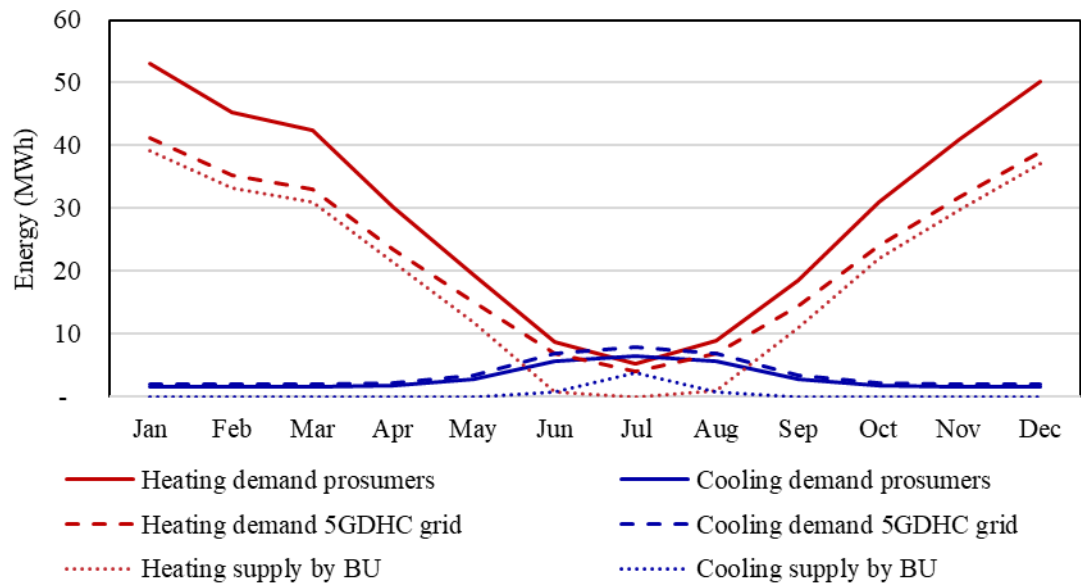


Figure 6.10: Example of BU balancing requirements for a fictitious 5GDHC scheme.

Heat losses must be accounted for in both 4GDH and 5GDHC networks. LOGSTOR's online calculator [207] is used to obtain the heat loss coefficients in (MWh/year) per meter of pipe for each pipe diameter. It uses system parameters such as soil heat transfer coefficient, soil cover and pipe characteristics [87]. The heat loss coefficients are also a function of fluid temperature and insulation series which are different for 4GDH and 5GDHC networks. Series 2 insulation is the selected solution for the 4GDH network and series 0 for the 5GDHC network, according to common practice [43,87].

For the CO₂ emission evaluation, the electricity emission factor used in CATHeaPS is not constant. This is due to the UK's national plan of increasing electricity generation from renewable energy to decarbonise the energy grid. The declining emission factor of the electricity network as projected by the UK's Department for Energy Security and Net Zero (DESNZ) is shown in Figure 6.11 [17]. Different factors are used for residential and commercial electricity consumptions. The emission factors for gas is set to 0.1835 kgCO₂/kWh [17].

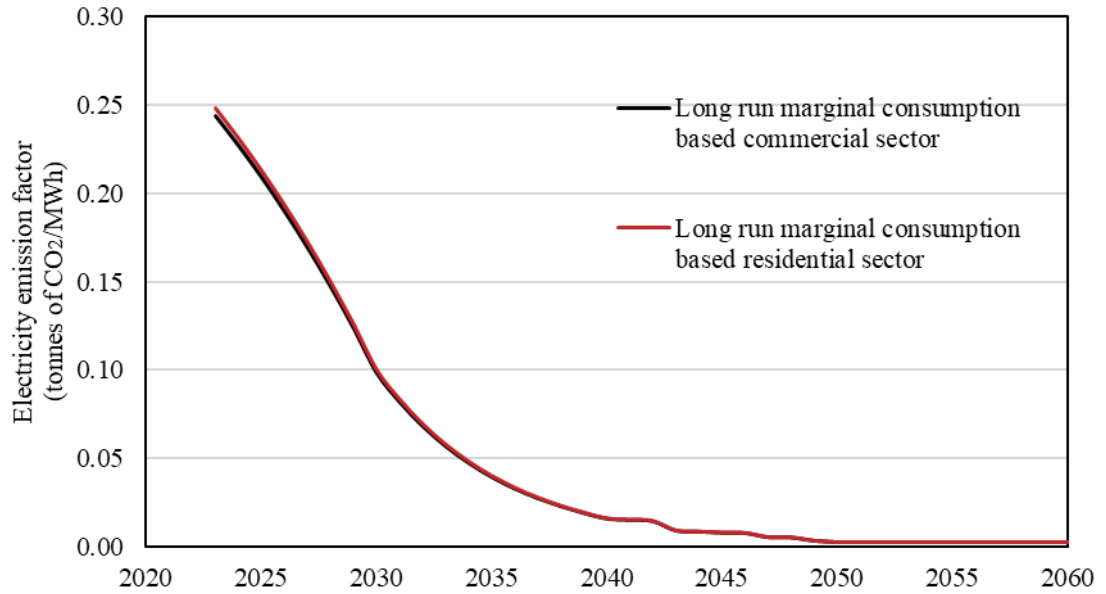


Figure 6.11: Electricity emission factors [17].

In this analysis, the development of the thermal source along with its specific economic, regulatory, hydrogeological and technical risks due to abstraction and deposition is not included. The reason for omitting these elements is the great variation of cost and technical details present depending on the nature of the technology which is highly project specific [28]. Therefore, the analysis considers everything after the point of abstraction.

6.2.4 Economic analysis in CATHeaPS

The economic analysis combines the results from all stages of the design to dictate the economic performance of the project, assessing the costs and revenues against energy, operation and maintenance costs. The economic performance is evaluated by the NPV and LCOE for a lifetime of 40 years [208], shown in equations 6.9 and 6.10. The NPV determines the present difference of the lifetime costs and revenues of the project, while the LCOE shows the present total cost per unit of energy consumed:

$$NPV = \sum \frac{-(CAPEX_{t_y} + OPEX_{t_y} + REPEX_{t_y} + Fuel\ Cost_{t_y}) + Revenues}{(1 + r)^{t_y}} \quad (6.9)$$

$$LCOE = \frac{\sum \frac{CAPEX_{t_y} + OPEX_{t_y} + REPEX_{t_y} + Fuel\ Cost_{t_y}}{(1+r)^{t_y}}}{\sum \frac{Energy\ Demand_{t_y}}{(1+r)^{t_y}}} \quad (6.10)$$

where *CAPEX* is capital expenditure, *OPEX* the operational expenditure, *REPEX* the replacement expenditure, *r* is the discount rate and *t_y* the number of years since the start of the project. Maximising NPV and minimising LCOE is desired for projects. CATHeaPS includes revenues as an option but only costs are considered in this analysis for comparison clarity, leading to always negative NPV values. The cost of decommissioning is not considered since it is assumed that residual liabilities are offset by residual value of assets [209].

The LCOE is selected as the key metric for the economic analysis due to its widespread use in literature for comparing different technologies [193], facilitating comparisons with national and international benchmarks such as UK benchmarks [17] and IEA benchmarks [210] for different heating and cooling technologies. This normalization of costs based on energy demand, combined with discounting future cash flows, provides a comprehensive view of the lifecycle costs associated with a technology. However, LCOE has several limitations. Its sensitivity to the magnitude of demand means that more energy-efficient properties, which have lower energy demands, can result in a higher LCOE for the same absolute cost. This can potentially misrepresent the economic viability of a technology. In additions, LCOE doesn't explicitly account for system size or economies of scale. A larger system might have a lower LCOE than a smaller one, even if the per-unit costs are similar. Therefore, the LCOE should be considered in conjunction the NPV and alongside considerations of system size, demand profiles, and other contextual factors. Comparing technologies based on similar demand profiles or energy efficiency levels is crucial for a fair assessment.

In addition, the concept of Social LCOE is introduced in the UK government's guidance on project appraisal and evaluation refer to as Green Book [193]. These social costs assign a cost to air quality impact and CO₂ emissions [211]. There are a range of costs that need to be included in a complete cash flow analysis, summarised in Table 6.3.

Table 6.3: Factors included in CATHeaPS supply options.

Cost Factors	4GDH&AC	5GDHC	ASHP	GB&AC
Discounted energy demand	X	X	X	X
Technology CAPEX	X	X	X	X
EC CAPEX	X	X	-	-
Building Connection CAPEX	X	X	-	-
Network CAPEX	X	X	-	-
Technology REPEX	X	X	X	X
EC REPEX	X	X	-	-
Building Connection REPEX	X	X	-	-
Network REPEX	X	X	-	-
Technology OPEX	X	X	X	X
EC OPEX	X	X	-	-
Building Connection OPEX	X	X	-	-
Network OPEX	X	X	-	-
Fuel cost	X	X	X	X
Social costs	X	X	X	X

The projections for the development of these costs over the years needs to be taken into consideration along with the relative value future cashflows will have compared to present ones. A discount rate thus needs to be used and published projections for energy prices to be included. For the UK, such projections are frequently published by DESNZ for different fuels [17]. A discount rate of 3.5% is used which is proposed for public led projects, while 7.0% would be typically expected for public/private collaborations [17,193]. In addition, the fuel cost projections are included in this study. Services projections are used for centralised equipment and non-residential properties. Residential projections are used in residential properties of decentralised supply options [17].

CAPEX and OPEX data used originate from DESNZ publications [212,213] and the Danish Energy Agency's cost database [189]. Interpolation methods are used when necessary, while Danish figures are transformed to UK figures by Eurostat's Purchasing Power Parities method [214]. Costs for utilities and miscellaneous items are included, accounting for ancillary plant associated with the network and EC (pumping; EC electricity costs and pipework; water treatment; pressurisation and expansion; and controls). Additional Costs for uplifts such as testing and commissioning, contingency, consultancy fees and design costs are included for all options in Technology, EC and Network CAPEX

using a figure of 30% [215]. REPEX is calculated based on the lifetime of the component, with 100% replacement assumed.

The electricity grid connection costs are not considered in the CAPEX figures for each technology. These include for potential upstream reinforcement such as transformers, switchgear and line changes of High Voltage (HV) or Extra High Voltage (EHV) grids. These costs are not included because they vary massively depending on the location of the project area and are unpredictable. Hence, it is advisable to contact the local Distribution Network Operator (DNO) [216,217]. However, typical figures are included for reference or if required to be used in a project valuation both for Low Voltage grid infrastructures with a high influx of HP [218] and for single points of connection (4GDH EC) of different capacities (in kVA) [219].

The key techno-economic data for CATHeaPS are also summarised in Chapter 12, Appendix C for clarity.

6.3 CATHeaPS verification

Given that no real operation data are available to allow for a complete model validation, the model can only be verified. The verification is split for the different supply options as shown in the following methodology subsection.

6.3.1 CATHeaPS verification methodology

For the 4GDH&AC supply option, the model is verified using the outputs from the conceptual design phase of a UK case study with slight modifications made and no georeferencing of the network to ensure confidentiality. The case study values used to verify the model are model outputs from commercial software, Energy Pro (version 4.8.526) [186] for energy flow analysis and System Rornet (version 8.1) [220] for hydraulic analysis. This network is referred to as Network 1. The verification is limited to 'heating only' districts since the project did not include cooling demands.

To verify the other supply options (5GDHC, ASHP and GB&AC), no data from commercial simulation models are available, so the theoretical results/analysis verification

approach is used [221]. If CATHeaPS' response to a controlled variation of the input parameters results in behaviour analogous to expectations based on relevant literature, the model is considered verified. For this verification process, the aforementioned network is used (Network 1), along with an additional fictional network with very different property characteristics. This network is referred to as Network 2.

To best study the performance of CATHeaPS, the networks are first analysed for 'heating only' districts and then cooling is introduced. The theoretical results/analysis verification approach is also used for studying the impact of cooling.

6.3.1.1 CATHeaPS verification methodology - Network 1

The building schedule of Network 1 is shown in Table 6.4, while the pipe schedule and network layout are shown in Table 6.5.

Table 6.4: Building schedule of Network 1.

Ref. Number	Connections	Class	Connection Year
1	12	Residential	2026
2	24	Residential	2026
3	367	Residential	2024
4	26	Residential	2024
5	59	Residential	2024
6	104	Residential	2024
7	17	Residential	2024
8	17	Residential	2024
9	45	Residential	2024
10	18	Residential	2024
11	38	Residential	2029
12	32	Residential	2025
13	18	Residential	2025
14	18	Residential	2025
15	32	Residential	2024
16	1	Public/Community	2029
17	2	Public/Community	2029
18	32	Residential	2025
19	2	Hotel	2024
20	1	Office	2024
21	1	Office	2024

Table 6.5: Pipe schedule and network layout for Network 1.

Pipe Diameter (DN) (mm)	Trench Length (m)	Layout
20	120	
25	0	
32	9	
40	142	
50	223	
65	154	
80	122	
100	127	
125	0	
150	313	

The key components that are investigated are the outputs from the energy demand assessment, the hydraulic analysis and the energy supply analysis. The economic outputs are also compared although their comparison depends on variations in cost values derived from supplier quotes specific to the project under consideration. The building schedule includes demand phasing, and the building density is set to match the network length of the case study. The SCOP for the HP is set to equal the one from the case study and the REPEX to 70% of original investment to obtain reliable results keeping the input parameters constant.

6.3.1.2 CATHeaPS verification methodology - Network 2

Network 2 is a fictional network, representing a typical small residential development with 70 detached residential houses. It comprises an equidistant linear network, with a total annual heating demand of 0.3GWh/year, and a building density of 60 buildings per hectare. The network layout and pipe schedule are shown in Table 6.6.

Table 6.6: Pipe Schedule and network layout for Network 2.

Pipe Diameter (DN) (mm)	Trench Length (m)	Layout
20	0	
25	13	
32	52	
40	90	

Pipe Diameter (DN) (mm)	Trench Length (m)	Layout
50	271	
65	478	
80	0	

6.3.2 CATHeaPS verification results and discussion

The verification outputs along with a discussion of the findings are presented below for both ‘heating only’ districts and heating and cooling districts.

6.3.2.1 ‘Heating only’ districts

The economic outputs for both Networks 1 and 2 are illustrated in Figure 6.12 (A) and (B) respectively. The LCOE is used as the Key Performance Indicators (KPI).

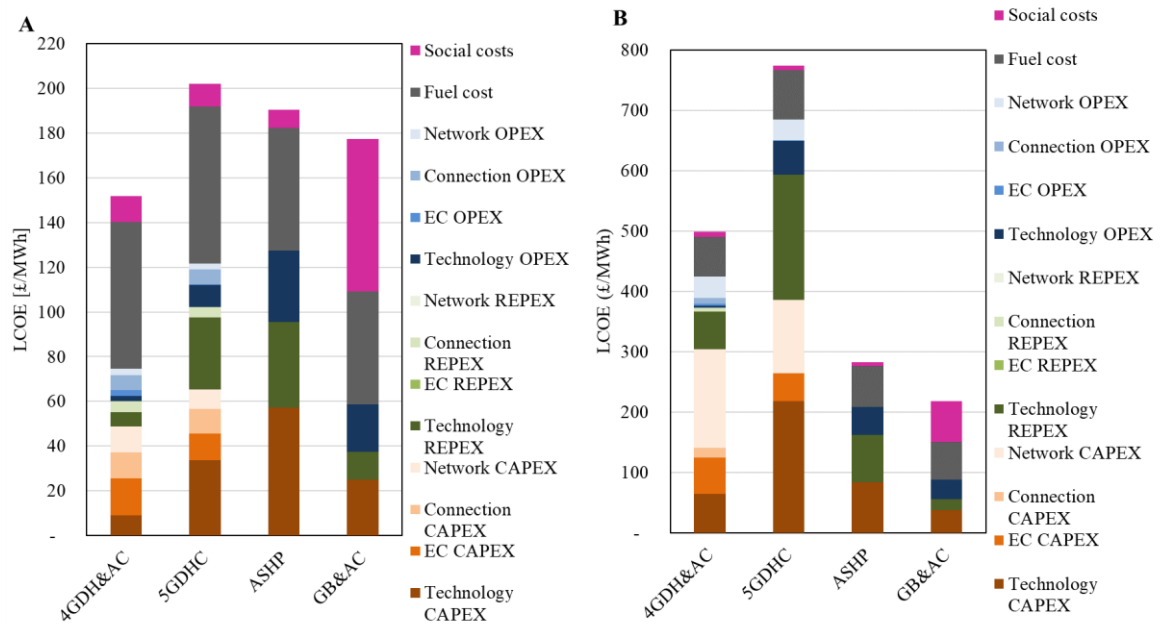


Figure 6.12: LCOE of Network 1 (A) and Network 2 (B) (heating demand).

As expected, for the network with the higher energy demand and number of properties (Network 1), centralised solutions perform better than decentralised ones and vice versa. 5GDHC performs poorly in both cases, since there is no cooling synergy to justify the additional costs from the BU’s equipment and EC costs. The fuel costs are the predominant cost element in Network 1 due to the high energy demand. For Network 2, infrastructure

elements (network and EC) are the key components of cost for the centralised solutions. For the decentralised options, the key parameters of cost are CAPEX for installation and replacement which due to economies of scale give a competitive advantage to centralised supply options for higher number of properties. Since centralised plantrooms are used for the 5GDHC option, the economies of scale apply to it as well when we have multiple connections per property as is the case for Network 1. Finally, the social costs are higher for the options using gas due to the decarbonisation of the electricity grid. These trends are in accordance with the research of [28,192,222] but a detailed verification of each supply option is conducted.

Network 1 outputs from the conceptual design phase using commercial software and the results given by CATHeaPS are shown in Table 6.7.

Table 6.7: 4GDH&AC supply option verification using Network 1 ('heating only' districts).

Item	Unit	Case study	CATHeaPS	Difference
Heating demand (Full built-out)	MWh/year	6,944	6,936	0%
Diversified peak demand	kW	4,940	5,015	2%
Heat losses (4GDH)	MWh/year	120	119	-1%
Pipe length (4GDH)	m	1,211	1,212	0%
Energy share of HP	%	83%	85%	
Phasing of demand		Yes	Yes	
HP size	kW	1,000	983	
Boiler back-up	kW	4,140	4,012	-3%
Electricity used (full built-out)	MWh/year	3,152	3,217	2%
CAPEX	k£	6,180	6,317	2%
OPEX	k£	3,713	3,602	-3%
REPEX	k£	3,120	3,215	3%
Energy costs	k£	16,525	16,459	0%
Social costs	k£	2,412	2,431	1%
Discounted expenditure (no social)	k£	17,633	18,142	3%
Discounted demand	MWh	131,881	129,448	-2%
LCOE	£/MWh	134	140	5%

Overall, CATHeaPS is within 5% discrepancy for all economic components. The key differences are in the network CAPEX where despite the similarity in length, there are differences in the pipe schedule with larger pipe diameter segments in the case study due to location of the loads in respect to EC. Finally, differences in electricity use come from the slightly different energy share of the HP.

For 5GDHC, the only relevant published data are found from the FLEXYNETS project. It is found that the LCOE of 5GDHC for ‘heating only’ districts lies between 100EUR/MWh and 150EUR/MWh [223]. CATHeaPS provides an output of 192£/MWh (228EUR/MWh) for Network 1, which represents a typical district-wide project area with multiple prosumers. The reason this is higher than literature, is that no BU is considered in FLEXYNETS and new buildings with high energy efficiency (and thus lower heating demands) are assumed in CATHeaPS. Without the BU costs (CAPEX, OPEX, REPEX and fuel for the BU and its equipment), the value of 126£/MWh is found (150EUR/MWh). This figure is within the FLEXYNETS range.

To verify the ASHP and GB supply options, a comparison with published LCOE data from an IEA assessment for residential properties [224] is conducted. Table 6.8 presents this comparison, including the theoretical LCOE ranges and the outputs from Network 2, which also comprises single residential properties.

Table 6.8: Verification of ASHP and GB using IEA published data [224].

Supply option	IEA Data	Network 2 Outputs	Network 2 outputs with triple annual heating demand benchmarks
ASHP	78-116 £/MWh (97-145 USD/MWh)	277 £/MWh	120£/MWh
GB	54-90 £/MWh (68-113 USD/MWh)	150£/MWh	84£/MWh

The IEA figures do not include ancillary costs, price projections nor social costs. More importantly though, they assume a heating demand of 13.0MWh/year, which is almost triple to the value accounted for in CATHeaPS for residential properties (4.6MWh/year). CAPEX is almost identical (8,781£/unit from IEA compared to 8,170£/unit for CATHeaPS). Therefore, it can be assumed that the two models have similar peak heating demands, but different annual heating demands with CATHeaPS using a considerable smaller annual heating demand figure. This is expected since the benchmark used for heating demand is accounting for new properties with the latest fabric efficiency measures being implemented, leading to considerably lower annual consumption [198]. If the same annual heating demand is used by tripling the heating demand benchmark in CATHeaPS, the LCOE excluding social costs of both ASHP and GB is near the high-end limit presented by IEA. All in all, it is decided to keep the annual heating demand benchmark of

50kWh/m² rather than tripling it since this is the state-of-the-art figure for new properties that are assessed in this research.

6.3.2.2 Heating and cooling districts

The models for Networks 1 and 2 are simulated again, only this time cooling is also considered. The impact of having cooling is shown in Figure 6.13.

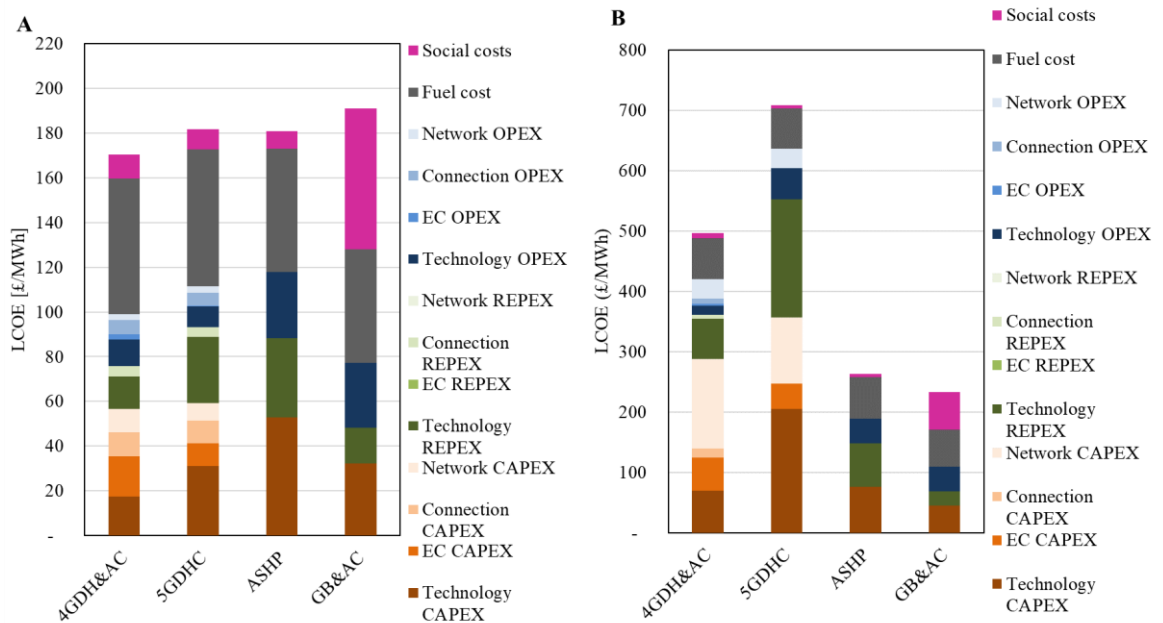


Figure 6.13: LCOE of Network 1 (A) and Network 2 (B) (heating and cooling demand).

For Network 1, a 598MWh/year annual cooling demand is introduced (9% of the heating demand) while for Network 2 this is 33MWh/year (10% of heating demand).

For Network 1, 4GDH&AC has an increased LCOE (14% increase) due to the introduction of the AC units (more CAPEX and REPEX for a small amount of cooling load). The same applies to the GB&AC option, where additional energy transformation equipment is required for a small cooling demand. The ASHP option has a reduction in its LCOE since it features reversible units, with a 5% decrease in its LCOE. The introduction of cooling has significantly improved the 5GDHC option. Its LCOE has decreased to 173£/MWh, a 10% decrease. This is due to the reversible BHPs, and the BU supplying less energy due to demand co-occurrence. The BU needs to add 580MWh less energy per year, which represents a nearly 10% reduction. No additional equipment is needed at BU level, since a

reversible ASHP is assumed. The BU’s energy supply share for Network 1 for ‘heating only’ is shown in Figure 6.14 and for heating and cooling is present in Figure 6.15.

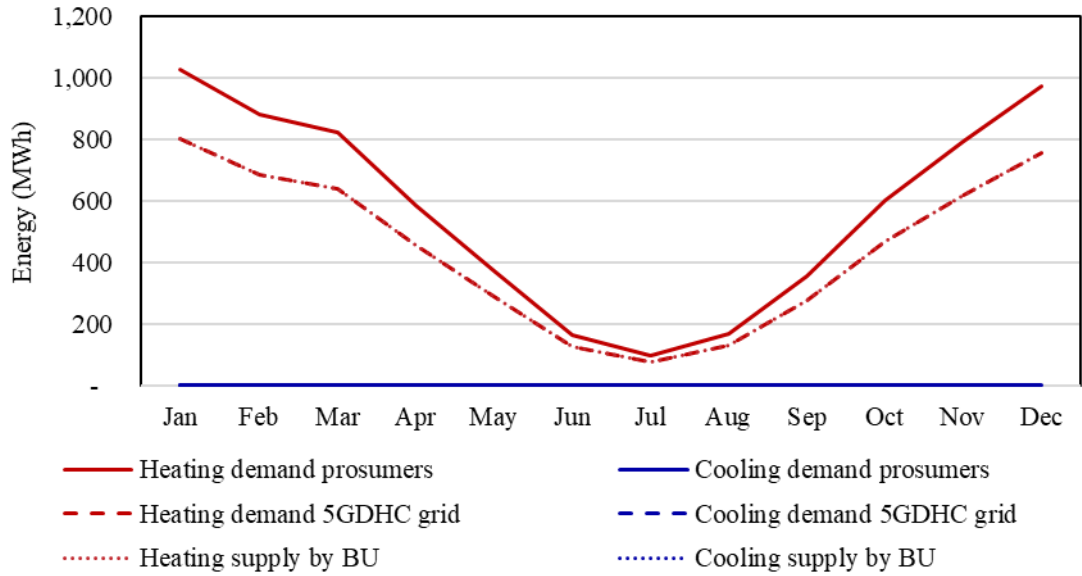


Figure 6.14: ‘Heating only’ scenario’s BU share for 5GDHC in Network 1.

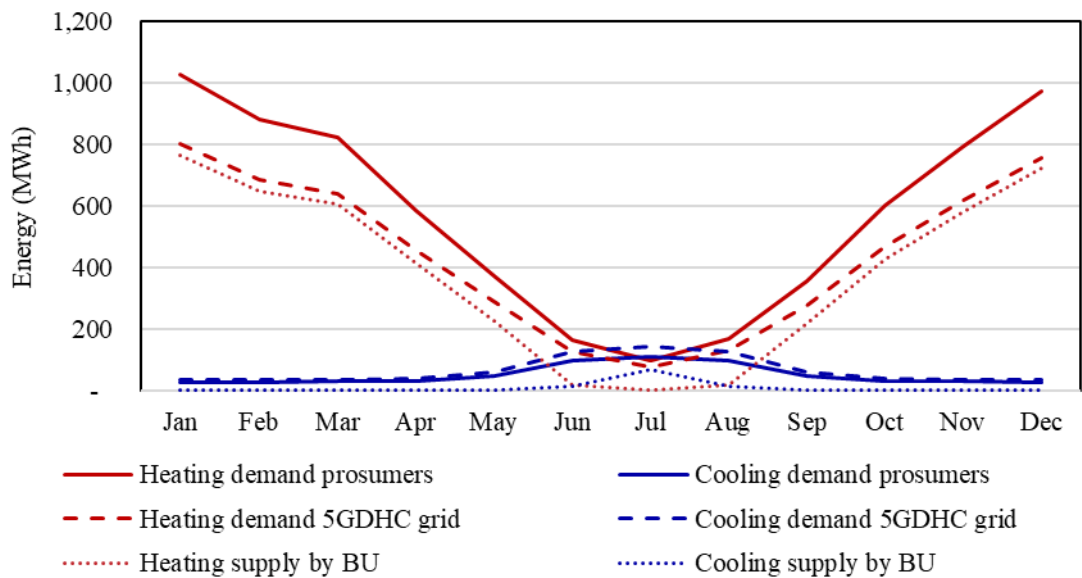


Figure 6.15: Heating and cooling scenario’s BU share for 5GDHC in Network 1.

For Network 2, the effect of introducing cooling is similar in percentages. However, the absolute difference is minimal, and the decentralised individual solutions remain better performing.

To further verify the model outputs for 5GDHC, the CAPEX share of different cost elements can be compared against published CAPEX data on a 5GDHC project in a college campus in New York [4]. This project features heating and cooling loads supplied by a 5GDHC system. The network consists of 34 buildings with a total demand of 25.5GWh/year of heating and 4.5GWh/year of cooling. No information is available on the details of the network's topology, nor its detailed economic performance other than the CAPEX share of the various components. CATHeaPS is simulated with 34 educational buildings, with the benchmarks calibrated so that the heating and cooling demand matched that of the project. The building density is also adjusted to match the length of the network (8,997m). The CAPEX share of the prosumer substation, centralised plant, and distribution network for both CATHeaPS and the published CAPEX data from Lauritsen et al. (2024) [4] are shown below in Table 6.9.

Table 6.9: Verification of 5GDHC using published CAPEX data [4].

Cost Cluster	Unit	Data from Lauritsen et al. (2024) [4]		CATHeaPS Outputs	
		Value	Share of total CAPEX	Value	Share of total CAPEX
Heating Demand	GWh/year	25.5	-	25.5	-
Cooling Demand	GWh/year	4.5	-	4.76	-
Network Length	m	8,997	-	8,779	-
Prosumer substations (BHPs, back-up boilers, pumps and TES) CAPEX	Thousand £	10,223	36%	7,620	30%
Centralised plant and storage CAPEX	Thousand £	12,687	45%	9,924	39%
Distribution network CAPEX	Thousand £	5,446	19%	8,040	31%
Total	Thousand £	28,356	-	25,584	-

CATHeaPS and the published data indicate a very similar CAPEX share, especially when considering cost variations occurring due to the different value chains between the UK and the USA. The only element with a large deviation is the network cost, with a 12% higher share than the one from CATHeaPS. This could be due to the project having different suppliers, hard vs soft dig and multiple complications that are present in a real project and cannot be accounted for in the high-level figures used in CATHeaPS. Overall, the

comparison between the CATHeaPS model outputs and published data demonstrates a good agreement for the 5GDHC system.

6.3.3 CATHeaPS verification sensitivity analysis

Other than investigating the economic outputs of the model against published data, it's important to analyse the sensitivity of the model to variations of its parameters. A sensitivity analysis investigates how changes in key input parameters affect the model outputs [225]. The One-Factor-at-a-Time sensitivity model will be followed which is the most used technique [226]. This is preferred due to its simplicity. Other than highlighting the sensitivity of the model, such an analysis would also indicate if there is a reasonable response to KPIs on system variations.

The analysed parameters are summarised in Table 6.10, each given a variation of -30% to 30% which is typical for feasibility stage work [183]. The sensitivity analysis is individually performed on each network where the output studied is the project's LCOE including social costs. The networks for conducting the feasibility study are Networks 1 and 2.

Table 6.10: Parameters included in the sensitivity analysis.

Parameters	Description of impact
CAPEX	A variation of all capital costs, which also influences the REPEX since the two are linked.
OPEX	Variation of the operational and maintenance costs.
Fuel Price Sensitivity	Variation of electricity and gas prices.
SCOP	Variation of the HP's SCOP. It depends on the inlet temperature. It affects the fuel cost for the HP, the CO ₂ produced (and thus the social costs) and the pipe sizing for the 5GDHC.
Discount Rate	Variation of the discount rate which is a way to quantify risk of future cashflows. By increasing it, future cashflows and energy supplied have a smaller value and thus a lesser impact on the LCOE.

The results of the sensitivity analysis for 'heating only' are shown in absolute terms in Table 6.11 and their relative impact on the LCOE can be seen in Figure 6.16. Heating and cooling demands are shown in Table 6.11 and Figure 6.17.

Table 6.11: Sensitivity analysis on 40-year LCOE with social costs for ‘heating only’.

Network 1												
Supply Option	Units	Base LCOE	CAPEX		OPEX		Fuel Price		SCOP		Discount Rate	
			-0.3	+0.3	-0.3	+0.3	-0.3	+0.3	-0.3	+0.3	-0.3	+0.3
4GDH&AC	£/MWh	152	137	166	147	156	132	171	169	143	137	175
5GDHC	£/MWh	152	137	167	148	157	134	171	170	143	138	175
ASHP	£/MWh	169	154	185	154	185	155	184	190	158	159	184
GB&AC	£/MWh	177	170	185	171	184	162	193	177	177	172	186
Network 2												
Supply Option	Units	Base LCOE	CAPEX		OPEX		Fuel Price		SCOP		Discount Rate	
			-0.3	+0.3	-0.3	+0.3	-0.3	+0.3	-0.3	+0.3	-0.3	+0.3
4GDH&AC	£/MWh	521	424	618	506	537	503	539	542	510	444	640
5GDHC	£/MWh	587	497	677	562	611	565	609	616	571	517	692
ASHP	£/MWh	282	257	307	257	307	262	303	312	267	264	309
GB&AC	£/MWh	218	207	229	208	227	199	236	218	218	210	230

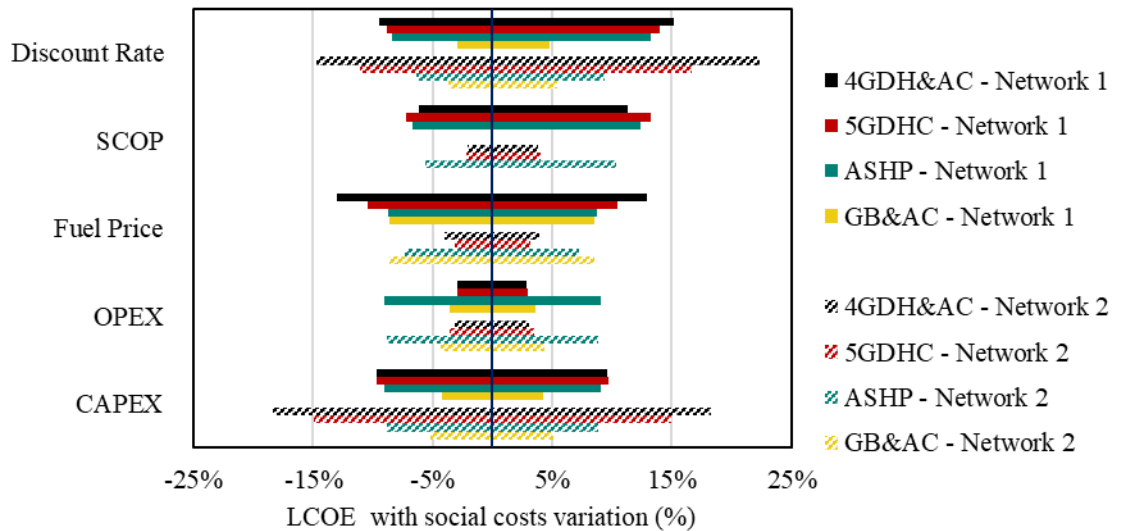


Figure 6.16: Normalised sensitivity analysis outputs (‘heating only’).

Table 6.12: Sensitivity analysis on 40-year LCOE with social costs for heating and cooling.

Network 1												
Supply Option	Units	Base LCOE	CAPEX		OPEX		Fuel Price		SCOP		Discount Rate	
			-0.3	+0.3	-0.3	+0.3	-0.3	+0.3	-0.3	+0.3	-0.3	+0.3
4GDH&AC	£/MWh	152	137	166	147	156	132	171	169	143	137	175
5GDHC	£/MWh	152	137	167	148	157	134	171	170	143	138	175
ASHP	£/MWh	169	154	185	154	185	155	184	190	158	159	184
GB&AC	£/MWh	177	170	185	171	184	162	193	177	177	172	186
Network 2												
Supply Option	Units	Base LCOE	CAPEX		OPEX		Fuel Price		SCOP		Discount Rate	
			-0.3	+0.3	-0.3	+0.3	-0.3	+0.3	-0.3	+0.3	-0.3	+0.3
4GDH&AC	£/MWh	521	424	618	506	537	503	539	542	510	444	640
5GDHC	£/MWh	587	497	677	562	611	565	609	616	571	517	692
ASHP	£/MWh	282	257	307	257	307	262	303	312	267	264	309
B&AC	£/MWh	218	207	229	208	227	199	236	218	218	210	230

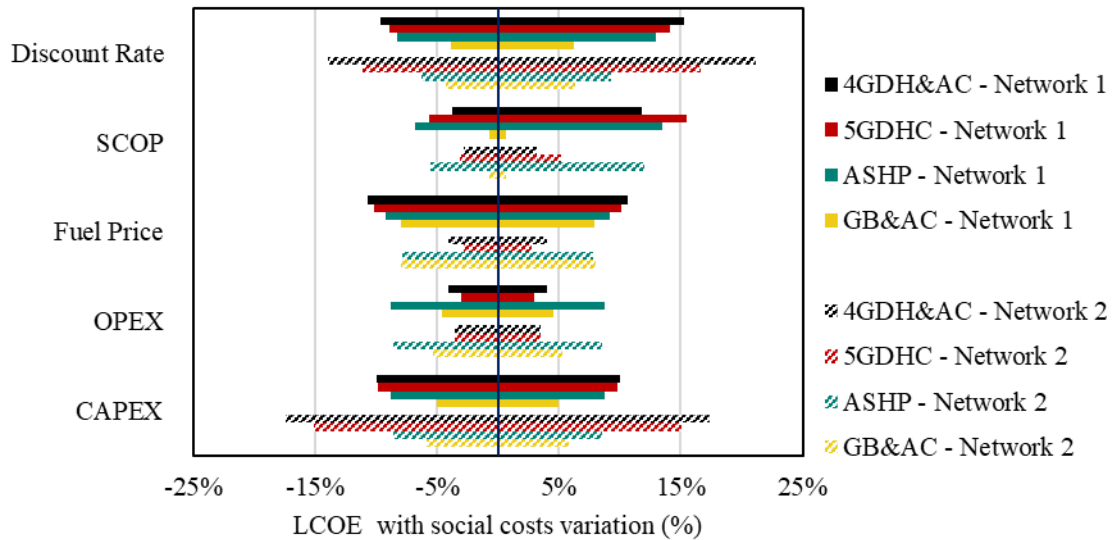


Figure 6.17: Normalised sensitivity analysis outputs (heating and cooling).

The analysis reveals that both ‘heating only’ and heating and cooling districts have an almost identical response to variable variations. Only 5GDHC and ASHP systems become slightly less sensitive to SCOP and fuel price variations. More importantly, smaller

networks are more sensitive to CAPEX fluctuations for centralised solutions. This is attributed to the inclusion of large, fixed investments for plant and network infrastructure. This can also be seen by the impact of the discount rate that reduces the impact of future energy demand, increasing the impact of expenditures on earlier years, and thus affecting projects irrespective of size for centralised solutions. Following the discount rate, for Network 1 the fuel price has the second largest impact on centralised networks since it's a large expenditure happening annually. Interestingly, the impact on the LCOE changes for Network 2 with a greater effect on ASHP and GB&AC options. This is since for smaller networks, the major cost component is CAPEX and fuel plays a minor role due to some fixed costs which are not linearly increasing with the capacity required (network, EC, building connections). Expectedly, the SCOP has a similar impact to the fuel price sensitivity since the two are linked. OPEX has the smallest impact for all options other than ASHP due to its low value. Overall, investment expenditures have the largest impact on small networks due to their low energy demands. Energy use related factors have the main impact on larger networks with the discount rate selected being critical irrespective of project area size.

Given that all behaviours can be justified and are logical, along with the discussions throughout this section, CATHeaPS is considered verified. Other than using it for bespoke projects, it is of interest to highlight how it can be used for conducting other economic and environmental analyses.

6.4 CATHeaPS for economic and environmental analyses

CATHeaPS offers the capability of analysing the economic and environmental behaviour of different project areas. Other than looking at bespoke project areas, it can be used to discover trends to provide preliminary indications to decision makers. In this work, an economic and an environmental analysis are conducted.

For the economic analysis, a break-even analysis is conducted. The break-even analysis examines the location of the break-even point (BEP). Break-even analysis is used in technology comparisons, to determine at what value of an independent variable one technology becomes more expensive than the other [192,227]. In the context of this study, the BEP is defined as the number of properties after which one supply approach becomes

economically better than another. An example of the BEP for a network is illustrated in Figure 6.18.

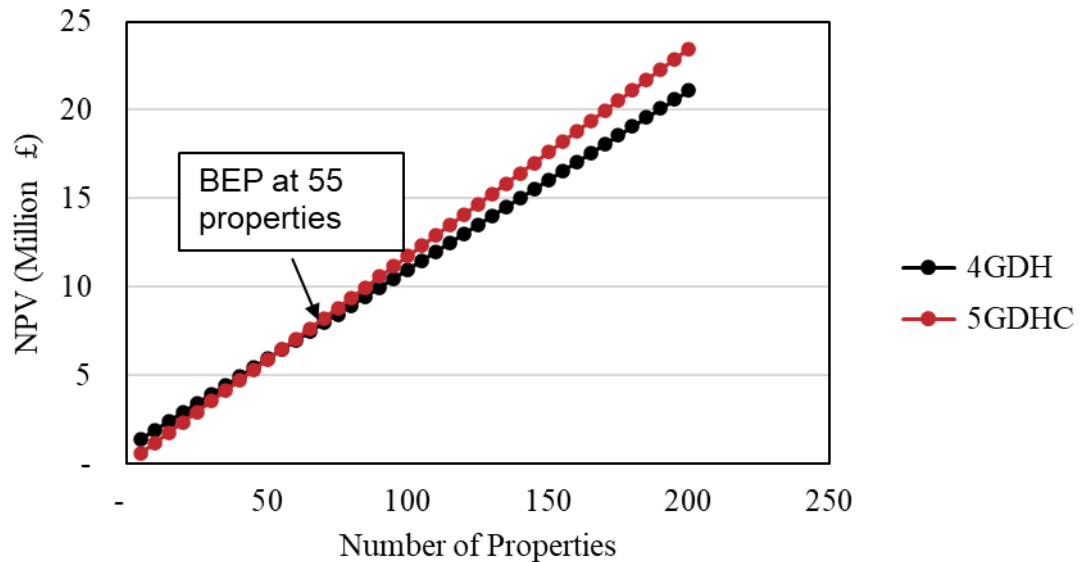


Figure 6.18: Break-even point example for 4GDH and 5GDHC networks.

To conduct a break-even analysis, the parameters of the project need to be set out and kept constant. By varying some system parameters while keeping the other constant, the fluctuation of the BEP can be mapped for all independent variables (property density and number of connections per property). In this work, a network with one consumer class (residential) and a uniform number of connections is preferred. This gives a simple system configuration that allows a clearer investigation of the BEP, avoiding interferences from consumer class and connection number related variables. The BEP is compared in pairs:

- 4GDH&AC – 5GDHC; 4GDH&AC – ASHP; 4GDH&AC – GB&AC
- 5GDHC – ASHP; 5GDHC – GB&AC
- ASHP – GB&AC

This BEP analysis can provide a preliminary indication to decision makers to evaluate projects.

For the environmental analysis, the CO₂ emissions of the supply options for different project input parameters and the relationships between them are investigated. To this aim,

a Monte Carlo simulation is used to explore the individual and combined effects of the four key project parameters on CO₂ emissions, following the methodology from Ioannou et al. (2020) [228]. Each input variable has the following probability distributions:

- Number of properties: uniform distribution between 10 and 100 properties.
- Density: uniform distribution between 10 and 75 properties per hectare.
- Consumer class: 50% probability for residential properties and 50% probability for non-residential properties. For the non-residential properties there is a uniform distribution between them, of 10% each.
- Connections per property: Dependent on consumer class to best represent reality:
 - For residential uniform distribution between 1 and 40 (detached houses or properties with multiple flats).
 - For non-residential properties fixed at 1.

Regarding their joint probability, each parameter is treated independently, having randomly selected values from their respective ranges. 10,000 project scenarios are generated in this manner and simulated in CATHeaPS to provide a comprehensive picture of the impact of each parameter on CO₂ emissions and their potential interactions.

For both the economic and environmental analyses, three project area scenarios are considered. They are selected to provide indications for the most typical scenarios that decisions makers may encounter in northern Europe. They also highlight the impact of cooling and system design to the overall performance. The cases considered are:

- a) **‘Heating only’ districts with access to an ambient temperature waste heat source**
 This scenario is typical for UK rural areas with access to water (river, lake or flooded mine), and it can shed light on when it’s better to prefer centralised over decentralised WSHPs. Cooling demand is not present in such scenarios. Since only heating is taken into consideration and a HEX is used to draw heat from the ambient temperature waste heat source. This simple approach requires no decentralised pumping, it requires only an abstraction centre with a HEX and a TES. Bidirectional flows are also not present, and decentralised pumping can be avoided. To distinguish from 5GDHC, and avoid confusion, the term Anergy Network (AN) is used for the decentralised system with building level WSHPs. Altogether, this AN has a unidirectional flow regime with

centralised pumping and decentralised WSHPs meeting only heating demands, taking heat from the hot line (10°C to 15°C) and supplying it to cold one (5°C to 10°C).

Figure 6.19 shows a schematic of the setup for the AN.

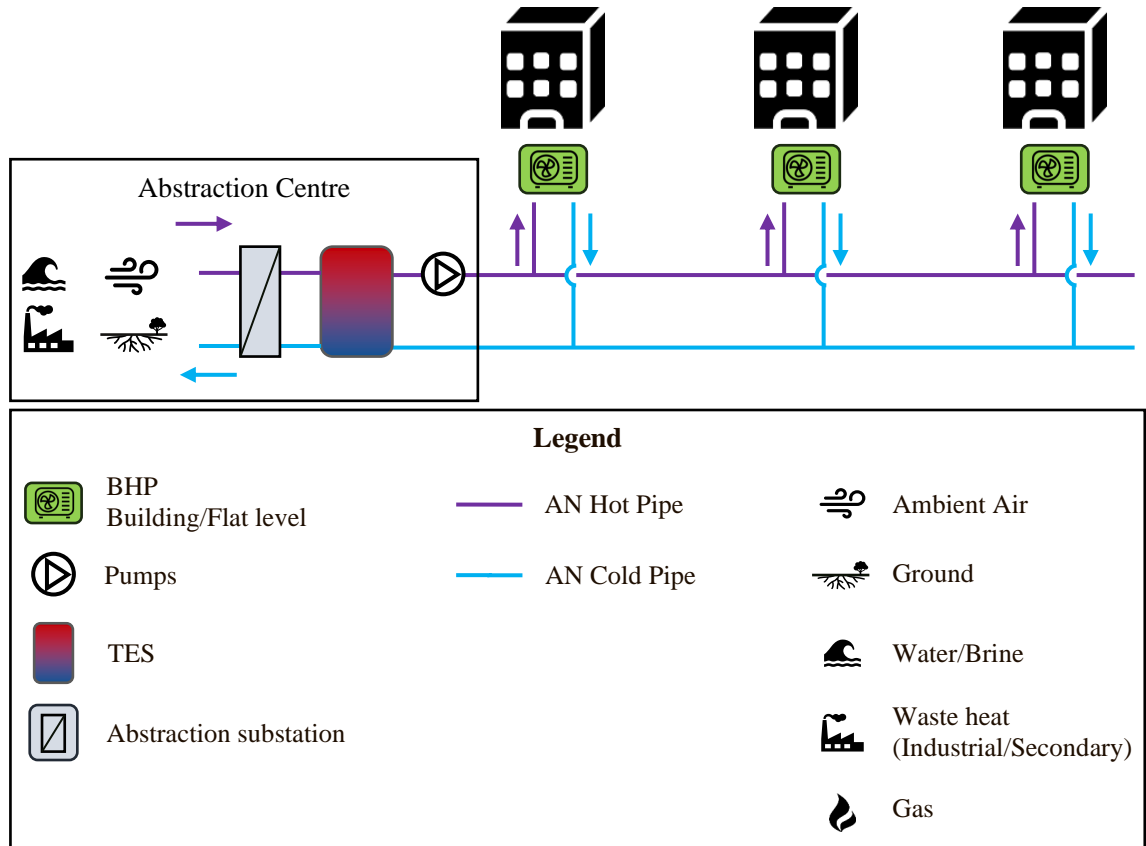


Figure 6.19: AN schematic.

The supply options for this setup include the same supply options described in this chapter, without cooling (4GDH, ASHP and GB). 5GDHC is replaced by AN. A schematic of the options is shown below in Figure 6.20.

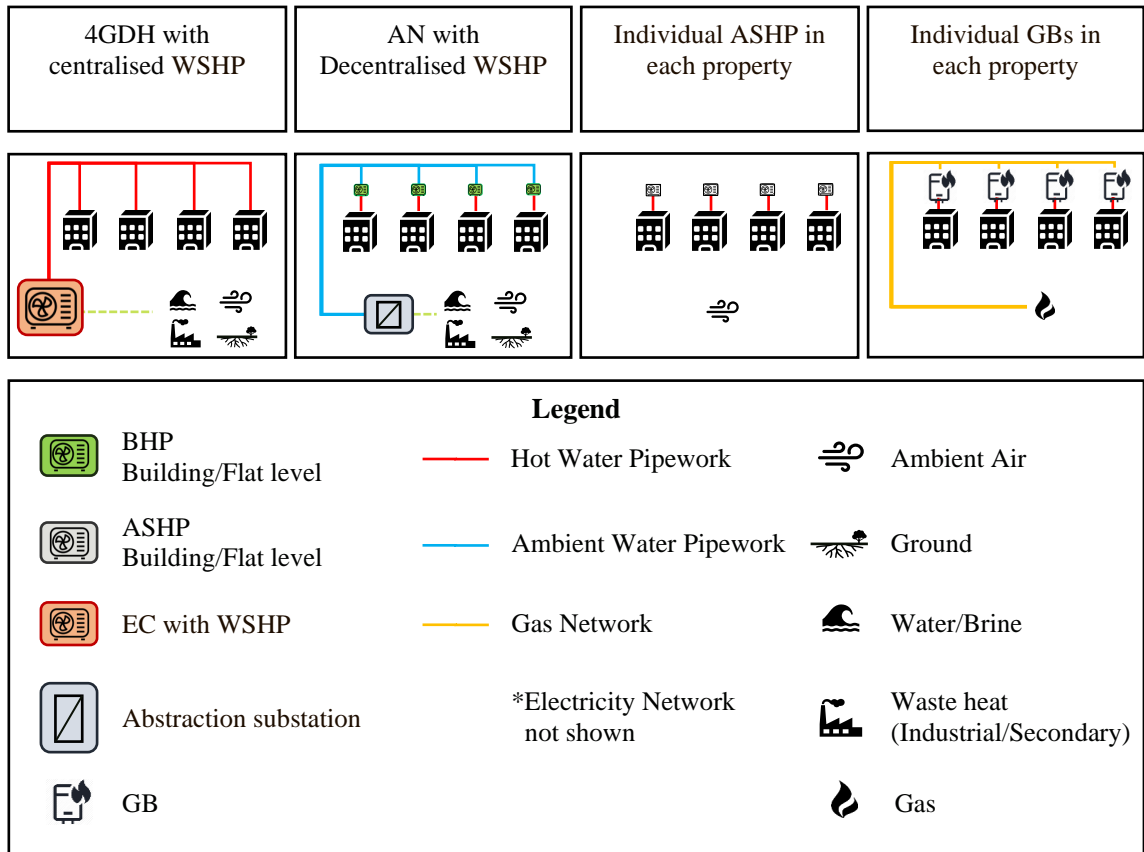


Figure 6.20: Supply options considered for ‘heating only’ districts with access to an ambient temperature waste heat source.

b) ‘Heating only’ districts

A heating demand only district with a BU featuring an ASHP for 5GDHC. This would be more typical for urban areas with little access to an ambient temperature waste heat source, where cooling demands are not present. The analysis will focus on the number of properties needed for different project characteristics and the sensitivity of the BEP on various project variables.

In this case, no access to an ambient temperature waste heat source is assumed.

Therefore, the 4GDH and 5GDHC options rely on a centralised ASHP for the EC and BU respectively. A schematic of the supply options is shown in Figure 6.21.

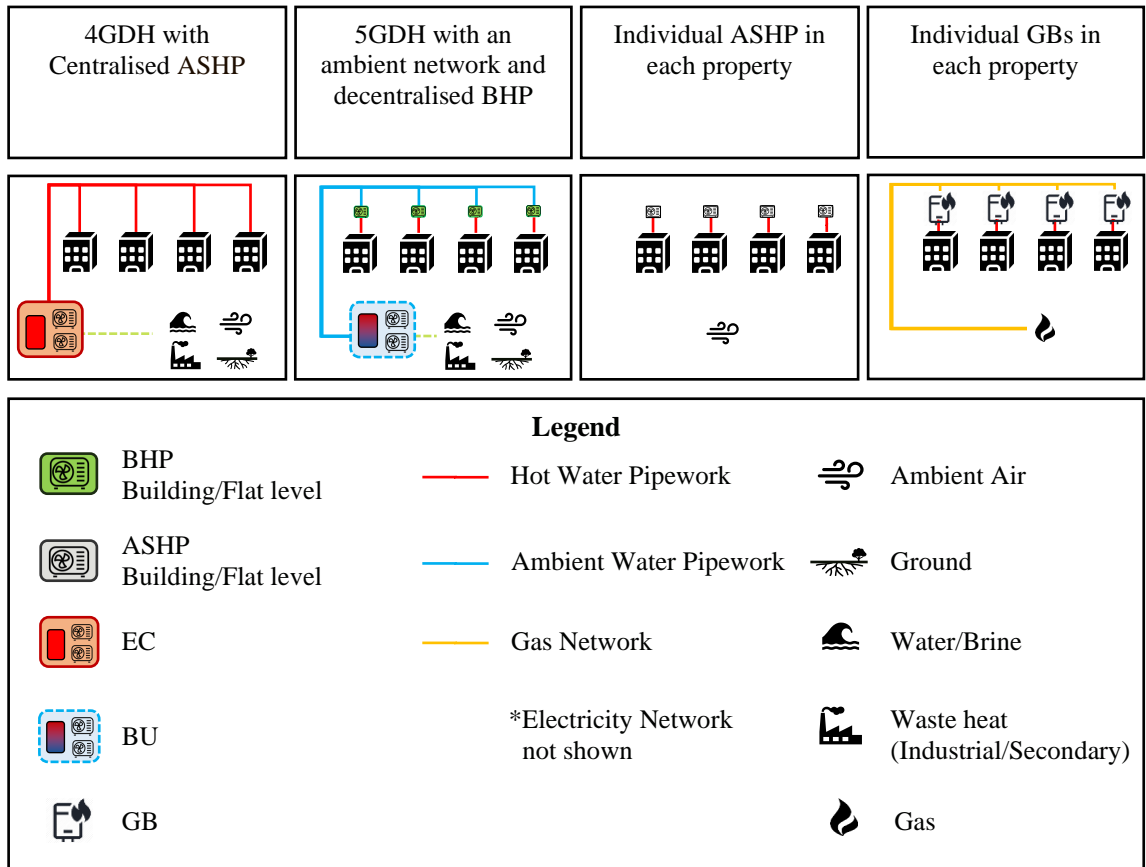


Figure 6.21: Supply options for ‘heating only’ districts.

c) Heating and cooling districts

A heating and cooling district with a BU featuring an ASHP for 5GDHC. This case would be typical for urban areas with new developments. The same setup as the one in (b) is used, only that this time AC units are introduced in the 4GDH and GB supply options. The supply options are shown below in Figure 6.22. CATHeaPS is used for variations in the share of annual cooling demand to the share of annual heating demand.

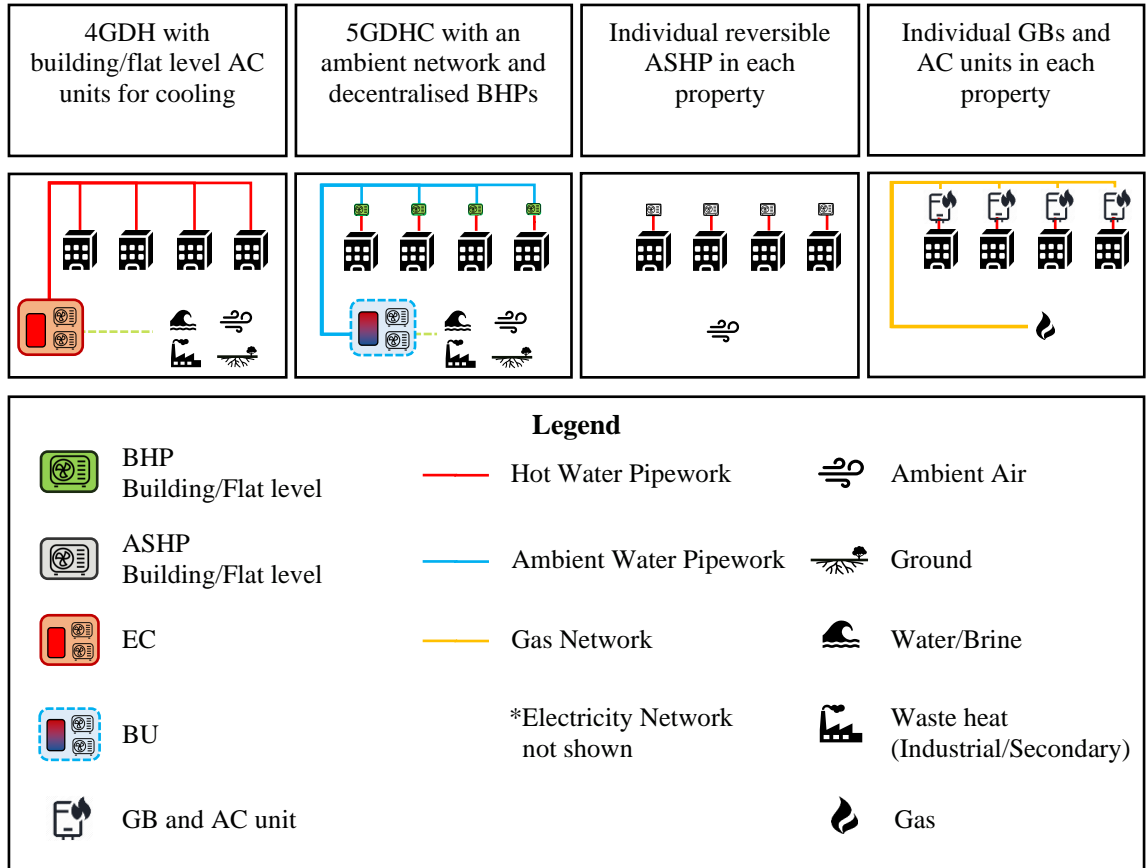


Figure 6.22: Supply options for heating and cooling districts.

6.5 CATHeaPS for economic analysis – BEP

The outputs of the BEP analysis are presented below for the aforementioned project area scenarios. All simulations are performed in the same laptop as the one mentioned in Section 5.2 using Excel, Microsoft 365 & Retail (Windows) version 2412. All simulations lasted between 1s and 3s, with the number of properties influencing the computational time. The average computational time to simulate up to 3,000 properties is shown in Table 6.13.

Table 6.13: Average computational time for CATHeaPS for different number of properties.

Number of properties	10	500	1,000	2,000	3,000
CPU time (s)	1	2	3	5	7

6.5.1 BEP of ‘heating only’ districts with access to an ambient temperature waste heat source

Figure 6.23 contains the graphical outputs from the BEP analysis for 4GDH - AN, 4GDH – ASHP, and 4GDH – GB.

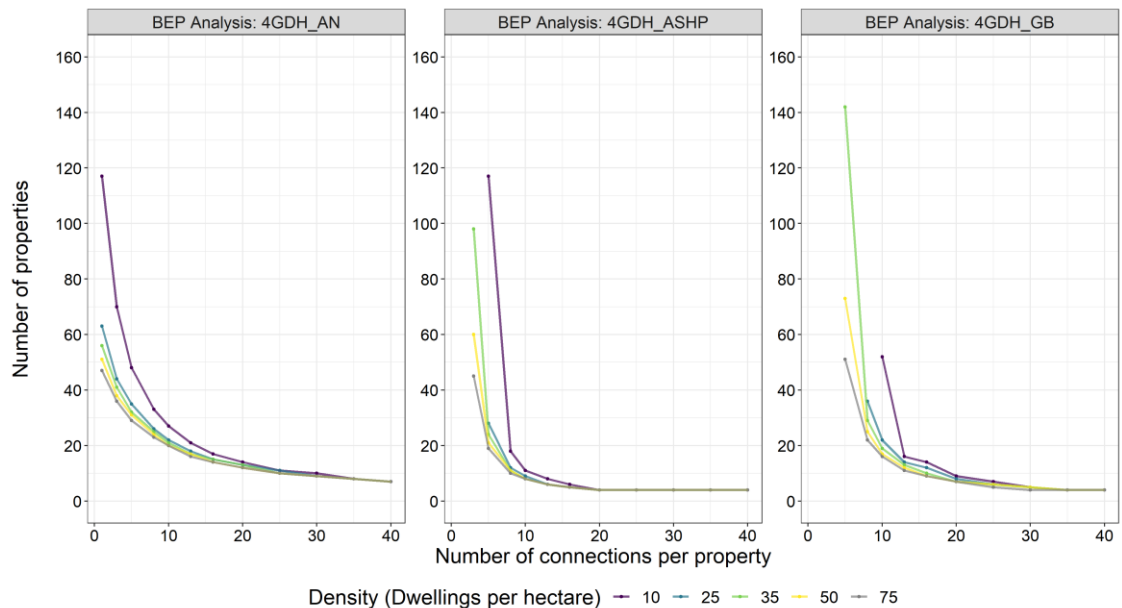


Figure 6.23: BEP for 4GDH to become more economical than other energy supply options.

The number of connections has the biggest impact on the BEP for all comparisons, while spatial density’s effect exponentially decreases as the number of connections increases. For the average spatial density of 35 properties per hectare, the BEP of 4GDH-AN ranges from 56 properties for 1 connection to 13 properties for 20 connections and reaching 7 properties when 40 connections per property are present. The ASHP always performs better when single houses are concerned, with the first BEP observed on 98 properties with 3 connections for 35 buildings per hectare which drops significantly for denser networks. After 5 connections, it takes only 18 properties for a BEP with 75 properties per hectare. Finally, for the comparison with GB, the BEP is similar to the ASHP only for more properties, with a BEP observed after 5 connections per property at 142 properties.

For the comparison of the AN with the ASHP and GB, density plays little role with the number of connections per property being the only influence. It takes 5-6 connections per property to reach a BEP for ASHP while 10-12 for GB. The reasoning for this is that the

key cost components are linearly increasing with more properties, namely the network and technology CAPEX for the AN and ASHP/GB respectively. ASHP-GB does not have a BEP since GB are always cheaper.

Combining the above, a preliminary performance comparison proposing which technology to use at different densities can be produced as shown in Figure 6.24 for a comparison with individual ASHP and Figure 6.25 for a comparison with individual GB.

It can be seen from these two figures that for sparse networks with a small number of connections per property individual solutions are preferable. For residential properties with one connection (detached houses), individual ASHP or GB always outperform centralised solutions. 4GDH is becoming more economically viable after at least 3 connections per property, performing better for denser networks while AN should not be used until there are at least 5 connections per property. After 5 connections per property for ASHP and 10 for GB, AN with a plantroom level HP should be considered in which case they are performing better than 4GDH on average up to project areas with 10-30 properties.

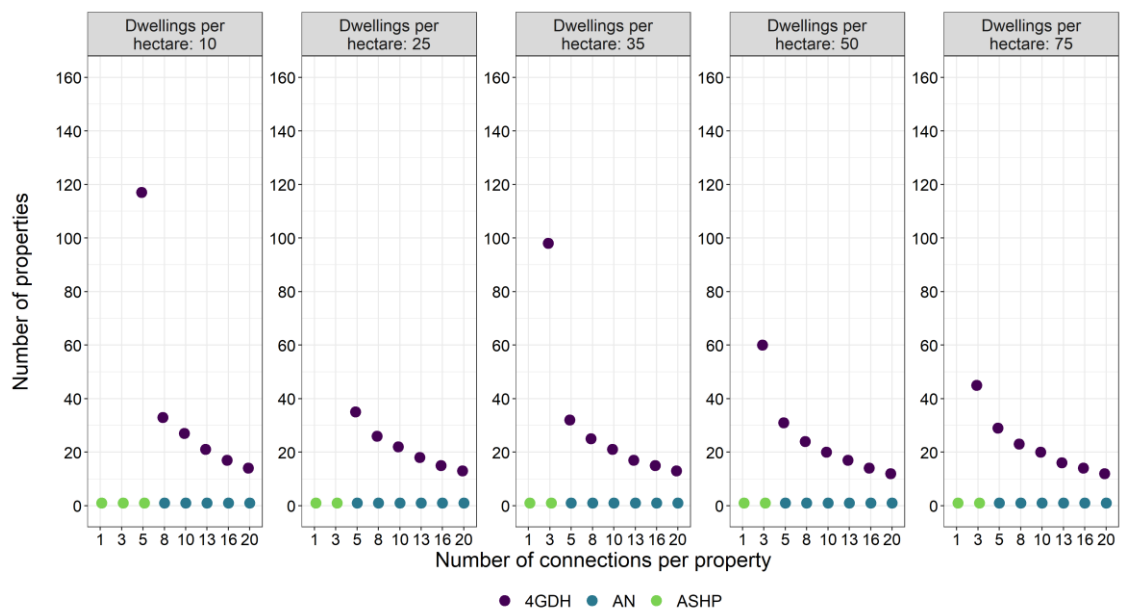


Figure 6.24: Preliminary energy supply performance comparison of ASHP-AN-4GDH.

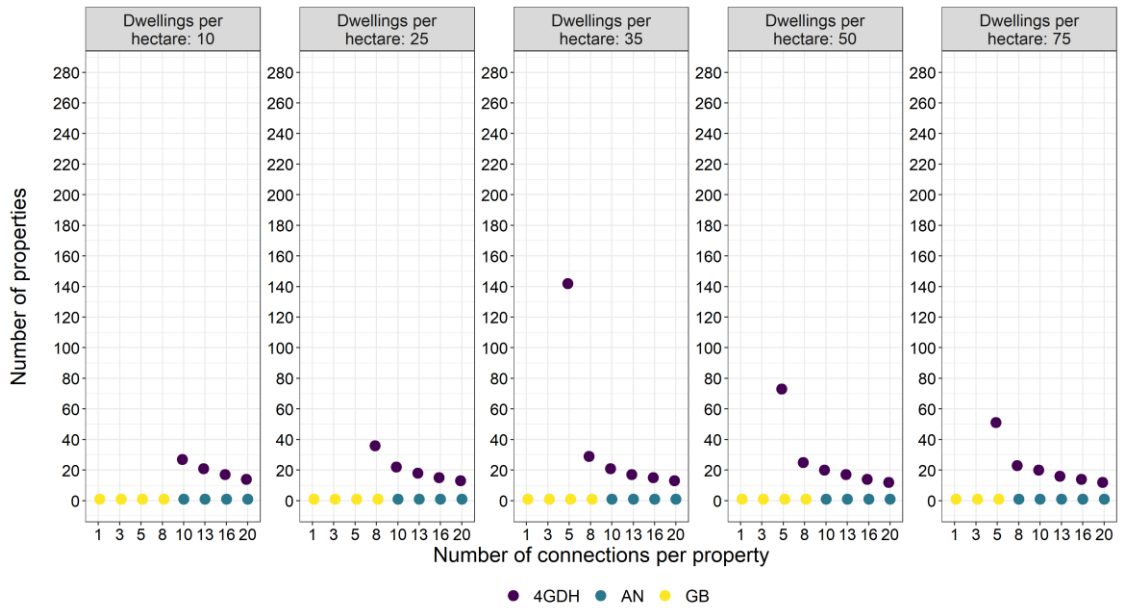


Figure 6.25: Preliminary energy supply performance comparison of GB-AN-4GDH.

A sensitivity of the BEP. The same variable variations, summarised in Table 6.10, are investigated for a +30% change. The outputs are shown in Figure 6.26 and Figure 6.27.

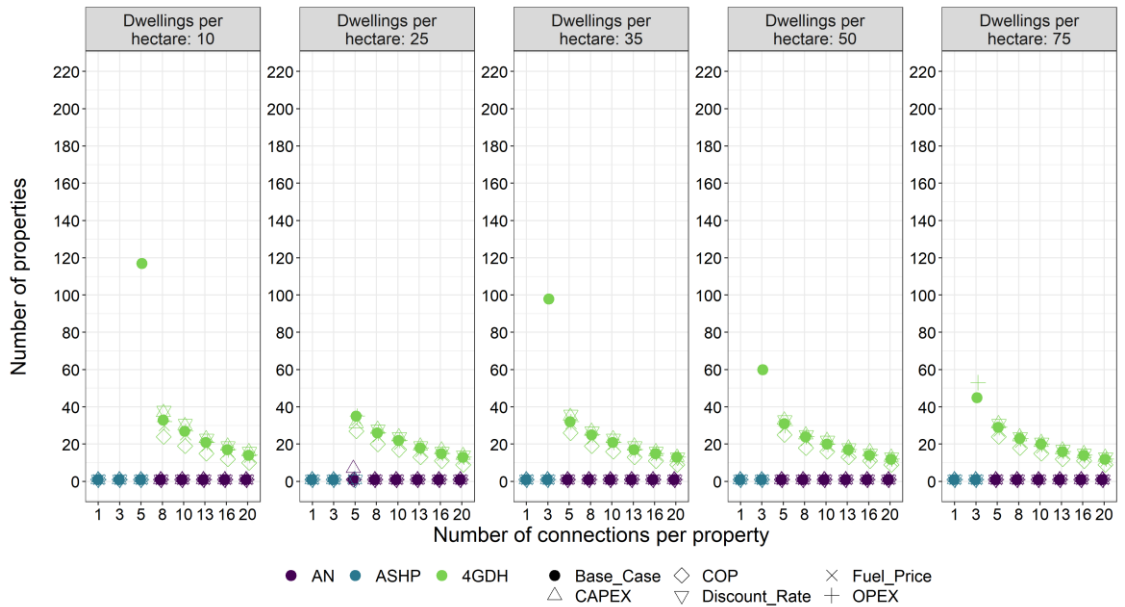


Figure 6.26: Sensitivity analysis on BEP for ASHP-AN-4GDH.

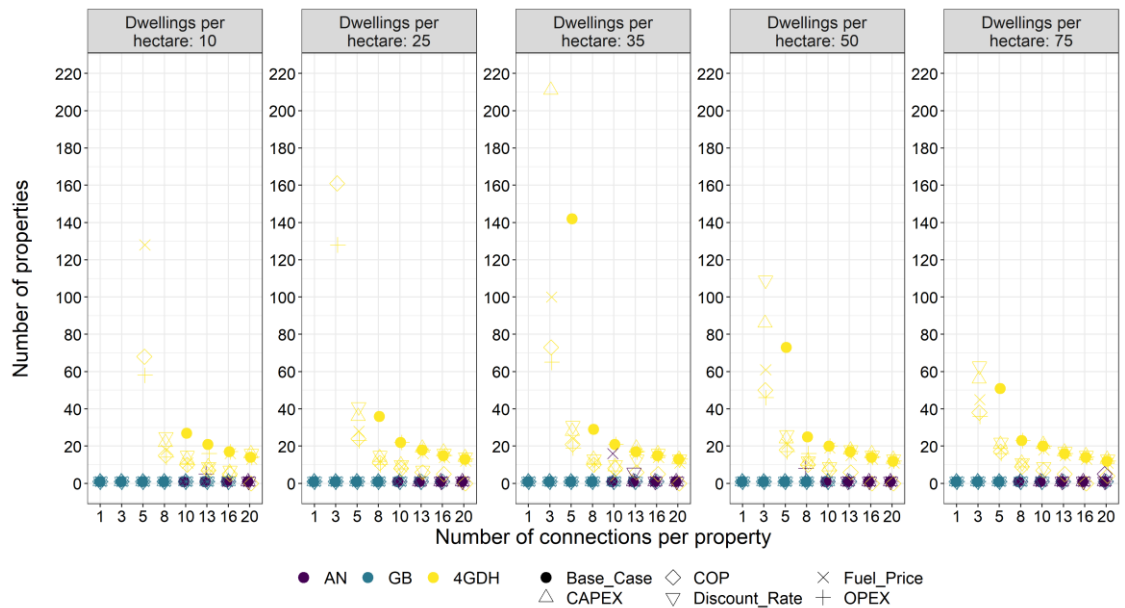


Figure 6.27: Sensitivity analysis on BEP for GB-AN-4GDH.

In both cases, the BEP remains stable across sensitivity variables for 1 connection. For the ASHP comparison, the BEP has very slight deviations from the original data. However, for the GB comparison, especially between 3 and 8 connections there is a great variation from the baseline values. After 10 connections, there is a decrease on the BEP value compared to the baseline, needing less properties for the 4GDH option to become more economically viable, especially for sparser networks. This is due to the delicate balance between 4GDH's CAPEX and the savings from reduced energy expenses. Therefore, especially when considering areas with 5 to 10 connections per property, it is recommended to conduct a bespoke analysis using CATHeaPS rather than solely relying on the BEP guidelines presented.

6.5.2 BEP of 'heating only' districts

Interestingly, there is no BEP for 5GDHC with 4GDH when 'heating only' and no directly usable waste heat source is present. This should come as no surprise since the benefit from 5GDHC comes from energy sharing between heating and cooling. When there is no cooling, 4GDH is always better than 5GDHC. These findings are in line with the outputs from Gudmundsson et al. (2022) [28] and Wirtz et al. (2020) [29], where they state that when there is no cooling, 4GDH always performs better than 5GDHC.

The BEPs for 4GDH-ASHP and 4GDH-GB remain almost unchanged since the only difference is the HP switching from a WSHP to an ASHP. Since these are preliminary results, the outputs from Section 6.5.1 should be used.

6.5.3 BEP of heating and cooling districts

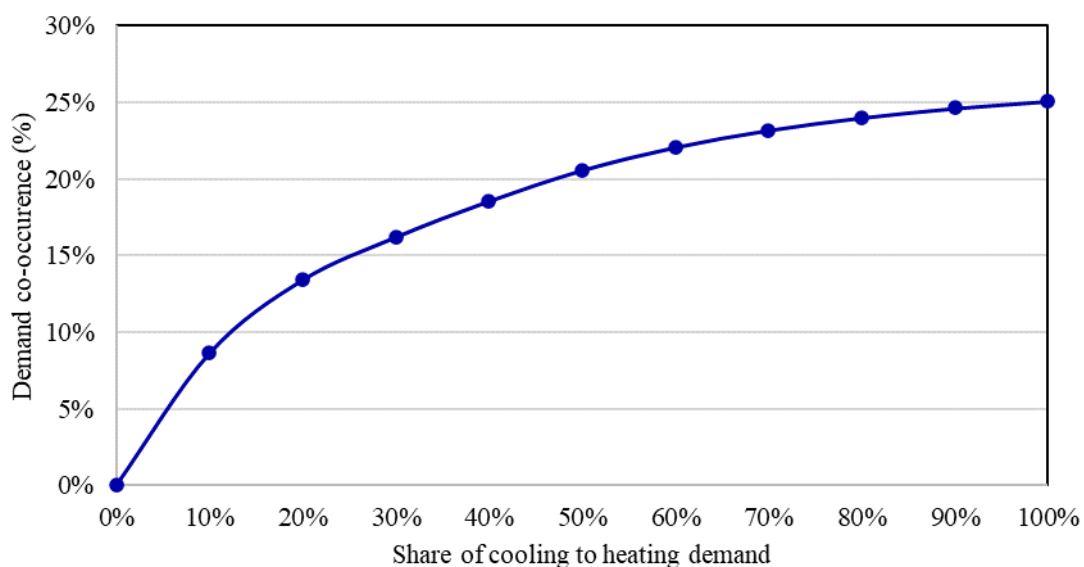
Finally, seeing that there is no BEP for the system when there is no cooling, an analysis is conducted by increasing the level of cooling. It is found that for 4GDH&AC compared to 5GDHC, the number of connections per property is the only variable affecting the output along with the share of cooling. For annual cooling to heating demand shares of 20% or less 4GDH&AC is always better. For annual cooling to heating demand shares of 50% or more 5GDHC is always better. For 30% and 40% annual cooling to heating demand shares, the building density impacts the preferred technology, due to the cost of the network. In addition, the number of connections has an impact, with higher number of connections leading to a better performing 5GDHC. This is due to the higher number of AC units needed for 4GDH&AC, impacting the CAPEX and fuel cost of 4GDH&AC. The outputs on which network is more economical for a cooling share of 30% and 40% for different building densities and connections per property is shown in Table 6.14.

However, these shares represent the annual share of cooling, not the DOC. This depends on the hourly profiles of the demands rather than the annual benchmarks. The DOC is irrespective of the number of connections, since the same hourly profiles are used. The DOC for different shares of cooling demand using CATHeaPS profiles is shown in Figure 6.28.

It's clear that a logarithmic trendline is present, showing that for increased levels of annual cooling shares, the DOC does not linearly increase. For example, the demand profile and BU contribution for an annual cooling to heating share of 10% and 50% are shown below in Figure 6.29 and Figure 6.30.

Table 6.14: 4GDH&AC vs 5GDHC for different shares of cooling demand.

Annual cooling demand share (% of heating)	Building density (dwellings/hectare)	Connections per property				
		1	2	3	4	5
$\leq 20\%$						
	10-75	4GDH&AC	4GDH&AC	4GDH&AC	4GDH&AC	4GDH&AC
30%						
	10	4GDH&AC	4GDH&AC	5GDHC	5GDHC	5GDHC
	25	4GDH&AC	4GDH&AC	4GDH&AC	4GDH&AC	5GDHC
	35	4GDH&AC	4GDH&AC	4GDH&AC	4GDH&AC	5GDHC
	50	4GDH&AC	4GDH&AC	4GDH&AC	4GDH&AC	4GDH&AC
	75	4GDH&AC	4GDH&AC	4GDH&AC	4GDH&AC	4GDH&AC
40%						
	10	4GDH&AC	4GDH&AC	5GDHC	5GDHC	5GDHC
	25	4GDH&AC	4GDH&AC	4GDH&AC	4GDH&AC	5GDHC
	35	4GDH&AC	4GDH&AC	4GDH&AC	4GDH&AC	5GDHC
	50	4GDH&AC	4GDH&AC	4GDH&AC	4GDH&AC	4GDH&AC
	75	4GDH&AC	4GDH&AC	4GDH&AC	4GDH&AC	4GDH&AC
$\geq 50\%$						
	10-75	5GDHC	5GDHC	5GDHC	5GDHC	5GDHC

**Figure 6.28: DOC for different annual shares of cooling and heating demand.**

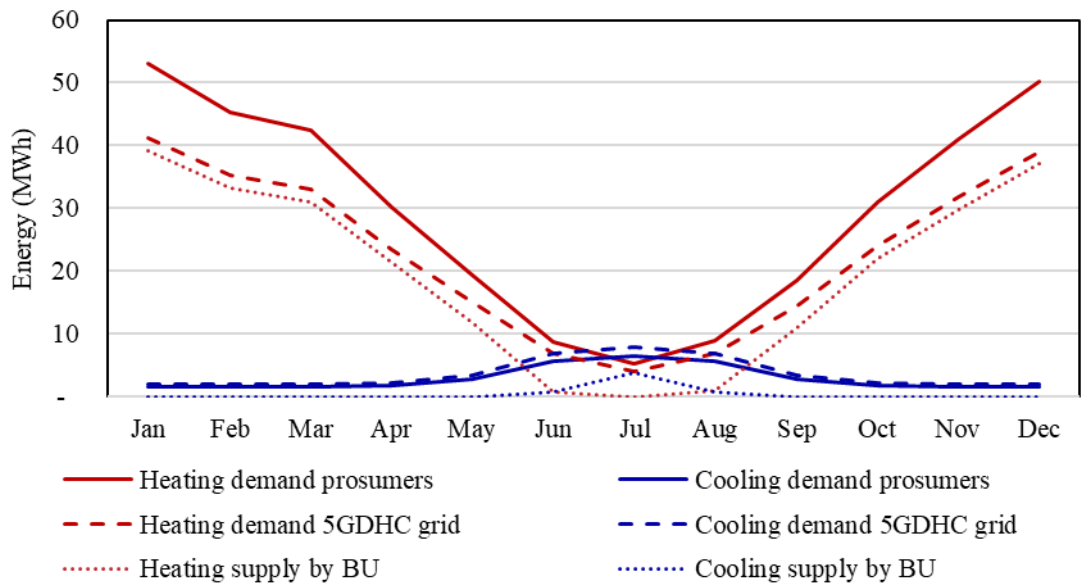


Figure 6.29: Heating and cooling demands overlaid on the BU's share. Annual cooling demand is 10% of the annual heating demand.

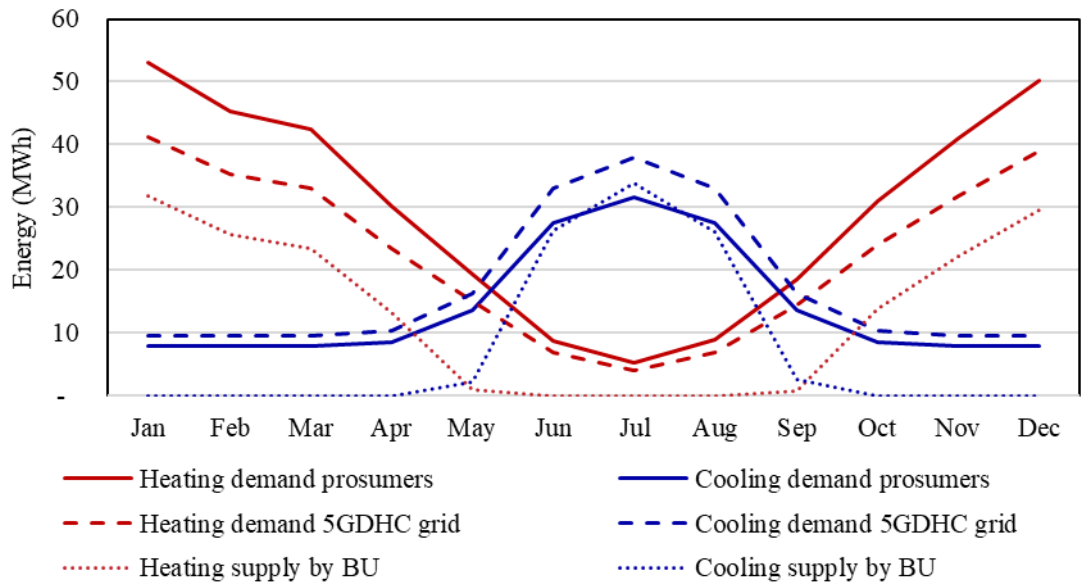


Figure 6.30: Heating and cooling demands overlaid on the BU's share. Annual cooling demand is 50% of the annual heating demand.

Most of the cooling demand is in summer, which is why increasing its annual share, does not linearly increase the DOC. Therefore, when having a network with heating and cooling demands, it's crucial to capture their hourly profiles to yield a precise economic performance of 5GDHC.

Having identified these trends, the preliminary performance comparison for different shares of cooling demand to heating demand is investigated. They are shown in Figure 6.31 for ASHP and Figure 6.32 for GB&AC. The cooling shares considered vary between 10% and 50% of heating demand.

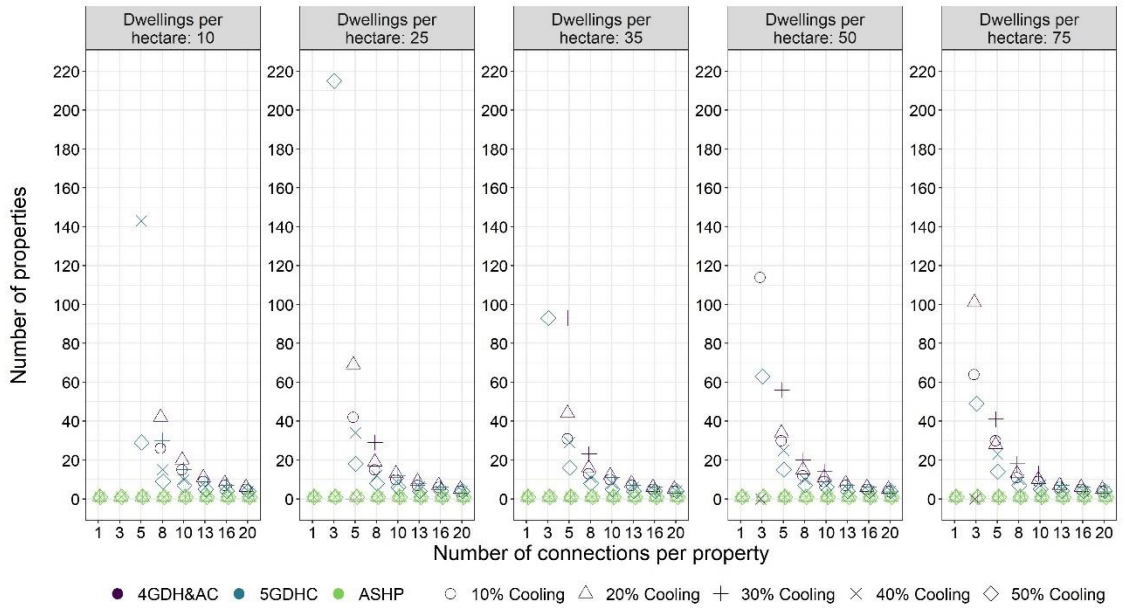


Figure 6.31: Preliminary energy supply performance comparison of ASHP-5GDHC-4GDH&AC for annual cooling demand of 10% to 50% of heating demand.

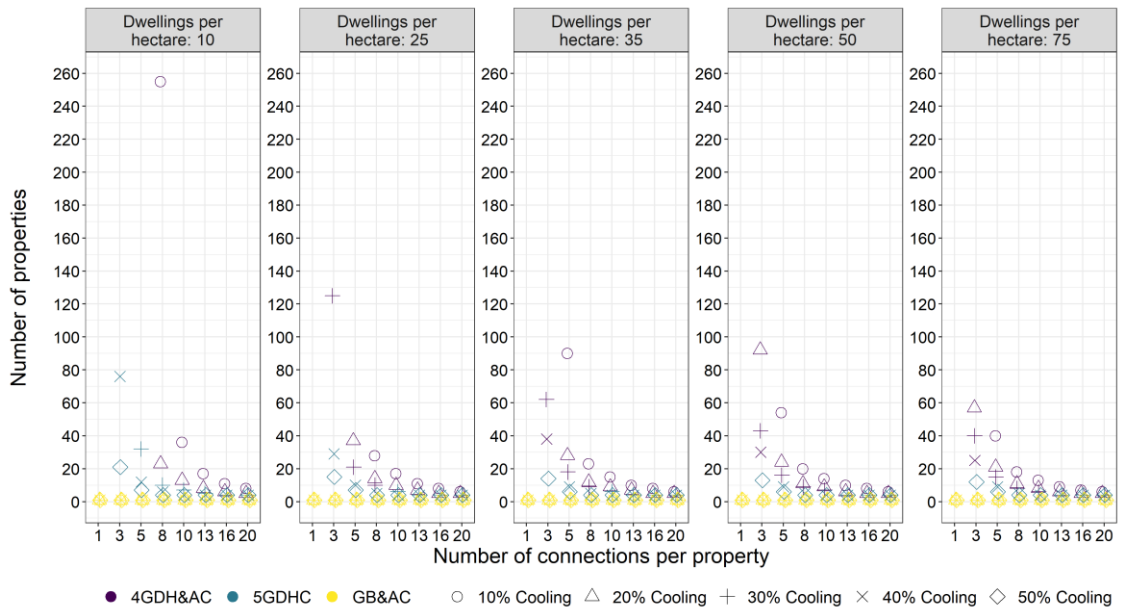


Figure 6.32: Preliminary energy supply performance comparison of GB&AC-5GDHC-4GDH&AC for annual cooling demand of 10% to 50% of heating demand.

In both cases the BEP remains stable across annual cooling demand shares for 1 connection. Irrespective of the level of cooling, the individual options (GB&AC or ASHP) are always better than more centralised solutions. The BEP drops for higher connections per property as expected, with the impact of the level of cooling decreasing. Similar to the ‘heating only’ districts analysis, the BEP is less than 20 properties for higher than 8 connections per property, with the range between 3 and 8 connections per property having large fluctuations. The BEP also reduces for higher levels of cooling share, since there is more energy used by the properties for similar infrastructure costs. It can also be seen that there is a transition from 4GDH&AC to 5GDHC from 30% to 40% cooling, as expected from Table 6.14.

6.5.4 Discussion of BEP outputs and wider considerations.

The results are in line with literature on comparisons of 5GDHC with 4GDH solutions. When there is no cooling, 5GDHC performs worse than 4GDH for any network configuration. An annual cooling to heating demand share of 30% (with a DOC of 16%) is needed for 5GDHC to start performing better for higher number of connections per property. For an annual cooling to heating demand share of 50% (with a DOC of 21%), 5GDHC performs always better than 4GDH&AC. These findings are also in line with the work of Wirtz et al. (2020) [29], who proposed that a DOC of 30% is needed for 5GDHC to perform better than 4GDH solutions.

It is important to highlight some technical considerations that are not fully captured by the results. Centralised solutions can benefit from bespoke agreements on energy prices (electricity and gas) and be less prone to fluctuations of energy prices. Having many individual HP increases the amount of refrigerant that is required, increasing the environmental impact and limits the selection of refrigerants that can be used (since they are located near residential properties). In addition, noise (from the evaporators) and space constraints (from the units, the risers and the TES) are present in decentralised solutions (both for individual dwellings and centralised plantrooms in apartment complexes). Additionally, fire hazard risk management needs to be considered for individual ASHP when considering space available which significantly limits their application in larger residential complexes. Defrosting in individual ASHP can be another issue with additional controls and electricity costs required during winter months. Maintenance of multiple

individual units can also be problematic when one stakeholder owns all assets (an ESCo) as well metering and billing. With decentralised solutions it's easier to phase the CAPEX to match demand development and potentially discount large components of CAPEX. It is also not required to have a network of pipes that requires underground space and coordination with other utilities as well as risks of prohibitive obstacles in planning approvals (such as archaeological spaces). Therefore, it is crucial to consider all choices when deciding which energy supply option is more appropriate rather than limiting oneself to the economic performance.

6.6 CATHeaPS for environmental analysis – Monte Carlo simulations

The CO₂ emissions heavily depend on the SCOP used for each technology and the type of back up boilers used for 4GDH, whether they are electric or gas. For this analysis, electric boilers are assumed. As before, the level of cooling for the heating and cooling demand scenario is set to 50% of the heating demand. The outputs for all three project area scenarios are shown in Figure 6.33 while Figure 6.34 also includes the GB&AC emissions.

It is found that the relative CO₂ emissions of the networks remain constant, with GB/GB&AC emissions being higher by a factor of 10. This is because energy use is directly linked to asset efficiency, with network losses having a small impact due to the assumed insulation levels. The other supply options relative environmental performance changes between the different scenarios (A to C), due to the role of the BU and the impact of cooling. The normalised variations with respect to the GB/GB&AC supply options are calculated and it is found that the ASHP always has the second largest emissions due to the lower SCOP. Furthermore, Plot A shows that 4GDH has higher CO₂ emissions than AN (31% higher) due to larger heat losses in the network and lower SCOP (caused by a minimum 5°C higher supply temperature to account for thermal losses in the TES and the network) [229]. When a BU is introduced in scenario B, the emissions from the added ASHP in the BU and the parasitic loads lead to higher emissions for 5GDHC (12%). Finally, when cooling is introduced, there is more variation in the normalised CO₂ emissions due to the GB and AC units having different efficiencies. In this case, 5GDHC has slightly lower emissions than 4GDH&AC (10% smaller).

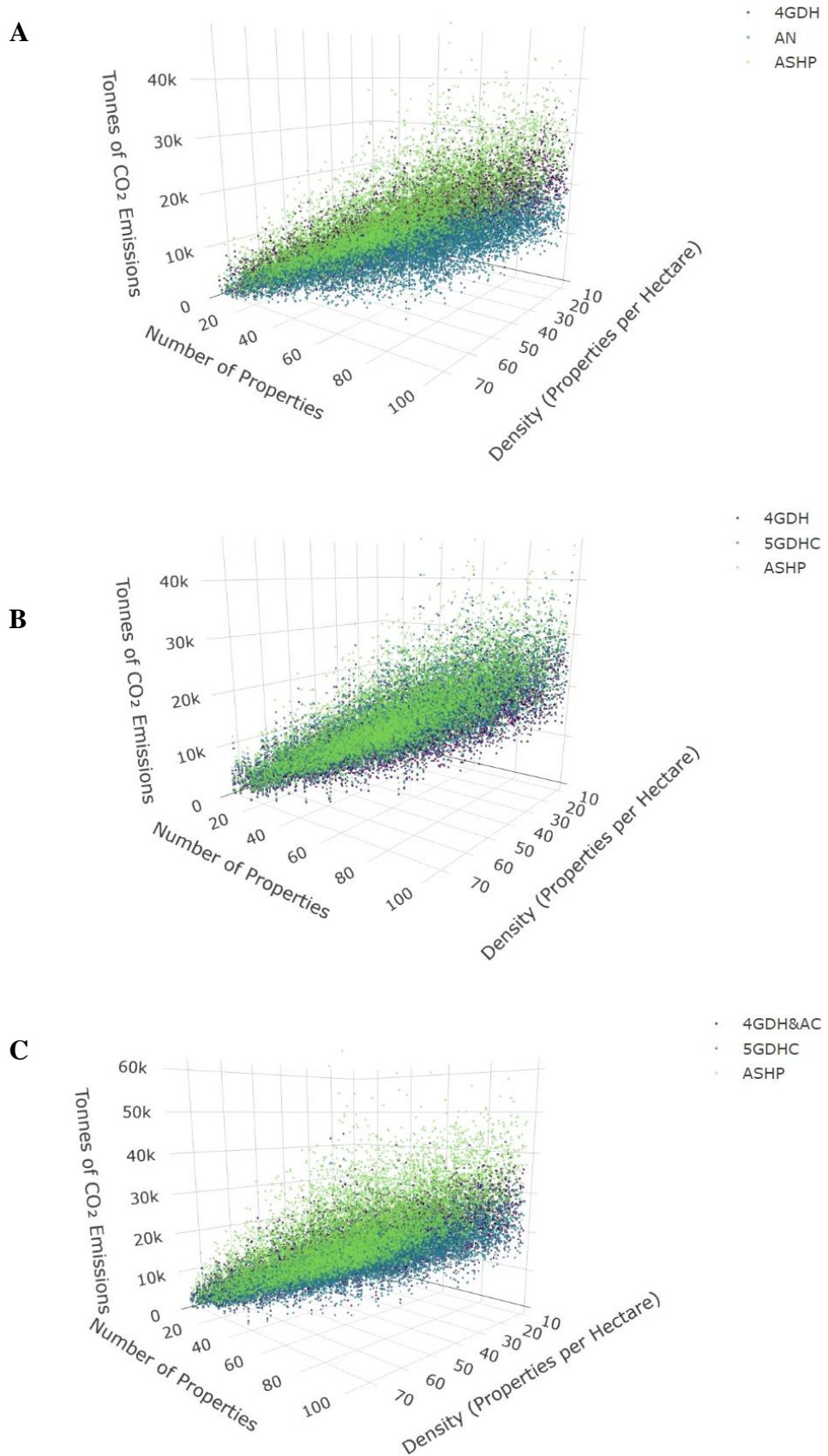


Figure 6.33: CO₂ Emissions from Monte Carlo simulations excluding GB&AC (A) ‘heating only’ districts with access to an ambient temperature waste heat source, (B) ‘heating only’ districts and (C) heating and cooling districts.

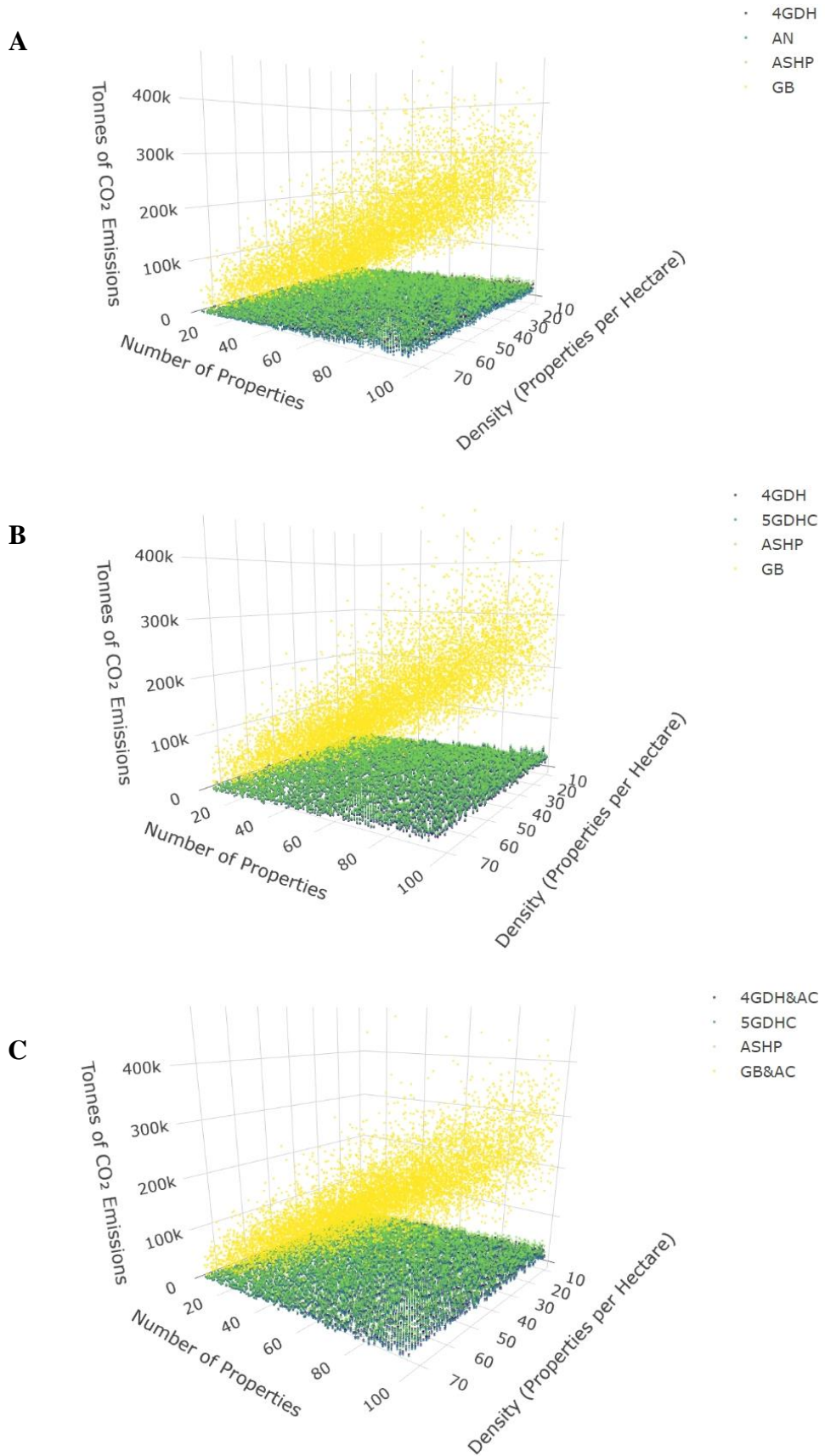


Figure 6.34: Emissions from Monte Carlo simulations (A) ‘heating only’ districts with access to an ambient temperature waste heat source, (B) ‘heating only’ districts and (C) heating and cooling districts.

The 3D plots in Figure 6.33 and Figure 6.34 also show that the CO₂ emissions are varying equally with the number of properties and the property density. To quantify the impact of these two parameters on CO₂ emissions, the normalised standard deviation method is employed. A higher value of normalised standard deviation indicates a larger impact on CO₂ emissions (greater variability).

Since there are two parameters that affect the CO₂ emissions, their respective impact can be studied by keeping one constant and observing the effect of the other in isolation. For example, to study the impact of the housing density, the normalised standard deviation is studied at different number of properties. Figure 6.35 shows the normalised standard deviation of CO₂ emissions for both a variation of the number of properties (Plots A) and property density (Plots B). For all 3 project area scenarios a similar behaviour is observed. The normalised standard deviation is oscillating around 55% for all plots. This indicates that the two variables equally affect the CO₂ emissions, without one being more dominant than the other.

6.6.1 Discussion of environmental analysis outputs

This economic analysis provides some insights on the CO₂ emission behaviour of the analysed supply energy systems. However, further factors can be accounted for when examining the environmental performance. These include the implication of project-specific characteristics, life-cycle assessments and the wider impact on the electricity grid.

Firstly, the use of the SCOP is a first indicator of the CO₂ emissions however, in real world applications, many parameters can impact this figure. Operational details and system design will impact the operating hours of different units, as well as start-stop cycles and back-up unit contribution. The bespoke demand profiles and consumer class mixing need to be studied since they will impact the DOC, influencing 5GDHC's environmental performance. Additionally, exploring the impact of different refrigerants and their impact on the SCOP is advised.

This analysis focuses on operational CO₂ emissions, but a complete characterisation would require a complete life cycle assessment. In such an assessment, the number of HPs and ancillary equipment needed in decentralised systems would heavily favour centralised

systems due to reduced material use. Another item that is not captured in the operational CO₂ emissions is the required power requirement from the electricity grid. Solutions with reversible units and centralised energy transformation assets, require lower electric capacity. This can help avoid the installation of additional electricity generation units (PVs, wind turbines etc.), leading to lower overall CO₂ emissions due to reduced material use.

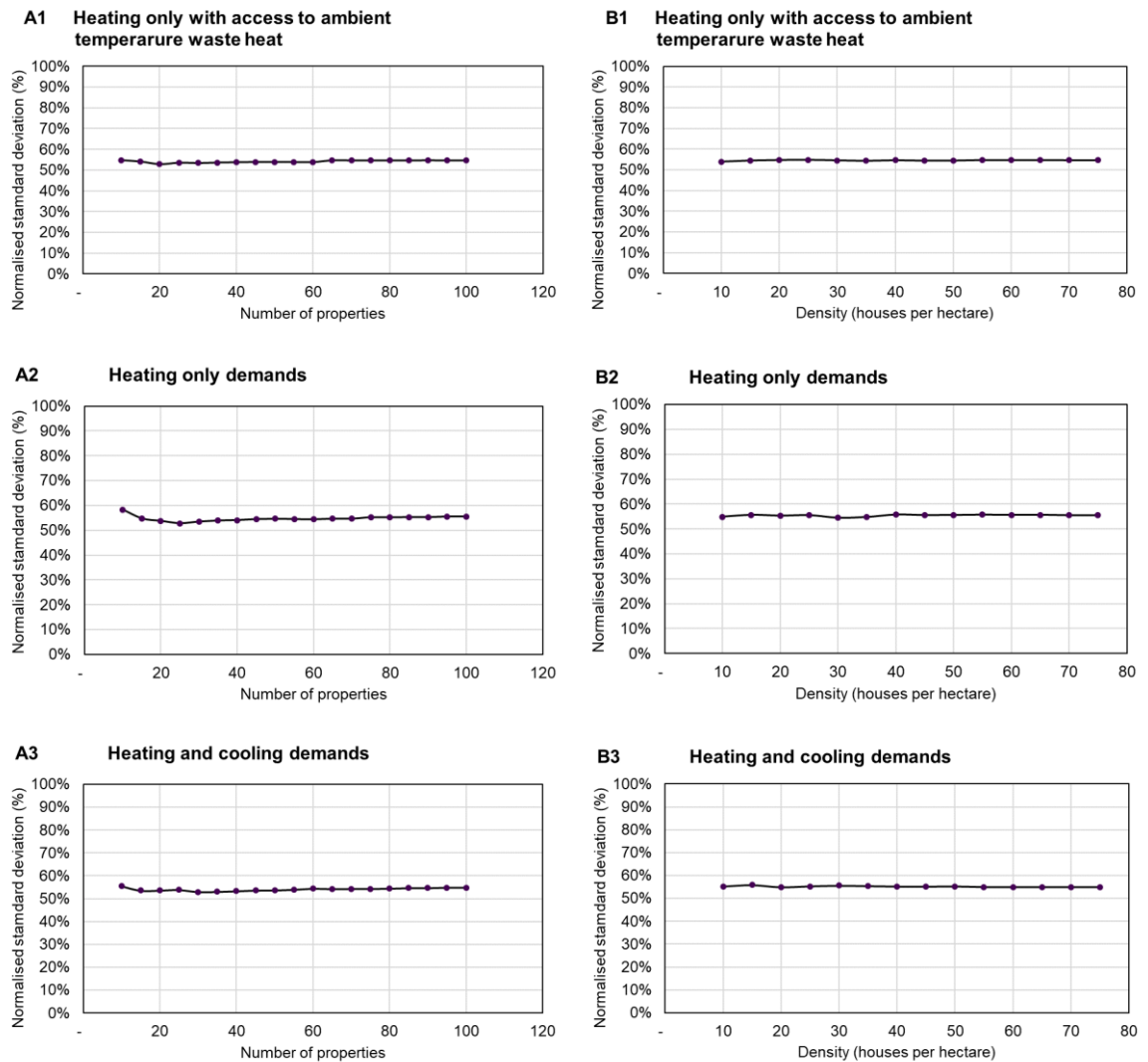


Figure 6.35: Normalised standard deviation of CO₂ emissions for all three scenarios when (A) the number of properties is kept constant and (B) when the density is kept constant.

Finally, the required space requirements that could be used for renewable energy generation need to be considered. Specifically, decentralised ASHP solutions require roof or garden space for their evaporators (dry air coolers). Freeing up this space by preferring a centralised approach could allow the installation of PV for renewable energy generation, reducing the electricity grid's carbon content.

6.7 Discussion on CATHeaPS limitations and future improvements

CATHeaPS is a novel simulation model that, like any other, possesses some inherent limitations on its functionality. In this section the key limitations are discussed along with key areas for future improvements of the model.

A comprehensive validation study using metered data from an operational network would enhance its reliability. Such validation would not only bolster the model's credibility but also enable further refinement and expansion of its capabilities. Regarding the network topology, a critical aspect of the hydraulic modelling is that all networks studied are linearised. It is common to have intricately shaped networks, consisting of multiple branches and loops. While the capacity to input 2D networks by specifying each property's Cartesian coordinates is available, it should be noted that the hydraulic analysis would need to be updated as part of future developments. Alternatively, network linearization could be used, allowing the use of the current hydraulic analysis. Linearization is a technique that is used in potable water networks where branches and loops are taken as black boxes that the system sees as a single heat node. To perform this simplification, intricate matrix calculations are required along with the construction of a sophisticated algorithm [230]. The incorporation of the capability to solve for non-linear networks is a crucial future improvement and its results should be compared to the ones outlined in this study. Such a feature would also allow the performance of a network alignment study.

Furthermore, future efforts should be directed towards including the capacity for mixed network analysis, comprising centralised and decentralised WSHPs at different levels of thermal zoning. The analysis of such a network is more complicated and is not included due to the scope of this project which is the comparison of different energy supply options. In addition, since SCOP is one of the major components that influences the economic performance of the 4GDH&AC, 5GDHC and ASHP options as the sensitivity analysis displayed, a seasonal profile analysis of the water source temperature should be carried out to obtain a realistic SCOP for the WSHPs. Plastic pipes could be used for the 5GDHC which have a lower CAPEX but could have limitations on the diameters that can be achieved. In addition, the hydraulic sizing of the 5GDHC needs verifying. Despite being

unidirectional, the direct connection to evaporators rather than HEXs found in 4GDH networks might lead to adjustments needed in the hydraulic design. Retrofitting is beyond the scope of this research but it could be incorporated in future work, following an evaluation of the associated costs and technical differences such as the potential flow and return temperature increase [43]. 4GDH networks with centralised GBs are not included as a counterfactual scenario since the study is focused on new markets where individual GBs are common practice. While this supply option could be built into future iterations of CATHeaPS, it is not compatible with the net zero targets. Cost and technical characteristics for the thermal sources should be added for future iterations, allowing the user to select the water type or input their own data since these costs are highly project specific.

Having established CATHeaPS' functionality and verified it, it's important to use it for a real case study. Chapter 7 illustrates how CATHeaPS can be used for assessing a real project. It also uses the ProHMo models along with a more detailed network routing exercise to inform its demand, energy supply and hydraulic assessments.

7 Case Study: D2 Grids Ambient Loop Project in Clyde Gateway, Glasgow

In this chapter, an assessment of a real-world project with potential for 5GDHC implementation is conducted. This is the expansion scenario of D2 Grids Ambient Loop Project in Clyde Gateway, Glasgow. The developed design, control methodologies and models (ProHMo models and CATHeaPS) are used to quantify the techno-economic performance of 5GDHC against other supply options. An introduction of the study area's characteristics is followed by the energy-supply scenario build-up. An energy demand assessment is performed along with an energy supply assessment for the Dalmarnock WWTP. A detailed analysis on the 5GDHC system's design and operation is then shown as well as the key design decisions for the alternative energy supply options. The outputs of the techno-economic analysis of all scenarios are then presented, followed by a thorough discussion on their interpretation and the other factors that should be considered in the decision-making process. This case study was selected because it represents a typical scenario for 5GDHC implementation: a new mixed development with heating and cooling demands located near a low-temperature waste heat source. This configuration is common in many urban settings, making the assessment methodology applicable to a wide range of project areas with similar characteristics.

7.1 Introduction to the case study

The first step in designing and assessing a 5GDHC system for this case study is an understanding of the project area. This includes existing infrastructure and the building schedule for the development. In addition, identifying potential opportunities for utilising ambient temperature waste heat sources/sinks is needed to fully characterise the project area. These elements can inform and shape the scope of the work.

7.1.1 Case study background

The D2 Grids Ambient Loop Project is being developed by Clyde Gateway who are the organisation tasked to deliver one of Scotland's biggest regeneration programmes. The regeneration area is located in the east end of Glasgow, shown below in Figure 7.1.

The project is helping deliver new infrastructure including residential, commercial, retail, leisure and education over the next 25 years. The Dalmarnock WWTP is identified as a key opportunity for recovering waste heat from its final effluent, with an abstraction HEX already installed [231]. Currently, the waste heat is used to supply a Sewer Water Source Heat Pump (SWSHP) located in the Red Tree Magenta building. The SWSHP is sized for supplying only this building but there is space capacity in the plantroom for more SWSHPs to supply a potential future 4GDH network. A plastic pipe is used to connect the WWTP with the SWSHP with a DN355 diameter. A schematic of the current setup including the WWTP, and existing EC is shown below in Figure 7.2.

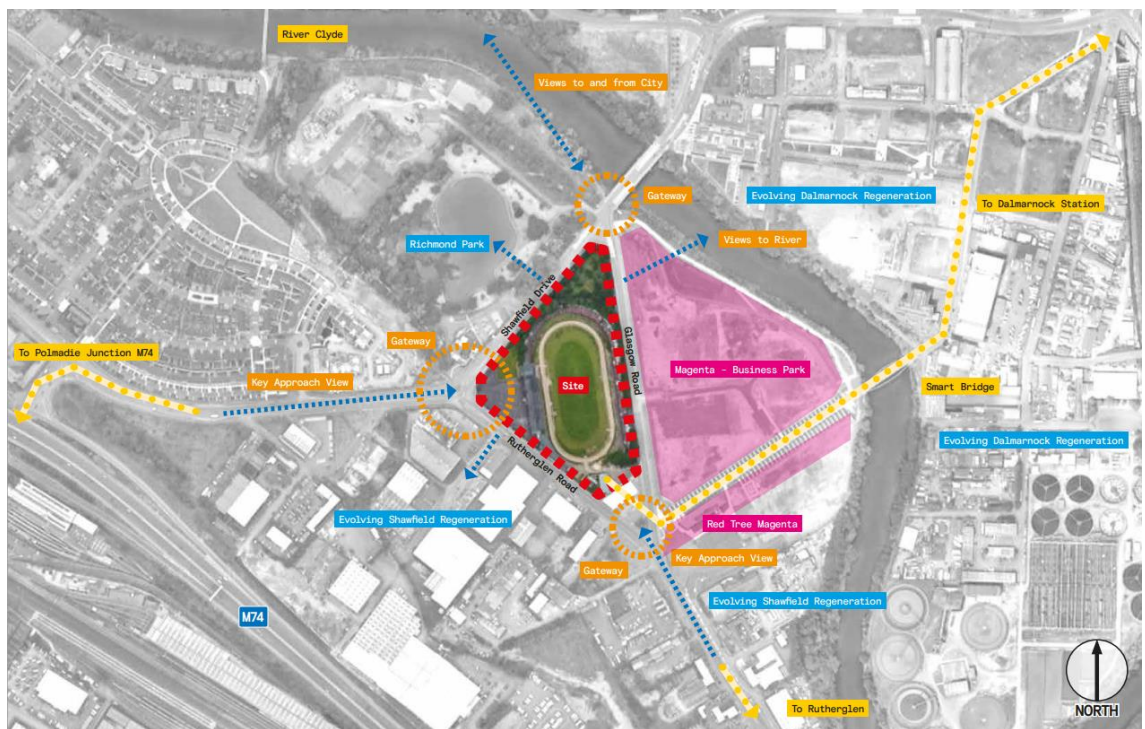


Figure 7.1: Project regeneration area in Glasgow [232].

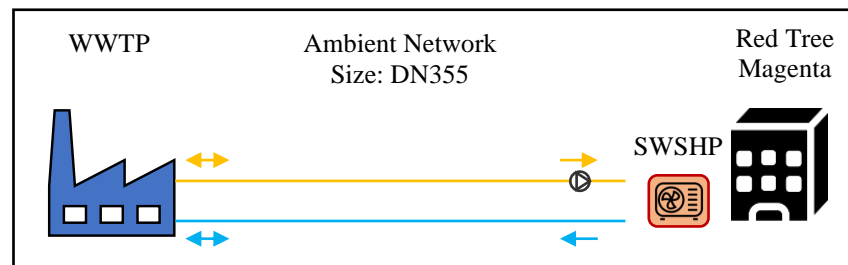


Figure 7.2: Constructed ambient network, EC and WWTP abstraction point [233].

As part of the future developments that will be constructed in the next 25 years, there are questions as to what is the best way to provide heating and cooling. A map of the proposed

development to be considered is shown below in Figure 7.3, with the labels capturing the construction year of the properties.

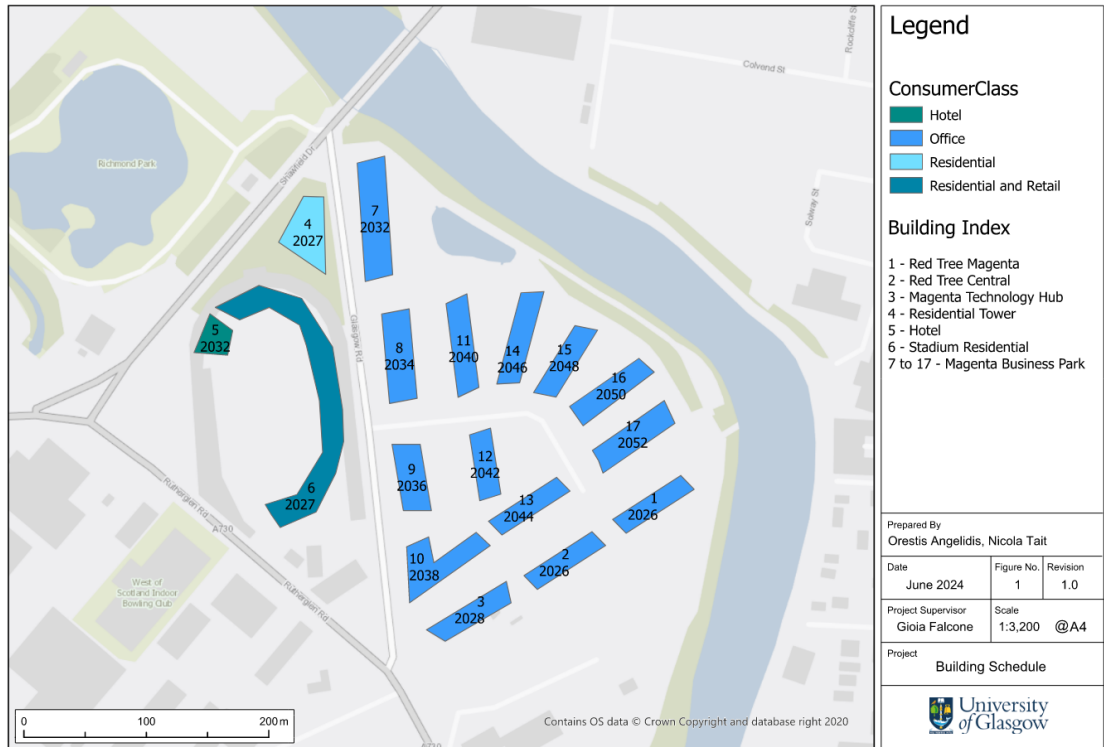


Figure 7.3: Building schedule for case study.

7.1.2 Supply options in case study project area

Clyde Gateway is interested on the potential techno-economic feasibility of 5GDHC, along with a design that can effectively utilise the WWTP as a heat source/sink. The possible supply options are similar to the ones already mentioned in Chapter 6 and are:

- **5GDHC** - An ambient temperature network with decentralised reversible BHPs and TES at building level for both heating and cooling demands, treating the WWTP as a prosumer (Figure 7.4)
- **4GDH&AC** - 4GDH for meeting heating loads, with the WWTP acting as a source for a centralised SWSHP. Individual AC units are meeting the cooling loads of the buildings (Figure 7.5).
- **ASHP** - Individual reversible ASHPs at property level for meeting heating and cooling loads; no utilisation of the WWTP is made (Figure 7.6).

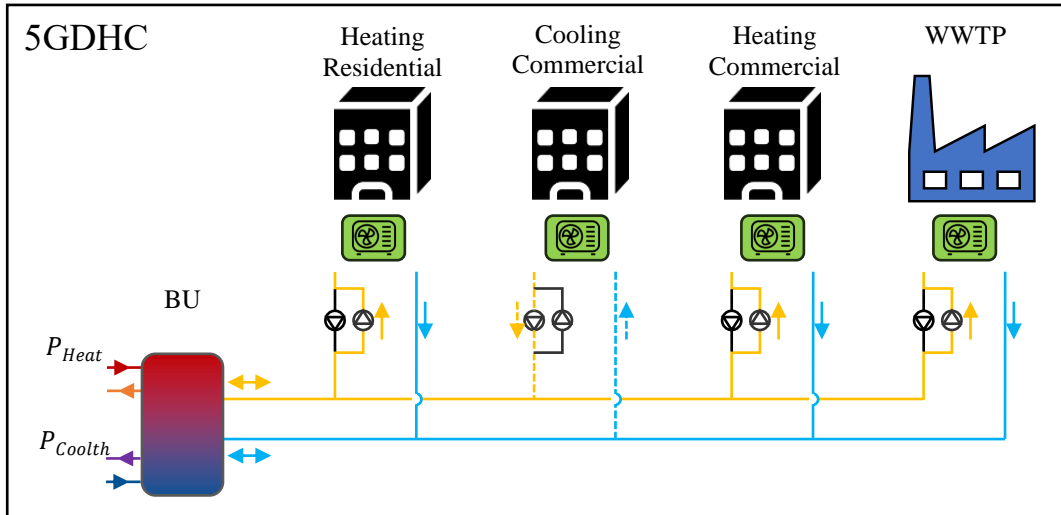


Figure 7.4: 5GDHC Network with decentralised BHP plantrooms.

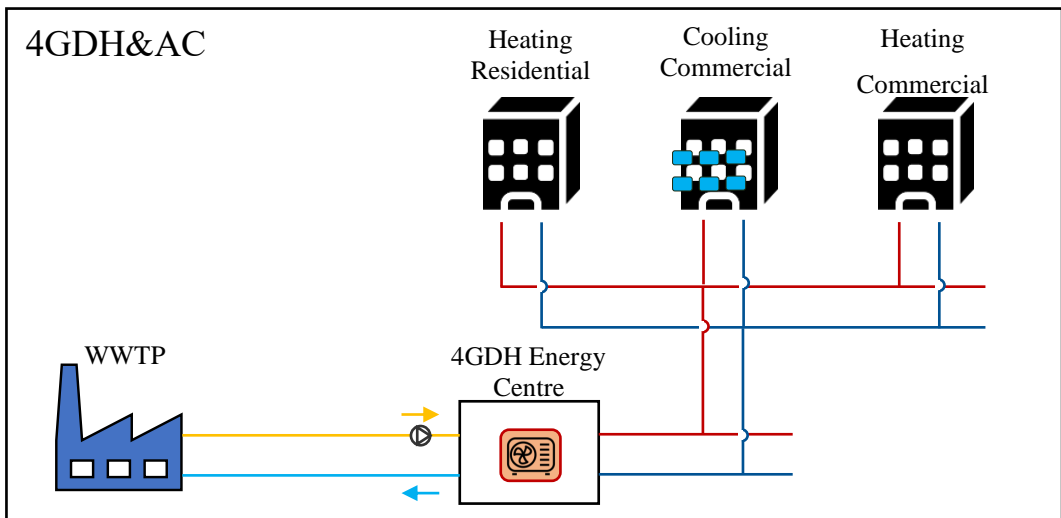


Figure 7.5: 4GDH network with centralised EC and individual AC for cooling.

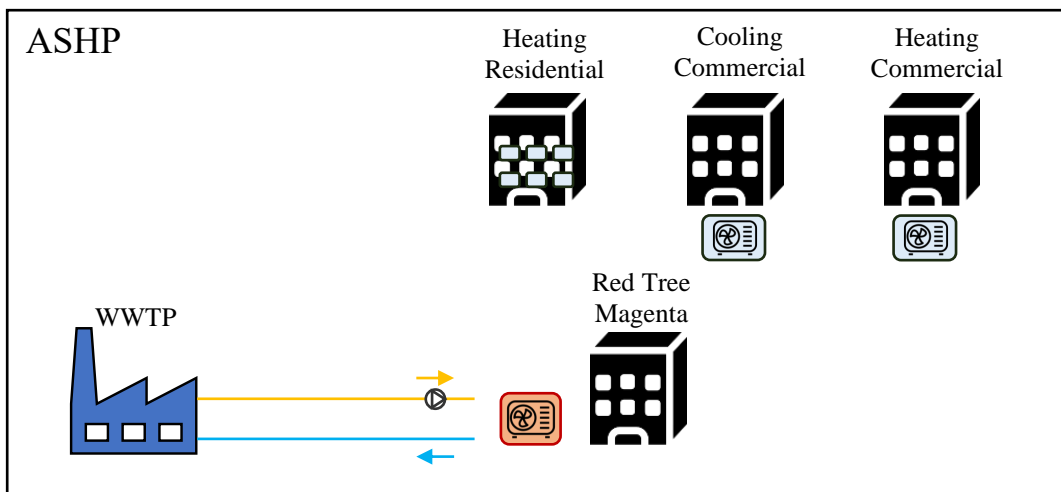


Figure 7.6: Reversible ASHPs on building level for heating/cooling.

7.1.3 Case study aim and objectives

The aim of this chapter is to provide a complete conceptual design for a 5GDHC system in Clyde Gateway's planned regeneration area in Glasgow, quantifying its techno-economic feasibility against counterfactual supply options. To complete this task, the developed hydraulic designs and control philosophy are applied, along with a combination of the developed models (ProHMo and CATHeaPS). The KPIs used for assessing the supply options include economic and environmental indicators as well as a discussion on the impact to the electricity grid based on installed capacity. This chapter's objectives are found in Table 7.1.

Table 7.1: Case study objectives.

Topic	Objectives
Demand Assessment	<p>Establish the building schedule for analysis.</p> <p>Review the building types and their characteristics of each building within the scheme.</p> <p>Produce hourly energy profiles for all buildings (using ProHMo models).</p>
WWTP Supply Assessment	<p>Quantify the capacity of the WWTP.</p> <p>Identify methods for utilising the waste energy and provide appropriate designs.</p>
5GDHC System	<p>Develop 5GDHC system designs with fitting control philosophies that details how the buildings will draw and discharge heat from and to the network.</p> <p>Provide a detailed analysis of prosumer plantroom level technology mix and asset sizing for each 5GDHC scenario.</p> <p>Conduct detailed thermofluid modelling (using ProHMo models) to yield energy flows and electricity requirements per prosumer plantroom for each 5GDHC scenario.</p> <p>Conduct hourly energy flow analysis for identifying BU's supply requirement and thus sizing technology mix for each 5GDHC scenario.</p> <p>Review the potential route options and the study area in GIS to identify a preferred network route and topology for each 5GDHC scenario.</p> <p>Carry out hydraulic modelling to determine the pipe sizing for each 5GDHC scenario (using CATHeaPS).</p>
Counterfactual Supply Options	<p>Conduct equipment sizing, energy flow and hydraulic analysis for each supply option (using CATHeaPS).</p>
Techno-economic Modelling	<p>Compare the techno-economic performance 5GDHC scenarios against counterfactual supply options (using CATHeaPS).</p> <p>Conduct an environmental analysis for CO₂ emissions (using CATHeaPS).</p>

Topic	Objectives
Data Analysis	Identify the impact on the electricity grid (peak power and energy demand requirements). Conduct economic sensitivity analysis for cost variables and WWTP available capacity.

The analysis includes phasing, heating and cooling demands, mix of consumer classes and a low temperature waste heat source. Beyond demonstrating how the developed methodologies and models can be used in such an analysis, this chapter sheds light on different design parameters and highlights constraints and opportunities that need to be considered in a 5GDHC system.

7.2 Energy demand assessment of case study project area

First, the energy demand assessment for the project area is conducted. The building schedule shown in Table 7.2 is composed using information received from Clyde Gateway.

Table 7.2: Building schedule of project area.

Building name	Consumer class	Year of connection	Building area (sqm)
Red Tree Magenta	Office	2026	3,750
Red Tree Central	Office	2026	4,780
Magenta	Office	2028	3,000
Technology Hub			
Residential Tower	Residential	2027-2028 with 50 flats per year (100 flats total)	9,000
Stadium Hotel	Hotel	2032	3,600
Stadium Residential	Residential	2027-2035, 50 flats per year (450 flats total)	40,500
Stadium Retail	Retail	2027	700
Magenta Business	Office	2032 to 2052 with a building per 2 years (11 offices total)	46,120
Park			

To develop accurate hourly demands of the buildings, including space heating, space cooling and DHW demands, bespoke Modelica models are developed. The Green City library is used to yield each building's space heating and cooling demands. The simulations require to first define each building's characteristics. These include total floor

area, number of floors and flanking characteristics. Furthermore, the building insulation levels and resulting U values are defined. They are in line with the Energy Saving Regulation, found in the Energy Act 2016 (Commencement No. 1 and Savings Provisions) Regulations 2016 [234]. The terminal units are set to modern radiators with area specific heating power of 15W/m^2 . The reference temperature for the living zone for residential and commercial buildings is set to 21°C for heating and 23°C for cooling, in line with the international standards for thermal comfort levels [120]. The assumed flow temperature for the terminal units is 40°C with a 10°C ΔT for space heating and 8°C with a 7°C ΔT for space cooling [43].

For the ambient conditions, a CFSR2 dataset is used for the weather station near Kessington and Summerston, on river Kelvin, with coordinates 55.91N and 4.30W . This dataset provides hourly information for atmospheric temperature ($^\circ\text{C}$), wind speed (m/s), and humidity (g/kg). For direct and diffused solar irradiance (W/m^2), the Surface Radiation Data Set - Heliosat (SARAH) - Edition 2.1 is used [235] for the same coordinates. The ambient temperature and solar radiation are shown in Figure 7.7.

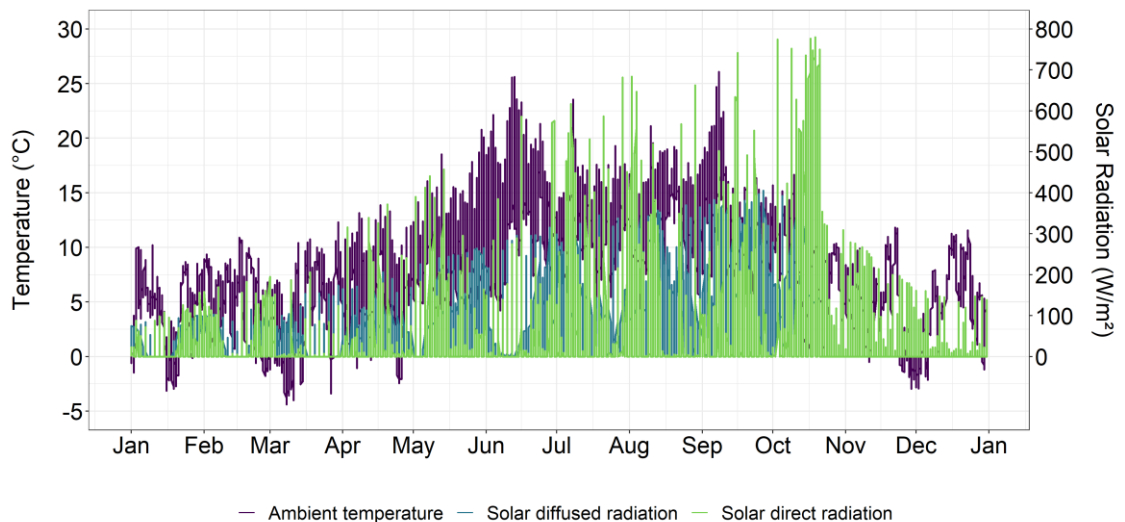


Figure 7.7: Ambient air temperature, solar direct and diffused radiation.

For the DHW demand of the residential properties, the profiles need to be generated using a statistical basis because DHW is delivered from a centralised plant at building level. This process is similar to the diversification factor described in Section 6.2.2, but since an hourly profile is required, the open access DHWcalc tool is used. It allows for an hourly estimation of the design water demand in l/min based on probability functions [236]. The

DHW demands are modelled as multi-family houses, using the cumulated frequency method (based on the integral of the probability function) of seasonal and daily variations. Step functions for the amount of draw off and the time interval are set in accordance with the developers' recommendations [236]. The step function values are seen in Figure 7.8.

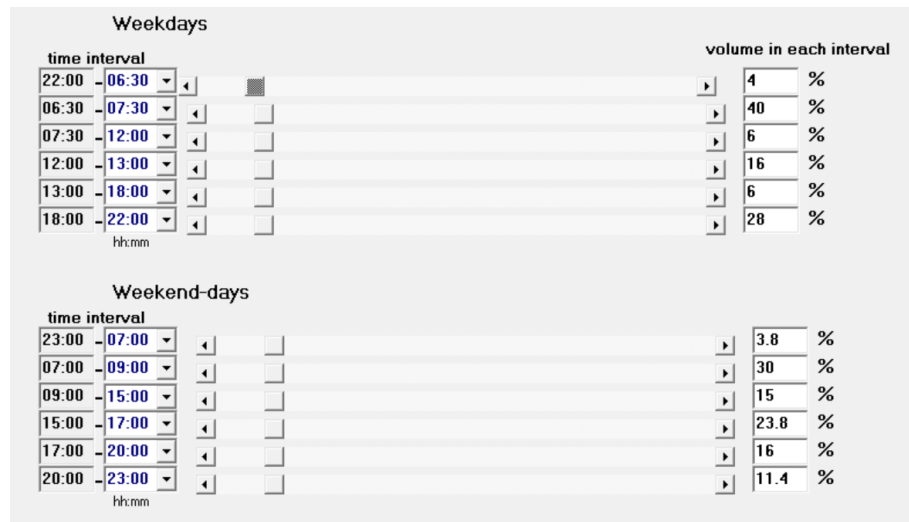


Figure 7.8: Values for step functions probability method for DHW demand analysis.

Using these inputs, the prosumers behaviour is simulated for a year in Modelica. The outputs are shown in Table 7.3, while Figure 7.9 and Figure 7.10 show the area specific energy demand and peak demand per building respectively.

Table 7.3: Demand assessment outputs.

Building	Space heating (MWh/year)	DHW (MWh/year)	Space cooling (MWh/year)	Peak space heating (kW)	Peak DHW (kW)	Peak space cooling (kW)
Red Tree Magenta	88	-	31	154	-	109
Red Tree Central	108	-	40	138	-	132
Magenta Technology Hub	74	-	24	136	-	90
Residential Tower	97	126	24	159	22	227
Stadium Hotel	86	-	32	185	-	108
Stadium Residential	445	575	87	355	98	862
Stadium Retail	11	-	8	12	-	23
Magenta Business Park	1,084	-	377	957	-	1,324
Total	1,994	700	621	-	-	-

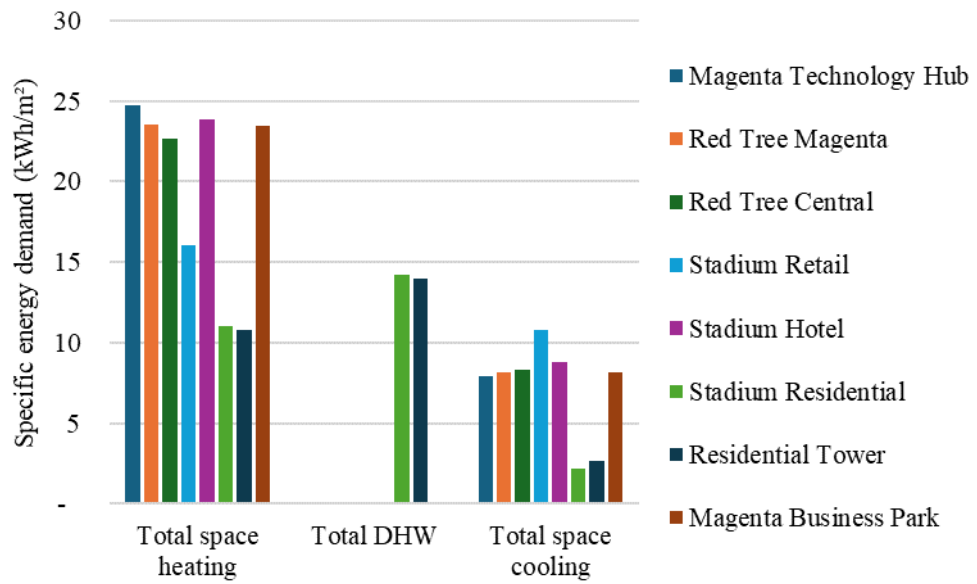


Figure 7.9: Specific Energy demand per building.

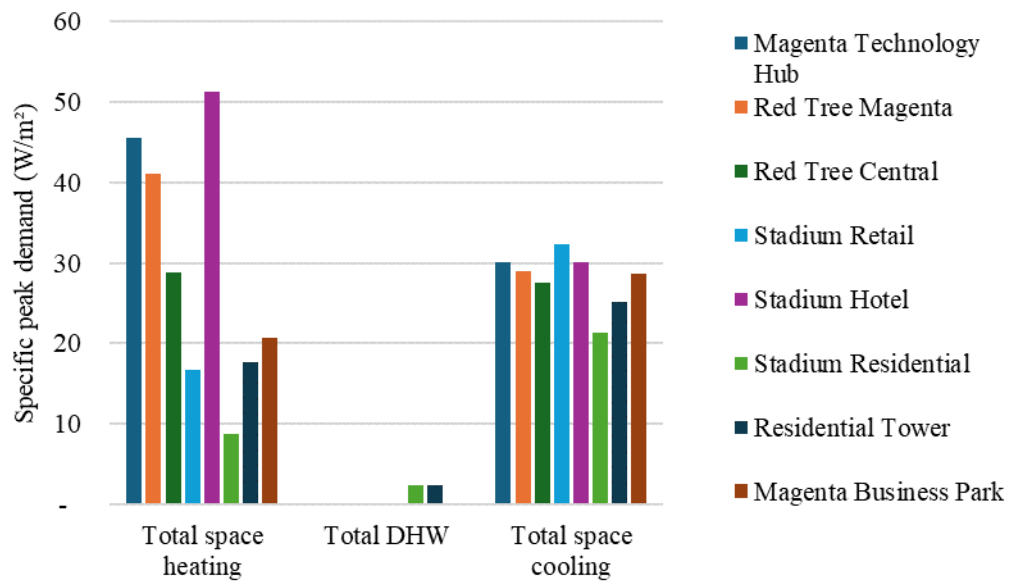


Figure 7.10: Specific peak demand per building.

These outputs are compared against published building standards for new buildings. Most regulations in the UK request a figure of 15-30kWh/m² for heating, and a total energy use of 35-40kWh/m² for planning permissions [237]. Observing that all outputs from Figure 7.9 are within this range verifies the results. What is of further interest is the annual profile of these demands, which is shown in Figure 7.11.

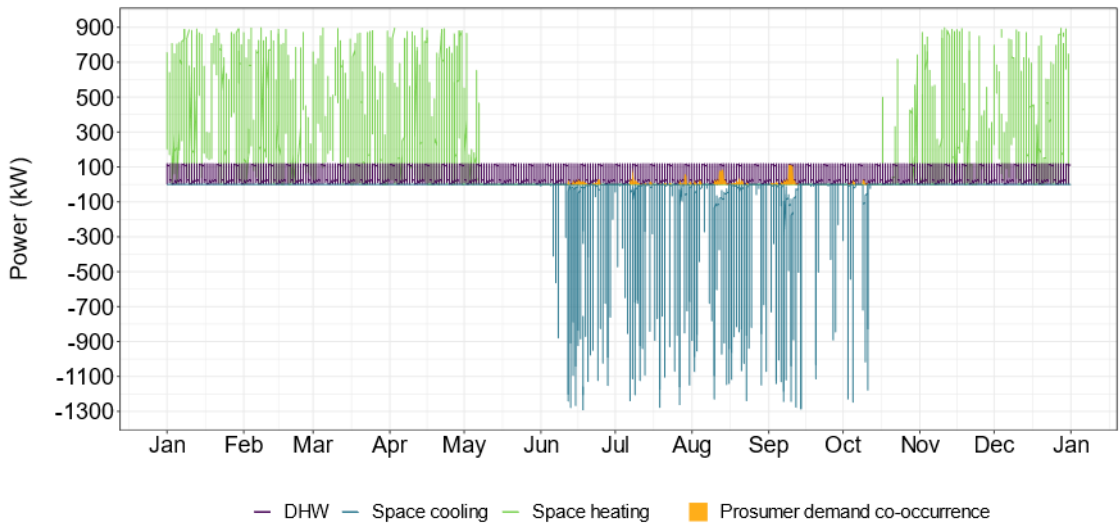


Figure 7.11: Total annual heating and cooling demand and their co-occurrence (DOC).

Figure 7.11 highlights that there is a clearly seasonal demand profile with cooling demands during summer and heating demands during the winter. This is in line with demand profiles of common European building stock as discussed in Zhang et al. (2023) [30]. The DOC is 114MWh/year for full built-out, which represents 3.4% of the total energy demand. Finally, the phasing of the demand (shown in Table 7.2) is considered. The annual heating and cooling demand for each year until full built-out is shown in Figure 7.12.

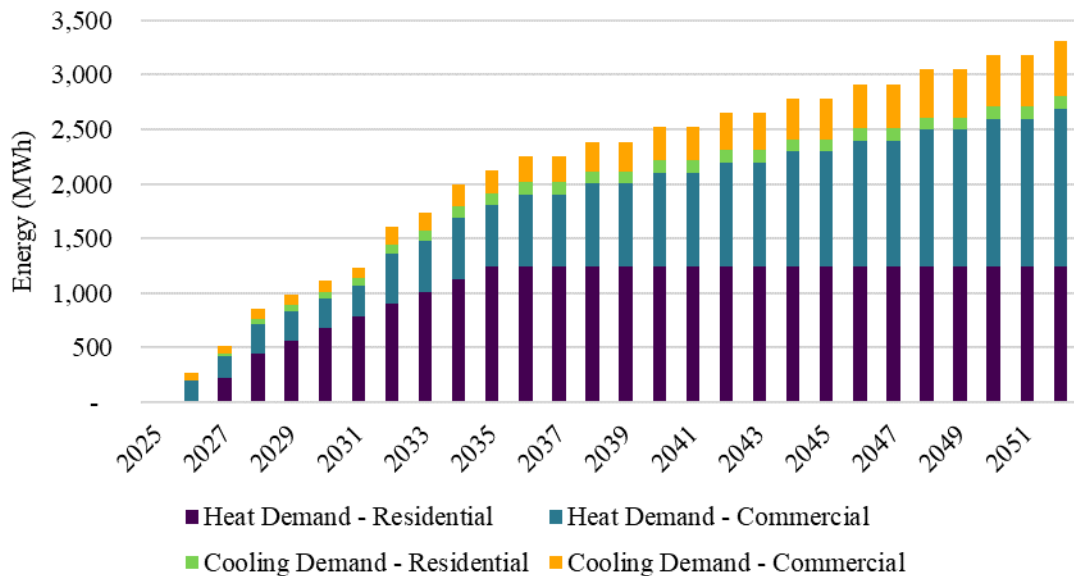


Figure 7.12: Demand phasing from start year to full built-out.

7.3 WWTP waste heat utilisation

Waste heat utilisation from the WWTP's final effluent can greatly benefit a 5GDHC system, by acting as a heat source during winter, and a heat sink during summer. However, to be able to extract/deposit heat, the final effluent's temperature and existing infrastructure need to be studied. Clyde Gateway supplied data for the WWTP's final effluent temperatures for March 2017 to April 2019. Using them, the average daily final effluent temperatures are determined and shown in Figure 7.13.

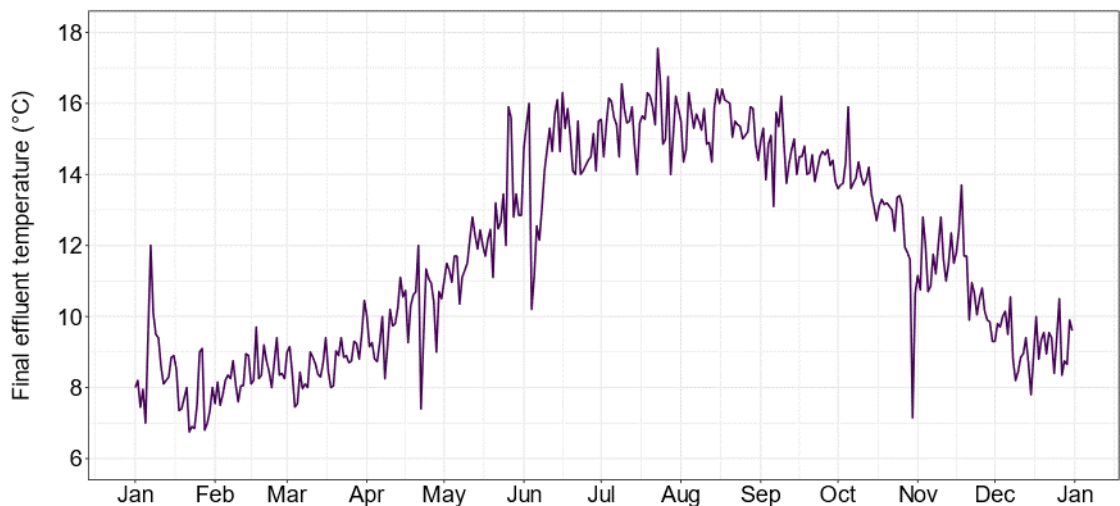


Figure 7.13: Average daily final effluent temperature.

The installed pipe for abstracting and circulating the final effluent through the installed HEX is DN150. Assuming a pressure drop limit of 250Pa/m, the maximum flow available for a temperature of 8°C is 48kg/s using equation 6.4 in Section 6.2.2. For utilising this WWTP capacity, there are two options available. Either the ambient network connects directly to the WWTP, acting as a prosumer, or it acts as the source for a SWSHP charging the BU's TES. Since there is no space in the WWTP plantroom, the SWSHPs will need to be in the EC near the Red Tree Magenta building. In each case, a different behaviour of the system will be present, along with a different network design and topology. This leads to two scenarios that need to be investigated as to how to utilise the WWTP for 5GDHC, also captured in a schematic in Figure 7.14:

- a) Scenario 1 (referred to as 5GDHC-1): Use of existing HEX at the WWTP plant. Appropriate network temperatures are needed to use the WWTP as a heat source during winter and as a heat sink during summer.
- b) Scenario 2 (referred to as 5GDHC-2): WWTP acts as a heat source/sink for a reversible SWSHP in the BU. The SWSHP acts as the main charging unit for the BU's TES.

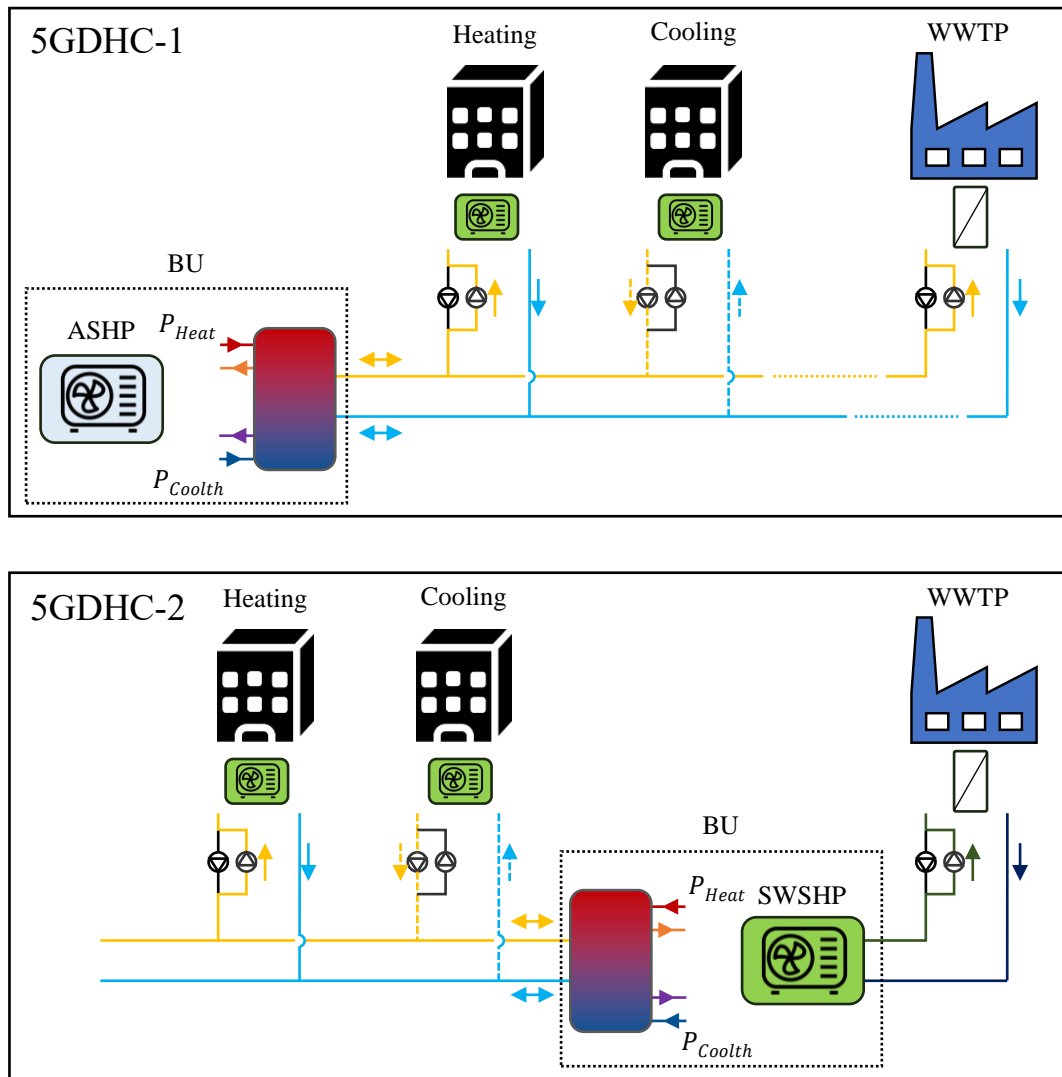


Figure 7.14: 5GDHC scenarios for using the WWTP as a heat source/sink.

For 5GDHC-1, the ambient network's temperature regime needs to be set so that heat can be abstracted during winter and deposited during summer. Therefore, two temperature regimes are required during heating and cooling seasons. The following conditions need to be met when selecting the temperature spread, which should be read in conjunction to Figure 7.15:

- Minimum ΔT difference between sink and source of 2°C ($\Delta T_1 - \Delta T_2$).
- Keep the same ΔT difference across the HEX during heating and cooling (ΔT_3).
- Have the same ΔT on the network during heating and cooling (ΔT_4) for the evaporators to operate in both temperature regimes.
- The minimum temperature for the return of the final effluent ($T_{\text{out_WWTP}}$) is always above 4°C .
- WWTP for heating (winter): The hot line temperature in the ambient network ($T_{\text{hw_5GDHC}}$) is lower than the minimum temperature of the final effluent ($T_{\text{in_WWTP}}$).
- WWTP for heating (winter): The cold line temperature in the ambient network ($T_{\text{cw_5GDHC}}$) is lower than the final effluent return temperature ($T_{\text{out_WWTP}}$).
- WWTP for cooling (summer): The cold line temperature in the ambient network ($T_{\text{cs_5GDHC}}$) is higher than the final effluent inlet temperature ($T_{\text{in_WWTP}}$).
- WWTP for cooling (summer): The hot line temperature in the ambient network ($T_{\text{hs_5GDHC}}$) is higher than the final effluent return temperature ($T_{\text{out_WWTP}}$).

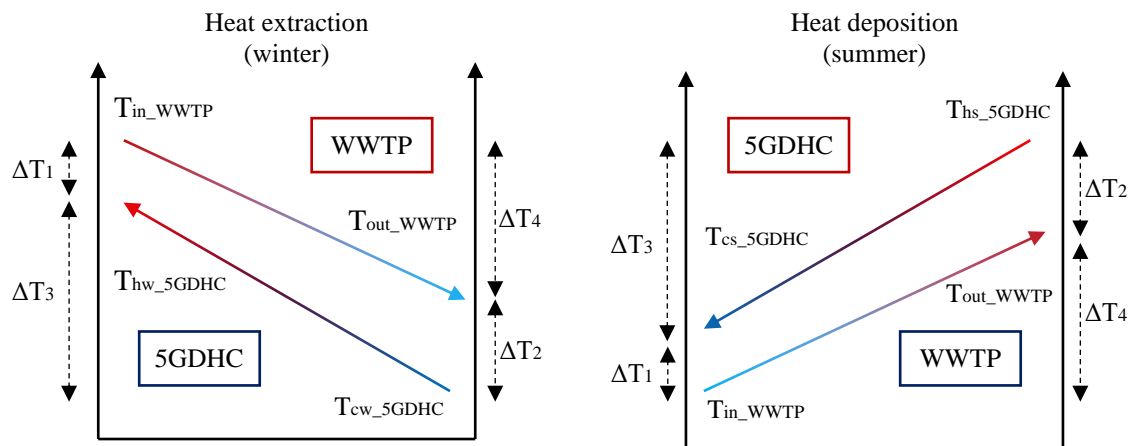


Figure 7.15: 5GDHC-1 restrictions for utilising WWTP through a HEX.

To determine the temperature profiles of the ambient network, a histogram of the temperature spread in the final effluent is studied, shown in Figure 7.16.

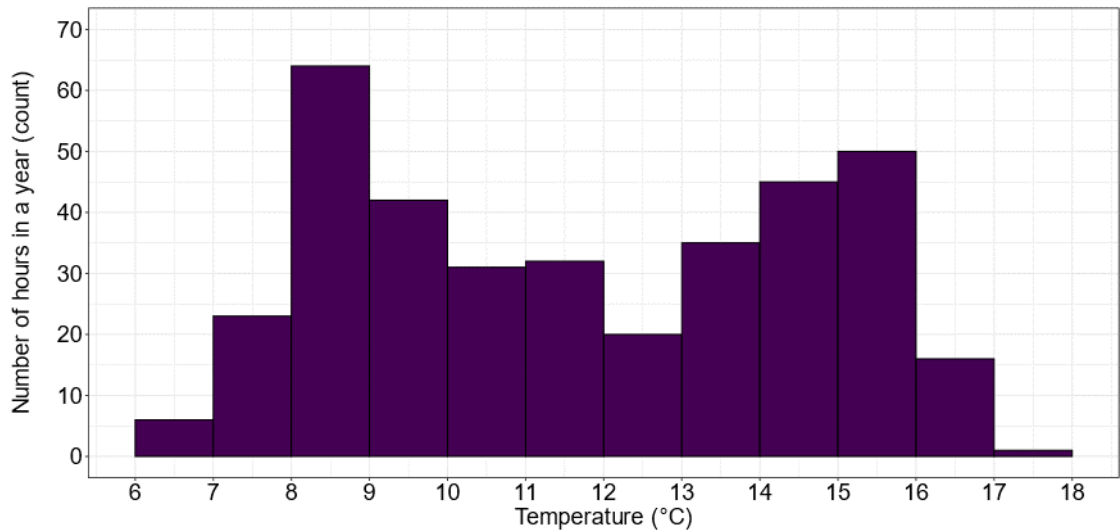


Figure 7.16: Histogram of WWTP's final effluent flow temperatures.

To maximise the number of final effluent temperatures that allow heat extraction, the ambient network hot line temperature (T_{hw_5GDHC}) needs to be lower than the final effluent's temperature. To satisfy all the conditions mentioned, a temperature profile of 7°C to 2°C for the 5GDHC is proposed (ΔT of 5°C), with a final effluent temperature difference (ΔT_4) of 3°C. A minimum operation temperature of 8°C is set for the final effluent, allowing the return to always stay above the minimum final effluent return temperature of 4°C. To ensure the medium in the ambient network does not freeze, a 20% glycol with 80% water mixture is used [238], dropping the mixture's freezing temperature to -10°C. When cooling is needed from the final effluent, the cutoff temperature of 17°C is used based on the histogram. To satisfy condition (g), the cold line of the ambient network (T_{cs_5GDHC}) is set to 17°C. To keep the same ΔT in the network as per condition (b), the hot line temperature of the ambient network (T_{hc_5GDHC}) is set to 23°C. Figure 7.17 shows the ambient temperature profile for heating (October to May) and cooling (June to September) season.

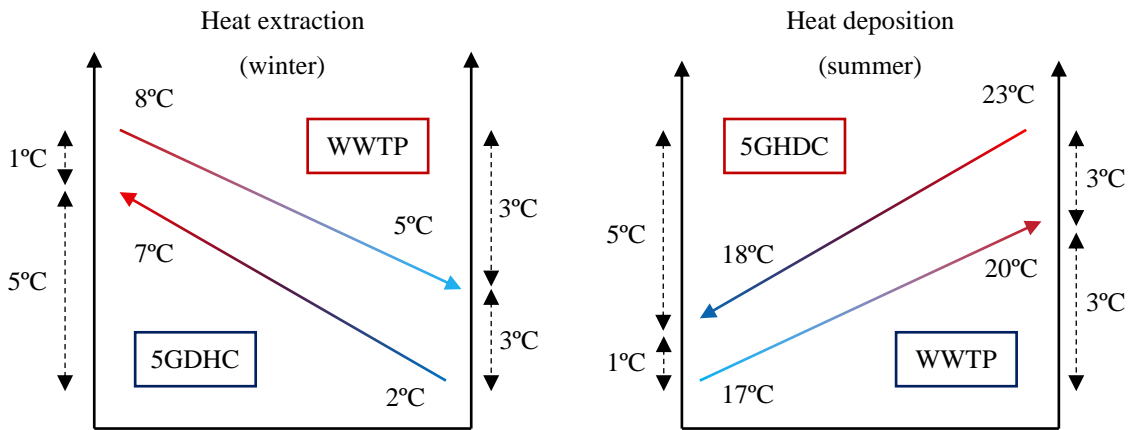


Figure 7.17: 5GDHC-1 temperature profile during heating and cooling season.

For this temperature profile, the available power can be calculated for each timestep based on the Logarithmic Mean Temperature Difference (LMTD) and the HEX’s surface area.

$$LMTD = \frac{\Delta T_1 - \Delta T_2}{\ln \left(\frac{\Delta T_1}{\Delta T_2} \right)} \tag{7.2}$$

$$Q = A_{HEX} LMTD h_o \tag{7.3}$$

where Q is the available power from the WWTP, A_{HEX} is the surface area of the WWTP’s HEX and h_o is the heat transfer coefficient of the medium. The 20% glycol with water mixture has a h_o of 5,000W/m²K at high Reynolds numbers [238]. The A_{HEX} is 20m² according to the data provided from Clyde Gateway. Figure 7.18 shows the resulting daily available power from the final effluent, and respective flow and return temperatures.

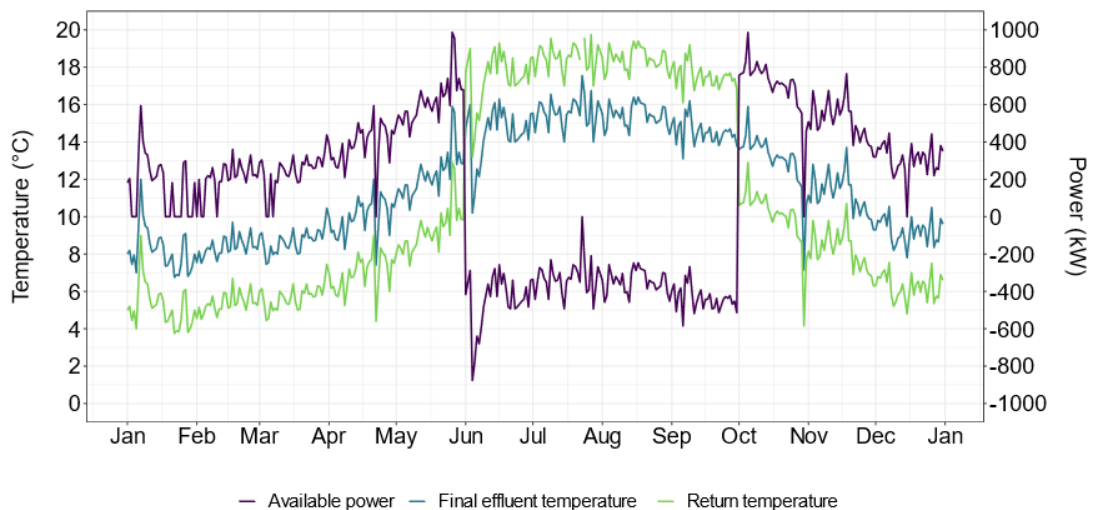


Figure 7.18: WWTP’s final effluent and temperature profile and available thermal power.

In 5GDHC-1, by treating WWTP as a prosumer (cooling prosumer during winter and heating prosumer during summer), the potential energy share from the WWTP gives a DOC of 38.4% with an additional DOC of 3.4% coming from building demand co-occurrence. This is shown in Figure 7.19 and Figure 7.20.

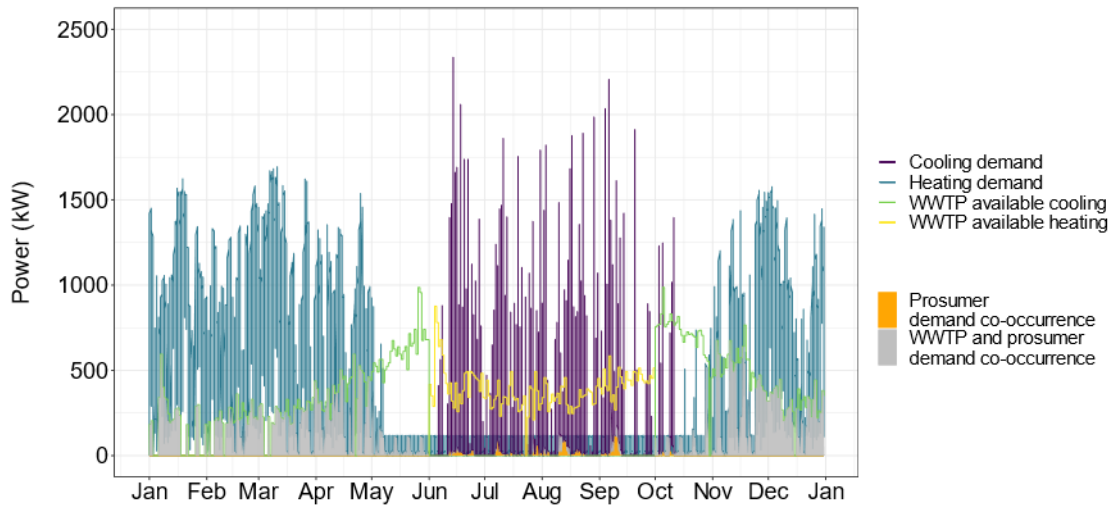


Figure 7.19: Building heating and cooling demands, WWTP energy share and demand co-occurrence.

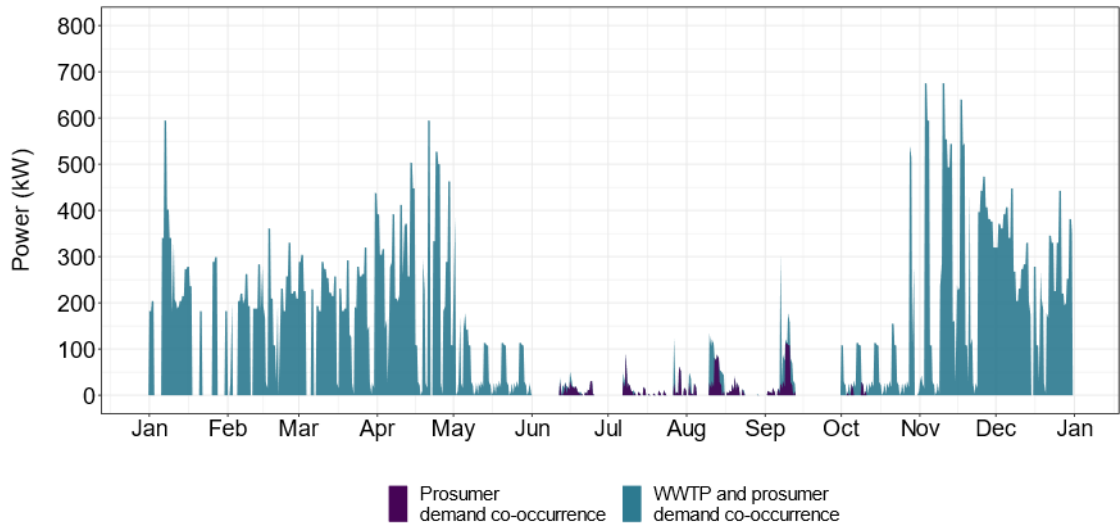


Figure 7.20: Demand co-occurrence from prosumer demands and WWTP.

For scenario 5GDHC-2, the ambient network is split into two parts. One comprises the existing ambient pipework (DN355) from the WWTP to Red Magenta, which will act as a feed to the SWSHP in the BU. This will keep the same temperature characteristics as the

ones detailed above, along with the same capacity availability. The other comprises the ambient network for 5GDHC, which in this scenario can follow the more typical 15°C to 20°C temperature range for the cold and hot lines respectively.

7.4 5GDHC design and operation for case study

To complete the design of the 5GDHC system and characterise its operation, a stepwise methodology is followed. It starts from the demand assessment, and uses its outputs to design the prosumer substations, BU and ambient network. It leverages the prosumer and BU models from the ProHMo library in a series of steps. This combined methodology, comprises a combination of ProHMo and CATHeaPS along with GIS mapping. This methodology is shown in Figure 7.21 and described below.

(1) Demand assessment in Modelica

The demand assessment outputs from Section 7.2 are obtained and set to demand profiles, similar to the experimental demands from the PHIL discussed in Section 5.1. They have an hourly timestep and include space heating, space cooling and DHW.

(2) Prosumer simulation

The demands from the demand assessment advise an asset sizing exercise for prosumer level equipment. The ProHMo prosumer models are then used for the prosumers' energy supply analysis, providing hourly power requirements (heating and cooling) and electricity use. The $T_{GridFix}$ control regime is used, assuming a constant ambient grid temperature profile. This allows to simulate the prosumers' behaviour separately to the BU, assuming the hot and cold line temperatures are constant to the setpoint values. These are:

- 5GDHC-1:
 - Winter operation (Oct – May) hot line at 7°C and cold at 2°C
 - Summer operation (Jun - Sep) hot line at 23°C and cold at 18°C
- 5GDHC-2 has a constant seasonal profile with the hot line temperature at 20°C and cold line at 15°C.

Methodology for generating inputs for the techno-economic analysis of 5GDHC against counterfactual supply technologies in CATHeaPS.

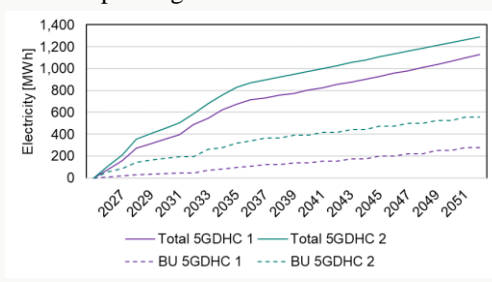
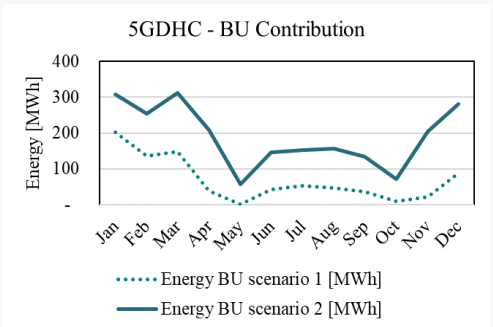
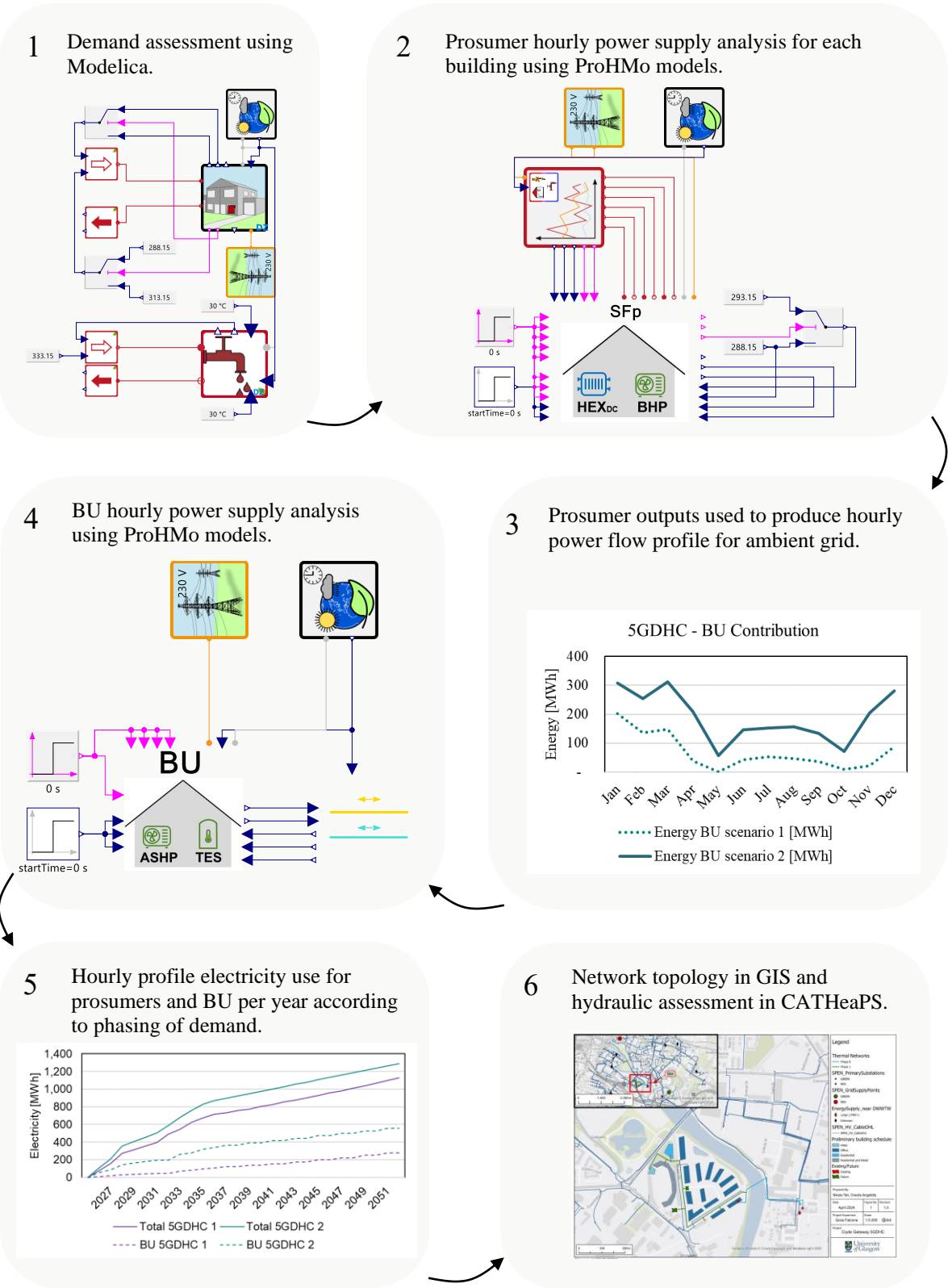


Figure 7.21: Methodology of 5GDHC design for yielding inputs for TEM.

(3) BU power demand

The net demand seen by the BU for each hourly timestep is thus yielded for each year of the phased development. Similar to step (1), the power and net flowrate are set as a demand for the BU. This allows for sizing the BU equipment and determining its mix of technologies required, designed for the full built-out.

(4) BU simulation

The BU ProHMo model is then used, with the hourly BU share of heating and cooling set as a power input. The models need to be slightly altered to account for the mix of technologies for each scenario. Their control setpoints are also set to account for the network temperatures and prioritisation of operation. This allows for a complete characterisation of the power flows present in the system for each year of the development.

(5) Total energy use

The outputs from steps (2) and (4) are compiled to get the annual electricity use for each scenario, at prosumer and BU level for both heating and cooling supply.

(6) Network hydraulic analysis

Finally, a network routing exercise is conducted in GIS considering 5GDHC-1 and 5GDHC-2 bespoke characteristics. A hydraulic assessment is conducted in CATHeaPS, sizing the pipes for each 5GDHC scenario based on the temperature and power profiles as well as the network topology.

Altogether, the outputs of this exercise provide information about plant capacities, electricity use and network sizing. They are used as inputs in CATHeaPS to quantify the techno-economic performance of both 5GDHC scenarios.

The proposed stepwise simulation uses a different modelling architecture than the one used in the experimental validation section. This is because that modelling architecture is suited for the detailed analysis of 5GDHC systems, but it is not appropriate for this conceptual design stage. That model architecture excels at creating digital twins but requires precise network sizing and specifications (including resistance elements) for accurate pump selection and a thorough hydronic balancing exercise. Here, the primary focus is understanding the techno-economic performance of the system. Therefore, the proposed

simplified approach utilizing hourly timesteps is employed to reduce computational times without affecting the accuracy of the power flow behaviour characterisation of the system.

All Modelica simulations are conducted in the same computing environment as the one mentioned in Chapter 5 (laptop with 12 physical cores and 16 logical processors, running Simulation X version 4.2 at Microsoft Windows 10 Enterprise). CVODE C compiled integration algorithm is used, with an equidistant timestep of 60min, simulating 365 days.

7.4.1 Analysis and simulation of prosumers for 5GDHC

To determine the heating and cooling requirements for the prosumers, the ProHMo prosumer models are used. They are modified so that they can supply cooling to commercial customers with 8°C flow and 15°C return terminal units. For the heating terminal units, low temperature heating is assumed with a 40°C flow and 30°C return. DHW is supplied from a separate riser, having a 60°C flow and 35°C return. One TES for heating and one for cooling is used, with the control parameters having the same rule-based approach as the one explained in Section 3.3.3. A reversible BHP is used, charging either the heating or the cooling TES, with priority given to the Heating TES to avoid legionella concerns. A schematic of the prosumer setup is shown in Figure 7.22.

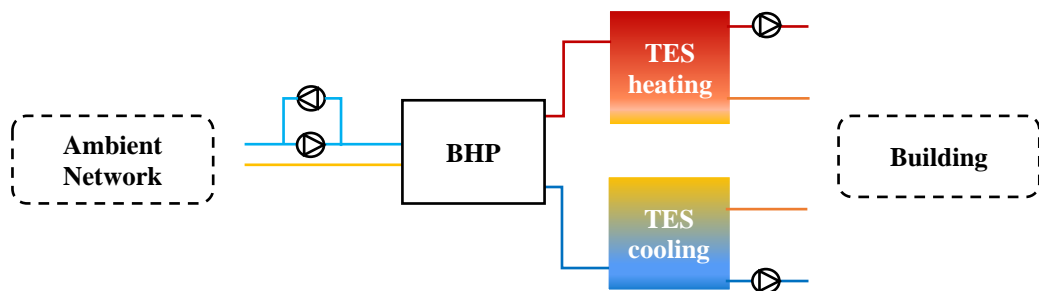


Figure 7.22: Prosumer setup schematic.

As mentioned, $T_{GridFix}$ control regime is assumed, allowing for a simpler assessment using only the thermal components of the system. It is assumed that the hot and cold line remain at the temperature setpoints (5GDHC-1: cold line 2°C and hot line 7°C in winter and cold line 18°C with hot line 23°C in summer, 5GDHC-2: cold line 15°C and hot line 20°C throughout the year). This allows for a simulation with hourly timesteps (60min) of each prosumer substation separately using the prosumer models from ProHMo, as shown in Figure 7.23. A variable modulation factor is used for the BHP as discussed in Section

3.3.3. The turndown ratio is set to 10%, matching the value of the BHP unit used in the experiment. The nominal COP is set to 4.5 for heating and the nominal EER to 5.0 for cooling according to Kim et al. (2021) [239], where a similar system of water to water reversible HP for communal systems is used. The SCOP and Seasonal EER (SEER) will vary from the nominal value based on the inflow temperature changes and the modulation factor. Therefore, 5GDHC-1 is expected to have lower SCOP than 5GDHC-2, due to heating operation during winter where the ambient network's hot line temperature is 7°C.

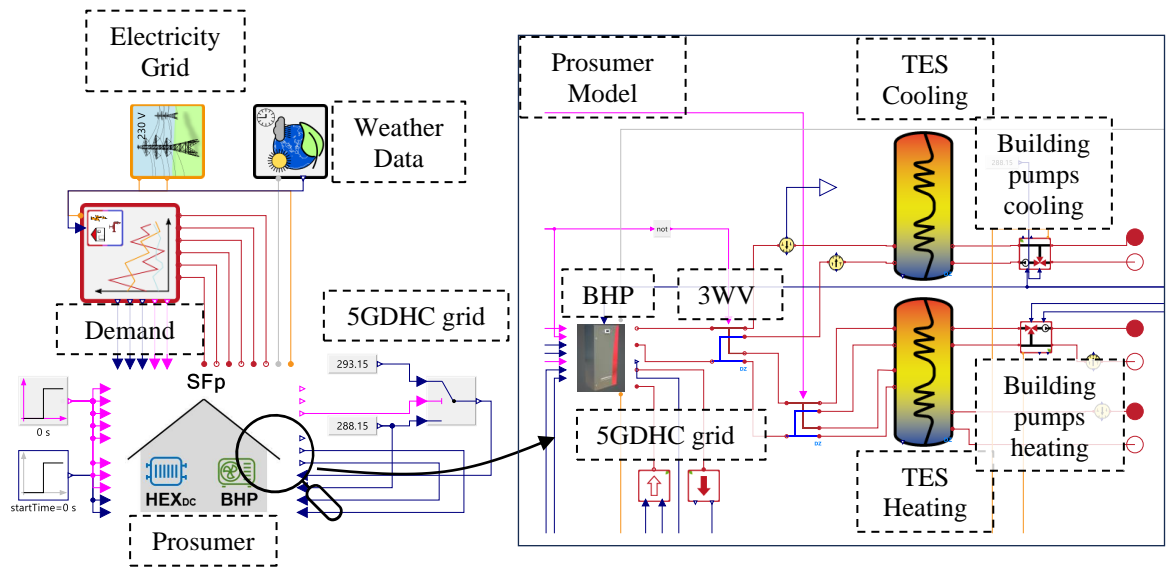


Figure 7.23: Prosumer simulation using ProHMo models.

To accurately simulate prosumer behaviour, details of the asset capacity are needed. These are yielded from the demand assessment outputs. For the TES, a 30min discharge at peak demand is assumed and a diameter to height ratio of 2.5 to ensure thermal stratification within the TES [43]. The TES volume is calculated using equation 7.1:

$$V_{TES} = \frac{\rho(P_{th}t_{dis})}{\Delta T_{TES}c_p n_{TES}} \quad (7.1)$$

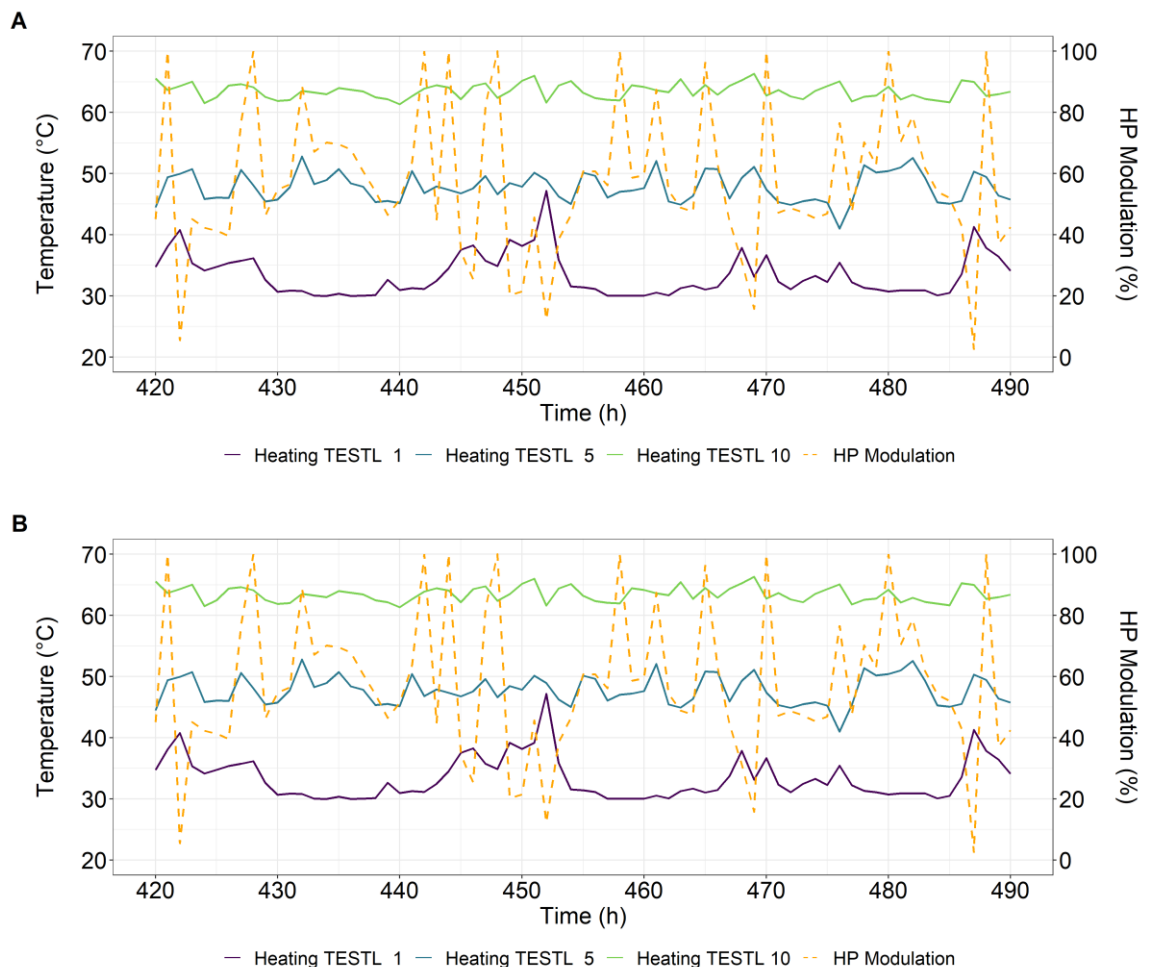
where V_{TES} is the volume of the TES needed to supply the peak demand (P_{th}) for a discharge period (t_{dis}). ΔT_{TES} is the temperature difference of the TES system (35°C for the heating TES and 7°C for the cooling TES) and n_{TES} the efficiency of the TES (90%).

For the BHP capacity, the peak load is used for both heating and cooling, found from the maximum of the hourly power demands from the demand analysis, shown in Table 7.4.

Table 7.4: Capacity of BHP and TES.

Building	BHP heating (kW)	BHP cooling (kW)	TES heat (m3)	TES cooling (m3)
Red Tree Magenta	160	110	2.2	11.2
Red Tree Central	140	140	2.0	9.8
Magenta Technology Hub	140	100	2.0	9.8
Residential Tower	180	230	2.5	12.6
Stadium Hotel	190	110	2.7	13.3
Stadium Residential	420	870	5.9	29.3
Stadium Retail	20	30	0.3	1.4
Magenta Business Park	960	1330	13.4	67.0

The average computational time for the prosumers is 5.6min, with some units having more starts and stops due to large BHP capacity compared to demands encountered. An example of how the TES and the BHP are working to meet the demand is shown in the figures below for both heating (Figure 7.24) and cooling (Figure 7.25) operation.

**Figure 7.24: BHP and Heating TES operation for meeting heating requirements.**

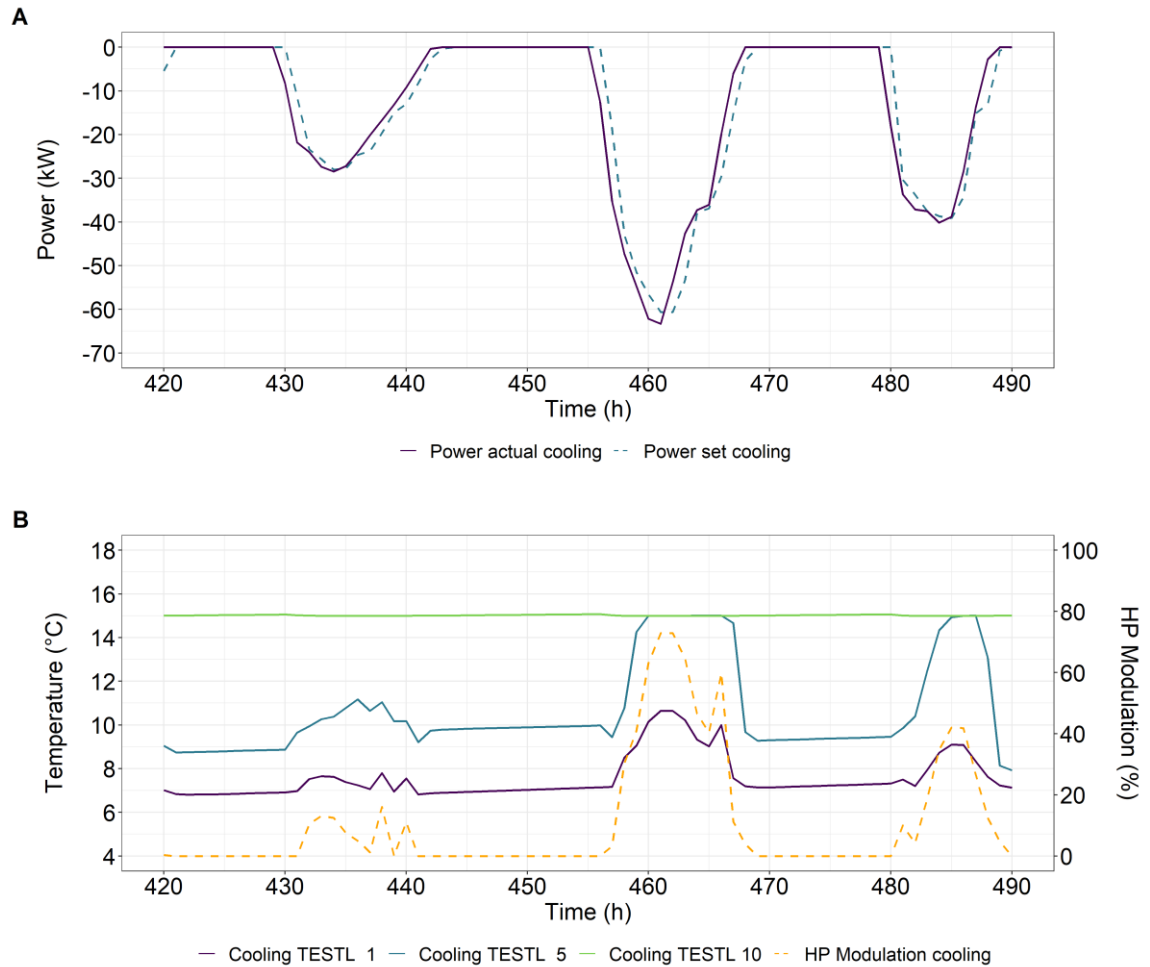


Figure 7.25: BHP and Cooling TES operation for meeting cooling requirements.

The power demands are met for space heating, DHW and space cooling. There is a slight delay between power supply and power demand for space heating and space cooling, but the energy demanded and supplied is perfectly matching. The effect of this slight mismatch has no impact on thermal comfort since the internal temperature is not sensitive to minor time delays, unlike DHW. The BHP is varying its modulation with the TESTLs temperature values as expected, allowing for a smaller number of starts and stops (none for heating operation and 3 for cooling in a period of 30h). These profiles indicate a smooth operation. From these simulations, the annual electricity use, and SCOP can be yielded for each scenario, shown in Table 7.5 along with the respective CPU time.

Energy demands for space heating, space cooling and DHW are met for all buildings. The annual electricity use for the BHP ranges from 7MWh/year for the Stadium Retail to 363MWh/year for the Magenta Business Park for 5GDHC-1. The SCOP ranges from 3.6 to 4.0 for 5GDHC-1 and from 3.9 to 4.8 for 5GDHC-2. The average SCOP is 3.9 for

5GDHC-1 and 4.5 for 5GDHC-2, while the average SCOP difference between the two scenarios is 14% higher for 5GDHC-2, due to the higher network temperatures. This spread of the SCOP among the buildings has to do with the operation of the BHP in different modulation factors throughout the year, and the number of starts. An optimisation of the technology mix and the sizing of the BHPs and the TESs could lead to higher SCOPs. The total electricity use for each year is shown in Figure 7.26.

Table 7.5: Electricity use and SCOP of BHP in prosumer substations.

Building	5GDHC-1 electricity (MWh/year)	5GDHC-2 electricity (MWh/year)	5GDHC-1 SCOP	5GDHC-2 SCOP	SCOP Difference (%)	CPU time (min)
Red Tree	32	27	3.9	4.6	6%	3.5
Magenta						
Red Tree Central	41	33	3.8	4.6	19%	3.6
Magenta	27	25	3.9	4.3	9%	3.4
Technology Hub						
Residential Tower	70	64	3.6	3.9	8%	4.1
Stadium Hotel	31	27	4.0	4.5	13%	3.4
Stadium	282	252	3.9	4.4	12%	4.2
Residential						
Stadium Retail	7	5	3.8	4.7	19%	3.4
Magenta Business	363	305	4.0	4.8	16%	3.8
Park						
Total	853	738	3.9	4.5	14%	-

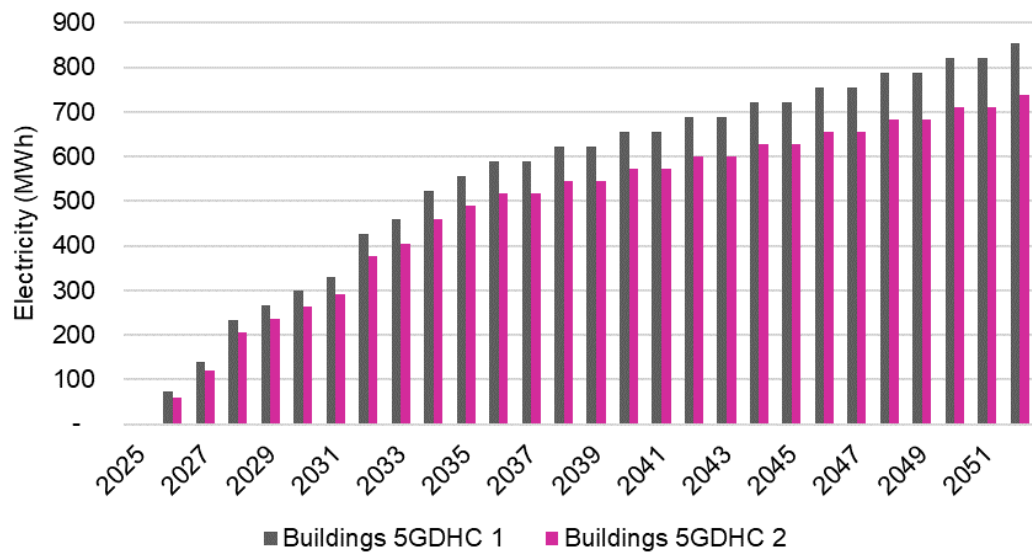


Figure 7.26: Electricity use for buildings for each year accounting for phasing.

This exercise results in hourly data for heating and cooling requirements from the ambient grid for each prosumer's BHP for each year of the project. These are used to calculate the net requirements for the BU, allowing energy equipment sizing and, through simulations, yielding their annual electricity requirements.

7.4.2 Analysis and simulation of BU for 5GDHC

To find what the BU needs to supply in each timestep to thermodynamically balance the network, the net power requirement is found. Due to the development's phasing, different buildings and share of demands need to be accounted for each year.

For 5GDHC-1 scenario, other than the prosumers, the WWTP is treated as a prosumer. Depending on its power availability, it supplied the needed heating or cooling in the system, with the remainder met by the BU. The net power that the BU needs to supply for full built-out for 5GDHC-1 and 5GDHC-2 is shown in Figure 7.27.

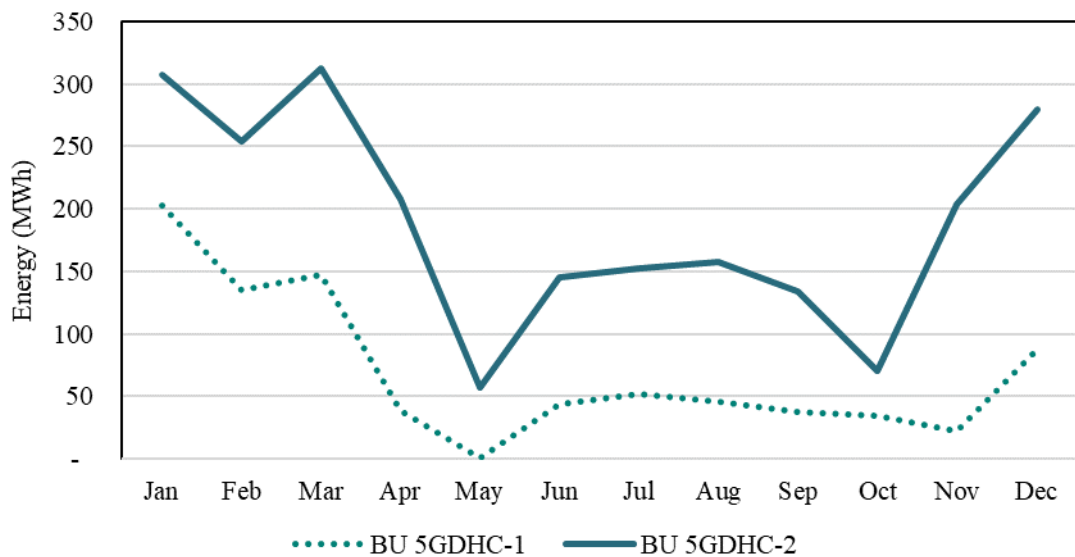


Figure 7.27: Energy supply from BU for 5GDHC-1 and 5GDHC-2 for full built-out.

As expected, for scenario 5GDHC-1 there are increased demand synergies between heating and cooling due to the WWTP acting as a prosumer. In fact, the BU for 5GDHC-1 needs to supply 823MWh/year during full built-out (693MWh/year of heating and 130MWh/year of cooling). The BU of 5GDHC-2 needs to supply 2,284MWh/year (1,719MWh/year of

heating and 565MWh/year of cooling). This is 64% less energy required for 5GDHC-1, 60% less for heating and 77% less for cooling.

Using these hourly power demands, along with the net hourly flowrate from the prosumers, the BU ProHMo models can be used to determine the electricity consumption for 5GDHC-1 and 5GDHC-2. The two BU models include different equipment and control strategies since for 5GDHC-1 only an ASHP is needed while for 5GDHC-2 a SWSHP is meeting the base load with an ASHP meeting any remaining demands. The limitation for the SWSHP is the minimum capacity available during winter as established in Section 7.3, being 180kW. Therefore, a 200kW capacity unit is used with the remainder of the peak being supplied by the ASHP. A schematic of the models used is shown in Figure 7.28 while a table with the capacities of the equipment is found in Table 7.6.

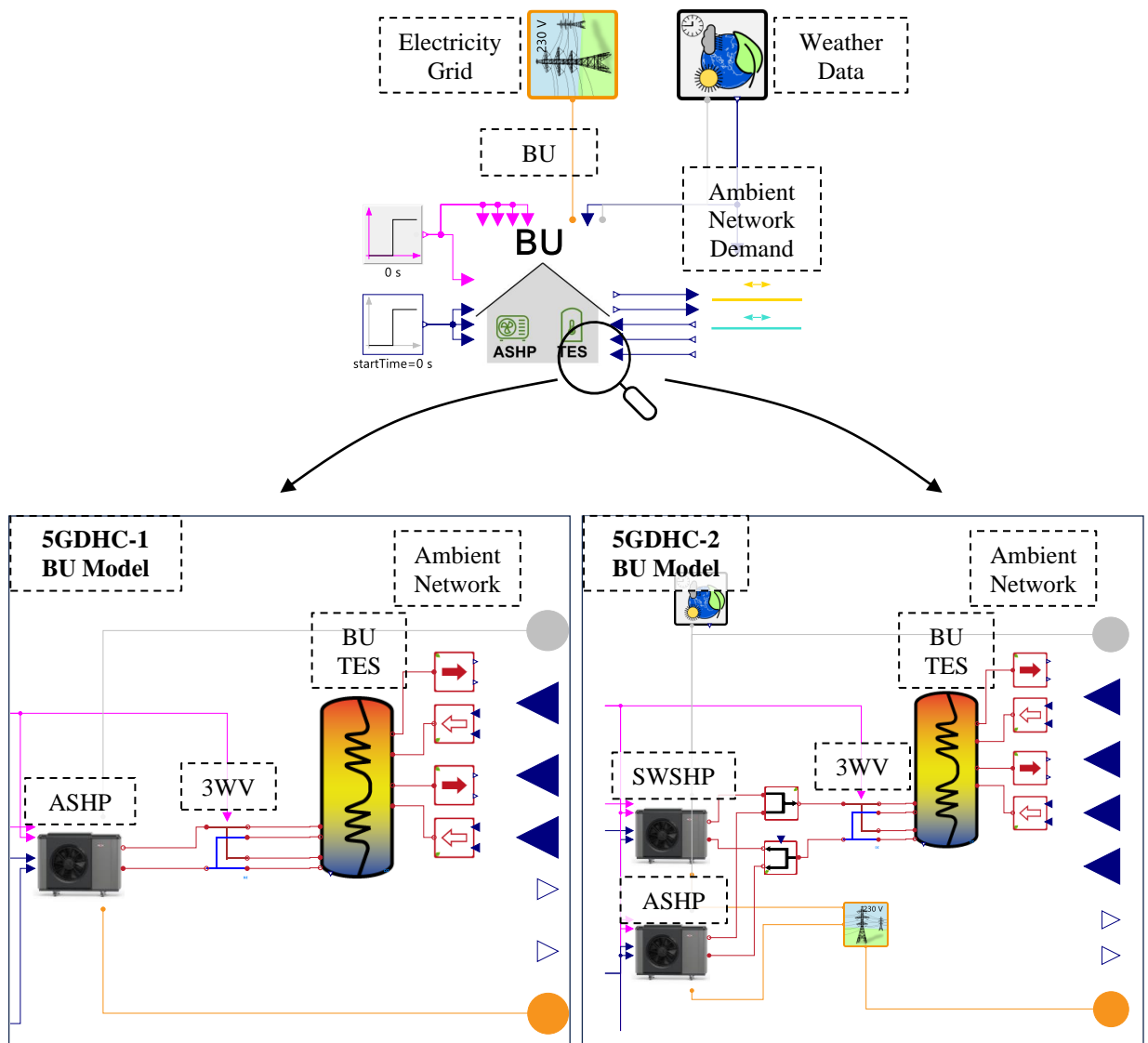


Figure 7.28: BU Models in ProHMo.

Table 7.6: Plant sizing for BU for 5GDHC-1 and 5GDHC-2.

Item	Units	5GDHC-1	5GDHC-2
BU peak heating	kW	599	601
BU peak cooling	kW	933	1,113
SWSHP capacity	kW	-	200
ASHP capacity	kW	933	1,113
TES	m ³	91	109

For the controls, the same rule-based approach using the specified TESTLs temperature values and the flow direction as shown in Section 3.3.4 is used for both 5GDHC-1 and 5GDHC-2. The control setpoints are altered to fit the temperature profile of the network during winter/summer for 5GDHC-1 as well as the priorities for the SWSHP and ASHP in 5GDHC-2. By giving a lower temperature setpoint for starting for the ASHP, it allows it to act as a back-up unit, in case the SWSHP cannot supply enough power.

Table 7.7: Control setpoints for ASHP and SWSHP in the BU based on TES temperature.

Control setpoints	5GDHC-1 ASHP	5GDHC-1 ASHP	5GDHC-2	5GDHC-2 ASHP
	Winter	Summer	SWSHP	
$T_{set,BU,StartHeat}$	6.0°C	22.0°C	20.0°C	19.5°C
$T_{set,BU,StopHeat}$	9.0°C	25.0°C	22.0°C	22.0°C
$T_{set,BU,StartCool}$	2.0°C	18.0°C	15.0°C	15.5°C
$T_{set,BU,StopCool}$	0.0°C	16.0°C	13.0°C	13.0°C

Finally, the nominal COP is set to 8.0 for the SWSHP according to Gudmundsson et al. (2021) [27] for systems supplying ultra-low temperature heat networks, and the COP for the ASHP to 6.0 to account for the lower source inlet temperatures [240]. The nominal EER is set to 5.0 for both the ASHP and the SWSHP, since the similar inlet and outlet values as the BHP values are present.

The simulations' outputs for full built-out are shown in Table 7.8, where the Seasonal Performance Factor (SPF) captures both the SEER and SCOP. The average computational time for 5GDHC-1 is 2.38 minutes and for 5GDHC-2 is 6.33 minutes. The higher times for 5GDHC-2 are due to the added complexity of having another energy transformation unit in the BU model.

Table 7.8: Energy use for BU for full built-out.

Item	Units	5GDHC-1	5GDHC-2
CPU time	minutes	5.6	5.8
Heating SWSHP	MWh/year	-	672
Cooling SWSHP	MWh/year	-	254
Electricity for heating SWSHP	MWh/year	-	85
Electricity for cooling SWSHP	MWh/year	-	56
SCOP SWSHP heating	constant	-	7.9
SEER SWSHP cooling	constant	-	4.5
SPF SWSHP total	constant	-	6.6
Number of starts	constant	-	748
Heating ASHP	MWh/year	684	1,015
Cooling ASHP	MWh/year	131	324
Electricity for heating ASHP	MWh/year	113	182
Electricity for cooling ASHP	MWh/year	28	72
SCOP ASHP heating	constant	6.1	5.6
SEER ASHP cooling	constant	4.6	4.5
SPF ASHP total	constant	5.8	5.3
Number of starts	constant	1,010	1,473
Total BU electricity use	MWh/year	141	395

The energy demanded from the BU is met in both cases:

- 5GDHC-1:
Heating demand of 693MWh/year, ASHP supply of 684MWh/year
Cooling demand of 130MWh/year, ASHP supply of 131MWh/year
- 5GDHC-2:
Heating demand of 1,719MWh/year, supply of 1,688 (SWSHP: 672MWh/year and ASHP: 1,015MWh/year)
Cooling demand of 565MWh/year, supply of 578MWh/year (SWSHP: 254MWh/year and ASHP: 324MWh/year)

The slight discrepancies in supply and demand of heating/cooling originate from the heat gains/losses from the TES (discrepancies less than 2%). An ambient temperature of 18°C is assumed for the plantroom along with a heat conductance of 7W/K in accordance with the experimental apparatus shown in Section 5.1. The number of starts indicates a smooth operation of all HP units, since they correspond to a daily average of 2 to 3 starts per day.

The SWSHP has the smoothest operation with only 748 starts (approximately twice per day) since it is given priority in the system controls. The total SPF for the ASHP in 5GDHC-2 is slightly lower due to the greater temperature differences in source/sink temperature, the higher number of starts and prolonged operation in lower capacities than its design power (as it has a top-up role). Finally, the total electricity use for full built-out from the energy transformation units is 141MWh/year for 5GDHC-1 and 395MWh/year for 5GDHC-2, meaning 5GDHC-2 requires 180% more electricity than 5GDHC-1.

An example of how the BU's energy transformation units and TES are operating in 5GDHC-2 is shown in Figure 7.24 and Figure 7.25. They capture hours 30 to 70 (corresponding to the first days of January) to illustrate the operation of the two HPs according to the TESTLs temperature values (Figure 7.29) and the power & energy in and out of the TES (Figure 7.30).

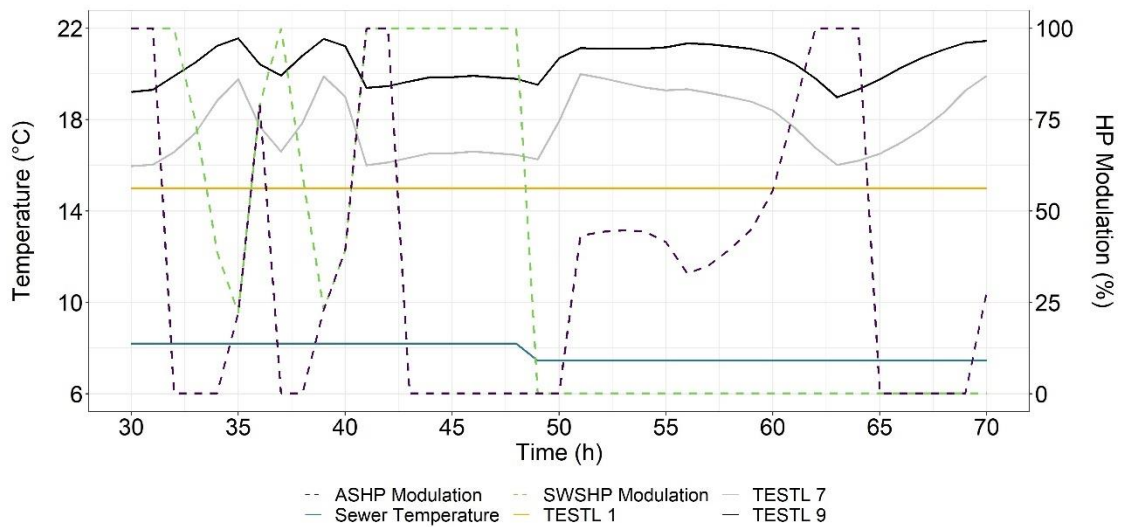


Figure 7.29: Operation of 5GDHC-2 BU units during hours 30 to 70.

It can be seen in Figure 7.29, that SWSHP has priority. For example, in the 35h to 45h period, the ASHP has a lower modulation factor, acting as a back-up unit the temperature drops below the ASHP temperature setpoint for TESTL 9. When there is a temperature lower than 8°C in the final effluent (hour 48), the SWSHP stops operating and the ASHP is solely responsible for charging the TES.

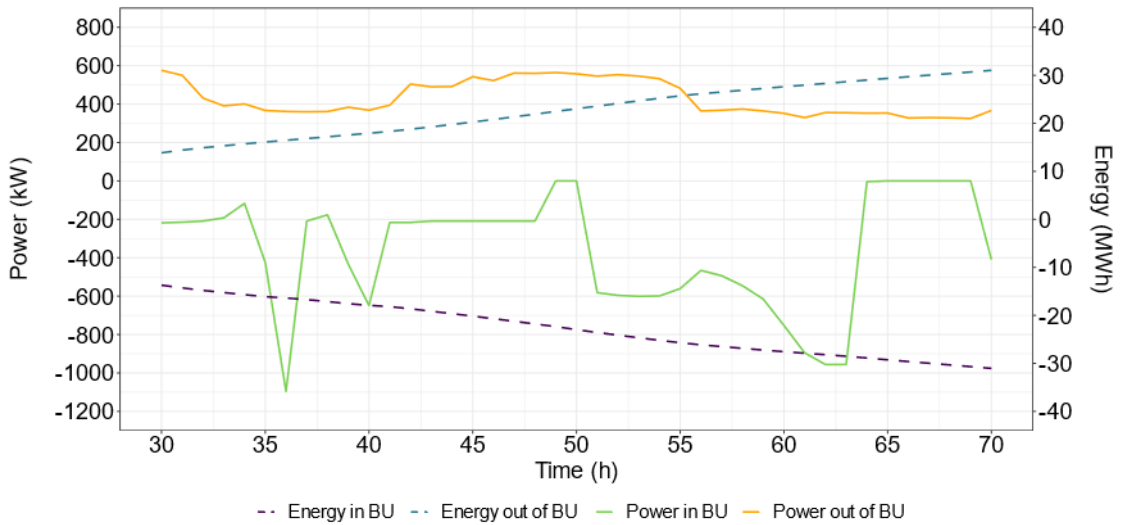


Figure 7.30: 5GDHC-2 BU's TES power and energy profile during hours 30 to 70.

In Figure 7.30 there is a variation on the power in and out of the TES at every time step. However, the thermal inertia of the TES allows for the energy in and out to be equal at all times. In other words, the TES offers a hydraulic separation and a buffer between supply and production.

Furthermore, for 5GDHC-1 the TES has a different temperature profile in summer and winter, as aforementioned. Figure 7.31 illustrates that the TES remains stratified with the top and bottom TESTL temperatures staying within the assigned control setpoints. The seasonal profile of the grid is followed by the TES, with the temperature regime changing between start of June and start of October (cooling season).

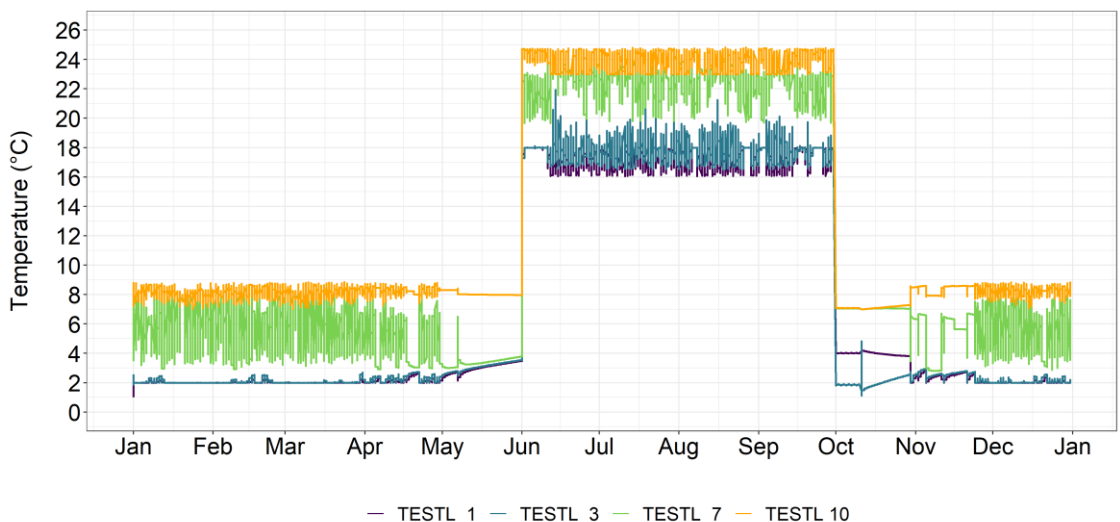


Figure 7.31: Annual temperature profile in BU's TES.

Having tested the operation of the BU for full built-out, the annual electricity use at BU level can be found for each year of the project. The only thing that is changing in the models are the input demands, with the equipment kept the same. This led to the total electricity consumption per year, shown in Figure 7.32. The values are shown next to the building level electricity use for the BHPs, along with the total electricity use for each 5GDHC's energy transformation units.

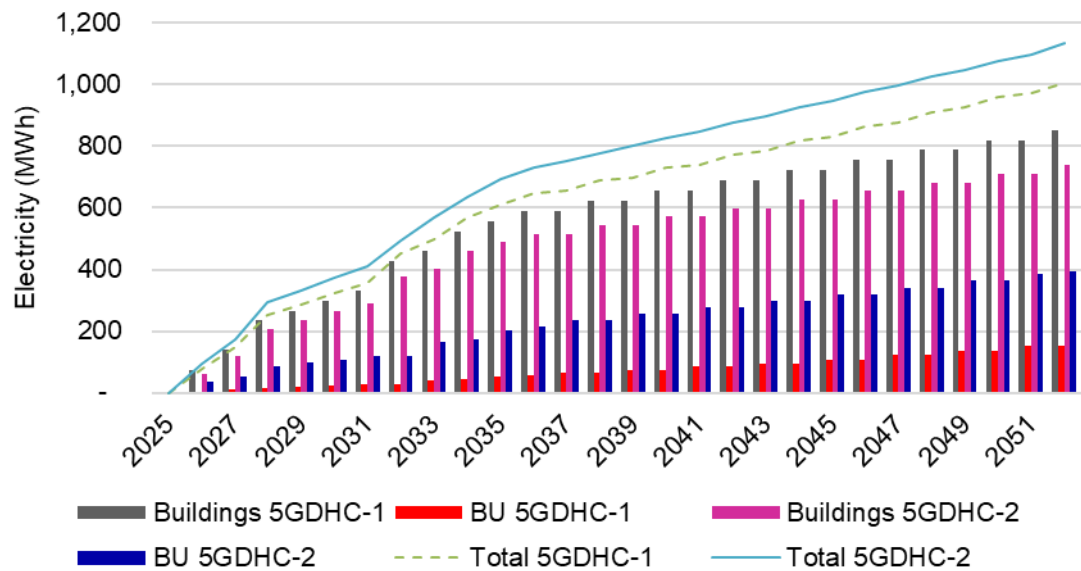


Figure 7.32: Energy transformation units' electricity use for 5GDHC-1 and 5GDHC-2.

As expected, the electricity use is lower for the first years of the project due to the low thermal demand. Despite the difference in the amount of heating and cooling that the BU needs to supply in 5GDHC-1 and 5GDHC-2, the overall electricity use is not that different. The reason for this are the lower SPF of the ASHP compared to the SWSHP and the higher electricity use of the prosumer BHPs due to lower ambient network temperatures as discussed in Section 7.4.1. Overall, for full built-out, the electricity use for 5GDHC-2 is higher than 5GDHC-1 by 133MWh/year (12% higher electricity use).

7.4.3 Energy share of the WWTP for 5GDHC

Having characterised each 5GDHC system, it is important to analyse the respective energy share from the WWTP. The energy use of the WWTP can be found from the HEX's efficiency from equation 7.2:

$$P_{th_{WWTP}}(t) = \frac{P_{th_{sink}}(t)}{n_{HEX}} \quad (7.2)$$

where $P_{th_{WWTP}}$ is the power in/out from the WWTP's final effluent in a timestep (t), n_{HEX} is the HEX's efficiency and $P_{th_{sink}}$ is the power out/in the sink. For 5GDHC-1, $P_{th_{sink}}$ is the 5GDHC ambient grid while for 5GDHC-2 is the feed for the SWSHP. As aforementioned, for 5GDHC-1, the net demand on a timestep t is compared to the available WWTP capacity and is used accordingly. For 5GDHC-2, since the SWSHP is sized at 200kW to account for the minimum limitation of the WWTP power (for a temperature of 8°C on the final effluent), the power drawn has a cap at 180kW. For 5GDHC-2, $P_{th_{sink}}$ is found from the ProHMo models and depends on the SWSHP's behaviour at the given timestep, as shown in equation 7.3 for heating and equation 7.4 for cooling:

$$P_{th_{sink_{he}}}(t) = P_{th_{SWSHP_{he}}}(t) \left(1 - \frac{1}{COP_{SWSHP}(t)}\right) \quad (7.3)$$

$$P_{th_{sink_{co}}}(t) = P_{th_{SWSHP_{co}}}(t) \left(1 + \frac{1}{EER_{SWSHP}(t)}\right) \quad (7.4)$$

where $P_{th_{SWSHP_{he}}}$ is the heat power output of the SWSHP and COP_{SWSHP} the COP of the SWSHP for a timestep t . During the SWSHP's cooling operation, its power output ($P_{th_{SWSHP_{co}}}$) is used along with the EER (EER_{SWSHP}). For full built-out, Table 7.9 captures the annual energy share of the WWTP for 5GDCH 1 and 5GDHC-2.

Table 7.9: Share of energy from WWTP.

Item	5GDHC-1 (MWh/year)	5GDHC-2 (MWh/year)	Difference (%)
WWTP heating demanded ($E_{sink_{he}}$)	883	587	50%
WWTP heating supplied ($E_{WWTP_{he}}$)	929	618	
WWTP cooling demanded ($E_{sink_{co}}$)	584	310	88%
WWTP cooling supplied ($E_{WWTP_{co}}$)	615	327	
Total WWTP energy demanded (E_{sink})	1,466	898	63%
Total WWTP energy supplied (E_{WWTP})	1,544	945	

There are significant variations in the heating supplied by the WWTP in the two scenarios, due to the 200kW capacity of the SWSHP for 5GDHC-2. For 5GDHC-2, the BU's TES in 5GDHC-2 is decoupling the power demanded from the power supply as shown in Figure

7.30. However, it's not sufficient to allow the SWSHP to meet the large peaks of the demand (especially for cooling), leading to a prolonged operation of the ASHP. For heating where power demands are closer to the capacity of the SWSHP, the difference between 5GDHC-1 and 5GDHC-2 is significantly smaller (50% compared to 88%). Therefore, there is a smaller utilisation of the WWTP in 5GDHC-2. Having a higher minimum capacity for the WWTP would allow a higher utilisation for 5GDHC-2. Therefore, waste heat sources with a flatter power availability annual profile would be critical for 5GDHC-2 unlike 5GDHC-1.

7.4.4 Ambient network sizing for 5GDHC

Another key variation that needs to be considered is the hydraulic design of 5GDHC. The topology of the ambient network for 5GDHC-1 and 5GDHC-2 is different as well as the network temperatures, leading to a different hydraulic sizing. To obtain the ambient network topology, the placement of the BU is critical. The ideal placement of the BU is in the centre of the network to allow for smaller pipe sizes, by splitting the network in branches rather than having one large spine.

For 5GDHC-1, there are no constraints for the placement of the BU. Upon discussions with Clyde Gateway, the BU is placed at the middle of the network, to allow for a split of the load in two main branches. One plantroom is allocated to the Magenta Business Park while the existing plantroom in the Red Tree Magenta building services only that building. The network layout is shown in Figure 7.33. For 5GDHC-2, the BU is placed in the Red Tree Magenta building. This is done to minimise the distance of the WWTP to the SWSHP, to avoid the additional pipework cost and space uptake. The network layout for this case is shown in Figure 7.34.

To determine the pipe diameters for each case, the same methodology to the CATHeaPS algorithm shown in Figure 6.5 is used. In this case, the placement of the loads in the grid is not linearised, the actual pipe lengths and load locations are used from the GIS maps. Ordnance Survey map data are used in GIS for network distance calculation. Medium characteristics for water with 20% glycol mix are used at the respective network temperatures [241]. These include density, viscosity, specific thermal capacity and freezing

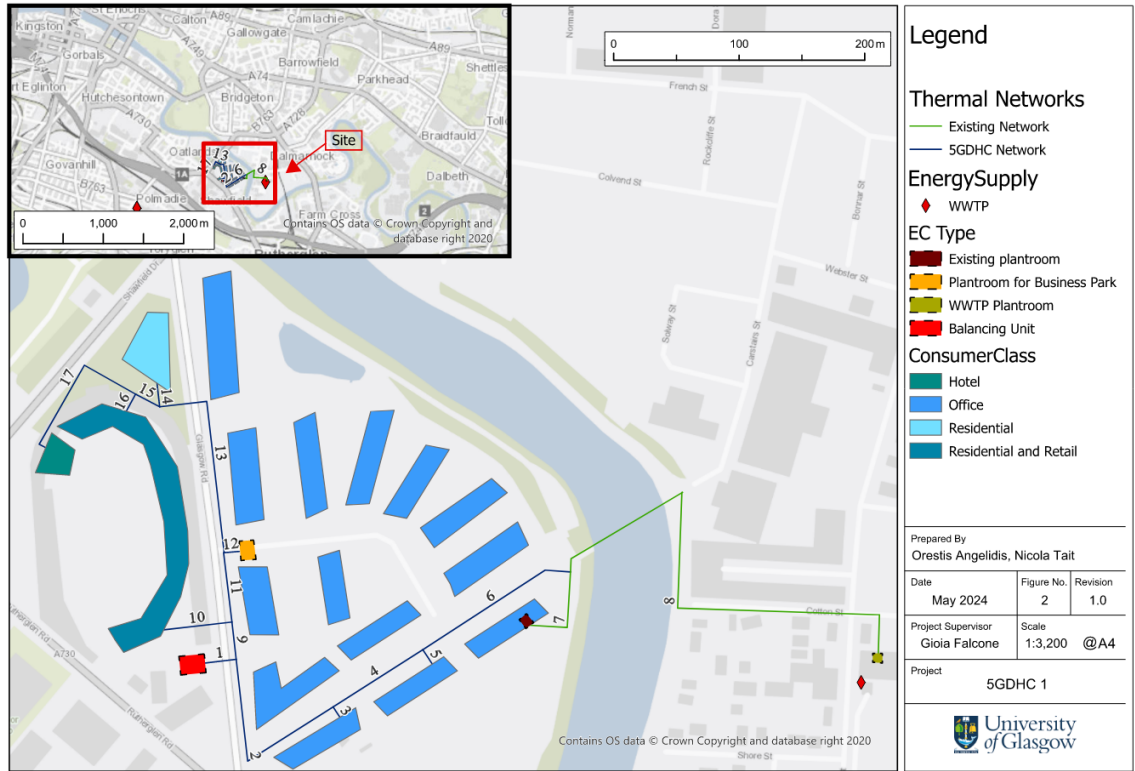


Figure 7.33: 5GDHC-1 network layout.

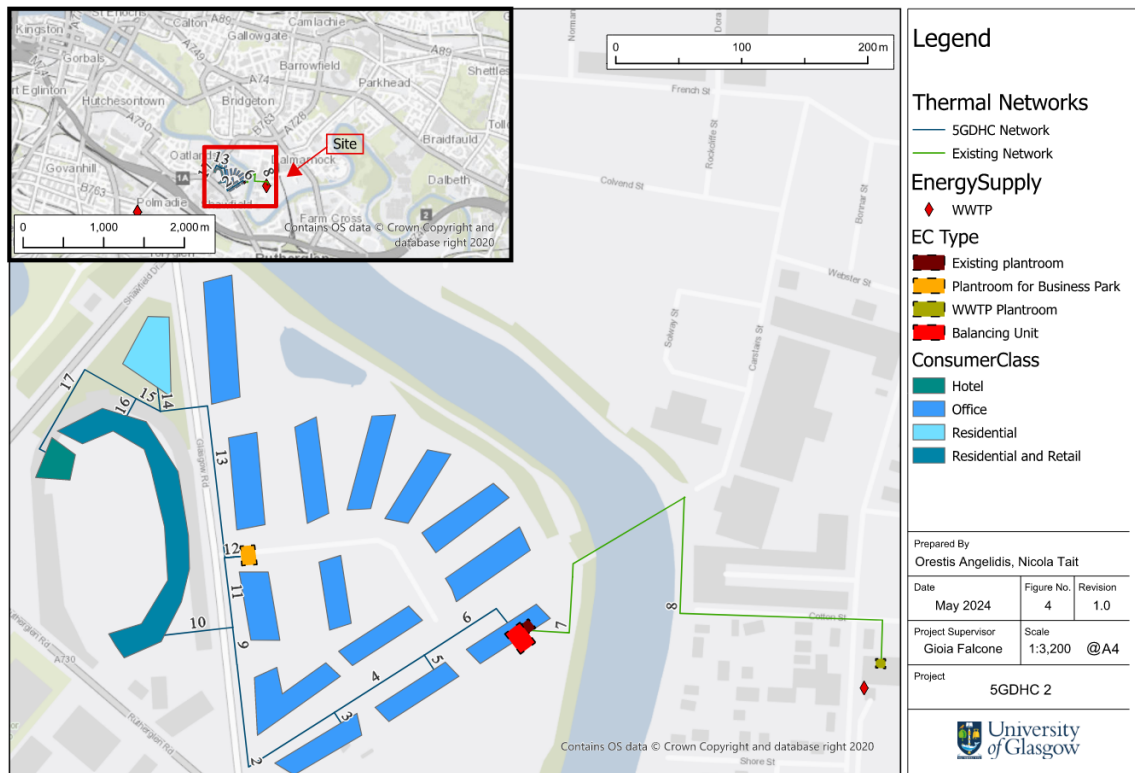


Figure 7.34: 5GDHC-2 network layout.

temperatures. A design pressure drop of 250Pa/m is used. The resulting pipe diameters along with trench lengths are shown below for both scenarios, in Table 7.10.

Table 7.10: Trench lengths and pipe diameters for each topology.

Pipe Segment Identifier	Total trench length (m)		Pipe Diameters (DN)	
	5GDHC-1	5GDHC-2	5GDHC-1	5GDHC-2
1	62	-	250	-
2	289	289	200	200
3	29	29	80	65
4	151	151	200	200
5	29	29	80	65
6	241	151	200	200
7	138	138	355*	355*
8	712	712	355*	355*
9	53	53	250	200
10	97	97	150	125
11	98	98	200	150
12	22	22	150	150
13	283	283	100	100
14	45	45	100	100
15	39	39	80	80
16	36	36	65	50
17	222	222	80	65
Total new pipework	1,834	1,544	-	-

*Existing pipes

It is seen that 5GDHC-1 has more trench length that needs to be installed, with an additional 290m. Additionally, the pipe diameters are equal or higher in each segment for 5GDHC-1. This is due to the lower network temperatures in the heating season and the WWTP's function as a prosumer connected to the main ambient network. Using these internal diameters and assuming 100% fill level in the pipe, the total glycol amount needed for 5GDHC-1 is 12m³. For 5GDHC-2, only the BU to WWTP segment needs glycol, resulting to 6m³. The BU's TES volume must also be added to calculate the total glycol requirements. Using the calculated 91m³ and 109m³ for 5GDHC-1 and 5GDHC-2 (Equation 7.1), the total glycol needed in each system can be found. The total glycol volume sums to 30m³ for 5GDHC-1 and 34m³ for 5GDHC-2. A set of schematics for summarising the hydraulic analysis outputs are provided in Figure 7.35 and Figure 7.36, including pipe diameters and design power requirements.

Network Details 5GDHC-1

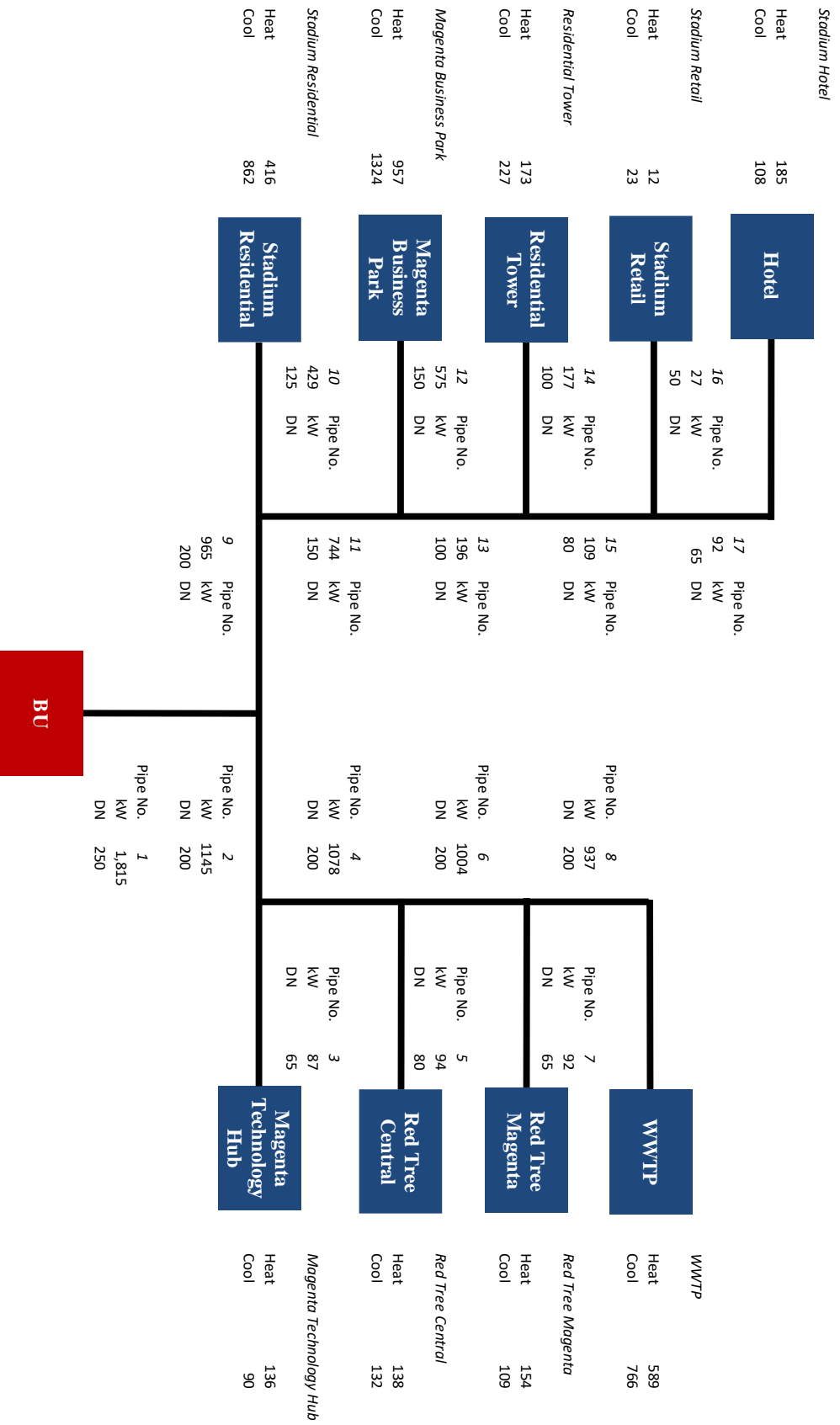


Figure 7.35: Network topology 5GDHC-1.

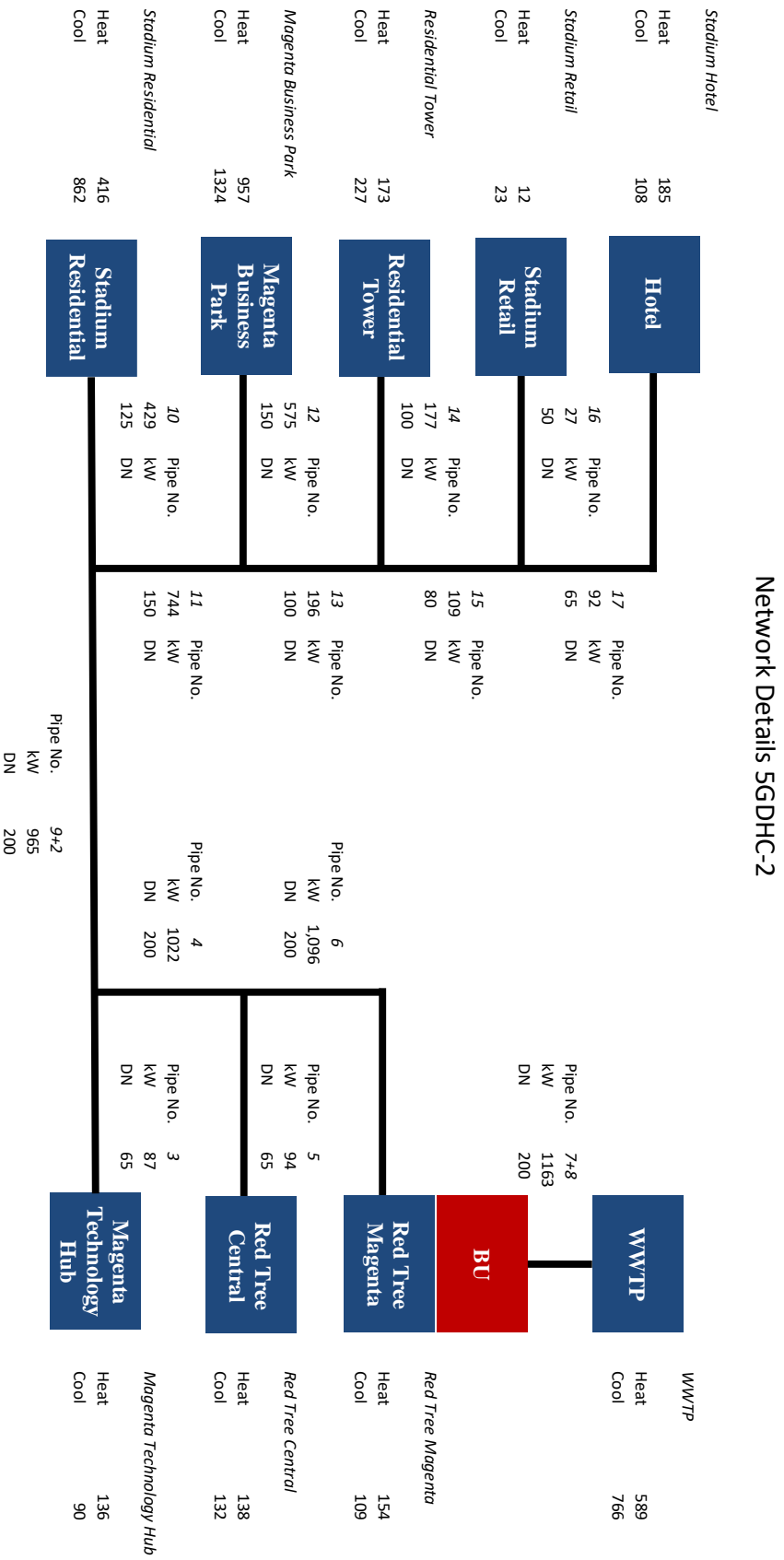


Figure 7.36: Network topology 5GDHC-2.

7.5 Techno-economic modelling of case study

Having completed the design and technical analysis of the two scenarios for 5GDHC, the data can be used in CATHeaPS to analyse their techno-economic performance. Slight alterations are made to CATHeaPS to allow for these inputs to be used.

For the other supply options (4GDH with individual AC units for cooling and building level ASHPs for heating and cooling) CATHeaPS data are used, as presented in Chapter 6. For 4GDH&AC, the EC has a SWSHP fed by the WWTP and a top-up ASHP similar to 5GDHC-2, only that a 4GDH network is used instead of an ambient one. The network topology is the same as for 5GDHC-2, changing the temperature profile to 60°C flow and 40°C return and including only heating demands. The resulting pipe schedule for the 4GDH&AC option is shown in Table 7.11. The equipment sizing for the 4GDH&AC and ASHP supply options are shown in Table 7.12 and Table 7.13 respectively.

Table 7.11: Trench lengths and pipe diameters for 4GDH&AC option.

Pipe Segment Identifier	Total trench length (m)	Pipe Diameters (DN)
1	-	-
2	289	125
3	29	50
4	151	125
5	29	50
6	151	125
7	138	355*
8	712	355*
9	53	125
10	97	65
11	98	100
12	22	100
13	283	50
14	45	50
15	39	50
16	36	40
17	222	50

*Existing pipes

Table 7.12: 4GDH&AC supply option equipment sizing.

Building	SWSHP capacity (kW)	ASHP capacity (kW)
EC	200	1,080
Building	Heating peak for sizing HIU/Substation (kW)	Cooling peak demand for sizing AC units (kW)
Red Tree Magenta	180	110
Red Tree Central	190	130
Magenta Technology Hub	170	90
Residential Tower	43 (per flat)	6 (per flat)
Stadium Hotel	180	110
Stadium Residential	43 (per flat)	6 (per flat)
Stadium Retail	80	20
Magenta Business Park	1,120	1,320

Table 7.13: ASHP supply option equipment sizing.

Building	ASHP capacity (kW)
Red Tree Magenta	180
Red Tree Central	190
Magenta Technology Hub	170
Residential Tower	43 (per flat)
Stadium Hotel	180
Stadium Residential	43 (per flat)
Stadium Retail	80
Magenta Business Park	1,120

Regarding the SPF of the equipment, the data from CATHeaPS is used. For the SWSHP, a heating SCOP of 3.4 is used according to Kim et al. (2021) [239], where experimental measurements are taken for a real SWSHP (181kW) system, covering a period of 2 years. The SWSHP had a similar inlet temperature profile (average of 9°C for winter months) to 5GDHC-1. In addition, the temperature profile of sink and source is the same as for the BHPs of the prosumers in 5GDHC-1 during winter so their average SCOP of 3.9 is in line with the literature. The cooling SEER for the AC units is set to the minimum European standard of 4.6 according to EN 14825. For the ASHP scenario, the values from CATHeaPS are used, including the ancillary electric resistance for DHW production [242]. The reason the ASHP's SEER values are lower than the EC units is that they are reversible ASHPs, limiting the refrigerant and compressor selection to operate for heating and cooling modes. These are summarised below in Table 7.14.

Table 7.14: SPF for counterfactual energy supply scenarios.

Item	SCOP/SEER/Efficiency/SPF	Source
ASHP individual SPF heating	2.0	[242]
ASHP building level SPF heating	2.9	[243]
4GDH&AC - SWSHP centralised	3.4	[239]
ASHP individual SEER cooling	3.5	[244]
ASHP building level SEER cooling	3.5	[244]
Individual AC SEER	4.6	[245]

Phasing is included for all options, with network and EC CAPEX coming in on year 0. The CAPEX for building level equipment (BHPs, ASHPs, ACs, HIUs and substations) happen one year before the connection of the respective building. For REPEX, 100% of the CAPEX is assumed, taking into consideration the lifetime and the installation year of the unit. No abstraction cost is included for the energy from the WWTP. A 40-year project assessment period is used, with a start year in 2025.

Outputs for the electricity use and CO₂ emissions are first presented, followed by a thorough discussion of the economic performance of the scenarios. Finally, a sensitivity analysis is conducted.

7.5.1 Electricity use and CO₂ emissions of supply options considered in the case study

First, the electricity use for full built-out for each of the supply options is analysed. Other than the energy transformation unit electricity use, the parasitic loads for pumping are included. The parasitic loads (pumping, controls and auxiliaries) are set to 2.9% for 4GDH and 7.0% for 5GDHC due to the lower temperature difference between the hot and cold line (similar to 4GDC) [246]. The lower temperatures lead to larger flows in the network to meet the same demand as in 4GDH and thus higher electricity needs for pumping. The electricity at full built-out with parasitic loads is shown in Figure 7.37.

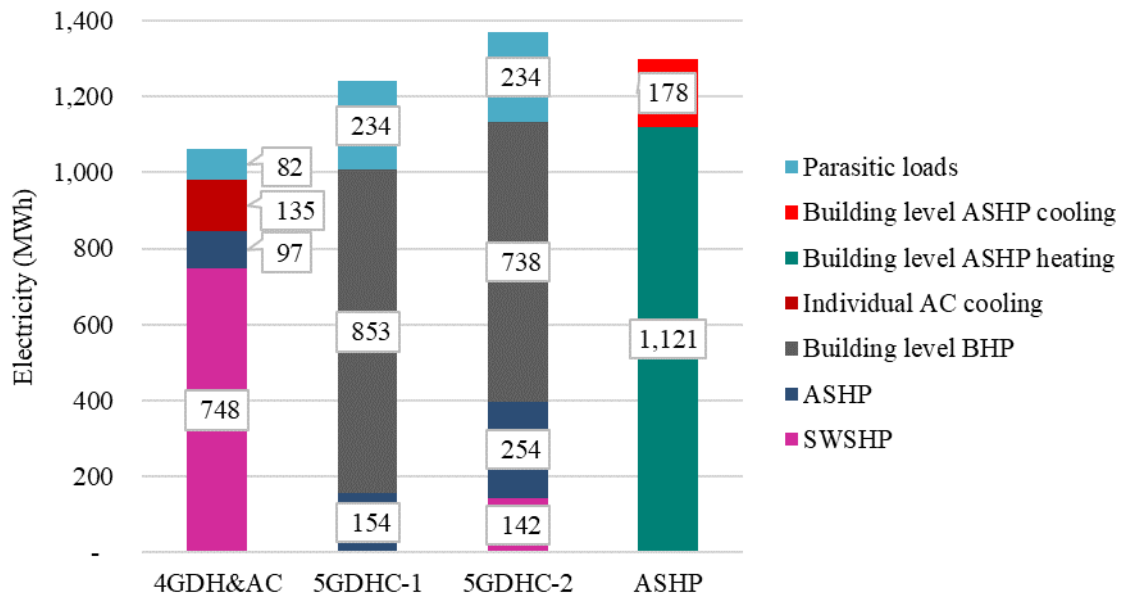


Figure 7.37: Total electricity use for different supply options at full built-out.

As already discussed, scenario 5GDHC-2 requires more electricity overall than 5GDHC-1 bringing its electricity use to 1,369MWh/year including 234MWh/year of parasitic loads. Interestingly, the 4GDH&AC case is performing best since despite the energy transformation units having approximately the same electricity consumption as 5GDHC-1 (980MWh/year compared to 1,007MWh/year), the smaller parasitic loads lead to lower overall emissions. Even the ASHP scenario performs better than 5GHDC 2. The reason for this is that not only a single unit is used for both heating and cooling but there are multiple stages, leading to more system inefficiencies.

Furthermore, the total CO₂ emissions per year along with the cumulative emissions are shown in Figure 7.38. This considers the decarbonisation of the grid, leading to 4GDH&AC having the least emissions with 709 tonnes of CO₂, followed by 5GDHC-1 with 790 tonnes of CO₂. 5GDHC-2 and ASHP have the highest emissions with 880 tonnes of CO₂ and 920 tonnes of CO₂ respectively.

However, other than the energy consumption and the CO₂ emissions, the impact on the electricity grid from a capacity perspective needs to be studied (kVA required). The electric capacity is found from the simulation models for 5GDHC, while for the other supply options by dividing the rated capacity by the SCOP/SEER for the 4GDH&AC and ASHP energy units. The output on electric capacity is shown in Figure 7.39.

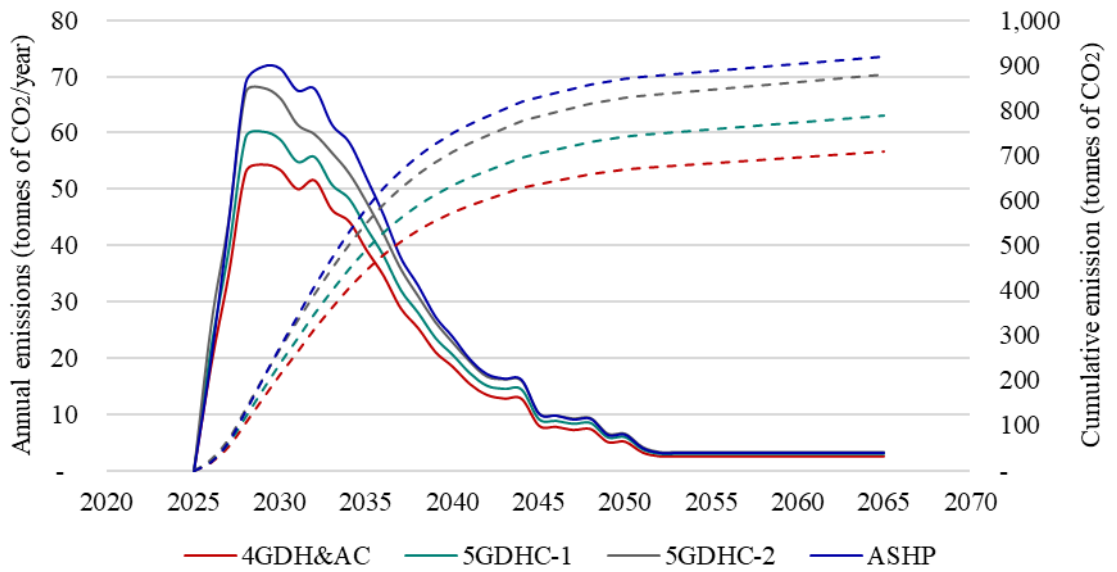


Figure 7.38: Annual (solid) and cumulative (dashed) CO₂ emissions for each supply option.

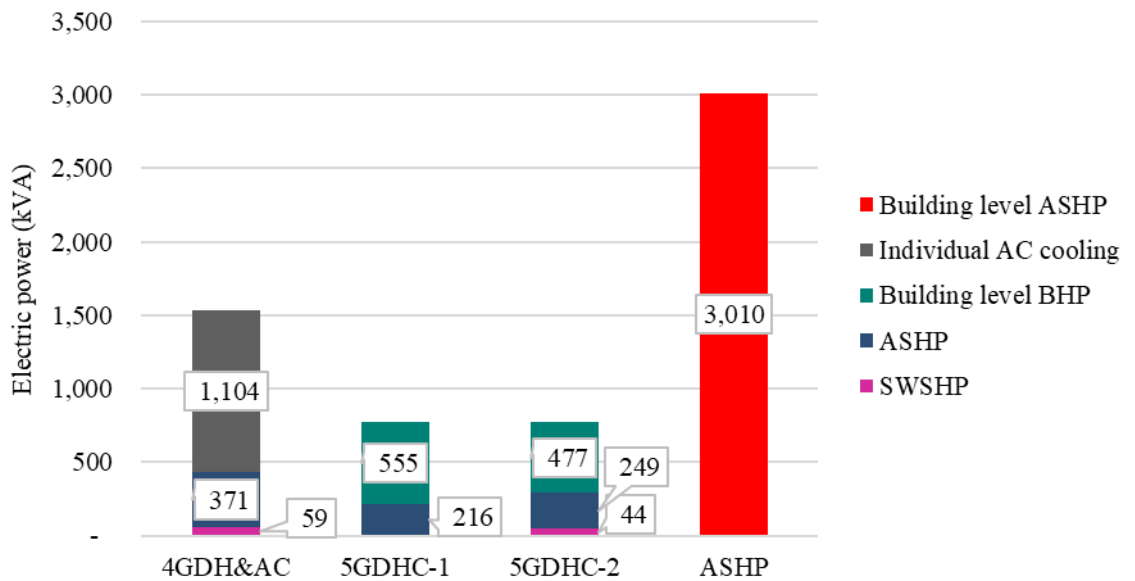


Figure 7.39: Installed power capacity for each supply option.

There are variations on the total electric power capacity requirements, ranging from 1.5MVA for 4GDH&AC and 3.0MVA for ASHP to 0.8MVA for 5GDHC-1 and 5GDHC-2. Overall, the solutions with decentralised, individual units (4GDH&AC due to the AC units for cooling and ASHP due to individual ASHPs) have a large electric capacity requirement, even though their individual impact is small. To study the potential impact on the grid, the local infrastructure constraints must be studied.

After communications with the local DNO, Scottish Power Energy Networks, details on the local electricity network infrastructure are received. These include the primary substation capacity (33kV), and the grid supply points (transformers for 132/33kV) that supply them. In addition, they include information on the EHV (nominal voltage of 33kV) export capacity as well as the HV Overhead Lines (OHL) (nominal voltage of 11kV) capacity. Figure 7.40 shows these data, with a traffic light system used for the capacity constraints.

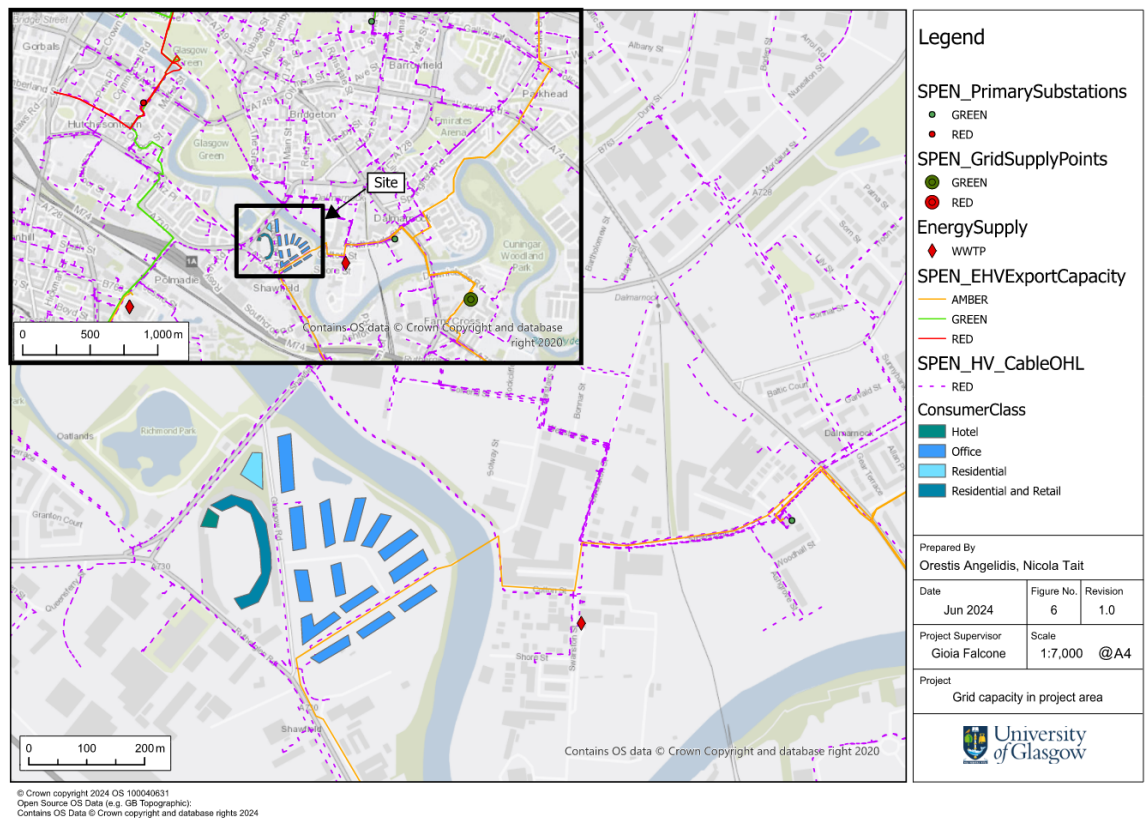


Figure 7.40: Electricity grid capacity in project area.

The grid supply point located in Dalmarnock are in the green category since they have a firm capacity (committed level of available electric power) of 90MVA and currently a maximum load of 36MVA. The primary substation in Ashgrove Road which is supplied by the Dalmarnock supply point is also in the green category since it has a firm capacity of 21MVA and a maximum load of 14MVA, leaving an availability of 7MVA. This should be sufficient for all supply options, however, there could be contractual agreements already in place, limiting the power availability. It can also be seen that all OHL lines are close to their limit capacity, meaning that large additional electricity demands could lead to OHL reinforcements. No costs for upgrading the grid are included in the economic performance

analysis for any of the scenarios since the extent of the OHL refurbishments is unknown and discussions are needed to agree on who bears this cost. The EHV capacity is of low interest since no electric power is supplied back to the grid.

Altogether, it's important to analyse both electricity use and installed electric capacity requirements. 4GDH&AC offers the lowest emissions and electricity use in the network but due to the use of AC units for cooling is linked with high-capacity requirements. 5GDHC solutions use the same infrastructure for heating and cooling requirements and due to the high SCOPs have lower electric capacity requirements. Due to existing constraints in the network, supply options with a lower electric capacity requirement could avoid considerable costs for upgrading the electricity grid.

7.5.2 Economic performance of supply options considered in the case study

The levelised outputs of the techno-economic analysis are shown in Table 7.15 and Figure 7.41, while the total absolute costs are shown in Table 7.16.

Table 7.15: CATHeaPS outputs – LCOE components.

Item	Units	4GDH&AC	5GDHC-1	5GDHC-2	ASHP
Discounted energy demand	MWh	47,548	47,548	47,548	47,548
Technology CAPEX	£/MWh	53	39	52	91
EC CAPEX	£/MWh	11	3	18	-
Connection CAPEX	£/MWh	18	17	17	-
Network CAPEX	£/MWh	53	50	30	-
Technology REPEX	£/MWh	28	35	48	85
EC REPEX	£/MWh	-	-	-	-
Connection REPEX	£/MWh	8	7	7	-
Network REPEX	£/MWh	-	-	-	-
Technology OPEX	£/MWh	21	9	11	48
EC OPEX	£/MWh	2	0	0	-
Connection OPEX	£/MWh	10	10	10	-
Network OPEX	£/MWh	9	9	7	-
Fuel cost	£/MWh	43	48	53	70
Social costs	£/MWh	3	4	4	4
Total LCOE	£/MWh	257	227	253	294
Total LCOE with social	£/MWh	260	230	257	298

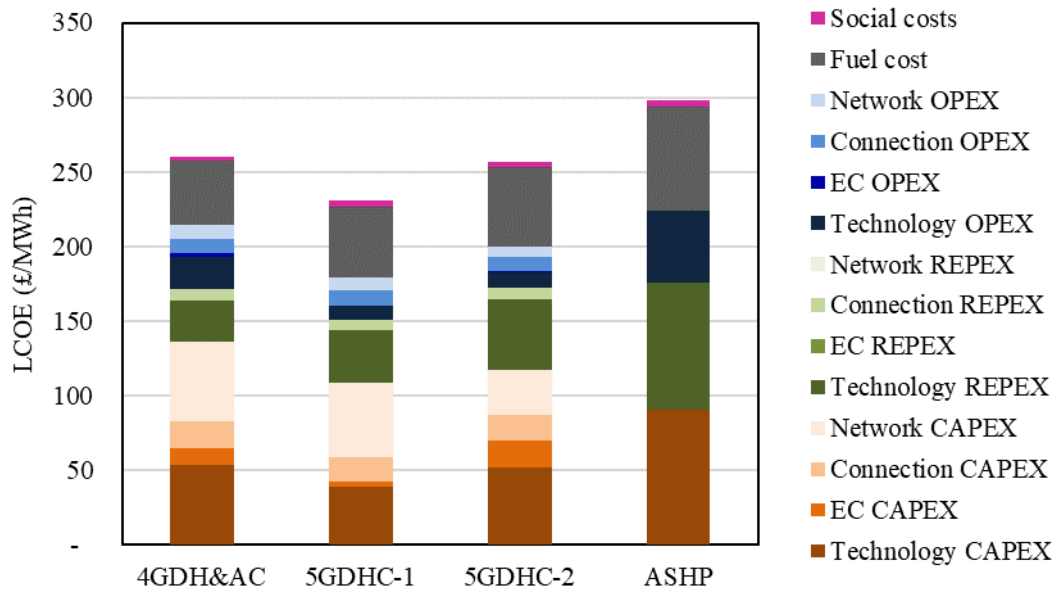


Figure 7.41: CATHeaPS outputs – LCOE.

Table 7.16: CATHeaPS outputs – total absolute costs.

Item	Units	4GDH&AC	5GDHC-1	5GDHC-2	ASHP
CAPEX	Thousand £	6,885	5,565	5,961	5,112
OPEX	Thousand £	4,177	2,600	2,607	4,702
REPEX	Thousand £	4,123	4,689	5,933	9,861
Energy Costs	Thousand £	4,363	4,938	5,460	6,931
Social costs	Thousand £	214	239	266	277
Total Cost	Thousand £	19,548	17,792	19,962	26,607
Total Cost with social	Thousand £	19,762	18,031	20,228	26,884

The best performing scenario is 5GDHC-1 with a LCOE of 227£/MWh. 5GDHC-2 has the second lowest LCOE with 253£/MWh. The 4GDH&AC scheme is the next best performing option with an LCOE of 257£/MWh and lastly the ASHP option has a LCOE of 294£/MWh.

Firstly, a comparison of the two 5GDHC options is made. The additional energy use for the 5GDHC-2 (53£/MWh compared to 48£/MWh for 5GDHC-1) led to a large capacity requirement. The CAPEX for the EC is 18£/MWh for 5GDHC-2 compared to 3£/MWh for 5GDHC-1. It also led to a smaller technology CAPEX for the BU, with 39£/MWh compared to 52£/MWh. 5GDHC-1 has higher network CAPEX arising from its different topology (pipes need to account for the WWTP load since there is no hydraulic separation as in 5GDHC-2 and 4GDH&AC) and lower temperature requirements. The CAPEX for the

network is 30£/MWh for 5GDHC-2, compared to 50£/MWh for 5GDHC-1. The remaining costs are similar, since no major system variations are present. Overall, the CAPEX for the two cases is similar (higher network cost for 5GDHC-1 balanced out by higher technology cost for 5GDHC-2) but the REPEX is different (35£/MWh compared to 48£/MWh for 5GDHC-2), since there are 2 HPs in the BU for 5GDHC-2 that need to be replaced every 15 years (twice in the project lifetime).

DH&AC performs approximately as well as 5GDHC-2. The network CAPEX is greater than 5GDHC-2 (53£/MWh compared to 30£/MWh) despite having the same topology. The smaller pipe diameters (averaging 2 sizes smaller for 4GDH&AC compared to 5GDHC-2 based on Table 7.10 and Table 7.11) are insufficient to offset the higher cost of steel with series 2 insulation compared to uninsulated plastic pipework. The technology CAPEX is similar to 5GDHC-2 (53£/MWh), since the cost of the individual AC units are to a degree negating the benefits of centralisation for the heating equipment. Interestingly, the EC costs are higher for 5GDHC-2 (18£/MWh compared to 11£/MWh). This occurs because in 5GDHC-2 there are larger TES space requirements (more volume required), and since the SWSHP and ASHP need to meet both heating and cooling demands, they have a higher capacity rating. The REPEX is also slightly higher for 4GDH&AC than 5GDHC-2 since many of the AC units need to be replaced twice in the period of 40 years (15-year lifetime) and there are many individual units due to the number of flats in the residential buildings (550 AC units for residential properties). The fuel costs are also lower than 5GDHC-1. 4GDH&AC's system SPF is higher, due to having bespoke units for cooling and heating and not having to break down the energy upgrade to two stages (BU and prosumer level). In addition, there are lower parasitic loads from smaller volumes of water being circulated in the network.

The building level ASHP option is the worst performing option, with a LCOE 23% higher than 5GDHC-1. Despite the fact that the ASHP option can take advantage of the phasing of demand, allowing for the CAPEX of its assets to come in later years, the large number of units lead to the total CAPEX and REPEX to be slightly higher than all other options. Its levelised CAPEX is 176£/MWh compared to 172£/MWh for 4GDH&AC, 151£/MWh for 5GDHC-1 and 172£/MWh for 5GDHC-2. Residential properties are the main reason for this cost, with 550 properties requiring individual ASHPs including fittings, small buffer tank and electric cylinder for DHW and controls but excluding heat distribution system.

The lower heating SPF for the residential ASHPs due to the need for the electric resistance in the small buffer tanks to meet DHW demands is also leading to a high fuel cost, with 70£/MWh. Therefore, the benefit of phasing costs by having individual units does not counter the effect of lower SPF and higher cumulative costs from decentralising the equipment.

7.6 Sensitivity analysis of case study variables

A sensitivity analysis is conducted on key TEM variables such as CAPEX and discount rate as well as on the WWTP available capacity.

7.6.1 Sensitivity analysis of techno-economic variables

Similar to Section 6.3.3, the analysed parameters for the systems' sensitivity are summarised in Table 7.17. Each is given a variation of -30% to 30% which is typical for feasibility stage work [183]. The sensitivity analysis is individually performed on each network where the output studied is the project's LCOE including social costs.

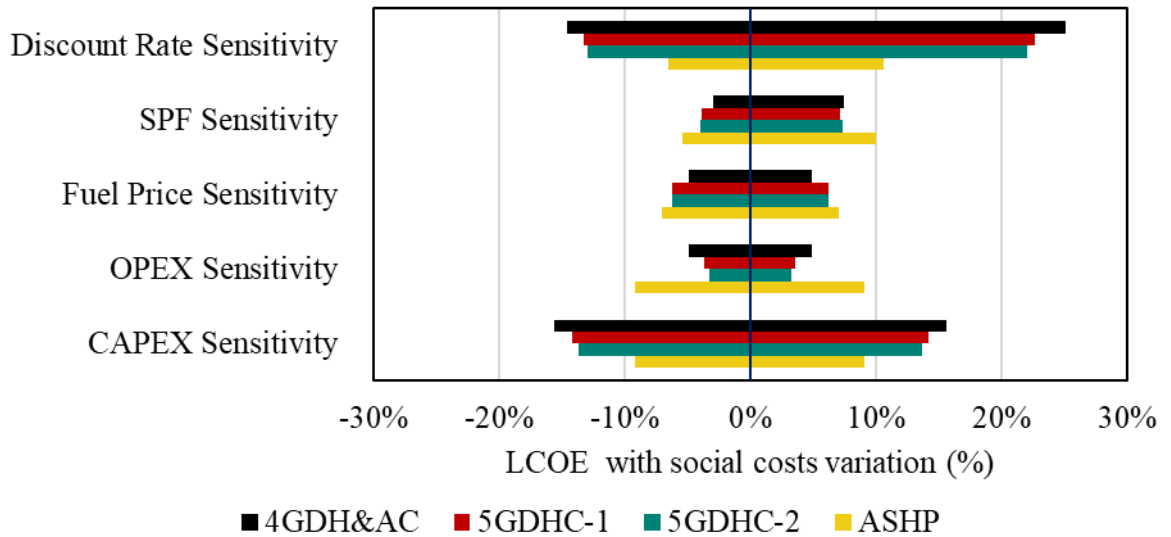
Table 7.17: Parameters included in the sensitivity analysis.

Parameters	Description of impact
CAPEX	A variation of all capital costs, which also influences the REPEX since the two are linked.
OPEX	Variation of the operational and maintenance costs.
Fuel Price Sensitivity	Variation of electricity and gas prices.
SPF	Variation of the HP's SCOP & SEER. It affects the fuel cost for the HP and the CO ₂ produced (and thus the social costs).
Discount Rate	Variation of the discount rate which is a way to quantify risk of future cashflows. By increasing it, future cashflows and energy supplied have a smaller value and thus a lesser impact on the LCOE.

The results of the sensitivity analysis are shown in absolute terms in Table 6.11 and their relative impact on the LCOE can be seen in Figure 6.16.

Table 7.18: Sensitivity analysis on 40-year LCOE with social costs.

Supply Option	Baseline LCOE (£/MWh)	CAPEX Variation (£/MWh)		OPEX Variation (£/MWh)		Fuel Price Variation (£/MWh)		SCOP Variation (£/MWh)		Discount Rate Variation (£/MWh)	
		+0.3	-0.3	+0.3	-0.3	+0.3	-0.3	+0.3	-0.3	+0.3	-0.3
4GDH&AC	260	220	301	247	273	247	273	253	280	222	326
5GDHC-1	252	198	263	222	239	216	245	221	247	200	283
5GDHC-2	257	222	292	249	265	241	273	247	276	224	314
ASHP	298	271	325	271	325	277	319	282	328	278	330

**Figure 7.42: Normalised outputs of sensitivity analysis on LCOE with social costs.**

The biggest impacts are the variables related to CAPEX. Especially for the options with centralised CAPEX coming in at the beginning of the project (4GDH&AC and 5GDHC-1 and 2) where no phasing is applied, the discount rate has the largest impact. When it increases by 30%, meaning that future cashflows have a smaller impact, it leads to a 25% increase in the LCOE for 4GDH&AC, 22% for 5GDHC-1 and 21% for 5GDHC-2. The electricity use affecting variables (SPF and the Fuel price) also have a large impact when they increase by 30%. Especially for the ASHP case where the fuel costs have a larger share of the total LCOE, they can increase the LCOE by 10% and 7% respectively.

Overall, investment expenditures have the largest impact on the centralised options due to phasing while energy use related factors have the main impact on ASHP option with the discount rate selected being critical for both.

7.6.2 Sensitivity analysis of WWTP capacity

The effect of changing the available capacity from the WWTP is investigated, by applying a $\pm 50\%$ variation on the hourly available power. For 5GDHC-2, the only difference will be the SWSHP's share of supply but for 5GDHC-1, the effect on the BU demand needs to be studied. This impact on the co-occurrence of the WWTP available power and the prosumers' demand for 5GDHC-1 is shown in Figure 7.43.

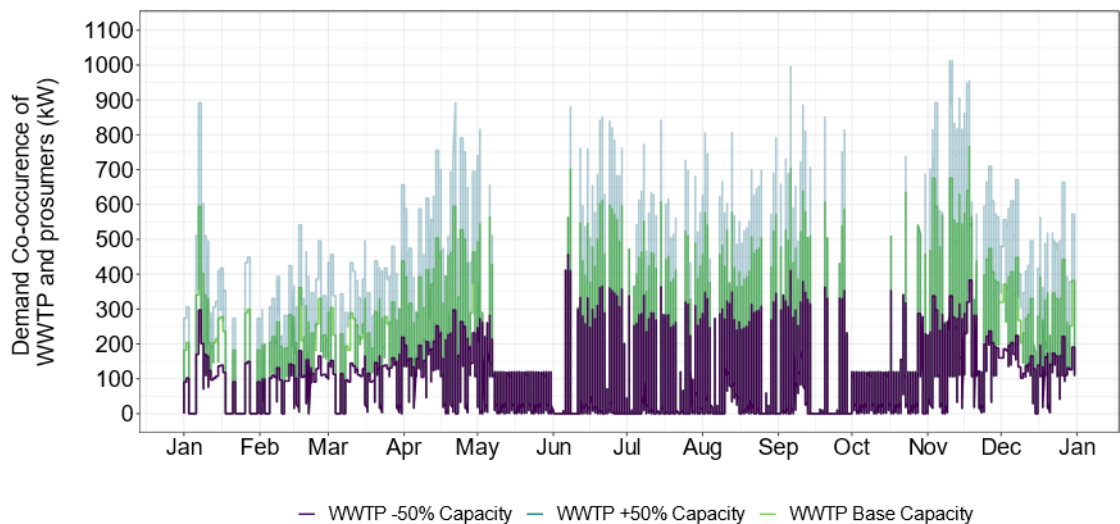


Figure 7.43: WWTP capacity sensitivity on co-occurrence of building demand and WWTP available power.

The DOC increases to 52.1% for +50% WWTP capacity and drops to 28.1% for -50% capacity from the base case of 41.8% co-occurrence. The new demand the BU needs to meet for 5GDHC-1 is shown in Table 7.19.

Table 7.19: 5GDHC-1 BU's new demand.

Total	Base	-50% WWTP capacity	+50% WWTP capacity
Annual BU heating added [MWh/year]	693	1,093	451
Annual BU cooling added [MWh/year]	130	306	52
Total BU demand [MWh/year]	823	1,399	502

The WWTP share has a large impact on the demand requirements from the BU, with the total requirement increasing by 69% when the WWTP's capacity is halved and decreasing by 39% when the WWTP capacity is increased by 50%.

The ProHMo models for the BU are re-simulated for both scenarios 5GDHC-1 and 5GDCH 2, with the new BU demand for 5GDHC-1 and a new WWTP available capacity and SWSHP size for 5GDHC-2. The new energy share for the BU's equipment along with the new full built-out electricity used are shown in Table 7.20.

Table 7.20: Impact on BU's energy supply for WWTP sensitivity.

Item	Units	5GDHC-1			5GDHC-2		
		Base	-50%	50%	Base	-50%	50%
Heating SWSHP	MWh/year	-	-	-	672	373	957
Cooling SWHSP	MWh/year	-	-	-	254	104	307
Heating ASHP	MWh/year	684	1,077	444	1,015	1,336	733
Cooling AHSP	MWh/year	131	313	55	324	472	273
Electricity for heating SWSHP	MWh/year	-	-	-	85	47	123
Electricity for cooling SWSHP	MWh/year	-	-	-	56	22	67
Electricity for heating ASHP	MWh/year	113	182	73	182	236	132
Electricity for cooling ASHP	MWh/year	28	66	12	72	102	60
Total electricity use	MWh/year	141	249	85	395	408	382
Total electricity use variation from base	%	-	-76%	40%	-	-3%	3%

The biggest impact is on 5GDHC-1, where the WWTP directly impacts the share of energy the BU needs to supply. When the WWTP available capacity increases by 30% and the DOC reaches 41.8%, the electricity use drops by 76%. Adversely, when there is 50% less available WWTP capacity and the DOC is at 28.1%, the electricity use increases by 40%. For 5GDHC-2, there is a significant change on the SWSHP and ASHP shares, but since the SPFs for them are high, the effect on the overall electricity use is minimal (3% variation from base scenario).

Regarding the economic performance of the scenarios, the impact is seen on the fuel use and the required BU capacity (and thus CAPEX). The LCOE variation can be seen below in Table 7.21.

Table 7.21: Impact of WWTP capacity on LCOE.

Item	Units	5GDHC-1			5GDHC-2		
		Base	+50%	-50%	Base	+50%	-50%
Technology CAPEX	£/MWh	39	39	39	52	54	50
EC CAPEX	£/MWh	3	2	6	18	18	18
Connection CAPEX	£/MWh	17	17	17	17	17	17
Network CAPEX	£/MWh	50	50	50	30	30	30
Technology REPEX	£/MWh	35	35	36	48	50	46
EC REPEX	£/MWh	-	-	-	-	-	-
Connection REPEX	£/MWh	7	7	7	7	7	7
Network REPEX	£/MWh	-	-	-	-	-	-
Technology OPEX	£/MWh	9	9	10	11	12	11
EC OPEX	£/MWh	0	0	0	0	0	0
Connection OPEX	£/MWh	10	10	10	10	10	10
Network OPEX	£/MWh	9	9	9	7	7	7
Fuel cost	£/MWh	48	46	52	53	53	54
Social costs	£/MWh	4	3	4	4	4	4
Total LCOE	£/MWh	227	224	234	253	259	251
Total LCOE with social	£/MWh	230	228	238	257	262	255

Both 5GDHC-1 and 5GDHC-2 are slightly influenced by the WWTP capacity, with the LCOE changing by approximately 3%. Interestingly, an opposite influence is observed. For 5GDHC-1, when the capacity decreases by 50%, more energy needs to be supplied by the BU. This leads to a higher EC CAPEX and fuel cost. The peaks remain relatively unchanged since they occur when the WWTP is not operating so the size of the ASHP also remains unchanged as seen by the identical technology CAPEX. For 5GDHC-2, when the WWTP capacity drops, the additional electricity use from the ASHP is minor as aforementioned. The benefit from having a lower capacity in the SWSHP (half) is seen by a drop in the technology CAPEX, since the ASHP remains unchanged (sized for the peak of the network). The energy share from the BU remains unchanged (same demand) so the EC cost is unchanged for 5GDHC-2.

7.7 Discussion on case study outputs

To further interpret these results, a discussion on other miscellaneous factors that need to be considered in the decision-making process is conducted. Then, a wider analysis of the techno-economic performance of all options is presented, followed by a discussion on ways to render 5GDHC economically viable for areas with low heating and cooling demand co-occurrence. Lastly, limitations and proposal for future work is also presented.

7.7.1 Miscellaneous factors affecting supply option selection

Space constraints, system complexity and expansion flexibility need to be taken into consideration and influence the decision-making process. These are discussed below.

Space constraints can be a critical parameter for deciding on a supply option, especially for dense urban areas. On the one hand, 5GDHC requires a very large TES in the BU (100m^3 in this case), to ensure thermal stratification due to the small ΔT of 5K. A height to diameter ratio of 2.5 is recommended to keep stratification which as shown in the ProHMo models is sufficient. A height of 10m with a 3.7m diameter is used which could be difficult to secure in an urban area. Due to the TES height requirement, it would also be difficult to have such a TES in an inside space. Having such an outside space availability creates further planning complications and potentially uses valuable space. Furthermore, the decentralised TESs for the BHPs would also lead to a significant footprint requirement in the prosumer plantrooms. On the other hand, by using BHPs at prosumer level, there is no need for evaporators (dry air coolers) on roofs or balconies (for individual flats) compared to the ASHP and AC units. This reduced space requirements on the roofs could be critical for buildings with limited roof space, or ones that aim to place PVs on their roofs to comply with building standards. In addition, dry air coolers are noisy, which can be a problem in residential areas due to noise restrictions.

System complexity is higher for 5GDHC systems since multiple control elements are present due to the decentralisation of the prosumer pumps. As mentioned in Section 4.6.2 scaling up the proposed hydraulic design to a larger network with multiple prosumers introduces challenges related to pump sizing and network expansion. Each prosumer pump needs to be able to circulate the water to the BU if no other pump is connected. Inefficient

pump operation at normal load conditions could be encountered, and lead to a variation on the sizing and operation of the prosumer pumps, depending on their proximity to the BU. The flexibility for future network expansion could also be compromised, where the introduction of new pumps may result in a different system characteristic curve regime. This could potentially impact the pump operation of existing prosumers and impact the system's hydraulic balance.

7.7.2 Overall techno-economic performance of supply options considered in the case study

All options result in a high LCOE (lowest one is 227£/MWh for 5GDHC-1), considerably higher than GB equivalent costs (80£/MWh [224]). The main reason for this is the high cost of electricity and the low energy use for the new, energy efficient buildings. Energy efficient buildings allow for reducing energy use and emissions, but they can result in higher costs per unit of energy supplied. This is because CAPEX, REPEX and OPEX have fixed cost elements.

For individual residential properties supplied by individual solutions such as ASHP, the DHW peak is irrespective of building standards, unlike space heating/cooling demands. Therefore, a high capacity and high CAPEX and REPEX are needed, despite the low overall energy demand. This trend can be seen when examining published LCOE figures from IEA (2021) [224] for a typical residential property (90m²) with individual ASHPs. In the calculations resulting to a 110£/MWh figure for the LCOE, 13MWh/year of heating consumption are assumed, out of which 11MWh/year are for space heating and 2MWh/year for DHW. In comparison, using the residential benchmarks from this study (15kWh/m²), the space heating demands for a similar property are closer to 1MWh/m². This difference of 10MWh/m² (91%) highlights the drop in energy demand in well insulated new buildings.

For centralised approaches, the low demand makes it difficult to justify the high CAPEX of their infrastructure (pipe network, ECs and consumer connections). In addition, it is difficult to take advantage of phasing of demand, since there are a lot of upfront CAPEX elements. This is highlighted from the discount rate sensitivity, where for centralised solutions (4GDH&AC and 5GDHC), the LCOE increases by over 20% when the discount

rate is increased from 3.5% to 4.5%. Therefore, the added flexibility that 5GDHC offers for phasing of assets, and utilisation of reversible energy transformation units for supplying heating and cooling fits well with the reduced new building demands.

7.7.3 5GDHC for areas with low heating and cooling demand co-occurrence

For project areas where higher demand co-occurrence is present, 5GDHC-2 would perform considerably better since its primary electricity use comes from the BU unlike 5GDHC-1. If the DOC is low as in this case study, using a direct HEX is better for utilising low temperature waste heat in 5GDHC systems. Especially if the waste heat source is located close to the demands, since it would be limiting additional network costs. However, if the heat source is far from the demand, hydraulically isolating that section and using a concept similar to 5GDHC-2 is recommended, to limit the flows the rest of the ambient network sees. Another issue that needs to be accounted when comparing waste heat capture is control complexity. Thus, the level of demand co-occurrence and project area topology need to be studied before deciding on an option.

Other than utilising low temperature waste heat sources, a way to bridge the seasonality of demand are large seasonal TES. As discussed in Section 2.4.1, an equipment free BU allows for charging the BU's TES through a hot and a cold well, charged during summer and winter respectively. Such a configuration would significantly lower emissions and energy use from the BU's energy transformation equipment. It could significantly improve the system's techno-economic performance. It could also allow for a better sector coupling through using the BU's energy transformation equipment to charge it using curtailed wind as shown in Brown et al. (2023) [105]. However, the system complexity rises for such a system, with the need of a detailed hydrogeological assessment of the project area. Space restrictions, CAPEX and regulatory limitations could also present implementation barriers.

Therefore, it is argued that access to low temperature waste heat sources located near the demands along with the use of seasonal TES could render 5GDHC economically viable even when there is low co-occurrence of heating and cooling. A bespoke assessment is needed for their utilisation in project areas, to highlight their technical and economic viability.

7.7.4 Limitations of the case study analysis

This work required a conceptual level design, with a focus on the annual energy use of the models and the examination of multiple scenarios. The full 5GDHC architecture shown in Chapter 5 comprising the ProHMo hydraulic components, is not appropriate due to the detail needed and the computational times. For future design stages, it is recommended to complete a detailed hydraulic design and simulate the system's behaviour for full built-out. It would also be recommended to develop some simplified hydraulic Modelica components that could neglect pressure to connect the prosumers and BU components instead of conducting the simulation in steps. Studying the impact of physical distance and time delays on the capacity of the WWTP to balance the network is recommended.

Furthermore, other than not including a seasonal TES and an equipment-free BU, this analysis did not consider more complicated control regimes for the operation of the BHPs and the BU equipment. The simple rule-based controls based on TESTLs temperatures, could be replaced by more complex controls such as MPC or other demand response controllers as the ones used in Buffa et al. (2020) [112], to quantify their impact on overall energy use. The effect of sector coupling is analysed based on installed capacity, but a live operation with the electricity grid could be conducted. Such an analysis could comprise a study on the impact of 5GDHC to electricity grid frequency control and the impact of the number of prosumers on the network's operation.

Finally, at a later design stage, investigations could expand on the impact of a wider technology mix, in terms of technologies considered and their possible combinations. This could involve optimising the capacity and number of technologies at prosumer and BU level, and the underlying control strategy. Additional technologies like electric chillers, electric boilers, solar thermal and variable refrigerant flow units can be evaluated to provide a more comprehensive analysis on their role in the system's performance. Levels of centralisation of the demand and thermal zoning for different clusters could also be studied, creating a hybrid scenario of all supply options.

This case study has been critical in combining the findings of this research and applying them to a real project. Chapter 8 draws a cohesive conclusion of the thesis and presents the wider context of the findings and the pathways for future research.

8 Conclusion, Context and Future Research

Decarbonising the heating and cooling sector in a holistic way is a crucial challenge to meet the energy trilemma of low cost, low emissions, and high security of supply. This research focuses on exploring and quantifying the potential of 5GDHC for a holistic decarbonisation.

A detailed SLR highlights key 5GDHC research gaps on hydraulic design and operation standardisation, quantified techno-economic boundary conditions and a business structure redefinition. To address them, novel hydraulic designs and operational methodologies are presented and experimentally validated in this thesis. Suitable open access simulation models for all 5GDHC components are developed and experimentally validated to capture the proposed designs. A detailed open access TEM is also produced to allow for detailed techno-economic assessments of 5GDHC against other decarbonisation supply options. Finally, a real-world case study with heating and cooling loads and a waste heat source/sink during the winter/summer is used to demonstrate the application of the developed models and methodologies. It also allows for a wider discussion on the miscellaneous factors that need to be considered when assessing 5GDHC systems for real world applications. The outputs of this thesis facilitate the understanding of 5GDHC, elucidating key identified research gaps and ultimately assisting the efforts for a holistic energy system decarbonisation.

In this final chapter, a discussion on the overall outputs of the thesis is conducted by evaluating each RO. The broader context of the results and the contribution to the field is also presented. Lastly, pathways for future research are analysed.

8.1 Conclusion

The key outputs for each of the ROs are outlined below.

RO 1. Evaluate 5GDHC's opportunities and shortfalls for holistic energy system decarbonisation. Focus on the characteristics of operation as well as its technical and business-related features that could facilitate a holistic approach to decarbonising the

energy grid. An SLR and stakeholder interviews (policymakers, industry and academic experts) will be used.

An SLR of 5GDHC systems for holistic decarbonisation is conducted, combining fragmented research on key technical and business topics, and superimposing it onto views from 18 leading industrial and academic professionals in the field.

Findings suggest that the high seasonal heating and cooling demand co-occurrence is crucial to help minimise operational costs. 5GDHC's economic performance benefits from phased developments and varying levels of retrofitting within the project area. This is particularly true for new markets where centralised infrastructure does not exist, and industrial high temperature waste heat sources are not located near the demands. In such cases of scattered low temperature waste heat sources, the use of 5GDHC could be a viable option. However, these are benefits highly subject to the operating costs and the overall system efficiency which in turn are highly dependent on the complicated physics of operation. Bidirectionality of flow leads to multiple control issues that give rise to hydraulic instabilities and control complexities. Determining a coherent system-wide design that includes pumping, pipe, and substation hydraulics, as well as a centralised BU for thermodynamic and hydraulic balancing are crucial. In addition, creating an overall control methodology to encompass that design is critical. The control strategy is tied to individual energy substations' operation, thus impacting the electricity grid due to the use of HPs. Creating controls that optimise HP operation through TES at a substation level and DSM practices could allow development of a smart HP grid. This HP grid could take sector coupling a step forward by coordinating with the electrical utilities to provide voltage control and frequency balancing opportunities. At the same time, it could offer peak shaving and demand shifting potentials. Furthermore, the economic feasibility of 5GDHC heavily relies on creating fitting business models, legal frameworks, and modes of financing, which are currently lacking.

Having a limited number of prosumers would limit the technical risks and permit the balancing of energy sharing and demand diversification. Creating zones of heating and cooling demands of similar consumer classes would be a smart way of combining 5GDHC with the benefits of 4GDH and 4GDC. Such a combined approach could allow a phased, bottom-up energy system development that is appropriate for new markets. It would also

provide construction flexibility and facilitate novel asset ownership and tariff structures. 5GDHC must be viewed as a tool in the arsenal of decarbonisation solutions. Further research is required on quantifying beneficial operation boundaries, hydraulic design, operation standardisation and business structure redefinition.

RO 2. Investigate 5GDHC hydraulic designs, focusing on maximising energy synergies and sector coupling. Understand how the fitting of operating methodologies, comprising control philosophies and equipment interaction, can ensure hydraulic stability.

As established in the SLR, one of the main challenges in the design and operation of 5GDHC systems stems from their energy sharing aspect. The main problem in bidirectional networks can be traced to the interaction of the decentralised pumps. As a solution, an ambient network with very small pressure difference between the cold and hot pipes is recommended. Instead of using an active BU with a pump that meets the hydraulic misbalances of the system, a passive BU is proposed. In this case, the BU acts as an escape route for water, offering the path of least resistance. To avoid pump hunting, it is recommended to have pumps controlled by return temperature rather than by flowrate, as this will minimise the constant variation of the system's characteristic curve due to the pressure and flowrate variations from neighbouring pumps. A VSD pump is required for this design, with minimal use of valves for the regulation of flow. Two control philosophies are proposed, one where the temperature of the ambient grid is allowed to fluctuate ($T_{GridFloat}$) and one where it is kept constant ($T_{GridFix}$). For $T_{GridFix}$, the control of the prosumer primary pumps is the return temperature after the BHP/HEX_{DC}. For $T_{GridFloat}$, the control of the prosumer primary pumps when BHP is used is the flowrate, while for the HEX_{DC}, it is the tertiary flow temperature.

The proposed 5GDHC configuration along with the two bespoke control philosophies, $T_{GridFix}$ and $T_{GridFloat}$, are experimentally validated in the CoSES lab. Both control approaches focus on alleviating control instability and unstable prosumer interaction through the selection of control variables.

The experiment for both control philosophies lasted for 20 hours, and included periods of both heating and cooling, heating only, cooling only, and no demand. No control issues are

identified, with the BU maintaining hydraulic and thermodynamic balance, which allowed the system to meet the prosumer demands. The energy consumption of the BHP for these 20 hours is greater for $T_{GridFix}$ (13.5 kWh compared to 12.1 kWh), while having a lower SCOP (3.8 compared to 4.1). This is due to the fixed network ΔT (5K) spread being greater than the evaporator's ΔT (3.5K), leading to extended use of the BHP internal pump mixing the return with the flow. However, the grid temperatures are unstable for $T_{GridFlow}$. This could lead to prosumer interaction and higher electricity use due to fluctuating grid temperatures requiring the use of BHP rather than HEX_{DC}. The BU control using an ASHP led to multiple starts and stops as well as a large temperature range in the TES, indicating the importance of a well-designed and sized energy supply system configuration for the BU.

A thorough comparison of the control philosophies revealed the considerations for their design and implementation. On the one hand, $T_{GridFix}$ has better predictability and ease of applicability in terms of billing, since it minimizes prosumer interaction in terms of efficiency. However, it necessitates careful attention to evaporator/condenser sizing and their uniformity throughout the network to avoid inefficiencies as observed in the experiment. On the other hand, $T_{GridFloat}$ offers greater flexibility in asset selection and less sensitivity to grid temperature variations but introduces unpredictability of system behaviour. Selecting the control regime should be guided by a comprehensive evaluation of project characteristics. Irrespective of the control approach selected, some common considerations for the generalisability of findings for larger applications are highlighted regarding control stability, creation of hydraulic sub-cycles, pump operation and network expansion.

RO 3. Assess different modelling methodologies to accurately simulate 5GDHC's physics of operation along with the proposed hydraulic designs and operating philosophies. Emphasise the capacity to be used in different model architectures to allow the creation of 5GDHC digital twins and a higher-level system analysis.

The hydraulic designs and control strategies are replicated in the digital sphere by creating bespoke Modelica models for the prosumers, heating and cooling demands, ambient grid, and BU. The models allow detailed thermofluid analyses of 5GDHC systems with multiple

heating and cooling prosumers. The simulations can capture all hydraulic events including pressure variations and flow instabilities.

The prosumer and BU models comprise ‘thermal only’ connectors, which simplify the models, and reduces the computational time while ensuring high simulation accuracy. The ambient grid and the hydraulic interfaces of the prosumers and the BU include hydraulic components that capture the detailed thermofluid behaviour of flow bidirectionality, where ‘thermal only’ components would not be sufficient. Bespoke controls on equipment operation based on the specified TESTLs temperature values are proposed, for both the heating prosumer and the BU. Additional controls are generated for the operation of 3WVs and the logic of secondary and tertiary pumps based on prosumer demand. The energy transformation equipment uses experimentally validated digital twins from the ProHMo library. Suitable parameterisation is developed to allow users full control of the characteristics of the technical specifications of the equipment in the prosumer substations/demands. All models are made open access, with FMUs allowing their utilization in various coding environments via FMI. In addition to the models, simulation examples are also made open access, along with detailed commentary on all control logic implemented. Finally, a methodology for PHIL is presented, focused on utilising Modelica for experimental implementations with minimal hardware requirements.

For the experimental validation of the Modelica models, a digital twin of the 5GDHC experiment is constructed. A stepwise validation of the assembled digital twin demonstrates that the developed Modelica components effectively capture the behaviour of 5GDHC. The CPU time for the simulated 20h is 4.50min for $T_{GridFix}$ and 4.67min for $T_{GridFloat}$. For the Hy, HyP and HyPB validation cases, an R^2 exceeding 88% is found. The similarity of the results is also seen through an analysis of the overall system behaviour, including the replicant behaviour of all equipment modulation (valves, energy transformation units and TES). The full digital twin showed an energy profile very similar to the experimental one, with energy discrepancies being less than 3.1% for the BHP and 7.1% for the ASHP in both $T_{GridFix}$ and $T_{GridFloat}$ experiments. The key source of error is traced to the BU’s TES being simplified to a one-dimensional ‘thermal connector only’ model. A detailed hydraulic model could accurately capture the fluid dynamics of the TES and the interaction of the water stratification layers. The employed stepwise validation

methodology is recommended for future use of the models for creating digital twins of real systems.

RO 4. Examine TEMs for evaluating the LCOE of 5GDHC against other supply options, with a focus on transparency and ease of use to facilitate market uptake. They should allow for detailed economic and environmental comparisons of 5GDHC with other supply options. This can facilitate a techno-economic analysis to develop trends for what conditions are required to choose 5GDHC over other supply options for different project area variables.

This work introduces CATHeaPS, a TEM intended to capture the economic and environmental performance of 5GDHC and alternative supply quickly and effectively. The supply options included are 5GDHC; 4GDH with individual AC units for cooling loads (4GDH&AC); individual ASHP for both heating and cooling (ASHP); and individual GBs for heating with AC units for cooling (GB&AC).

CATHeaPS undertakes a complete energy demand, hydraulic and energy supply analysis. Bespoke algorithms allow the sizing of both network and equipment, while cost and technical data allow the construction of detailed cashflow models for a complete techno-economic assessment of all supply options. CATHeaPS offers the capacity for analysis of bespoke projects, by either simply inputting a preliminary building schedule or information from other software for the hydraulic and energy supply analysis. It also provides a comprehensive cost and technical database for 5GDHC systems. It's a flexible and editable model, offering a combination of simplicity, sufficient coding capacity (through VBA), and widespread availability.

CATHeaPS is verified through 2 case studies. Network 1 uses data from a conceptual design stage industrial case study from the UK. CATHeaPS outputs are analysed against outputs of specialised commercial software for Network 1. Network 2 comprises an imaginary small residential network. Both direct comparison of outputs and the theoretical results/analysis verification approaches are used, by assessing publicly available figures where appropriate. A direct comparison of the Network 1 outputs for 'heating only' showed that CATHeaPS is within 5% discrepancy for all economic components for the 4GDH&AC option. The theoretical results/analysis verification using both Network 1 and

Network 2 showed that the 5GDHC, ASHP and GB&AC outputs are reasonable and within the range of published figures. A sensitivity analysis on Network 1 and Network 2 outputs by varying several project parameters (discount rate, cost elements and SCOP) also produced logical responses from CATHeaPS.

Having verified the model, CATHeaPS is used to undertake economic and environmental analyses. These analyses are conducted to three scenarios: (i) a 'heating only' district with access to an ambient temperature waste heat source; (ii) a typical 'heating only' district; and (iii) a typical project area with heating and cooling demands.

For the economic analysis, a break-even analysis is conducted for project scenarios comprising residential properties. This exercise provides a preliminary guide on the number of properties needed for the cost of a specific energy supply option to become lower than another. Results suggest that the number of properties and the number of connections per property (flats per building) are the most impactful variables. As one would expect, 4GDH&AC performs best, having high energy demands with high density, while the effect of spatial density decreases exponentially with the number of connections. ASHP and GB&AC options are always more economic than centralised options, being viable for up to 5 and 10 connections per property, respectively. For scenario (a) 5GDHC performs best until 10-30 properties depending on the housing density, after which point 4GDH is always more economic. For the range of 3 to 10 connections per property, there is a great sensitivity to variables such as CAPEX, discount rate and COP, so a bespoke assessment is recommended. It is found that when there is no cooling, 5GDHC performs worse than 4GDH for any network configuration. An annual cooling to heating demand share of 30% (with a DOC of 16%) is required for 5GDHC to start performing better than 4GDH&AC for a higher number of connections per property. For an annual cooling to heating demand share of 50% (with a DOC of 21%), 5GDHC always performs better than 4GDH&AC. These findings are in line with the work of Wirtz et al. (2020) [29], who proposed that a DOC of 30% is needed for 5GDHC to perform better than 4GDH solutions.

For the environmental analysis, 10,000 Monte Carlo simulations are conducted to identify trends and relationships between the supply options. It is found that the relative CO₂ emissions of the networks remain relatively constant for all scenarios, with GB/GB&AC

emissions being higher by a factor of 10. ASHP always has the second largest emissions due to the lower SCOP. For scenario (a) 4GDH has higher CO₂ emissions than AN (31% higher) due to larger heat losses in the network and lower SCOP (caused by a minimum 5°C higher supply temperature to account for thermal losses in the TES and the network) [229]. When a BU is introduced in scenario (b), the emissions from the added ASHP in the BU and the parasitic loads lead to higher emissions for 5GDHC (12%). Finally, when cooling is introduced in scenario (c), there is more variation in the normalised CO₂ emissions due to the GB and AC units having different efficiencies. In this case, 5GDHC has lower emissions (10%) than 4GDH&AC.

RO 5. Utilise a case study to showcase the hydraulic design, system operation and techno-economic performance of a 5GDHC system using any developed methodologies and models.

The feasibility of 5GDHC for a new, large scale, mixed development project area, with access to a low temperature waste heat source is conducted for the extension scenario of the D2 Grids Ambient Loop Project in Clyde Gateway, Glasgow. It is found that, despite having different consumer classes with varying demand profiles and annual heating and cooling demands of similar magnitude, demand seasonality limits the opportunities for energy sharing between prosumers. The DOC is only 3.4% of the total energy demand, which signifies limited opportunities for 5GDHC.

Low temperature waste heat source can offer a solution for this discrepancy, by acting as a heat source during winter and a cooling source during summer. The temperature profile of the source and the abstraction limitations need to be taken into consideration in the design of the system. The available power fluctuates throughout the year depending on them (in this case from 180kW to 1,000kW). Two approaches are analysed, 5GDHC-1 treats WWTP as a prosumer connecting through a HEX and 5GDHC-2 treats WWTP as a source for a SWSHP to charge the BU's TES. 5GDHC-1 requires a seasonal temperature profile in the ambient grid, low enough to allow for heat transfer during the winter (2°C cold line to 7°C hot line) and the summer (18°C cold line to 23°C hot line). For 5GDHC-2, the conventional 15°C cold line to 20°C hot line can be used. This led to a higher energy use for the BU energy transformation equipment for 5GDHC-2, but a lower prosumer level energy use for the prosumer level BHPs.

A detailed techno-economic analysis shows that 5GDHC-1 is the most economic option. Its improvement over 5GDHC-2 in the overall LCOE is 10%. It is also better than the 4GDH&AC option, with a LCOE of 227£/MWh compared to 257£/MWh. This is mainly due to lower CAPEX and OPEX from having less units (550 AC units and an insulated network for 4GDH along with an EC). The ASHP option further highlighted the problems of decentralisation as having many individual units leads to a higher CAPEX and REPEX over a long period. In addition, by having individual units for both heating and cooling, the SPF is lower due to the need for a reversibility function of the ASHP and for an electric heater to help with the DHW production in the individual calorifiers.

5GDHC options are less energy efficient than the 4GDH&AC option, due to a lower overall SPF and higher parasitic loads. For 4GDH&AC, the centralisation of heat utilising the WWTP through a SWSHP and having individual AC units with a high SEER, allowing for the lower cumulative emissions (709 tonnes of CO₂), 11% less than 5GDHC-1 and 24% less than 5GDHC-2. However, having prosumer level reversible BHP units allows for a smaller electric capacity, potentially reducing the impact on the electricity grid. The 5GDHC options had a lower cumulative electric capacity, with 0.7VA for 5GDHC-1 and 5GDHC-2, with 4GDH&AC being 1.5MVA and ASHP 3.0MVA. An analysis of the capacity restrictions on the project area showed that there should be no issues with the supply capacity for the substations and primary transformers, but OHL reinforcements may be needed since they are at capacity. For optimising sector coupling, higher levels of centralisation and the use of the same units for both heating and cooling is recommended.

This work also discusses 5GDHC potential in a wider context. It presents miscellaneous factors that should be factored in, including space constraints, operational complexity, and expansion flexibility. It highlights the issue of high LCOE in new buildings, and how 5GDHC could provide flexibility in phasing the CAPEX by utilising reversible units. Design considerations in large scale developments illustrate how low demand co-occurrence can be tackled by utilising low temperature waste heat sources. Seasonal TESs are also proposed as a key strategy to bridge the seasonal demand gaps and improve 5GDHC's performance. Several limitations are acknowledged, due to the conceptual stage of the research, paving the way for future research. These include the analysis of hydraulic component behaviour, the impact of more complex control regimes for the prosumer

BHPs, the incorporation of an equipment free BU, and the investigation of a wider technology mix.

In summary, all ROs set out in Chapter 1 have been addressed in this thesis. The context of the findings and a synopsis of what they indicate for 5GDHC systems is presented in the following subsection.

8.2 Context

This research has shed light on the characteristics of 5GDHC systems, proposing designs and operating philosophies as well as quantifying their techno-economic performance against other supply options.

On the one hand, 5GDHC offers a greater range of benefits to developers other than the synergies of heating and cooling, which can reduce the overall electricity needs of the system. It allows for phased development, with the energy substations and pumping stations being present in individual plant rooms. This arrangement also makes managing the equipment easier for some stakeholders if the assets are present on their land. The localised energy supply also allows for incorporation of bespoke units for different prosumers, tailor-made for specific loads. For example, if a new residential development is adjacent to an existing hospital, the temperature requirements for the tertiary water will be different, implying that different HPs would be better suited for each. It also allows for higher flexibility to incorporate future energy transfer technologies to the scheme. Additionally, in areas with multiple sources of low temperature waste heat, 5GDHC could offer an easy pathway to decreasing the risk of their involvement, since they can connect at any point with localised plants. Finally, in areas where seasonal TES (such as ATEs) is present, seasonal heating and cooling demands could be superimposed, “creating” demand co-occurrence.

On the other hand, there are quite a few limitations, with the main one being the overall efficiency of the system. Energy sharing can lead to higher efficiency, however due to the seasonality of the loads and the energy losses from the BU offering thermodynamic balance, the overall system efficiency is typically low. In addition, equipment footprint could be higher than for centralised units since space allocation for TES is required both in

the centralised BU and the prosumer substations. This is especially true for ‘heating only’ districts; the TEM analysis showed that only for a small number of properties with multiple flats each it would be better to have 5GDHC than alternative supply options. Regarding the interface with the electricity grid, having multiple connection points could impose larger electric capacity requirements, with smaller benefits from peak shaving.

Altogether, there is a need to have a clear justification for implementing 5GDHC. It should not be seen as a continuation of individual ‘gas boiler mentality’ where GBs are replaced with HPs in every building/flat. 5GDHC excels at connecting heating and cooling loads, but it should be seen as a complementary system to 4GDH and plant room level solutions, being a connector between various heating and cooling systems in an area. In this way, the benefits of both worlds can be harnessed, further enabling thermal zoning and synergies between various sectors. It could even pave the way for alternative business models, where the paradigm of the prosumer’s role in a smart city is challenged.

8.3 Future research

The methodologies and models developed in this research offer a strong foundation for further research on 5GDHC. Specifically, the research pathways could steer towards additional investigations of hydraulic designs, improvements on the accuracy of the developed models and analyses on the benefits of and barriers to 5GDHC.

The proposed hydraulic design and control philosophy provide a basis for further development. Focus should be given on investigating the optimal hydraulic design configurations for addressing issues of low flows, the optimal number of BUs and the impact of their location on the overall stability and efficiency and the impact of network topology. Analysis on the effect of different control strategies on the overall system efficiency can also be studied, with potential communication between the individual agents and the overall system. In such a way, control strategies that include the impact on the grid frequency regulation and voltage control could be incorporated in the 5GDHC system. Research on optimally sizing the BU’s TES capacity and charging/discharging strategies is also recommended, identifying the impact of equipment based and equipment free charging approaches (ATES vs ASHP). Such research could consider system efficiency, applicability, robustness, and space requirements. Finally, an analysis of the system’s

sensitivity to different ambient network temperatures, both absolute and their difference is of interest. Such an analysis could consider different temperature setpoints for the ambient grid for different demand mixes and seasons.

The impact of connecting multiple prosumers should be investigated experimentally, to observe if any unexpected interactions occur. More specifically, investigations can highlight the occurrence of heat islands, areas of no and low flow as well as the creation and effect of hydraulic sub-cycles. Full scale implementations could test the developed control philosophies and simulation models in a real-world environment, presenting areas of concern or needed alterations. They would also provide insights into the actual level of energy sharing between heating and cooling.

Regarding the business models and policy frameworks, it is interesting to collaborate with stakeholders from both clients and industry to explore innovative business models that would best fit 5GDHC. The analysis could gravitate towards initiatives for participation, risk of connection quantification, optimised resource allocation and phasing as well as billing strategies and asset ownership. Structuring policy frameworks that can promote the adoption of smart systems and facilitate sector coupling would also be critical.

Finally, there is a range of tasks centred around the improvement of the developed models. Investigating co-simulation for faster and more efficient simulation of large 5GDHC without hindering the energy sharing accuracy is a priority. Creating detailed BU TES models for capturing the fluid dynamics of the TES is also required. Further, Modelica models can be developed to better understand the impact of various system components to system efficiency. Such developments could include models of ground conditions for the ambient network, detailed electricity grid components and building structures for different consumer types or other 4GDH networks. Furthermore, having an integration with GIS for CATHeaPS to automatically analyse a given network would facilitate its use and adoption by the industry.

In summary, the work conducted in this PhD is intended to act as a platform for future researchers. All the models and produced data are made open access, in the hope they open a wide range of possibilities for advancing research and uptake of smart thermal energy systems.

9 References

- [1] Angelidis O, Zinsmeister D. Experimental validation of a hydraulic design and control philosophies for 5th Generation District Heating and Cooling Networks 2024.
<https://doi.org/10.5525/gla.researchdata.1659>.
- [2] Zinsmeister D, Angelidis O. ProHMo: Prosumer House Model 2023.
<https://researchdata.gla.ac.uk/id/eprint/1639>.
- [3] Angelidis O. CATHeaPS: Centralisation Analysis Tool for Heat Pump Systems 2023.
<https://researchdata.gla.ac.uk/1638/>.
- [4] Lauritsen MK, Olofsson V, Thorpe R, Angelidis O, Bush R. Cost analysis of a typical 4th and 5th generation network. 2024.
- [5] Calvin K, Dasgupta D, Krinner G, Mukherji A, Thorne PW, Trisos C, et al. IPCC, 2023: Climate Change 2023: Synthesis Report. Contribution of Working Groups I, II and III to the Sixth Assessment Report of the Intergovernmental Panel on Climate Change [Core Writing Team, H. Lee and J. Romero (eds.)]. IPCC, Geneva, Switzerland. First. Intergovernmental Panel on Climate Change (IPCC); 2023.
<https://doi.org/10.59327/IPCC/AR6-9789291691647>.
- [6] European Commission. European Green Deal. Brussels: European Commission - Research & Innovation; 2019.
- [7] Erbach G, Roniger J. COP28 climate change conference: Outcomes. European Parliament; 2023.
- [8] International Energy Agency (IEA). Net Zero Roadmap: A Global Pathway to Keep the 1.5 °C Goal in Reach - 2023 Update. IEA; 2023.
- [9] Revesz A, Jones P, Dunham C, Davies G, Marques C, Matabuena R, et al. Developing novel 5th generation district energy networks. *Energy* 2020;201:117389.
<https://doi.org/10.1016/j.energy.2020.117389>.

- [10] Boesten S, Ivens W, Dekker SC, Eijdem H. 5th generation district heating and cooling systems as a solution for renewable urban thermal energy supply. *Advances in Geosciences* 2019;8.
- [11] Howarth N, Camarasa C, Lane K, Martin AR. Keeping cool in a hotter world is using more energy, making efficiency more important than ever – Analysis. IEA 2023. <https://www.iea.org/commentaries/keeping-cool-in-a-hotter-world-is-using-more-energy-making-efficiency-more-important-than-ever> (accessed July 24, 2024).
- [12] Eurostat. Use of renewables for heating and cooling 2024. https://doi.org/10.2908/nrg_ind_urhcd.
- [13] International Energy Agency. Empowering Cities for a Net Zero Future. IEA; 2021.
- [14] International Energy Agency. World Energy Outlook 2023. Paris: IEA; 2023.
- [15] Averfalk H, Benakopoulos T, Best I, Dammel F, Engel C, Geyer R, et al. Low-Temperature District Heating Implementation Guidebook: Final Report of IEA DHC Annex TS2 Implementation of Low-Temperature District Heating Systems. IEA DHC; 2021.
- [16] Zhang M, Millar M-A, Yu Z, Yu J. An assessment of the impacts of heat electrification on the electric grid in the UK. *Energy Reports* 2022;8:14934–46. <https://doi.org/10.1016/j.egy.2022.10.408>.
- [17] Department for Energy Security and Net Zero (DESNZ). Valuation of energy use and greenhouse gas emissions - Supplementary guidance to the HM Treasury Green Book on Appraisal and Evaluation in Central Government. London: UK Government; 2023.
- [18] Fridgen G, Keller R, Körner M-F, Schöpf M. A holistic view on sector coupling. *Energy Policy* 2020;147:111913. <https://doi.org/10.1016/j.enpol.2020.111913>.
- [19] Jokinen I, Lund A, Hirvonen J, Jokisalo J, Kosonen R, Lehtonen M. Coupling of the electricity and district heat generation sectors with building stock energy retrofits as a measure to reduce carbon emissions. *Energy Conversion and Management* 2022;269:115961. <https://doi.org/10.1016/j.enconman.2022.115961>.

- [20] Frederiksen S, Werner S. District Heating and Cooling. District Heating and Cooling. 1st ed., Sweden: Studentlitteratur; 2013.
- [21] Thorsen JE, Lund H, Mathiesen BV. "Progression of District Heating – 1st to 4th generation" 2018.
- [22] The four generations of district cooling Chart. Online: 2022.
- [23] Lund H, Werner S, Wiltshire R, Svendsen S, Thorsen JE, Hvelplund F, et al. 4th Generation District Heating (4GDH). *Energy* 2014;68:1–11. <https://doi.org/10.1016/j.energy.2014.02.089>.
- [24] Wirtz M. Bidirectional low temperature networks design methodology based on mathematical optimisation - poster 2019.
- [25] Buffa S, Cozzini M, D'Antoni M, Baratieri M, Fedrizzi R. 5th generation district heating and cooling systems: A review of existing cases in Europe. *Renewable and Sustainable Energy Reviews* 2019;104:504–22. <https://doi.org/10.1016/j.rser.2018.12.059>.
- [26] Cozzini M, D'Antoni M, Buffa S. District Heating and Cooling Networks Based on Decentralized Heat Pumps: Energy Efficiency and Reversibility at Affordable Costs. *Heat Pumping Technologies* 2018;36:5.
- [27] Gudmundsson O, Dyrelund A, Thorsen JE. Comparison of 4th and 5th generation district heating systems. *E3S Web Conf* 2021;246:09004. <https://doi.org/10.1051/e3sconf/202124609004>.
- [28] Gudmundsson O, Schmidt R-R, Dyrelund A, Thorsen JE. Economic comparison of 4GDH and 5GDH systems – Using a case study. *Energy* 2022;238:121613. <https://doi.org/10.1016/j.energy.2021.121613>.
- [29] Wirtz M, Kivilip L, Remmen P, Müller D. Quantifying Demand Balancing in Bidirectional Low Temperature Networks. *Energy and Buildings* 2020;224:110245. <https://doi.org/10.1016/j.enbuild.2020.110245>.
- [30] Zhang Y, Johansson P, Kalagasidis AS. Quantification of overlapping heating and cooling demand for the feasibility assessment of bi-directional systems over Europe. *Energy and Buildings* 2023;294:113244. <https://doi.org/wir>.

- [31] Sulzer M, Werner S, Mennel S, Wetter M. Vocabulary for the fourth generation of district heating and cooling. *Smart Energy* 2021;1:100003.
<https://doi.org/10.1016/j.segy.2021.100003>.
- [32] Denyer D, Tranfield D. Producing a systematic review. *The Sage handbook of organizational research methods*, Thousand Oaks, CA: Sage Publications Ltd; 2009, p. 671–89.
- [33] Abugabbara M, Javed S, Bagge H, Johansson D. Bibliographic analysis of the recent advancements in modeling and co-simulating the fifth-generation district heating and cooling systems. *Energy and Buildings* 2020;224:110260.
<https://doi.org/10.1016/j.enbuild.2020.110260>.
- [34] Ioannou A, Angus A, Brennan F. Risk-based methods for sustainable energy system planning: A review. *Renewable and Sustainable Energy Reviews* 2017;74:602–15.
<https://doi.org/10.1016/j.rser.2017.02.082>.
- [35] Juntunen JK, Martiskainen M. Improving understanding of energy autonomy: A systematic review. *Renewable and Sustainable Energy Reviews* 2021;141:110797.
<https://doi.org/10.1016/j.rser.2021.110797>.
- [36] Borri E, Zsembinszki G, Cabeza LF. Recent developments of thermal energy storage applications in the built environment: A bibliometric analysis and systematic review. *Applied Thermal Engineering* 2021;189:116666.
<https://doi.org/10.1016/j.applthermaleng.2021.116666>.
- [37] van Eck NJ, Waltman L. *VOSviewer Manual* 2020.
- [38] Leoni P, Geyer R, Schmidt R-R. Developing innovative business models for reducing return temperatures in district heating systems: Approach and first results. *Energy* 2020;195:116963. <https://doi.org/10.1016/j.energy.2020.116963>.
- [39] Ashish S. *How to Conduct an Interview for Research - The Complete Guide* 2020. Scripto Sphere 2020. <https://www.scriptosphere.com/how-to-conduct-an-interview-for-research-complete-guide/> (accessed January 25, 2022).
- [40] Maureen H, Anca V. *How to anonymise qualitative and quantitative data* 2021.

- [41] UK Data Service. Anonymising qualitative data. UK Data Service 2021. <https://ukdataservice.ac.uk/learning-hub/research-data-management/anonymisation/anonymising-quantitative-data/> (accessed December 20, 2021).
- [42] von Rhein J, Henze GP, Long N, Fu Y. Development of a topology analysis tool for fifth-generation district heating and cooling networks. *Energy Conversion and Management* 2019;196:705–16. <https://doi.org/10.1016/j.enconman.2019.05.066>.
- [43] Chartered Institution of Building Services Engineers (CIBSE). CP1 Heat networks: Code of Practice for the UK (2020). 2nd ed. London: Association for Decentralised Energy (ADE); 2020.
- [44] Buffa S, Fouladfar MH, Franchini G, Lozano Gabarre I, Andrés Chicote M. Advanced Control and Fault Detection Strategies for District Heating and Cooling Systems—A Review. *Applied Sciences* 2021;11:455. <https://doi.org/10.3390/app11010455>.
- [45] Blacha T, Mans M, Remmen P, Mueller D. Dynamic Simulation Of Bidirectional Low-Temperature Networks - A Case Study To Facilitate The Integration Of Renewable Energies, Rome, Italy: 2019, p. 3491–8. <https://doi.org/10.26868/25222708.2019.210670>.
- [46] Jensen LL, Trier D, Brennenstuhl M, Cozzini M, Serrano BG-U. Analysis of Network Layouts in Selected Urban Contexts. European Commission - Research & Innovation; 2016.
- [47] Gabrielli P, Acquilino A, Siri S, Bracco S, Sansavini G, Mazzotti M. Optimization of low-carbon multi-energy systems with seasonal geothermal energy storage: The Energy Grid of ETH Zurich. *Energy Conversion and Management: X* 2020;8:100052. <https://doi.org/10.1016/j.ecmx.2020.100052>.
- [48] Franzén I, Nedar L, Andersson M. Environmental Comparison of Energy Solutions for Heating and Cooling. *Sustainability* 2019;11:7051. <https://doi.org/10.3390/su11247051>.
- [49] Zeh R, Ohlsen B, Philipp D, Bertermann D, Kotz T, Jocić N, et al. Large-Scale Geothermal Collector Systems for 5th Generation District Heating and Cooling Networks. *Sustainability* 2021;13:6035. <https://doi.org/10.3390/su13116035>.

- [50] Sommer T, Mennel S, Sulzer M. Lowering the pressure in district heating and cooling networks by alternating the connection of the expansion vessel. *Energy* 2019;172:991–6. <https://doi.org/10.1016/j.energy.2019.02.010>.
- [51] Wetter M, Hu J. Quayside Energy System Analysis. Lawrence Berkeley National Laboratory; 2019.
- [52] Korsell L, Ydén T. Control Design for an Energy-Sharing Module of Next-Generation Thermal Energy System ectogrid™. MSc Thesis, ISSN 0280-5316. Lund University, 2021.
- [53] Sommer T, Sulzer M, Wetter M, Sotnikov A, Mennel S, Stettler C. The reservoir network: A new network topology for district heating and cooling. *Energy* 2020;199:117418. <https://doi.org/10.1016/j.energy.2020.117418>.
- [54] Andrés M, Thorsen JE, Buffa S, Firan ML, Regidor M, Fedrizzi R. Configuration and sizing of packaged substations. 2021.
- [55] Christian Johansson, Sofia Lettenbichle. Results of the STORM Project 2018.
- [56] Smulders E. The STORM project | The STORM project. The Storm Project 2021. <https://storm-dhc.eu/en> (accessed April 13, 2021).
- [57] Oevelen TV, Vanhoudt D, Johansson C, Smulders E. Testing and performance evaluation of the STORM controller in two demonstration sites. *Energy* 2020;197:117177. <https://doi.org/10.1016/j.energy.2020.117177>.
- [58] Johansson C, Bergkvist M, Geysen D, Somer OD, Lavesson N, Vanhoudt D. Operational Demand Forecasting In District Heating Systems Using Ensembles Of Online Machine Learning Algorithms. *Energy Procedia* 2017;116:208–16. <https://doi.org/10.1016/j.egypro.2017.05.068>.
- [59] Cubillo J, Cambronero MV, Ferrandis C. E2District demonstration experience; how to operate a DHC network in an efficient manner. *E2District*; 2019.
- [60] Lickleder T, Zinsmeister D, Lukas L, Speer F, Hamacher T, Perić VS. Control of bidirectional prosumer substations in smart thermal grids: A weighted proportional-integral control approach. *Applied Energy* 2024;354:122239. <https://doi.org/10.1016/j.apenergy.2023.122239>.

- [61] Schluck T, Kräuchi P, Sulzer M. Non-linear thermal networks – how can a meshed network improve energy efficiency?, Switzerland: CISBAT; 2015, p. 6.
- [62] Sommer T, Sotnikov A, Sandmeier E, Stettler C, Mennel S, Sulzer M. Optimization of low-temperature networks by new hydraulic concepts. *J Phys: Conf Ser* 2019;1343:012112. <https://doi.org/10.1088/1742-6596/1343/1/012112>.
- [63] Mugaguren ML, Martínez RG, Zabala VS. RELaTED, decentralized & renewable Ultra Low Temperature District Heating, concept conversion from traditional district heating. *IOP Conf Ser: Mater Sci Eng* 2019;609:052004. <https://doi.org/10.1088/1757-899X/609/5/052004>.
- [64] European Commission. The European Green Deal Investment Plan and Just Transition Mechanism explained. European Commission 2020. https://ec.europa.eu/commission/presscorner/detail/en/qanda_20_24 (accessed December 20, 2021).
- [65] Bünning F, Wetter M, Fuchs M, Müller D. Bidirectional low temperature district energy systems with agent-based control: Performance comparison and operation optimization. *Applied Energy* 2018;209:502–15. <https://doi.org/10.1016/j.apenergy.2017.10.072>.
- [66] Wirtz M, Kivilip L, Remmen P, Müller D. 5th Generation District Heating: A novel design approach based on mathematical optimization. *Applied Energy* 2020;260:114158. <https://doi.org/10.1016/j.apenergy.2019.114158>.
- [67] Wirtz M, Schreiber T, Mueller D. Survey of 53 Fifth-Generation District Heating and Cooling (5GDHC) Networks in Germany. *Energy Technology* 2022;10. <https://doi.org/10.1002/ente.202200749>.
- [68] Couturier S. Report on KPIs and monitoring strategy for district heating and cooling. European Commission - Research & Innovation; 2019.
- [69] Cozzini M, Trier D, Bava F, Fedrizzi R, Buffa S, Jensen LL, et al. FLEXYNETS Guide Book. European Commission - Research & Innovation; 2018.
- [70] Abugabbara M, Gehlin S, Lindhe J, Axell M, Holm D, Johansson H, et al. How to develop fifth-generation district heating and cooling in Sweden? Application review and

best practices proposed by middle agents. *Energy Reports* 2023;9:4971–83.
<https://doi.org/10.1016/j.egy.2023.04.048>.

[71] Gudmundsson O, Schmidt R-R, Dyrelund A, Thorsen JE. Economic comparison of 4GDH and 5GDH systems – Using a case study. *Energy* 2021;238:121613.
<https://doi.org/10.1016/j.energy.2021.121613>.

[72] Calise F, Cappiello FL, Cimmino L, Dentice d'Accadia M, Vicidomini M. A comparative thermoeconomic analysis of fourth generation and fifth generation district heating and cooling networks. *Energy* 2023;284:128561.
<https://doi.org/10.1016/j.energy.2023.128561>.

[73] Sayegh MA, Jadwiszczak P, Axcell BP, Niemierka E, Bryś K, Jouhara H. Heat pump placement, connection and operational modes in European district heating. *Energy and Buildings* 2018;166:122–44. <https://doi.org/10.1016/j.enbuild.2018.02.006>.

[74] Jones P, Dunham C, Davidson C. A roadmap to achieve 5th generation heat networks in the UK 2019.

[75] Sulzer M, Orehounig K, Knoeri C, Baldini L, Castello R, Chambers J, et al. Paradigm shifts for the Swiss building sector to shape the future energy system. Switzerland: SCCER FEEB&D; 2020.

[76] Vázquez MVC, Corscadden J, Marijuan AG, Barbagelata G, Hamann G, Grosjean M, et al. Integration of Renewables in DHC for Sustainable Living Workshop. *Proceedings* 2021;65:30. <https://doi.org/10.3390/proceedings2020065030>.

[77] Millar M-A, Elrick B, Jones G, Yu Z, Burnside NM. Roadblocks to Low Temperature District Heating. *Energies* 2020;13:5893. <https://doi.org/10.3390/en13225893>.

[78] Østergaard KK, Caramaschi M, Bryder K, Buhl L, Christiansen C holm, Pedersen MK. RELaTED D2.2 -Interconnection schemes for consumer installations. European Commission - Research & Innovation; 2019.

[79] Paardekooper S, Lund R, Vad Mathiesen B, Chang M, Petersen UR, Grundahl L, et al. Heat Roadmap Netherlands A low carbon heating and cooling strategy 2018.

- [80] Kadir S, Özkan S. EctogridTM : The competitiveness of a low temperature district heating network in Germany and United Kingdom. Master of Science Thesis. KTH Royal Institute of Technology, 2018.
- [81] Wahlroos M, Pärssinen M, Rinne S, Syri S, Manner J. Future views on waste heat utilization – Case of data centers in Northern Europe. *Renewable and Sustainable Energy Reviews* 2018;82:1749–64. <https://doi.org/10.1016/j.rser.2017.10.058>.
- [82] Fedrizzi R. How innovative district heating networks reduce the consumption of fossil energy. *Open Access Government* 2020. <https://www.openaccessgovernment.org/district-heating-networks-reduce-the-consumption-of-fossil-energy/98301/> (accessed May 26, 2021).
- [83] LIFE4HeatRecovery. LIFE4HeatRecovery newsletter #1 2019.
- [84] Menéndez J, Ordóñez A, Fernández-Oro JM, Loredó J, Díaz-Aguado MB. Feasibility analysis of using mine water from abandoned coal mines in Spain for heating and cooling of buildings. *Renewable Energy* 2020;146:1166–76. <https://doi.org/10.1016/j.renene.2019.07.054>.
- [85] Younger PL. Ground-Coupled Heating-Cooling Systems in Urban Areas: How Sustainable Are They? *Bulletin of Science, Technology & Society* 2008;28:174–82. <https://doi.org/10.1177/0270467607313963>.
- [86] Department for Energy Security and Net Zero (DESNZ). Research into barriers to deployment of district heating networks. Centre for Sustainable Energy for the Department of Energy & Climate Change; 2013.
- [87] LOGSTOR. Design Manual. 2019.
- [88] Volkova A, Pakere I, Murauskaite L, Huang P, Lepiksaar K, Zhang X. 5th generation district heating and cooling (5GDHC) implementation potential in urban areas with existing district heating systems. *Energy Reports* 2022;8:10037–47. <https://doi.org/10.1016/j.egy.2022.07.162>.
- [89] Brummer N, Midiere M. Procurement for 5gdhc: considerations on choosing for 5gdhc, the implications for procurement, and envisioning procurement’s role in the industrialization and scaling of 5gdhc. 2021.

- [90] Werner S. International review of district heating and cooling. *Energy* 2017;137:617–31. <https://doi.org/10.1016/j.energy.2017.04.045>.
- [91] Sun C, Liu Y, Li Y, Lin S, Gooi HB, Zhu J. Network-aware P2P multi-energy trading in decentralized electric-heat systems. *Applied Energy* 2023;345:121298. <https://doi.org/10.1016/j.apenergy.2023.121298>.
- [92] Guelpa E, Verda V. Demand response and other demand side management techniques for district heating: A review. *Energy* 2021;219:119440. <https://doi.org/10.1016/j.energy.2020.119440>.
- [93] Guelpa E, Marincioni L. Demand side management in district heating systems by innovative control. *Energy* 2019;188:116037. <https://doi.org/10.1016/j.energy.2019.116037>.
- [94] Plan Energi, Aalborg University. Technical and Economic Potential of Distributed Energy Storages for the Integration of Renewable Energy. Aalborg University; 2018.
- [95] Sveinbjörnsson D, Jensen LL, Trier D, Bava F, Hassine IB. Large Storage Systems for DHC Networks. European Commission - Research & Innovation; 2019.
- [96] Velvis H, Buunk RJ. District Aquifer Thermal Energy Storage (DATES), Netherlands: 12th IEA Heat Pump Conference; 2017, p. 11.
- [97] Buunk RJ. Introducing Dates 2017.
- [98] Jebamalai JM, Marlein K, Laverge J. Influence of centralized and distributed thermal energy storage on district heating network design. *Energy* 2020;202:117689. <https://doi.org/10.1016/j.energy.2020.117689>.
- [99] Al-Habaibeh A, Athresh AP, Parker K. Performance analysis of using mine water from an abandoned coal mine for heating of buildings using an open loop based single shaft GSHP system. *Applied Energy* 2018;211:393–402. <https://doi.org/10.1016/j.apenergy.2017.11.025>.
- [100] Loredó C, Ordóñez A, Garcia-Ordiales E, Álvarez R, Roqueñi N, Cienfuegos P, et al. Hydrochemical characterization of a mine water geothermal energy resource in NW

Spain. *Science of The Total Environment* 2017;576:59–69.
<https://doi.org/10.1016/j.scitotenv.2016.10.084>.

[101] Thakar K, Patel R, Patel G. Techno-economic analysis of district cooling system: A case study. *Journal of Cleaner Production* 2021;313:127812.
<https://doi.org/10.1016/j.jclepro.2021.127812>.

[102] Fischer D, Madani H. On heat pumps in smart grids: A review. *Renewable and Sustainable Energy Reviews* 2017;70:342–57. <https://doi.org/10.1016/j.rser.2016.11.182>.

[103] Brennenstuhl M, Hassine IB, Jobard X. Management of interaction with electricity and gas grid. *European Commission - Research & Innovation*; 2017.

[104] Prasanna A, Dorer V, Vetterli N. Optimisation of a district energy system with a low temperature network. *Energy* 2017;137:632–48.
<https://doi.org/10.1016/j.energy.2017.03.137>.

[105] Brown C, Desguers T, Lyden A, Kolo I, Friedrich D, Falcone G. Modelling Borehole Thermal Energy Storage using Curtailed Wind Energy as a Fluctuating Source for Charge. 2023 Stanford Geothermal Workshop, Stanford University; 2023.

[106] Zhang Z, Wang P, Jiang P, Liu Z, Fu L. Energy management of ultra-short-term optimal scheduling of integrated energy system considering the characteristics of heating network. *Energy* 2021;240:122790. <https://doi.org/10.1016/j.energy.2021.122790>.

[107] Iov F, Khatibi M, Bendtsen J. On the Participation of Power-To-Heat Assets in Frequency Regulation Markets—A Danish Case Study. *Energies* 2020;13:4608.
<https://doi.org/10.3390/en13184608>.

[108] Fransen M, Dubbeling T. ACM Position Paper: Marginal pricing for balancing energy. 2019.

[109] Glowacki Law Firm. Frequency Restoration Reserve (FRR) - Emissions-EUETS.com. European Union Emissions Trading Scheme – Legal Point of View 2021. <https://www.emissions-euets.com/internal-electricity-market-glossary/794-frequency-restoration-reserve-frr> (accessed February 7, 2022).

- [110] Qiu H, Vinod A, Lu S, Gooi HB, Pan G, Zhang S, et al. Decentralized mixed-integer optimization for robust integrated electricity and heat scheduling. *Applied Energy* 2023;350:121693. <https://doi.org/10.1016/j.apenergy.2023.121693>.
- [111] Cozzini M, Buffa S, Hassine IB, Vivian J. Low- and high-level controls for low temperature DHC networks. *European Commission - Research & Innovation*; 2018.
- [112] Buffa S, Soppelsa A, Pipiciello M, Henze G, Fedrizzi R. Fifth-Generation District Heating and Cooling Substations: Demand Response with Artificial Neural Network-Based Model Predictive Control. *Energies* 2020;13:4339. <https://doi.org/10.3390/en13174339>.
- [113] Bünning F, Wetter M, Fuchs M, Müller D. Bidirectional low temperature district energy systems with agent-based control: Performance comparison and operation optimization. *Applied Energy* 2018;209:502–15. <https://doi.org/10.1016/j.apenergy.2017.10.072>.
- [114] Li H, Wang SJ. Challenges in Smart Low-temperature District Heating Development. *Energy Procedia* 2014;61:1472–5. <https://doi.org/10.1016/j.egypro.2014.12.150>.
- [115] Saletti C, Gambarotta A, Morini M. Development, analysis and application of a predictive controller to a small-scale district heating system 2020. <https://doi.org/10.1016/j.applthermaleng.2019.114558>.
- [116] Hering D, Cansev ME, Tamassia E, Xhonneux A, Müller D. Temperature control of a low-temperature district heating network with Model Predictive Control and Mixed-Integer Quadratically Constrained Programming. *Energy* 2021;224:120140. <https://doi.org/10.1016/j.energy.2021.120140>.
- [117] Beder C, Blanke J, Klepal M. Towards Integrating Behaviour Demand Response into Simulation Based Heat Production Optimisation. *Proceedings* 2018;2:1125. <https://doi.org/10.3390/proceedings2151125>.
- [118] Edtmayer H, Nageler P, Heimrath R, Mach T, Hochenauer C. Investigation on sector coupling potentials of a 5th generation district heating and cooling network. *Energy* 2021;230:120836. <https://doi.org/10.1016/j.energy.2021.120836>.

- [119] Lucas A, Jansen L, Andreadou N, Kotsakis E, Masera M. Load Flexibility Forecast for DR Using Non-Intrusive Load Monitoring in the Residential Sector. *Energies* 2019;12:2725. <https://doi.org/10.3390/en12142725>.
- [120] DIN EN ISO 7730. Ergonomics of the thermal environment. Analytical determination and interpretation of thermal comfort using calculation of the PMV and PPD indices and local thermal comfort criteria: ISO International Standards; 2005. <https://doi.org/10.3403/30046382>.
- [121] Olivier S, Henry M, Chemali C. Market survey on available components. Heerlen, The Netherlands: 2020.
- [122] Boesten WI S. Transnational Roll-Out Strategy. Heerlen, The Netherlands: Open University; 2020.
- [123] Galindo Fernández M, Bacquet A, Bensadi S, Morisot P, Oger A. Integrating renewable and waste heat and cold sources into district heating and cooling systems. Luxembourg: Publications Office of the European Union; 2021.
- [124] Pellegrini M, Bianchini A. The Innovative Concept of Cold District Heating Networks: A Literature Review. *Energies* 2018;11:236. <https://doi.org/10.3390/en11010236>.
- [125] Gomez-Urbarri B, Fedrizzi R, Cozzini M, D'Antoni M. FLEXYNETS-TRADING policies. European Commission - Research & Innovation; 2018.
- [126] Rodolphe de B. Energy sector coupling session 2018.
- [127] Lickleder T, Zinsmeister D, Elizarov I, Perić V, Tzscheuschler P. Characteristics and Challenges in Prosumer-Dominated Thermal Networks. *J Phys: Conf Ser* 2021;2042:012039. <https://doi.org/10.1088/1742-6596/2042/1/012039>.
- [128] Venizelou V, Psara K, Pitsiladis G, Barrachina P, Stott R, Pieper N, et al. Plan for the deployment of the DRIMPAC solution and required equipment to pilot premises. European Commission - Research & Innovation; 2021.
- [129] “Integrated of Renewables in DHC for Sustainable Living Workshop” at Sustainable Places 2020. 2020.

- [130] A healthy economy should be designed to thrive, not grow. 2018.
- [131] Van der Bosch, H. Doughnut cities. Smart City Hub 2019.
<https://smartcityhub.com/governance-economy/doughnut-cities/> (accessed August 25, 2021).
- [132] Candelise C. Crowdfunding as a novel financial tool for district heating projects. European Commission - Research & Innovation; 2018.
- [133] Fernández Fuentes I, Barich A, Baisch C, Bodo B, Elíasson O, Falcone G, et al. The CROWD THERMAL Project: Creating Public Acceptance of Geothermal Energy and Opportunities for Community Financing. *Energies* 2022;15:8310.
<https://doi.org/10.3390/en15218310>.
- [134] Ioannou A, Falcone G, Baisch C, Friederichs G, Hildebrand J. A Decision Support Tool for Social Engagement, Alternative Financing and Risk Mitigation of Geothermal Energy Projects. *Energies* 2023;16:1280. <https://doi.org/10.3390/en16031280>.
- [135] Mihaylov S. Digital Single Market – Smartening Europe 2018.
- [136] Koller A. Smart Energy Systems – How digitalization is revolutionizing district energy 2018.
- [137] Rismanchi B. District energy network (DEN), current global status and future development. *Renewable and Sustainable Energy Reviews* 2017;75:571–9.
<https://doi.org/10.1016/j.rser.2016.11.025>.
- [138] Chemali C. 5th generation heating networks: A challenge to integrate the new business model. *Construction21Org* 2019. <https://www.construction21.org/articles/h/5th-generation-heatin-networks-a-challenge-to-integrate-the-new-business-model.html> (accessed May 17, 2021).
- [139] Faugeras A. State of the art report smart contract and blockchain. *GreenFlex*; 2019.
- [140] European Commission. ENCLUDE Energy Citizens for Inclusive Decarbonisation. ENCLUDE 2024. <https://encludeproject.eu/home> (accessed July 30, 2024).
- [141] Dunphy N, Lennon B, Quinlivan L, Revez A, Brenner-Fließer M. Intersectional analysis of emerging examples of energy citizenship 2023.

- [142] Dunphy NP, Revez A, Lennon B, Brenner-Fließer M. D2.2 Typology of Energy Citizenship(s). Enclude Project; 2023.
- [143] McGookin C, Süsser D, Xexakis G, Trutnevyte E, McDowall W, Nikas A, et al. Advancing participatory energy systems modelling. *Energy Strategy Reviews* 2024;52:101319. <https://doi.org/10.1016/j.esr.2024.101319>.
- [144] Angelidis O, Ioannou A, Friedrich D, Thomson A, Falcone G. District heating and cooling networks with decentralised energy substations: Opportunities and barriers for holistic energy system decarbonisation. *Energy* 2023;269:126740. <https://doi.org/10.1016/j.energy.2023.126740>.
- [145] Paarporn S. Decentralized pumping system. US6607141B2, 2003.
- [146] Dostal J, Havlena V. Modeling, optimization and analysis of hydronic networks with decentralized pumping. 2014 CACS International Automatic Control Conference (CACS 2014), Kaohsiung, Taiwan: IEEE; 2014, p. 269–74. <https://doi.org/10.1109/CACS.2014.7097200>.
- [147] Paarporn S. Local Pumping System. *ASHRAE Journal* 2000;42:26–32.
- [148] Wirtz M, Neumaier L, Remmen P, Müller D. Temperature control in 5th generation district heating and cooling networks: An MILP-based operation optimization. *Applied Energy* 2021;288:116608. <https://doi.org/10.1016/j.apenergy.2021.116608>.
- [149] Orehounig K, Evins R, Dorer V, Carmeliet J. Assessment of Renewable Energy Integration for a Village Using the Energy Hub Concept. *Energy Procedia* 2014;57:940–9. <https://doi.org/10.1016/j.egypro.2014.10.076>.
- [150] Schulze M, Friedrich L, Gautschi M. Modeling and optimization of renewables: applying the Energy Hub approach. 2008 IEEE International Conference on Sustainable Energy Technologies, Singapore, Singapore: IEEE; 2008, p. 83–8. <https://doi.org/10.1109/ICSET.2008.4746977>.
- [151] Abugabbara M. Modelling and Simulation of the Fifth-Generation District Heating and Cooling. Lunds Universitet; 2021.

- [152] Kuntuarova S, Lickleder T, Huynh T, Zinsmeister D, Hamacher T, Perić V. Design and simulation of district heating networks: A review of modeling approaches and tools. *Energy* 2024;305:132189. <https://doi.org/10.1016/j.energy.2024.132189>.
- [153] Wetter M, Treeck C van. IEA EBC Annex 60: New Generation Computing Tools for Building and Community Energy Systems. Lawrence Berkeley National Laboratory and RWTH Aachen University: IEA; 2017.
- [154] Wetter M, Zuo W, Nouidui TS, Pang X. Modelica Buildings library. *Journal of Building Performance Simulation* 2014;7:253–70. <https://doi.org/10.1080/19401493.2013.765506>.
- [155] Mueller D, Lauster M, Constantin A, Fuchs M, Remmen P. AixLib – An Open-Source Modelica Library within the IEA-EBC Annex 60 Framework. 2016.
- [156] Wüllhorst F, Maier L, Jansen D, Kühn L, Hering D, Müller D. BESMod - A Modelica Library providing Building Energy System Modules. *Modelica Conferences 2022*:9–18. <https://doi.org/10.3384/ECP211869>.
- [157] Hinkelman K, Wang J, Zuo W, Gautier A, Wetter M, Fan C, et al. Modelica-Based Modeling and Simulation of District Cooling Systems: A Case Study 2021. <https://doi.org/10.31224/osf.io/vpafs>.
- [158] Abugabbara M, Javed S, Johansson D. A simulation model for the design and analysis of district systems with simultaneous heating and cooling demands. *Energy* 2022;261:125245. <https://doi.org/10.1016/j.energy.2022.125245>.
- [159] van der Heijde B, Fuchs M, Ribas Tugores C, Schweiger G, Sartor K, Basciotti D, et al. Dynamic equation-based thermo-hydraulic pipe model for district heating and cooling systems. *Energy Conversion and Management* 2017;151:158–69. <https://doi.org/10.1016/j.enconman.2017.08.072>.
- [160] Zinsmeister D, Perić V. Implementation of a Digital Twin of the CoSES District Heating Prosumer Laboratory. *Energy Proceedings, Bochum, Germany: 2022*, p. 7.
- [161] Zinsmeister D, Lickleder T, Adldinger S, Christange F, Tzscheuschler P, Hamacher T, et al. A prosumer-based sector-coupled district heating and cooling

laboratory architecture. *Smart Energy* 2023;9:100095.
<https://doi.org/10.1016/j.segy.2023.100095>.

[162] Elizarov I, Lickleder T. ProsNet – a Modelica library for prosumer-based heat networks: description and validation. *J Phys: Conf Ser* 2021;2042:012031.
<https://doi.org/10.1088/1742-6596/2042/1/012031>.

[163] The Modelica Association. FMI 3.0 Implementers' Guide 2023.

[164] SensorShop24. Temperatursensoren PT (100 / 1000 / 500 / 2000) 2023.
<https://www.sensorshop24.de/temperatursensoren-pt-100-1000-500-2000> (accessed February 27, 2024).

[165] Endress + Hauser. Proline Promag E 100 electromagnetic flowmeter 2023.
<https://www.endress.com/en/field-instruments-overview/flow-measurement-product-overview/electromagnetic-flowmeter-promag-e100-5e1b> (accessed February 27, 2024).

[166] Ratiotherm. Heat pump storage tank Oskar^o WPS 2023. <https://ratiotherm-systems.com/schichtspeicher-oskar/waermepumpenspeicher/> (accessed February 29, 2024).

[167] WOLF. BSP & BSH Stratification cylinders 2023. <https://www.wolf.eu/en-de/products/stratification-cylinders> (accessed March 11, 2024).

[168] SWEP. B80 - SWEP 2023. <https://www.swep.net/products/B80/> (accessed February 27, 2024).

[169] IMP Pumps. NMT PLUS ER. IMP Pumps 2023. <https://imp-pumps.com/crpalke/nmt-plus-er/> (accessed February 27, 2024).

[170] Killus-technik. Elektrischer Durchlauferhitzer 9 Kilowatt aus Edelstahl. Killus-Technik 2023. <https://www.killus-technik.de/de/speichertechnik/speicher-zubehoer/elektro-heizstaebe-106/elektrischer-durchlauferhitzer-9-kilowatt-aus-edelstahl.html> (accessed March 11, 2024).

[171] Ratiotherm. WP Max-HiQ 2023. <https://ratiotherm-systems.com/waermepumpen/grundwasser-waermepumpe/wp-max-hiq/> (accessed February 27, 2024).

- [172] Grundfos. CME 1-2 A-R-G-E-AQQE S-A-D-N 2023. <https://product-selection.grundfos.com/uk/products/cm-cme/cme/cme-1-2-98394846> (accessed November 16, 2023).
- [173] WOLF. Wärmepumpe CHA 2023. <https://www.wolf.eu/waermepumpen> (accessed March 11, 2024).
- [174] Olszewski P, Arafeh J. Parametric analysis of pumping station with parallel-configured centrifugal pumps towards self-learning applications. *Applied Energy* 2018;231:1146–58. <https://doi.org/10.1016/j.apenergy.2018.09.173>.
- [175] Mason RL, Gunst RF, Hess JL. *Statistical design and analysis of experiments: with applications to engineering and science*. 2. ed. New York: Wiley-Interscience; 2003.
- [176] Zoltán S. Spakovszky. Thermodynamics and Propulsion, Chapter 18.5 Heat Exchangers. *Thermodynamics and Propulsion* 2023. <https://web.mit.edu/16.unified/www/FALL/thermodynamics/notes/node131.html> (accessed January 17, 2024).
- [177] Gülich JF. *Centrifugal Pumps*. Berlin, Heidelberg: Springer Berlin Heidelberg; 2010. <https://doi.org/10.1007/978-3-642-12824-0>.
- [178] SAUTER. Pressure transmitter DSU, DSI. Sauter-ControlsCom 2023. <https://www.sauter-controls.com/en/product/pressure-transmitter/> (accessed February 27, 2024).
- [179] SAUTER. Valve actuator with SAUTER Universal Technology (SUT) AVM 105S, 115S ► SAUTER Controls. Sauter-ControlsCom 2023. <https://www.sauter-controls.com/en/product/valve-actuator-with-sauter-universal-technology-sut/> (accessed February 27, 2024).
- [180] BENDER-Armaturen. 1431: CR-Brass Bevel seat Backflow-preventer Valve 2023. <https://www.bender-armaturen.de/en/valves-germany/cr-messing-marktmodelle/2019-10-18-03-38-47677450187-det.html> (accessed February 27, 2024).
- [181] Anderson TN, Duke M, Carson JK. Experimental determination of natural convection heat transfer coefficients in an attic shaped enclosure. *International*

Communications in Heat and Mass Transfer 2010;37:360–3.
<https://doi.org/10.1016/j.icheatmasstransfer.2010.01.008>.

[182] Hinkelman K, Wang J, Zuo W, Gautier A, Wetter M, Fan C, et al. Modelica-based modeling and simulation of district cooling systems: A case study. *Applied Energy* 2022;311:118654. <https://doi.org/10.1016/j.apenergy.2022.118654>.

[183] Department for Energy Security and Net Zero (DESNZ). HNDU Template Financial Model Detailed Model Specification and Technical Guide. March 2022; n.d.

[184] Building Research Establishment. Heat Networks for Oxford - City centre feasibility study. 2016.

[185] Sonvilla PM, López JV, Rosa DM de la, Reed PG, Holley M, Hinton T, et al. Thermos Thermal Energy Resource Modelling and Optimization System - District Heating & Cooling Case Studies. Thermos; 2021.

[186] EMD International A/S. User's Guide energyPRO 2017.

[187] nPro. Documentation - nPro. nPro - The Planning Tool for District Energy Systems 2023. <https://www.npro.energy/main/en/help> (accessed September 20, 2023).

[188] Larkery. Thermos UI 2023.

[189] Danish Energy Agency, Ramboll. District Heating Assessment Tool. Danish Energy Agency; 2017.

[190] Federico Bava, Daniel Tier. Pre-Design support tool for low-temperature DHC networks 2018.

[191] Molyneaux A, Leyland G, Favrat D. Environomic multi-objective optimisation of a district heating network considering centralized and decentralized heat pumps. *Energy* 2010;35:751–8. <https://doi.org/10.1016/j.energy.2009.09.028>.

[192] Wang Z. Heat pumps with district heating for the UK's domestic heating: individual versus district level. *Energy Procedia* 2018;149:354–62.
<https://doi.org/10.1016/j.egypro.2018.08.199>.

- [193] HM Treasury. The Green Book: Central Government Guidance on Appraisal and Evaluation. United Kingdom: HM Treasury; 2022.
- [194] Fuentes E, Arce L, Salom J. A review of domestic hot water consumption profiles for application in systems and buildings energy performance analysis. *Renewable and Sustainable Energy Reviews* 2018;81:1530–47. <https://doi.org/10.1016/j.rser.2017.05.229>.
- [195] Yao R, Steemers K. A method of formulating energy load profile for domestic buildings in the UK. *Energy and Buildings* 2005;37:663–71. <https://doi.org/10.1016/j.enbuild.2004.09.007>.
- [196] CIBSE. Energy benchmarks TM46. London: CIBSE; 2008.
- [197] CIBSE. Energy Efficiency in Buildings - CIBSE Guide F. 3rd ed. London: 2012.
- [198] Letcher M. Towards Low-carbon Housing Developments: a cumulative approach to reducing carbon emissions. Centre for Sustainable energy; 2005.
- [199] Department for Energy Security and Net Zero (DESNZ). The Non-Domestic National Energy Efficiency Data-Framework 2020 (England and Wales). London: 2020.
- [200] Ministry of Housing, Communities & Local Government. Floor Space in English Homes – main report. London: Ministry of Housing, Communities & Local Government; 2017.
- [201] National House Building Council. 8.1.5 Hot water service. NHBC Standards 2022, NHBC; 2022.
- [202] Dansk Standard. DS 439: 2009 Code of Practice for domestic water supply installations 2009.
- [203] Lauritsen AB, Andersen NB, Andreasen B, Drivsholm C, Hammer F, Ulbjerg F, et al. Varme Ståbi. 7th ed. Praxis - Nyt Teknisk Forlag; 2015.
- [204] Kensa Heat Pumps. Shoebox Heat Pump: Installation and Commissioning Manual 2017.

- [205] Chartered Institution of Building Services Engineers (CIBSE). Heating, ventilating, air conditioning and refrigeration: CIBSE guide B. London: Chartered Institution of Building Services Engineers; 2005.
- [206] Nkwetta D, Vouillamoz P-E, Haghghat F, Mankibi M, Moreau A, Daoud A. Impact of phase change materials types and positioning on hot water tank thermal performance: Using measured water demand profile. *Applied Thermal Engineering* 2014;67:460–8. <https://doi.org/10.1016/j.applthermaleng.2014.03.051>.
- [207] Logstor. Logstor Calculator 2022. <http://calc.logstor.com/en/energitaab/> (accessed October 3, 2022).
- [208] Ghafghazi S, Sowlati T, Sokhansanj S, Melin S. Techno-economic analysis of renewable energy source options for a district heating project. *International Journal of Energy Research* 2010;34:1109–20. <https://doi.org/10.1002/er.1637>.
- [209] Danish Energy Agency. The Danish Levelized Cost of Energy Calculator. 2014.
- [210] International Energy Agency. Heating. Paris: 2021.
- [211] Department for Energy Security and Net Zero (DESNZ), Triple Point, Heat Networks Investment Management. Green Heat Network Fund. London: Department for Energy Security and Net Zero (DESNZ); 2022.
- [212] Delta Energy and Environment, Department for Energy Security and Net Zero (DESNZ). The cost of installing heating measures in domestic properties. London: BEIS; 2018.
- [213] Department for Energy Security and Net Zero (DESNZ). Assessment of the Costs, Performance, and Characteristics of UK Heat Networks. London: 2015.
- [214] Eurostat. Comparative price levels for investment 2022.
- [215] AECOM. District Heating Feasibility Phase 2: Network Development and Financial Modelling. London Borough of Merton; 2018.
- [216] Thormann B, Kienberger T. Estimation of Grid Reinforcement Costs Triggered by Future Grid Customers: Influence of the Quantification Method (Scaling vs. Large-Scale

Simulation) and Coincidence Factors (Single vs. Multiple Application). *Energies* 2022;15:1383. <https://doi.org/10.3390/en15041383>.

[217] Klyapovskiy S, You S, Michiorri A, Kariniotakis G, Bindner H. Incorporating flexibility options into distribution grid reinforcement planning: A techno-economic framework approach. *Applied Energy* 2019;254:113662. <https://doi.org/10.1016/j.apenergy.2019.113662>.

[218] Meunier S, Protopapadaki C, Persson U, Sánchez-García L, Möller B, Wiechers E, et al. Cost and capacity analysis for representative EU energy grids depending on decarbonisation scenarios. *Zenodo*; 2021. <https://doi.org/10.5281/zenodo.4883664>.

[219] UK Power Networks. Common Connection Charging Methodology Statement 2022.

[220] Ramboll. System Rornet. Ramboll Group 2022. <https://ramboll.com/services-and-sectors/energy/district-energy/system-rornet> (accessed September 20, 2022).

[221] School of Informatics, The University Of Edinburgh. Computer science 4 & MSC Modelling And Simulation, Lecture 14 2003.

[222] Schaetzle WJ, Brett CE, Seppanen MS. Heat-pump-centered integrated community energy systems. Alabama Univ., University (USA). Bureau of Engineering Research; 1979. <https://doi.org/10.2172/5740509>.

[223] Cozzini M, D'Antoni M, Buffa S, Trier D, Jensen LL, Bava F, et al. FLEXYNETS Project Booklet. European Commission - Research & Innovation; 2018.

[224] International Energy Agency. Are renewable heating options cost-competitive with fossil fuels in the residential sector? – Analysis. Paris: IEA; 2021.

[225] Saltelli A. Sensitivity Analysis for Importance Assessment. *Risk Analysis* : An Official Publication of the Society for Risk Analysis 2002;22:579–90. <https://doi.org/10.1111/0272-4332.00040>.

[226] Saltelli A, Aleksankina K, Becker W, Fennell P, Ferretti F, Holst N, et al. Why so many published sensitivity analyses are false: A systematic review of sensitivity analysis practices. *Environmental Modelling & Software* 2019;114:29–39. <https://doi.org/10.1016/j.envsoft.2019.01.012>.

- [227] Ekren O, Ekren BY, Ozerdem B. Break-even analysis and size optimization of a PV/wind hybrid energy conversion system with battery storage – A case study. *Applied Energy* 2009;86:1043–54. <https://doi.org/10.1016/j.apenergy.2008.09.024>.
- [228] Ioannou A, Angus A, Brennan F. Stochastic financial appraisal of offshore wind farms. *Renewable Energy* 2020;145:1176–91. <https://doi.org/10.1016/j.renene.2019.06.111>.
- [229] Danish Energy Agency. Technology Data for power and heat production plants 2022.
- [230] Paluszczyszyn D, Skworcow P, Ulanicki B. Online simplification of water distribution network model. 2011.
- [231] Ramboll. Clyde Gateway D2 Grids Concept Design Report 2021.
- [232] Cooper Cromar. Shawfield Stadium – Planning Permission in Principle 2023.
- [233] Hulley and Kirkwood. Proposed Ambient Loop Network Layout 12701(56)-AL001 2022.
- [234] The Energy Act 2016 (Commencement No. 1 and Savings Provisions) Regulations 2016 2016. <https://www.legislation.gov.uk/ukxi/2016/602/regulation/1/made> (accessed May 13, 2024).
- [235] Pfeifroth U, Kothe S, Trentmann J, Hollmann R, Fuchs P, Kaiser J, et al. Surface Radiation Data Set - Heliosat (SARAH) - Edition 2.1 2019:7.5 TiB. https://doi.org/10.5676/EUM_SAF_CM/SARAH/V002_01.
- [236] Jordan U, Vajen K. DHWcalc: Program to generate domestic hot water profiles with statistical means for user defined conditions. *Proceedings of the ISES Solar World Congress*, vol. 12, Orlando, FL, USA: 2005.
- [237] Grainger C. Net Zero New Buildings 2021.
- [238] Djordjevic E, Kabelac S, SLOBODAN S. Mean heat transfer coefficients during the evaporation of 1,1,1,2-tetrafluoroethane (R-134a) in a plate heat exchanger. *Journal of the Serbian Chemical Society* 2007;72. <https://doi.org/10.2298/JSC0709833D>.

- [239] Kim M-H, Kim D-W, Han G, Heo J, Lee D-W. Ground Source and Sewage Water Source Heat Pump Systems for Block Heating and Cooling Network. *Energies* 2021;14:5640. <https://doi.org/10.3390/en14185640>.
- [240] Grassi W. *Heat Pumps*. Cham: Springer International Publishing; 2018. <https://doi.org/10.1007/978-3-319-62199-9>.
- [241] Preisegger E, Flohr F, Krakat G, Glück A, Hunold D. D4 Properties of Industrial Heat Transfer Media. In: VDI e. V., editor. *VDI Heat Atlas*, Berlin, Heidelberg: Springer Berlin Heidelberg; 2010, p. 419–512. https://doi.org/10.1007/978-3-540-77877-6_20.
- [242] Department of Energy & Climate Change. Performance of exhaust air source heat pumps: Summary of detailed monitoring results. 2013.
- [243] Danish Energy Agency, Energinet. Technology Data for Individual Heating Plants. 2021.
- [244] De Swardt CA, Meyer JP. A performance comparison between an air-source and a ground-source reversible heat pump. *International Journal of Energy Research* 2001;25:899–910. <https://doi.org/10.1002/er.730>.
- [245] Porrás F, Walter A, Soriano G, Ramírez AD. On the adoption of stricter energy efficiency standards for residential air conditioners: Case study Guayaquil, Ecuador. *Heliyon* 2023;9:e13893. <https://doi.org/10.1016/j.heliyon.2023.e13893>.
- [246] Lo ACW, Jones P, Yik FWH. Effects of pumping station configuration on the energy performance of district cooling systems. *Build Serv Eng Res Technol* 2017;38:287–308. <https://doi.org/10.1177/0143624416680019>.
- [247] AECOM, Delta Energy, University of Exeter. Cooling in the UK. Department for Energy Security and Net Zero (DESNZ); 2021.

10 Appendix A - Stakeholder interview details

The structure of the stakeholder interviews along with details on supporting documentation and consent form is presented in this section, followed by the actual documents. Interviews lasted approximately an hour, and all participants were provided with a participant information document detailing the purpose of the study, why they were invited to participate and the structure of the interview if they decide to take part. The structure of the interview is summarised below:

- Introduction (5 min)
- General question (5-10 min)
- Main Themes of research (20-30 min)
- Specific questions based on the stakeholder's background (10-20 min)
- End of Interview (5-10 min at the end)

In addition, the participant information sheet included potential risks and benefits of taking part, confidentiality statements and a detailed breakdown of how data will be stored and processed. A consent form was provided to all stakeholders to sign specifying the use of the accumulated data for academic research projects. It was also clearly stated that participants are free to withdraw from the study at any time without giving a reason and upon request their personal data can be erased or destroyed under their right to erasure.

10.1 Appendix A1 - Participant information sheet

Study title

Holistic approach of a 5th Generation District Heating and Cooling Network, coupling electricity and thermal networks.

1. Invitation paragraph

You are being invited to take part in a research study. Before you decide, it is important for you to understand why the research is being done and what it will involve. Please take time to read the following information carefully and discuss it with others if you wish. Ask me if there is anything that is not clear or if you would like more information. If you decide to take part in this study, you will be given a copy of this Participant Information Sheet and the signed consent form to keep.

2. What is the purpose of the study?

The interview will last for about an hour and be centred around the decarbonisation of the heat sector. More specifically the discussion will be centred around 5th Generation District Heating and Cooling systems to inform the literature's and industry's gap of knowledge and orient the study focus of the research.

The PhD's main research aim is to assess the environmental and economic benefits of a holistic 5th generation bidirectional flow ambient temperature network. It also aims to create an open-access model to better understand the operation of such a novel system and facilitate its industrial applications.

3. Why have I been invited to participate?

You have been invited to take part in this study because you are an expert on the field of district energy systems and your views would have a great impact on understanding the literature gap present.

4. Do I have to take part?

No, it is up to you to decide whether or not to take part. If you do decide to take part, you will be given this information sheet to keep and be asked to sign a consent form.

You are still free to withdraw at any time and without giving a reason. Upon request your personal data can be erased or destroyed under my right to erasure.

5. What will happen to me if I take part?

The interview will last for about an hour and the following structure will be followed.

- Introduction (5 min)
- General question (5-10 min)
 - What is your overall understanding of 5th Generation District Heating and Cooling Networks?
- Main Themes of research (20-30 min)
 - Comparison of 4GDH to 5GDHC. What are the key benefits and shortfalls?
 - What are the key physics of operation of a holistic bidirectional flow ambient temperature network?
 - What are your views on the modelling methodology for representation of the physics of operation of such an energy system? How can we minimise operation time and space?
 - What you think is the role of the thermal grid as a flexibility element to the electricity grid?
 - What you think is the role of energy storage and how can it lead to excess heat maximization?
 - What new business models are aware for this new technology that could facilitate decarbonisation?
- Specific questions based on your background (10-20 min)
 - These will be questions based on your own research/work
- End of Interview (5-10 min at the end)
 - Any questions for me? Anything I didn't ask about that you'd like me to know?

The interview will be recorded in the form of notes (no audio-video recording will be taken). These notes of your views will only be used to inform the literature's and industry's gap of knowledge and orient the study focus of the research.

6. What do I have to do?

Complete the interview.

7. What are the possible disadvantages and risks of taking part?

There are no potential disadvantages or harms in taking part in the study. However, your views/opinions on the themes identified above could be used on future publications.

8. What are the possible benefits of taking part?

You will receive no direct benefit from taking part in this study other than increasing your understanding on the topic of 5GDHC systems. The information that is collected during this study will give us a better understanding of the technology's benefits and shortfalls.

9. Will my taking part in this study be kept confidential?

All information which is collected about you, or responses that you provide, during the course of the research will be kept strictly confidential. As mentioned earlier, the interview will be recorded in the form of notes (no audio-video recording will be taken).

Personal data protection principles for your personal data (name, email, occupation, gender and age) will be followed throughout the project to ensure data security. Your data will be anonymised using the UK Data Service's text anonymization tool ([link](#)).

All data in electronic format will be stored on secure password-protected computers. No one outside of the research team or appropriate governance staff will be able to find out your name, or any other information which could identify you.

What will happen to my data?

Researchers from the University of Glasgow collect, store and process all personal information in accordance with the General Data Protection Regulation (2018).

The data will be stored in archiving facilities in line with the University of Glasgow retention policy of up to 10 years. After this period, further retention may be agreed or your data will be securely destroyed in accordance with the relevant standard procedures.

Your identifiable information might be shared with people who check that the study is done properly and, if you agree, in coded form with other organisations or universities to carry out research to improve scientific understanding. Your data will form part of the study result that will be published in expert journals, presentations, student dissertations/theses (if applicable) and on the internet for other researchers to use. Your name will not appear in any publication.

In case that any of your views/quotes are to be used in a publication they will be kept anonymised by simply presenting your general professional qualifications but no explicit occupation title (e.g. according to an industrial expert on heat pumps or a leading academic researcher on energy systems).

10. What will happen to the results of the research study?

If any of your views or direct quotes are used in a publication as a supporting element in the discussion section, you will be notified beforehand. The data will be anonymised. The inclusion in the publication will proceed only after having your consent. A copy of the publication will be sent to you when available.

11. Who is organising and funding the research?

Energy Technology Partnership (Public body)

Ramboll UK (Industrial Partner)

University of Glasgow

12. Who has reviewed the study?

The project has been reviewed by the College of Science and Engineering Ethics Committee.

Contact for Further Information

I can be contacted by email at xxxxxxxx@student.gla.ac.uk or at

xxxxxxxxxxxxxxxx@xxxxx.com

Thank you for reading this information sheet. If anything is unclear, please don't hesitate to contact me.

10.2 Appendix A2 - Consent form

CONSENT TO THE USE OF DATA

University of Glasgow, College of Science and Engineering Research Ethics Committee

I understand that **Orestis Angelidis** is collecting data in **the form of interview notes (no recordings)** for use in an academic research project at the University of Glasgow.

The topic of discussion will be on district energy systems and more specifically district heating and cooling networks. The interviews will only help to give a qualitative basis on the literature being reviewed to get a more holistic understanding of the knowledge gaps and potential biases present in various sectors.

None of these themes involve potentially sensitive topics and focus on my opinions on the future of the technology along with any potential issues of other nature they can identify.

I am free to withdraw from the study at any time and without giving a reason and upon request my personal data can be erased or destroyed under my right to erasure.

I give my consent to the use of data for this purpose on the understanding that (please put your initials after each statement to the respective box):

All names and other material (such as contact details, occupation, gender and age) likely to identify me will be anonymised.

The material will be treated as confidential and kept in secure storage at all times.

The material may be used in future publications, both print and online.

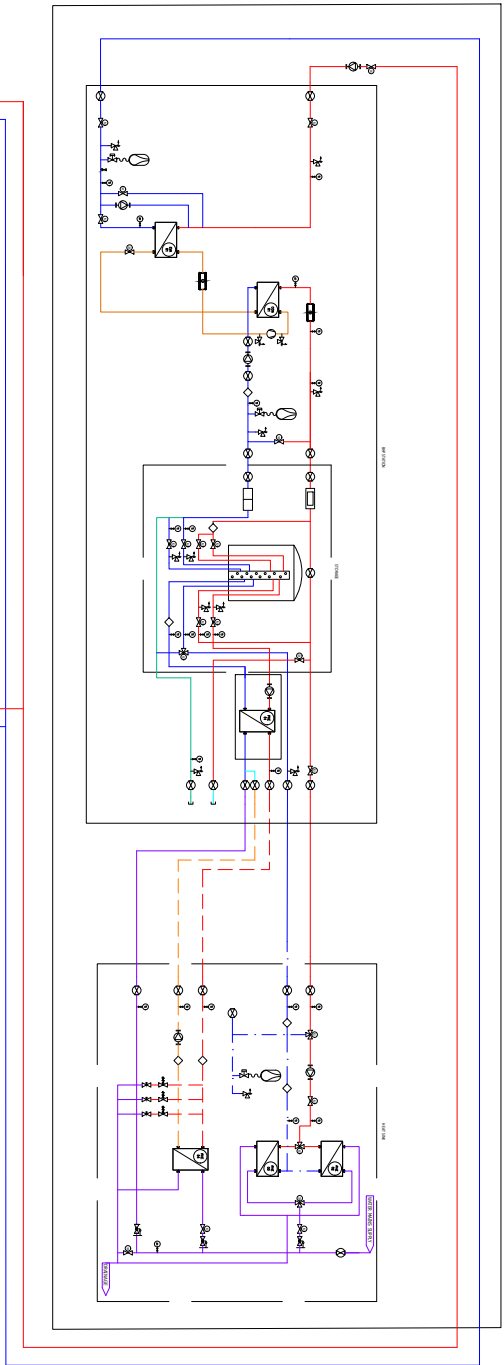
Signed by the contributor: _____ Date: _____

Researcher's name and email contact: Orestis Angelidis, xxxxxxxx@student.gla.ac.uk Supervisor's name and email contact: Gioia Falcone, Gioia.Falcone@glasgow.ac.uk Department address: University of Glasgow, School of Engineering, James Watt South Building, University of, Glasgow G12 8QQ

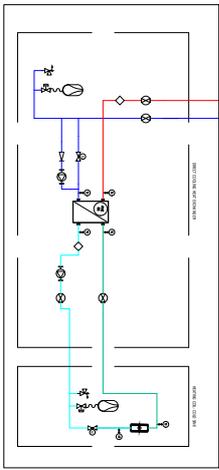
11 Appendix B – Experiment schematics, photos and drawings

11.1 Appendix B1 - P&ID

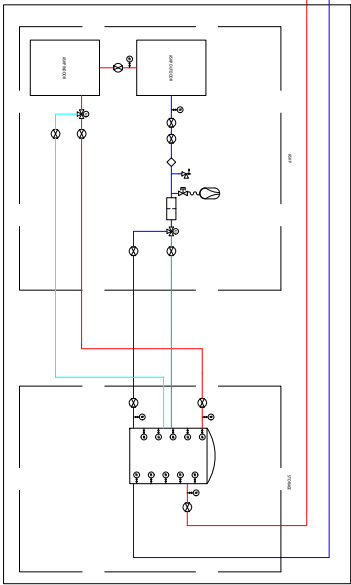
SF1 - BHP HEATING DEMAND



SF1 - HEX@C COOLING DEMAND



SF2 - BALANCING UNIT



LEGEND	
	WATER/STEAM
	GLYCOL
	COOLING WATER
	DOMESTIC HOT WATER
	RETURN WATER
	HEATING WATER
	CONDENSATE
	AIR SOURCE HEAT PUMP
	BOSTER HEAT PUMP
	CONDENSER
	DOMESTIC HOT WATER
	EVAPORATOR
	THERMAL ENERGY STORAGE
	WATER HEAT EXCHANGER
	SPACE COOLING
	SPACE HEATING
	WATER SOURCE HEAT PUMP
	TEMPERATURE DIFFERENCE

NONCIRCULAR	
	NONCIRCULAR
	WATER/STEAM
	GLYCOL
	COOLING WATER
	DOMESTIC HOT WATER
	RETURN WATER
	HEATING WATER
	CONDENSATE
	AIR SOURCE HEAT PUMP
	BOSTER HEAT PUMP
	CONDENSER
	DOMESTIC HOT WATER
	EVAPORATOR
	THERMAL ENERGY STORAGE
	WATER HEAT EXCHANGER
	SPACE COOLING
	SPACE HEATING
	WATER SOURCE HEAT PUMP
	TEMPERATURE DIFFERENCE

- NOTES
1. DRAWING NOT TO SCALE
 2. FINISHING INFO ON INDIVIDUAL COMPONETS AVAILABLE ONLINE AT: [www.rockwellautomation.com](#)
 3. DETAILED INFORMATION ABOUT THE CONTROL PHILOSOPHY CAN BE FOUND IN THE USER MANUAL FOR THE CONTROL SYSTEM.
 4. THIS SHEET IS TO BE USED FOR A SPECIFIC HEATING AND COOLING APPLICATION WITH SINGLE WINGS HEATING AND COOLING SEPARATION.
 5. SF1 - COOLING WATER IS CONNECTED TO THE TEST WATER USED TO BALANCE COOLING DEMAND AND A TEST TO EMULATE A BOSTER HEAT PUMP.
 6. SF2 - BHP FEEDBACK IN ASP AND A TEST TO EMULATE A BALANCING UNIT FOR COOLING DEMAND AND A TEST TO EMULATE A BOSTER HEAT PUMP.
 7. THE BHP MODEL AND THE ASP MODEL ARE NOT TO BE USED FOR DESIGN PURPOSES.
 8. THE BHP MODEL AND THE ASP MODEL ARE NOT TO BE USED FOR DESIGN PURPOSES.
 9. THE BHP MODEL AND THE ASP MODEL ARE NOT TO BE USED FOR DESIGN PURPOSES.
 10. THE BHP MODEL AND THE ASP MODEL ARE NOT TO BE USED FOR DESIGN PURPOSES.

11. ASP - AIR SOURCE HEAT PUMP
12. BHP - BOSTER HEAT PUMP
13. COM - CONDENSER
14. DHW - DOMESTIC HOT WATER
15. EVAP - EVAPORATOR
16. TES - THERMAL ENERGY STORAGE
17. WHE - WATER HEAT EXCHANGER
18. SC - SPACE COOLING
19. SH - SPACE HEATING
20. WSH - WATER SOURCE HEAT PUMP
21. DT - TEMPERATURE DIFFERENCE

PROJECT NAME	SCHEMATIC NUMBER
COOLING UNIT - SCHEMATIC PIPE AND INSULATION DIAGRAM (PID)	SC-001-001
CREATED BY	DESIGNER
REVISIONS	DESCRIPTION
DATE	VERSION

11.2 Appendix B2 – Equipment photos

11.2.1 Heating prosumer

For the heating prosumer, the grid side pump is sending the water through the BHP. On the return the water is also passing through a flow meter. After the BHP the heated water goes to the TES. From there, there are connections to the space heating and DHW loads.

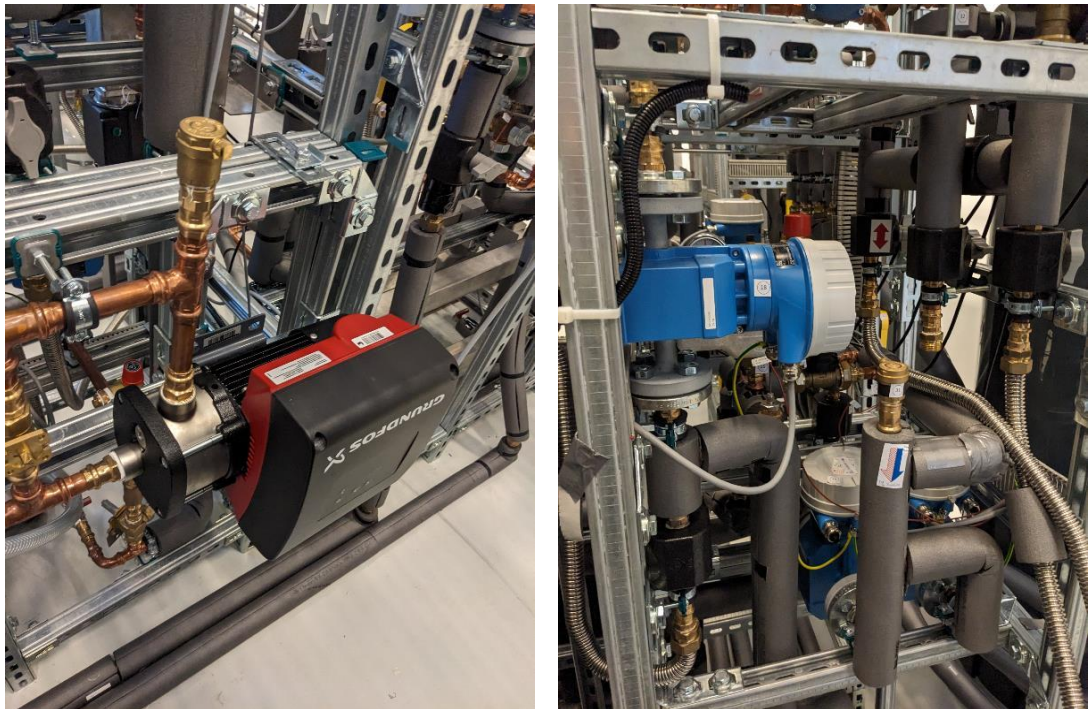


Figure 11.1: (Left) Grid pump for heating prosumer (Right) Flowmeter on the return of the BHP.

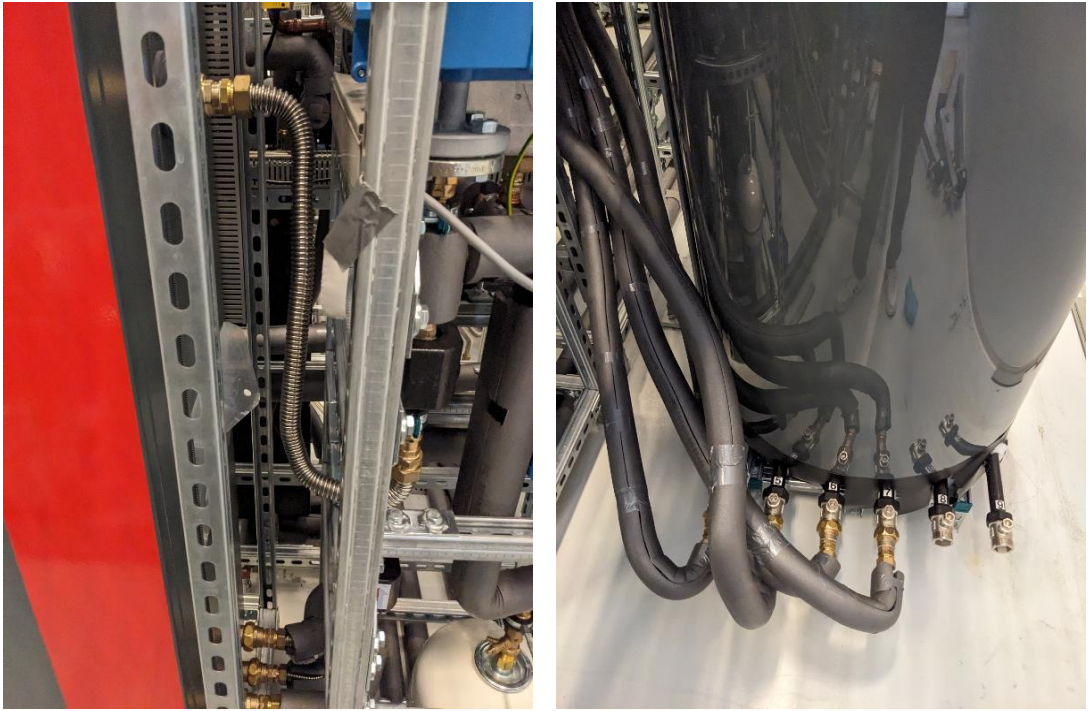


Figure 11.2: (Left) Connection to and out from the BHP (Right) Connection from the BHP to the TES.



Figure 11.3: Connection from the TES to the DHW and space heating loads.



Figure 11.4: Connection to the space heating and DHW loads, each having a HEX dedicated to it for the load emulation.

11.2.2 Cooling prosumer

The cold load emulated by a HC is shown below. The heated-up water from the HC is then returned to the HEX_{DC} . The pump on the grid side of the HEX_{DC} is shown in the last picture.



Figure 11.5: (Left) HC for replicating cooling prosumer (Right) HC inlet and outlet.

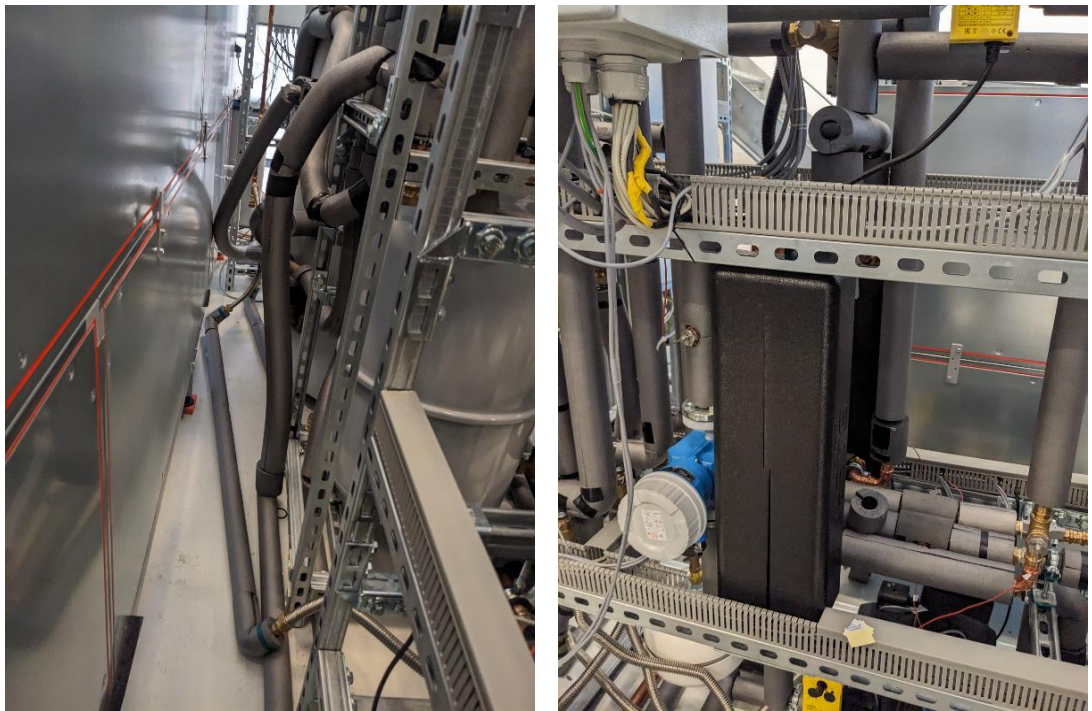


Figure 11.6: Connection to and from the HC, back to the HEX_{DC} (Right) HEX_{DC} and flowrate sensor.



Figure 11.7: Cooling prosumer grid pump.

11.2.3 ASHP and BU TES

The following pictures show the ASHP and the TES which is connected in series with it.



Figure 11.8: (Left) ASHP indoor and outdoor unit along with air chamber for air intake
(Right) BU TES.

11.2.4 Grid connector

The grid connection where the main intersection is located is shown below.

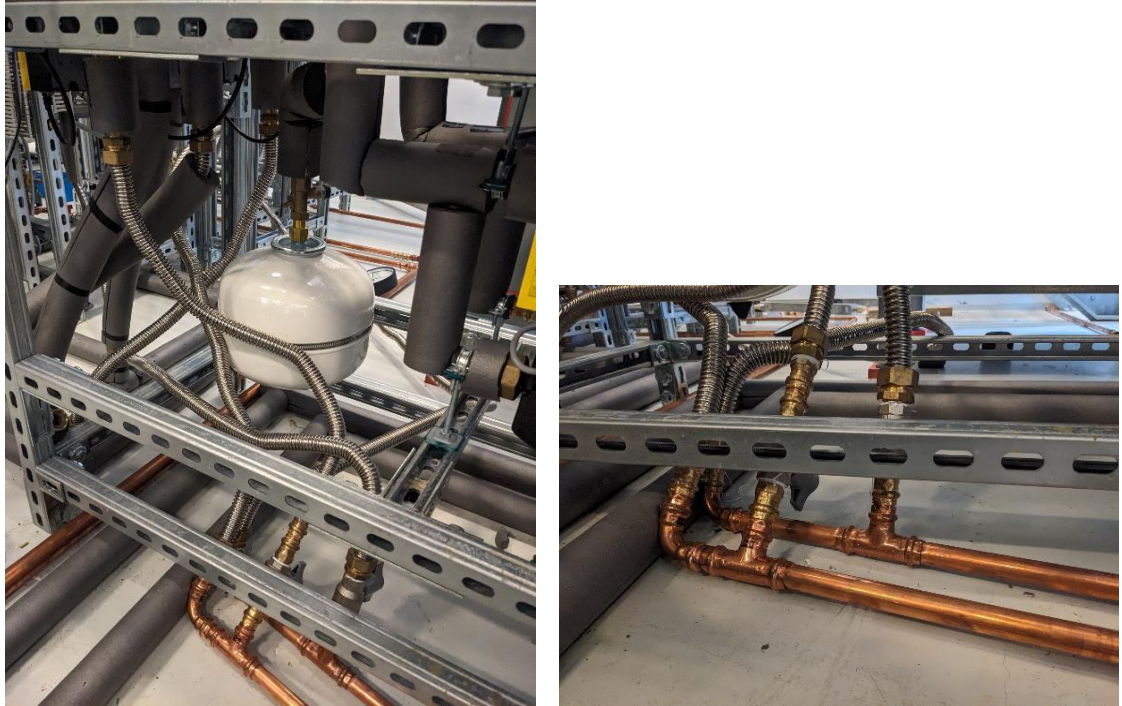


Figure 11.9: Grid connection (for hot and cold pipes), combining the BU TES, BHP and HEX_{DC} flows.

11.3 Appendix B3 – LabView screenshots

11.3.1 Main virtual instrument interface

The main Virtual Interface (VI) for the inputs recorded by the IC on the hardware is sent to VeriStand interface and from there, logged into Labview as inputs. These inputs are used in the Sub VIs which have individual control elements for the various components. The outputs from the SubVI control logic, are then exported back to VeriStand to be fed into the ICs for the new timestep. PHIL outputs are also sent to the ICs as shown on Figure 11.12.

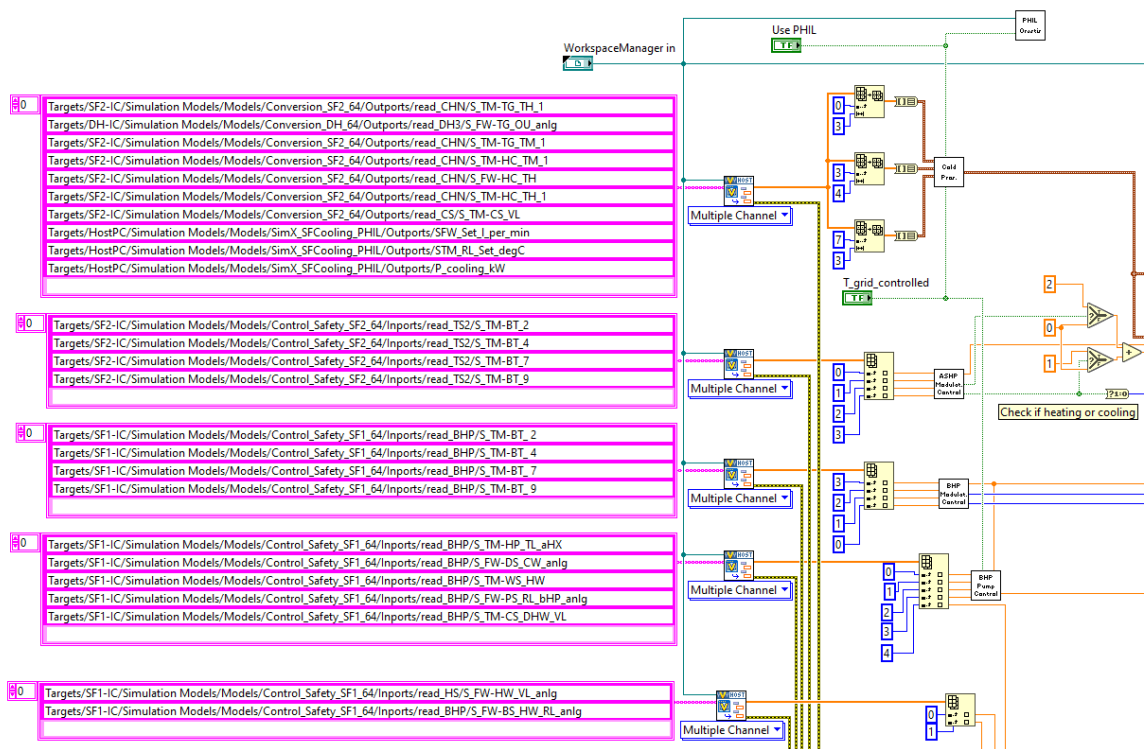


Figure 11.10: VeriStand inputs (from IC sensors) and LabView control sub-VIs.

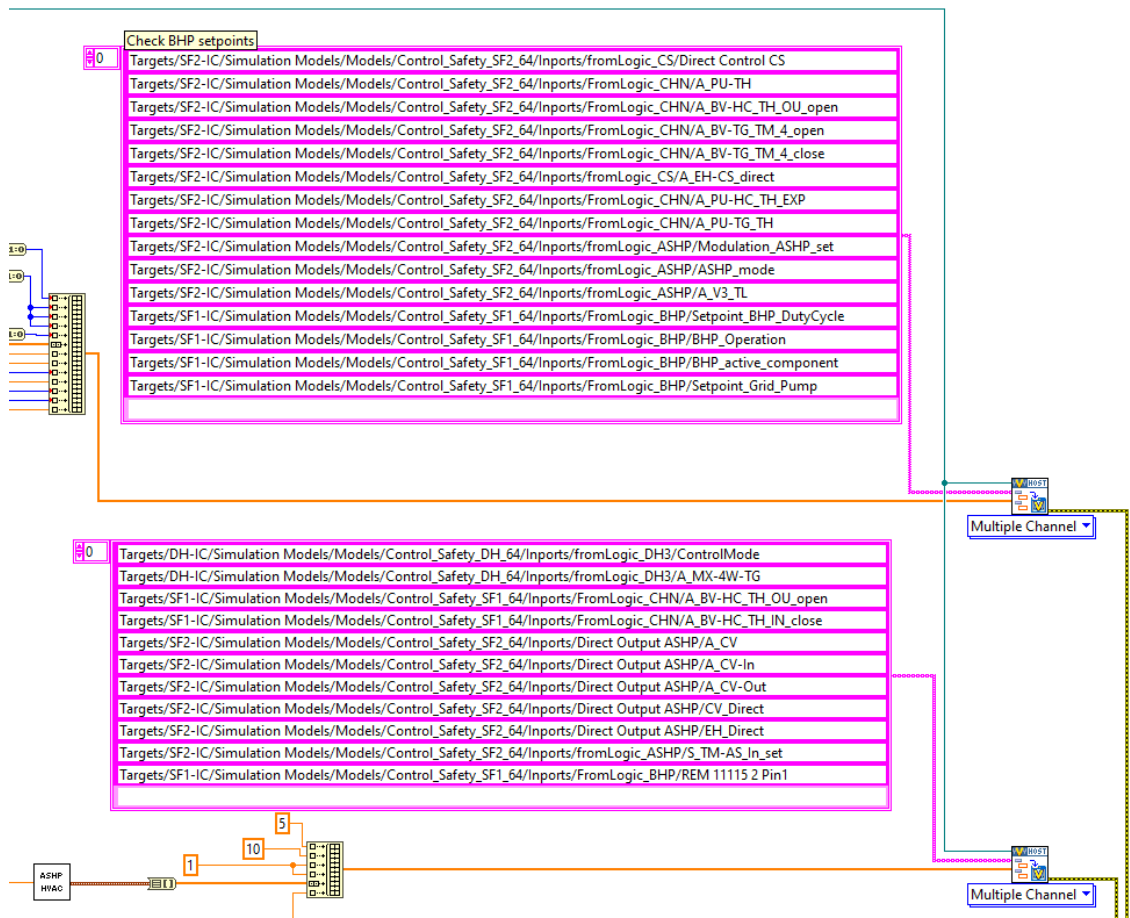


Figure 11.11: VeriStand outputs for IC.

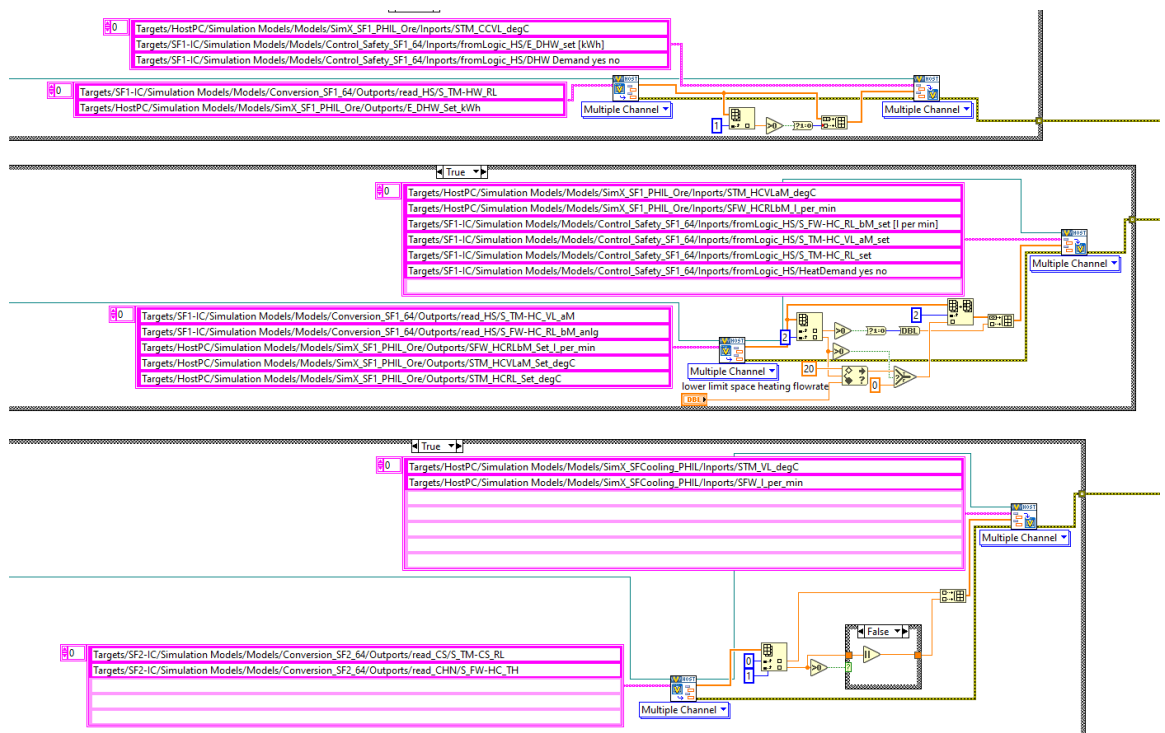


Figure 11.12: PHIL VeriStand outputs.

11.3.2 BU sub VI

The BU comprises the controls for the ASHP, showing the logic for when to turn off and when to turn on as shown in Figure 11.13 and Figure 11.14, while the parameters used in the logical steps are shown in Figure 11.15.

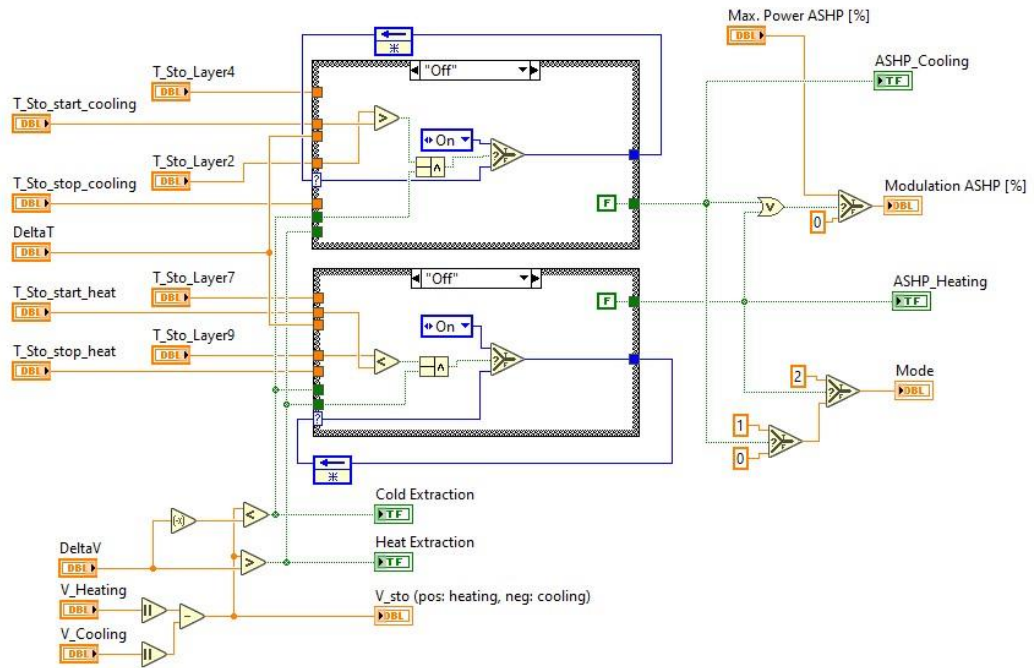


Figure 11.13: LabView control logic when the ASHP is off.

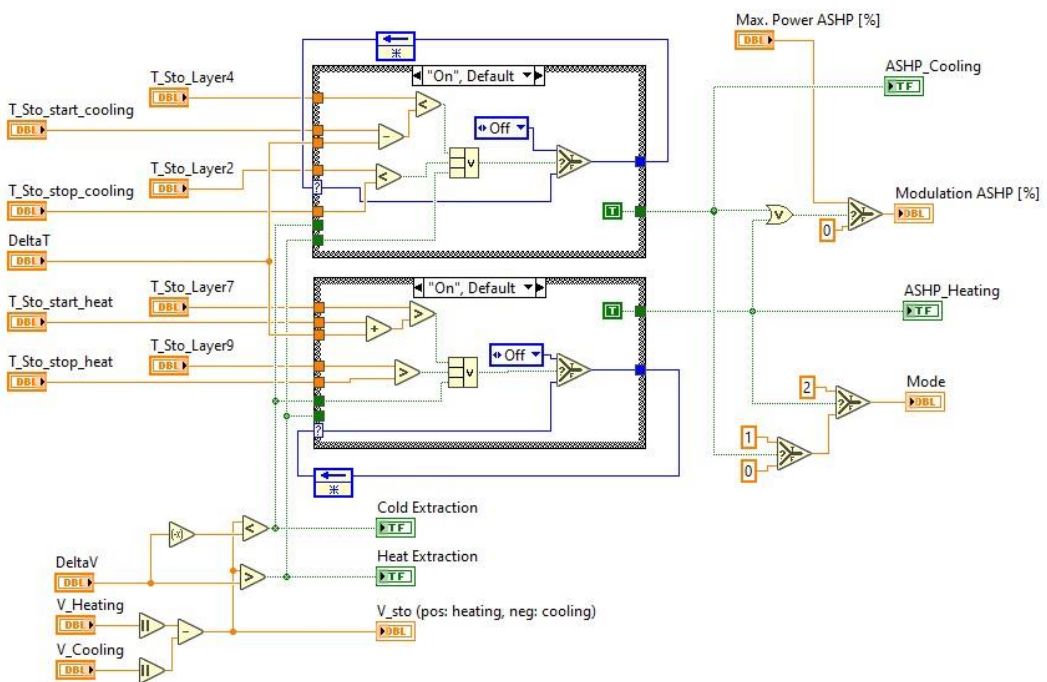


Figure 11.14: LabView control logic when the ASHP is on.

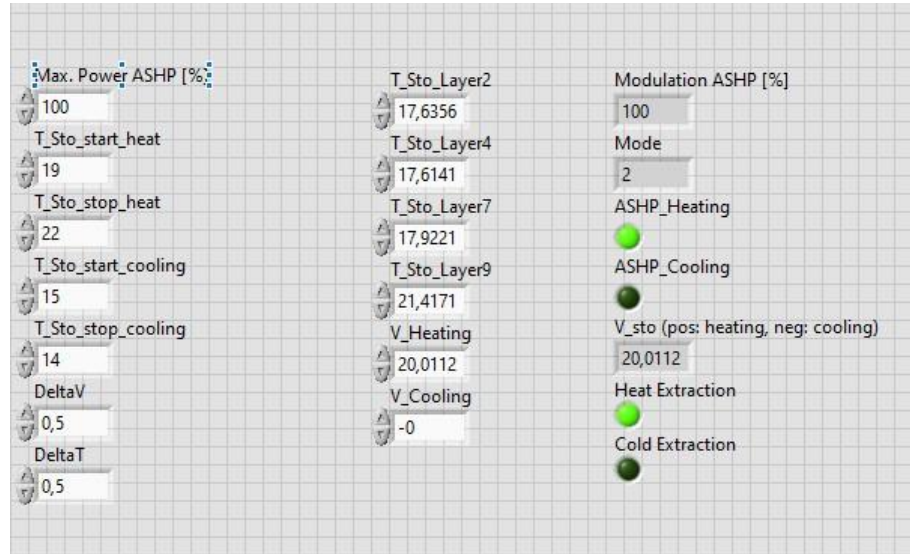


Figure 11.15: ASHP control parameters front panel.

From these figures it can be seen that the controls depend on the temperature within the TES.

11.3.3 Heating prosumer sub VI

Similar to the ASHP, the heating prosumer VI revolves around the BHP operation. The BHP operation is shown in Figure 11.16, Figure 11.17 and Figure 11.18. In addition, there is a VI for the grid pump for operation both under $T_{GridFloat}$ and $T_{GridFix}$, shown in Figure 11.19, Figure 11.20 and Figure 11.21. Finally, the DHW pump control is also included and shown in Figure 11.22.

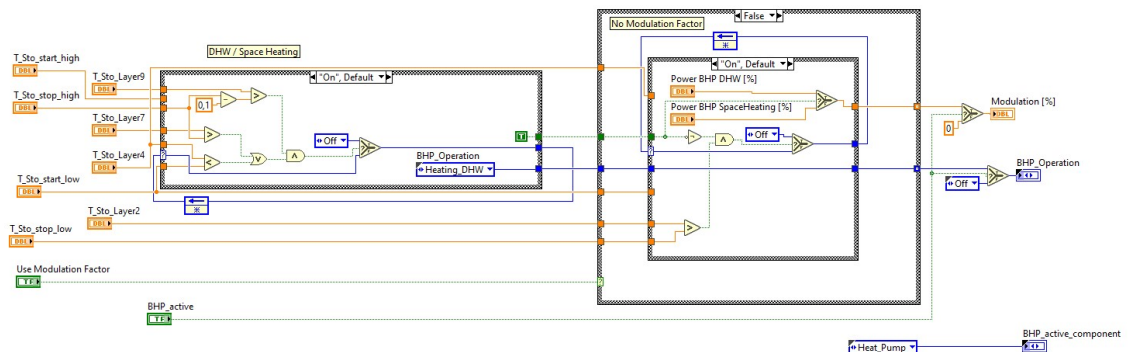


Figure 11.16: LabView control logic when the BHP is on.

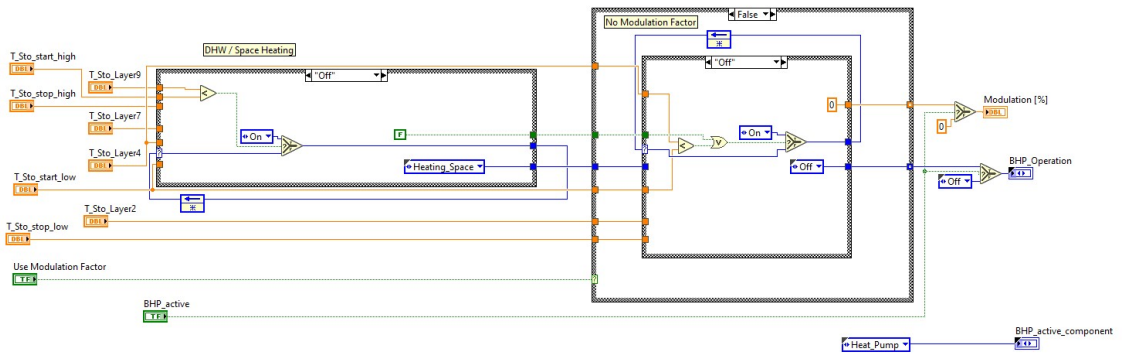


Figure 11.17: LabView control logic when the BHP is off.

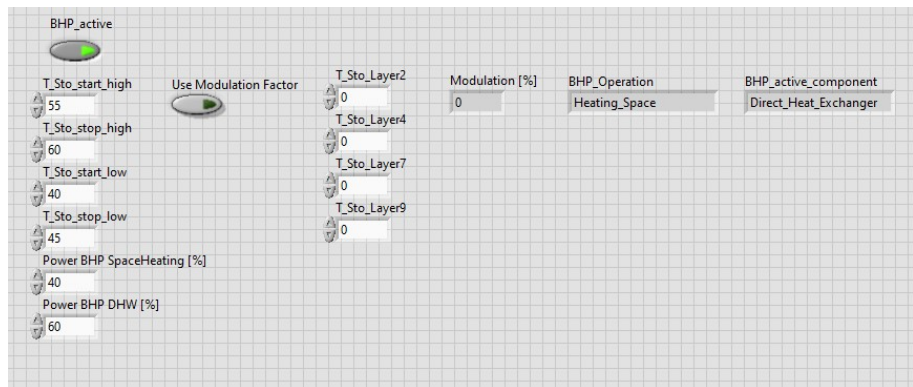


Figure 11.18: BHP control parameters front panel.

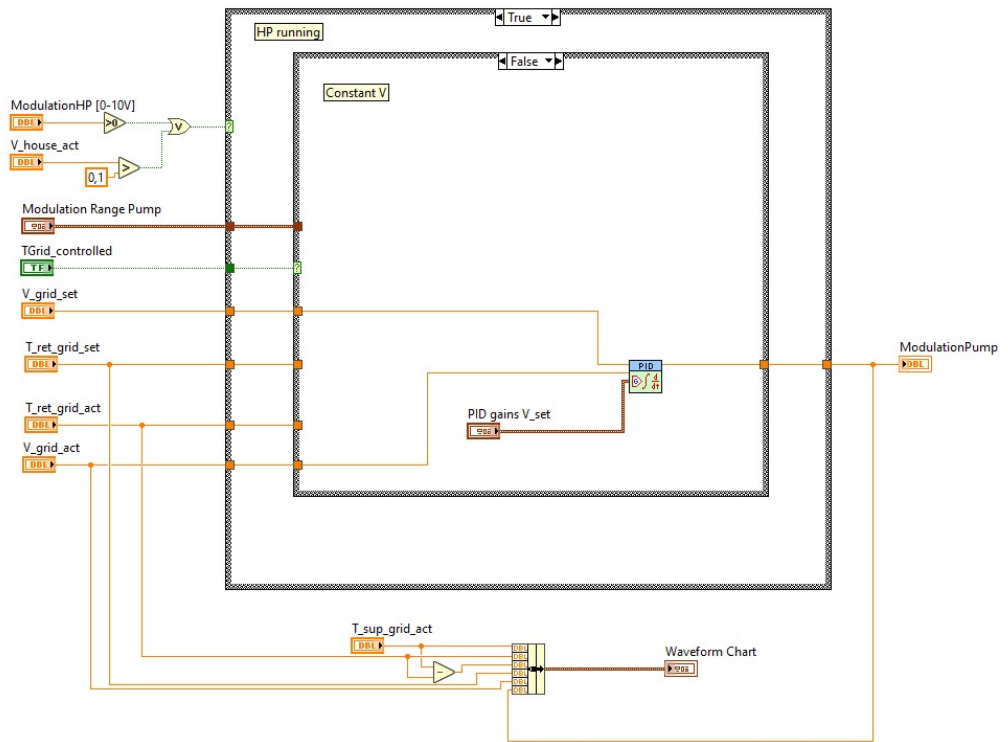


Figure 11.19: Heating prosumer grid pump control logic for $T_{GridFloat}$ (control on pump flowrate).

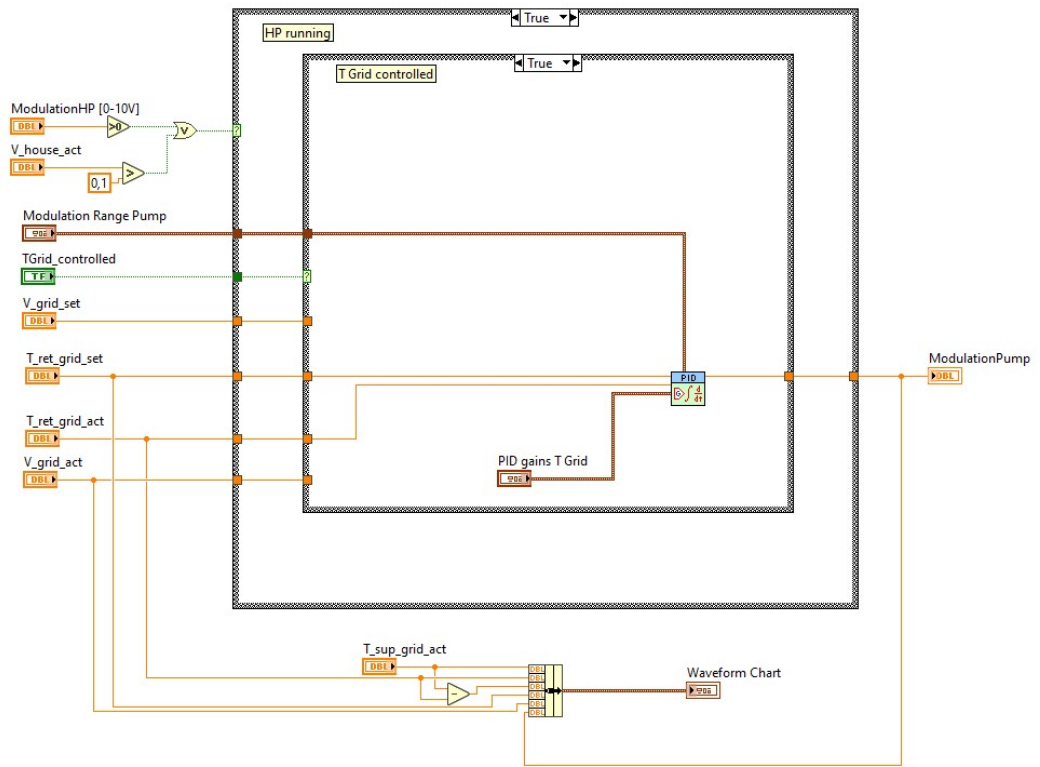


Figure 11.20: Heating prosumer grid pump control logic for $T_{GridFix}$ (control on return temperature).

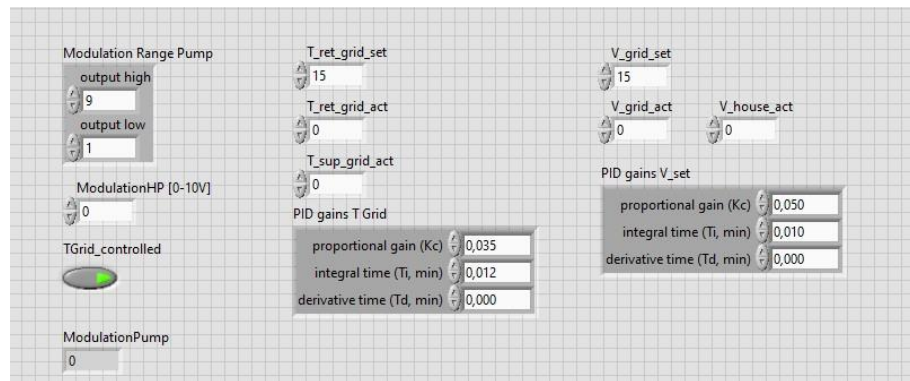


Figure 11.21: Heating prosumer grid pump control parameters front panel.

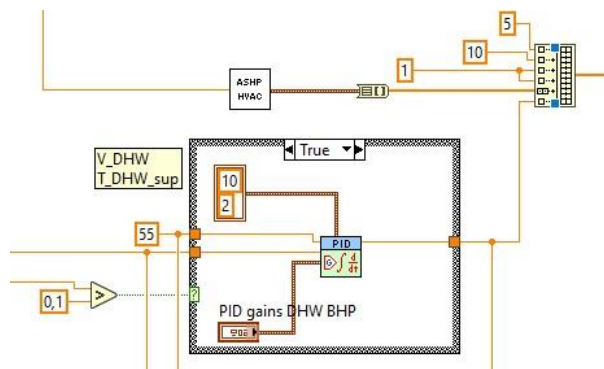


Figure 11.22: DHW control logic.

11.3.4 Cooling prosumer

For the cooling prosumer, the Sub VI includes controls for the grid pump and the heating coil operation. The heating coil operation is shown in Figure 11.23. In addition, there is a VI for the grid pump for operation both for $T_{GridFloat}$ and $T_{GridFix}$, shown in Figure 11.24, Figure 11.25 and Figure 11.26.

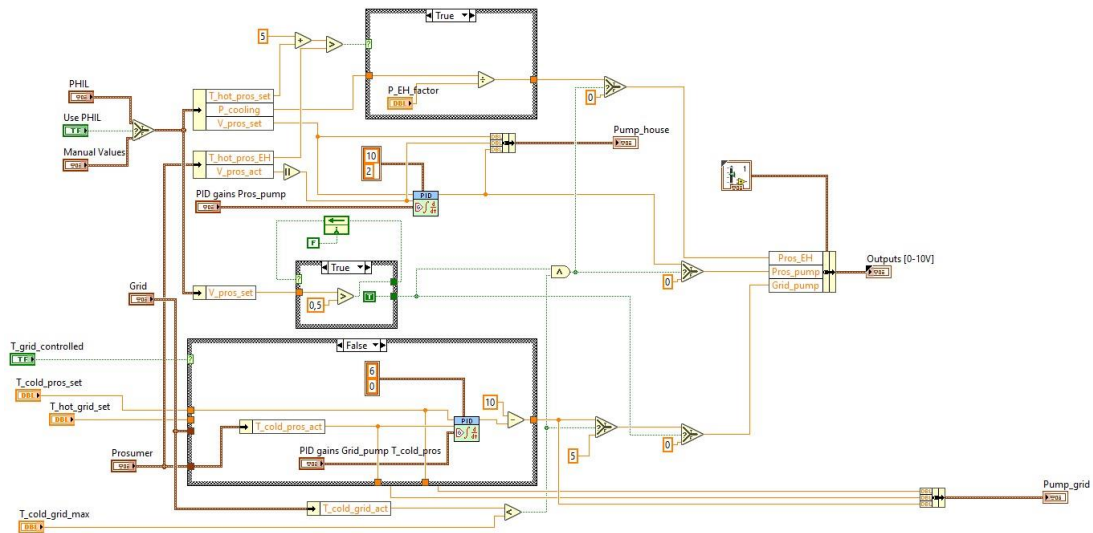


Figure 11.23: Heating coil operation and cold prosumer control logic.

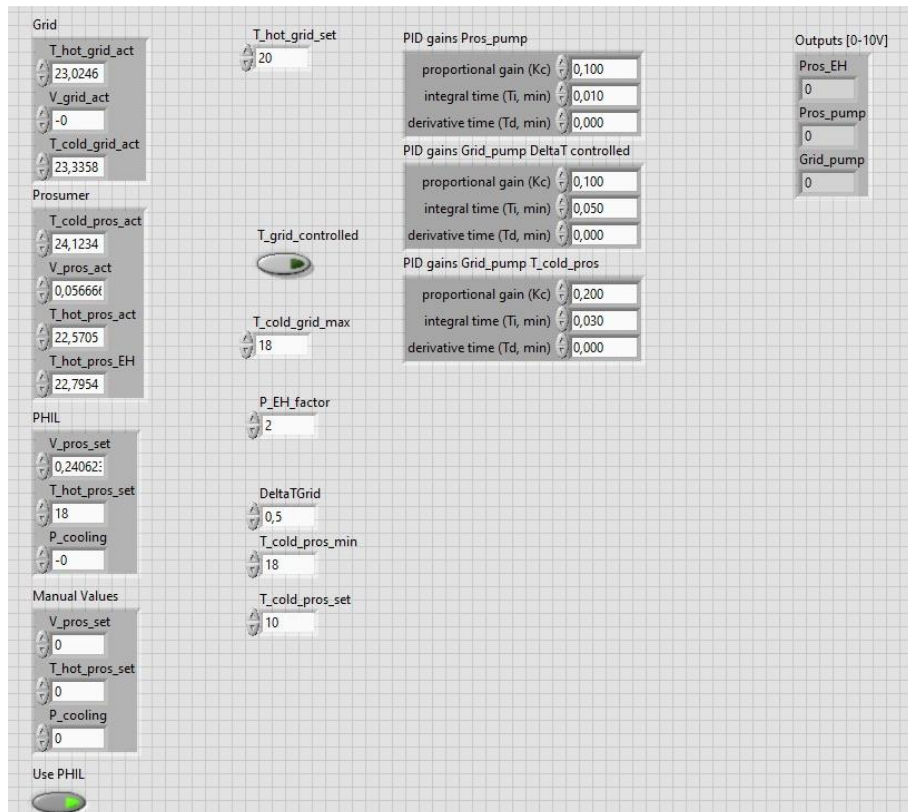


Figure 11.24: Cooling prosumer control parameters front panel.

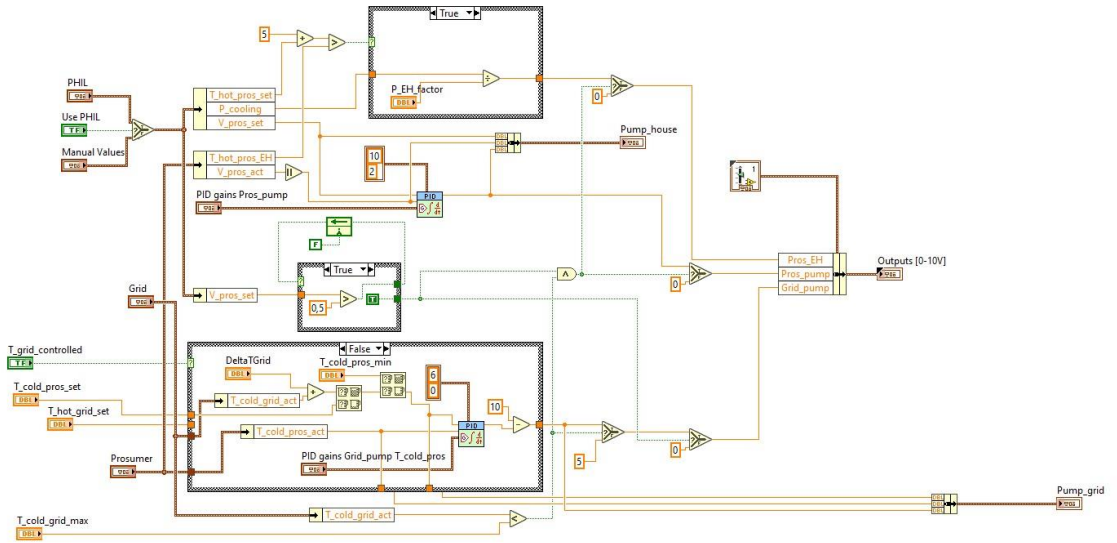


Figure 11.25: Cooling prosumer control logic for $T_{GridFloat}$ (control on flow temperature to heating coil).

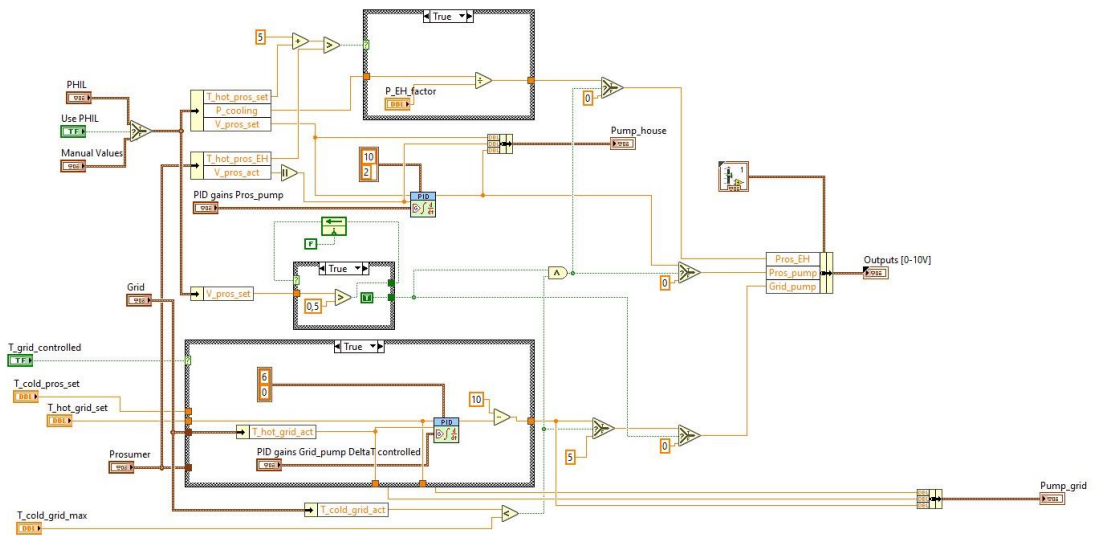


Figure 11.26: Cooling prosumer control logic for $T_{GridFix}$, (control on return temperature of HEX_{DC}).

12 Appendix C – CATHeaPS Data

The following tables capture the key techno-economic data used in CATHeaPS.

Table 12.1: Key technical data used in CATHeaPS.

Item	4GDH&AC	5GDHC	ASHP	GB&AC
Network Temperature	60°C – 40°C [43].	20°C – 15°C [144].	N/A	N/A
Network Insulation and pipe material	Pair of steel pipes Series 2 insulation [43].	Pair of steel pipes Series 0 insulation [43].	N/A	N/A
Parasitic Loads	3% of heating demand (MWh/year) including controls and pumping [213].	7% of energy demand (MWh/year) including controls and pumping [246].	N/A	N/A
Efficiency of supply units (SCOP, SEER, SPF)	ASHP EC SCOP: 3.2 [243] Gas boiler efficiency EC: 88% [229] Electric boiler efficiency EC: 99% [229] Individual AC unit SEER: 4.6 [245]	BHP: Heating SCOP: 4.5 [239] Cooling SEER: 5.0 [239] ASHP BU: Heating SCOP: 4.5 [239] Cooling SEER: 5.0 [239]	Individual reversible ASHP with calorifier: Heating SPF: 2.0 [242] Cooling SEER: 3.5 [242]	Gas boiler efficiency: 88% [243] Individual AC unit SEER: 4.6 [245]
Abstraction Point	Centralised HEX for pumping and abstraction point. Costs included in the WSHP CAPEX and OPEX.		N/A	N/A
Building Connection	Indirect system. HIUs for residential and substations for commercial properties.	When communal system, indirect space heating (HIU at each flat) and calorifier (with electric resistance) for DHW.	N/A	N/A
Technology Lifetime [28]	EC: 60 years Network: 60 years	BU: 60 years Network: 60 years	ASHP: 15 years	Gas boiler: 20 years

Item	4GDH&AC	5GDHC	ASHP	GB&AC
	ASHP: 15 years	BHP: 15 years		
	Boilers: 20 years	ASHP: 15 years		
	AC units: 15 years			
	HIU: 25 years			
	Substations: 25 years			

Table 12.2: Key cost data used in CATHeaPS.

Item	4GDH&AC	5GDHC	ASHP	GB&AC
Network CAPEX	1242 (£/m) [213].	Uninsulated pipework is 40% cheaper than insulated [28]. Pipe diameters are larger by ΔDN (depends on each project). Cost: $1,242(1 - \frac{0.4}{\Delta DN})$ (£/m)	N/A	N/A
Energy Supplying Technologies CAPEX	ASHP EC: 604,041 * $MW_{th}HP + 392,324$ (£) [229] Gas boiler EC: 45,477 (£/MW _{th}) [229] Electric boiler EC: 113,693 (£/MW _{th}) [229] AC Unit: Residential: 1,234£/unit Commercial: 318£/kW [247]	BHP: 492 * $kW_{th}HP + 10,052$ (£) [212,243] ASHP BU: 604,041 * $MW_{th}HP + 392,324$ (£) [229]	Individual ASHP: 297 * $kW_{th}HP + 6452$ (£) [212]	GB residential: 3,660 (£/unit) [212] GB plantroom: 107 (£/kW) [212] AC Unit: Residential: 1,234£/unit Commercial: 318£.kW
EC/BU/Plantroom CAPEX	Building and abstraction cost included in supplying technology costs. EC/Plantroom ancillary costs: 147 (£/MWh) [213]		N/A	N/A

Item	4GDH&AC	5GDHC	ASHP	GB&AC
Abstraction Point CAPEX	For this study, only the HEX cost is used, excluding all CAPEX associated with the thermal source. CAPEX for Abstraction HEX: 76 (£/kW) [28].		N/A	N/A
Building Connection CAPEX	Indirect HIU: 1,667 (£/unit) [28]. Substations: 68 (£/kW) [28].	Indirect HIU (for communal systems): 1,667 (£/unit) [28].	N/A	N/A
Additional Costs	30% of EC and network CAPEX [215]. Includes Testing and commissioning, Contingency, Consultancy & Design fees.		N/A	N/A
REPEX Share	Based on the lifetime of equipment shown above. 100% replacement assumed [213].			
Electricity grid connection CAPEX	These are not included because they vary massively depending on the location of the project area and are unpredictable. Contacting the local DNO is proposed for each specific project.			
Network OPEX	Variable 0.40 (£/MWh) [213]	Fixed 1% of Network CAPEX (£) [215]	N/A	
Energy Supplying Technologies OPEX	ASHP EC: -0.08* $MW_{th}HP + 2.02$ (£/MWh _{th}) [229] Gas boiler EC: 1,517 (£/MWh _{th}) [229] Electric boiler EC: 834 (£/MWh _{th}) [229] AC Units: Residential: 62£/unit Commercial: 16£/kW [247]	BHP: Residential Individual: 208 (£/unit) [212] Plantroom: 7 (£/kW) [212] ASHP BU: -0.08* $MW_{th}HP + 2.02$ (£/MWh _{th}) [229] Gas Boiler: 1,517 (£/MWh _{th}) [229]	ASHP Residential: 210 (£/unit) [212] Plantroom: 11 (£/kW) [212]	GB Residential: 146 (£/unit) [212] Plantroom: 3 (£/kW) [212]
EC/BU/Plantroom OPEX	Building and abstraction cost included in supplying technology costs. EC/BU/Plantroom ancillary costs: 2.5 £/MWh [213].		N/A	N/A

Item	4GDH&AC	5GDHC	ASHP	GB&AC
Abstraction Point OPEX	For this study, only the HEX cost is used, excluding all CAPEX associated with the thermal source. OPEX for Abstraction HEX: Variable 0.4 (£/kW) Fixed 0.2 (£/MWh) [28].		N/A	N/A
Building Connection OPEX	Indirect HIU: 1,667 (£/unit) [28]. Substations: 379 (£/unit) [28] and 0.19 (£/MWh) [28].	Indirect HIU (for communal systems): 1,667 (£/unit) [28].	N/A	N/A
Fuel Costs	Retail Electricity and Gas Prices (real 2022 p/kWh) with latest projections from DESNZ. Services projections used for 4GDH&AC and for commercial properties in 5GDHC, ASHP and GB&AC options, residential projections used in residential properties of 5GDHC, ASHP and GB&AC options [17].			
CO ₂ Emissions and associated costs	Carbon prices (real 2021 £/tCO ₂) and Air Quality Impact cost (real 2022 p/kWh) based on latest projections by DESNZ [17].			